



DEVELOPMENT AND CHARACTERIZATION OF COSMETIC APPLICATIONS FOR FUCOPOL

SÍLVIA DE ALMEIDA BAPTISTA

Master in Biotechnology

Master in Monetary and Financial Economy

DOCTORATE IN CHEMICAL AND BIOCHEMICAL ENGINEERING

NOVA University Lisbon

September 2022



DEVELOPMENT AND CHARACTERIZATION OF COSMETIC APPLICATIONS FOR FUCOPOL

SÍLVIA DE ALMEIDA BAPTISTA

Master in Biotechnology

Master in Monetary and Financial Economic

Adviser: Maria Filomena Andrade de Freitas

Assistant Professor, NOVA School of Science and Technology | FCT NOVA

Co-adviser: Filipe Manuel Rodrigues Leitão de Aguiar

CEO 73100, Lda.

Examination Committee:

Chair: Maria da Ascensão Carvalho Fernandes Miranda Reis,
Full Professor, NOVA School of Science and Technology | FCT NOVA

Rapporteurs: Anabela Cristina da Silva Naret Moreira Raymundo,
Associate Professor, School of Agriculture University of Lisbon (ISA)
Rita Palmeira de Oliveira,
Invited Assistant Professor, University of Beira Interior (UBI)

Adviser: Maria Filomena Andrade de Freitas,
Assistant Professor, NOVA School of Science and Technology | FCT NOVA

Members: Catarina Batista Fialho Rosado,
Associate Professor, University Lusófona (ECTS)
Luísa Alexandra Graça Neves,
Assistant Researcher, NOVA School of Science and Technology | FCT NOVA
Maria da Ascensão Carvalho Fernandes Miranda Reis,
Full Professor, NOVA School of Science and Technology | FCT NOVA

Development and characterization of cosmetic applications for FucoPol

Copyright © Sílvia de Almeida Baptista, NOVA School of Science and Technology, NOVA University Lisbon.

The NOVA School of Science and Technology and the NOVA University Lisbon have the right, perpetual and without geographical boundaries, to file and publish this dissertation through printed copies reproduced on paper or on digital form, or by any other means known or that may be invented, and to disseminate through scientific repositories and admit its copying and distribution for non-commercial, educational or research purposes, as long as credit is given to the author and editor.

This page was intentionally left blank

*To my greatest treasure,
Maria da Conceição Baptista & José Baptista*

*To my love,
André Freches*

This page was intentionally left blank

AGRADECIMENTOS

Esta tese não teria sido possível sem a orientação e ajuda de várias pessoas que de uma forma ou de outra contribuíram e estenderam a sua valiosa ajuda na preparação e conclusão deste estudo. É um gosto transmitir a minha gratidão a todos eles em meu humilde reconhecimento.

Em primeiro lugar, quero fazer um agradecimento muito especial à minha orientadora Professora Doutora Filomena Freitas pela exemplar orientação que me permitiu crescer cientificamente durante este processo. Agradeço a disponibilidade com que me recebeu e integrou no grupo BIOENG enquanto aluna de mestrado da Universidade da Beira Interior, assim como por me ter sugerido como investigadora à 73100, Lda. após a conclusão do mestrado. Ao longo de 10 anos, agradeço a partilha do seu conhecimento científico e críticas construtivas que me permitiram superar dúvidas e reformular decisões. Não posso deixar de destacar o seu positivismo, perseverança e dedicação que de uma forma muito clara, calma, objetiva e motivadora conduziram ao aperfeiçoamento da presente tese. A sua boa disposição e serenidade permitiram o melhor ambiente que alguém pode desejar enquanto desenvolve um trabalho desta complexidade. Destaco a sua conduta humana, apoio e incentivo sempre demonstradas em momentos difíceis e decisivos que resultaram sempre num forte estímulo para prosseguir o caminho que culmina nesta tese. Agradeço pela sua garra e por me ter defendido em todos os momentos. Saliento ainda a minha profunda gratidão e o privilégio que sinto pela amizade que construímos e que se projetará muito para além deste tempo. O meu reconhecimento para toda a vida.

À direção da 73100, Lda. em especial ao meu coorientador Dr. Filipe Aguiar pelo financiamento do plano doutoral que levou ao desenvolvimento desta tese. Agradeço a oportunidade e confiança depositada ao longo dos meus 9 anos de casa, assim como a inteira disponibilidade sempre demonstrada. Agradeço o apoio e as circunstâncias que me proporcionaram realizar este trabalho, dando-me liberdade científica para atingir os objetivos.

À Professora Doutora Maria Ascensão Reis pela qual tenho uma admiração profunda pelo seu percurso académico e científico. Agradeço pela aceitação no seu grupo de investigação BIOENG enquanto aluna de mestrado da Universidade da Beira Interior, facultando-me de imediato a possibilidade de executar o trabalho laboratorial nos seus laboratórios, permitindo o início da minha experiência científica e as oportunidades que advieram daí. Saliento a sua simpatia e por me fazer sentir sempre como parte do grupo.

À Universidade NOVA de Lisboa, em especial ao Senhor Reitor João Sàágua pela dispensa de pagamento de propina do presente ano letivo devido aos constrangimentos e constantes impedimentos causados pela pandemia de COVID-19 que tornaram impossível o normal decorrer do plano de investigação, durante os períodos de confinamento e meses posteriores.

À Universidade da Beira Interior e a todos os que foram meus docentes pela excelência científica e rigor de desempenho que proporcionou ser o que sou hoje. Agradeço àquela que foi a minha casa durante 6 anos pelo conhecimento e ferramentas que me enriqueceram e prepararam para este percurso. Deste tempo ficaram as bases científicas, as recordações maravilhosas e as amizades que perduram. Só

quem passa pela UBI e por todo o espírito académico e interpessoal sabe o que realmente significa. Tenho o maior orgulho de ter sido formada nesta instituição. Para sempre no meu coração.

Ao Grupo de investigação BIOENG por me ter recebido e por me ter tratado como elemento integrante do grupo. Agradeço tudo o que este grupo me proporcionou: novos conhecimentos e experiência científica, momentos de diversão, amizades e o mais importante, o amor da minha vida. A minha gratidão para toda a vida.

À Doutora Cristiana Torres, ao Professor Doutor Vítor Alves, ao Professor Doutor Jorge Silva, ao João Pereira, à Cátia Gil e ao Bruno Guerreiro agradeço as contribuições científicas prestadas na publicação de artigos científicos. Agradeço todos os ensinamentos, esclarecimentos, sugestões e diálogos científicos que em muito contribuíram para a qualidade desta tese.

À minha amiga e madrinha de casamento Ana Luísa Arquilino, agradeço pelos 28 anos de amizade, paciência, motivação, gargalhadas, cumplicidade e apoio nos momentos difíceis. Saliento a contagiante boa disposição que proporcionaram a vivência de momentos felizes e de descontração.

Aos meus amigos Élia Mota, Francisco Marques, Adriana Afonso, Madalena Marçal, Joana Santos e Ana Sapina agradeço as aventuras, boa disposição, longas conversas, incentivo e apoio.

Às minhas amigas Patrícia Reis e Diana Araújo agradeço o suporte, ajuda, momentos de boa disposição e acima de tudo pelo carinho. Agradeço a partilha de conhecimentos e ao espírito de grupo com que sempre me brindaram e enriqueceram.

Aos meus colegas do grupo BIOENG agradeço o bom acolhimento e disponibilidade continuada, em especial à Patrícia Freitas, Rita Bernardino, Asiyah Esmail e Ana Teresa Rebocho pela boa disposição no laboratório, entreajuda e incentivo. Agradeço ainda todo o apoio, partilha, paciência, sorrisos e alegrias. Um muito obrigado pela amizade e camaradagem.

À Filipa Baptista agradeço por ter sido a melhor aluna que se pode ter, pela ajuda e boa disposição.

Aos meus sogros agradeço o apoio e ajuda durante este último ano.

Ao André, agradeço de coração a inestimável paciência, tempo interminável, ajuda preciosa, apoio emocional e amor. Saliento o privilégio que sinto por partilhar a vida com uma pessoa tão especial e pelo que temos construído. Agradeço por ter sido o melhor colega, amigo, namorado e agora marido e por me fazer tão feliz. Pela sua capacidade de me tranquilizar e mostrar sempre o lado positivo de tudo, impedindo que desmoralizasse, especialmente nos períodos mais críticos. Agradeço por encher o meu coração de amor e tornar a minha vida mais leve, saudável e completa. O meu amor para sempre.

Finalmente, quero fazer um agradecimento muito especial à minha Mãe e ao meu Pai, sendo este o agradecimento mais importante para mim.

Nada do que possa escrever neste agradecimento descreve o que os meus pais significam para mim e como eles são importantes na minha vida. O apoio incondicional que me deram ao encarar este projeto e com o qual me ajudaram e continuam a ajudar a avançar sempre em frente, fomentando a conclusão dos objetivos a que me proponho, sempre rumo a um crescimento saudável e feliz. Agradeço por me terem proporcionado uma casa feliz, uma família coesa e amor incondicional. Os sacrifícios, paciência e apoio ao longo da vida. A presença nos momentos difíceis, conselhos certos e incentivo que me fazem acreditar que é possível superar todos os desafios. Por acreditarem sempre em mim.

Tudo o que sou hoje, devo aos meus pais. São as pessoas que me enchem o coração e a razão do meu viver. Estarei eternamente grata e amarei para sempre aqueles que são as melhores pessoas que conheço. O meu coração para sempre.

Bem haja a todos!

This page was intentionally left blank

"If people feel they understand the world around them, or, probably, even if they have the conviction that they could understand it if they wanted to, then and only then are they also able to feel that they can make a difference through their decisions and activities".

Frank Oppenheimer

This page was intentionally left blank

ABSTRACT

The constant development of new technologies and the interest in the incorporation of novel sustainable ingredients has rendered the cosmetic industry as one of the fastest growing industrial sectors. Consumers' demand for the utilization of biodegradable ingredients has precipitated the utilization of natural polymers as stabilizers in newly developed emulsions. Due to its unique properties, FucoPol has great potential to be used in various topical applications, i.e., as stabilizer, sensorial improvement promoter, and drug delivery polymer.

The main objectives of this study were the development and characterization of FucoPol-based emulsions for safe topical application, using production methods focused on cost-reduction, and further investigating the resulting system's behaviour under *in vitro* conditions.

FucoPol extraction was successfully optimized by ultrafiltration using a 30 kDa molecular weight cut-off (MWCO) membrane that allowed for a 37% reduction of the total water consumption and a 55% reduction of the extraction time. This improved downstream procedure resulted in a 10% increase in product recovery with higher purity, without impacting FucoPol's sugar and acyl groups composition, molecular mass distribution or thermal degradation profile.

As deacylation is known to alter the functional characteristics in various polysaccharides (e.g., xanthan gum), an alkaline treatment was developed and implemented to obtain a deacylated form of FucoPol (d-FucoPol). Deacetylation and desuccinylation were effectively achieved with 0.02 M NaOH, at 60 °C for 15 minutes, with no impact on the biopolymer's sugar composition, pyruvyl group content and average molecular weight. Nonetheless, d-FucoPol displayed novel properties, differing from the native FucoPol mainly in its viscoelastic properties. d-FucoPol's solutions' apparent viscosity decreased by 68%, but they were not affected by the pH, maintaining the similar apparent viscosity in a wide range of pH values, a contrasting behaviour with native FucoPol. Although d-FucoPol displayed emulsification activity (EA) for olive oil similar to FucoPol, for an oil:water ratio of 2:3, the emulsions were less viscous (the zero-shear viscosity decreased from 46.5 to 13.92 Pa.s). Therefore, further studies were conducted with the native FucoPol, given its properties were more suitable for the envisaged applications.

To understand the emulsion forming mechanisms and stabilizing capacity of FucoPol, preliminary tests were performed using two aqueous solutions of FucoPol (0.5 wt.% and 1.0 wt.%) with four hydrophobic compounds (olive oil, almond oil, paraffin oil and castor oil), at different oil/water (O/W) weight ratios. Response surface methodology (RSM) was used to define the optimal concentration ranges for FucoPol, olive oil, and α -tocopherol. Emulsions containing olive oil and α -tocopherol were successfully stabilized with FucoPol with optimal emulsification for FucoPol concentration in the range 0.7–1.3 wt.% and olive oil contents of 20–30 wt.%.

Oil-in-water (O/W) emulsions containing olive oil (30 wt.%) and α -tocopherol (2.5 wt.%) stabilized by FucoPol were formulated. Formula composition was designed using RSM approach to determine the contents of FucoPol (1.5 wt.%), cetyl alcohol (1.5 wt.%) and glycerine (3.0 wt.%) that resulted in high emulsification index after 24 hours ($E_{24} \geq 97.6\%$), concomitant with an apparent viscosity of

8.72 Pa.s (at a shear rate 2.3 s^{-1}), with a solid-like behaviour ($G' > G''$), and a droplet size of $6.12 \mu\text{m}$ and Zeta-potential of -98 mV .

Development of FucoPol-based emulsion with L-ascorbic acid (5.0 wt.%, 8.0 wt.%, 1.0 wt.% and 15 wt.%) was performed using olive oil or almond oil. The L-ascorbic acid concentration for each formulation was chosen considering the results obtained for olive oil (8.0 wt.% L-ascorbic acid with a $\eta=2.71 \text{ Pa.s}$, at 2.30 s^{-1}) and almond oil (15 wt.% L-ascorbic acid with $\eta=5.15 \text{ Pa.s}$, at 2.30 s^{-1}) using the apparent viscosity value as a decision factor. The L-ascorbic acid addition induced a lower stability to the formulations, by decreasing the emulsions' apparent viscosity, firmness, cohesiveness and adhesivity, causing a change in the viscoelastic behaviour as well ($G'' > G'$).

The validation of the FucoPol-based cream, named F-cream, was successfully performed. The formulation-cream proved to be suitable for topical use according to the rheological assessment and stability throughout the study period (2 months). *In vitro* studies also demonstrated that the F-cream was suitable for topical application, presented antioxidant, photoprotective, and regeneration effect, without relevant cytotoxicity.

Keywords: polysaccharides, FucoPol, biopolymer extraction, response surface methodology (RSM), O/W emulsions, cosmetic formulations, topical application.

RESUMO

A indústria cosmética é um dos setores industriais com maior crescimento e constante evolução, investindo em novas tecnologias e incorporação de novos ingredientes inovadores. A crescente preocupação dos consumidores com ingredientes naturais, resulta na crescente procura de produtos biodegradáveis e sustentáveis. Tendo em conta as suas propriedades únicas, o FucoPol apresenta potencial para ser empregue em diversas aplicações tópicas, seja como estabilizador, promotor sensorial e agente de libertação controlada de fármacos.

Esta tese teve como principais objetivos o desenvolvimento e caracterização de emulsões seguras à base de FucoPol para aplicação tópica, de custo reduzido e com propriedades regeneradoras.

Foi otimizado o método de extração para a recuperação do FucoPol com sucesso usando o método de ultrafiltração com uma membrana de 30 kDa. A otimização do processo permitiu uma redução de 37% no consumo total de água e uma redução de 55% no tempo de extração. Esta alteração no processo conduziu não só o aumento da recuperação de produto (cerca de 10%), assim como um aumento do grau de pureza, sem afetar a composição, distribuição de massa molecular ou perfil de degradação térmica do biopolímero.

A deacilação é uma reação química que potencia propriedades funcionais em vários polissacáridos (como por exemplo a goma xantana). Nesse sentido, foram testadas diferentes condições (concentração, temperatura e tempo) para atingir o tratamento alcalino ideal. As condições ideais para a deacilação e a desuccinilação foram alcançadas nas condições de 0,02M de NaOH, a 60 °C durante 15 minutos, sem afetar a composição e o peso molecular médio do biopolímero. Neste estudo, foi também avaliado o efeito na viscosidade aparente, força iónica, temperatura e pH.

Foi realizado um estudo preliminar para avaliar a capacidade de formação e estabilização de emulsões contendo FucoPol (0,5% e 1,0% (*m/m*)) para quatro compostos hidrofóbicos (azeite, óleo de amêndoas doces, parafina e óleo de ricínio), em diferentes razões de massa óleo/água (O/A). Emulsões contendo FucoPol, azeite e α -tocoferol foram desenvolvidas utilizando a metodologia de superfície de resposta. O FucoPol (0,7-1,3% (*m/m*)) mostrou capacidade de estabilização de emulsões constituídas por azeite (20-30% (*m/m*)) e α -tocoferol, obtendo-se um índice de emulsificação ideal.

Foram formuladas emulsões O/A com 30 % (*m/m*) de azeite e 2.5 % (*m/m*) de α -tocoferol estabilizadas com FucoPol. A composição da fórmula foi desenvolvida usando a metodologia de superfície de resposta para determinar a concentração ideal de FucoPol (1,5% (*m/m*)), álcool cetílico (1,5% (*m/m*)) e glicerina (3,0% (*m/m*)) com o objetivo de atingir um alto índice de emulsificação após 24 horas ($E_{24} \geq 97,6\%$), concomitante com uma viscosidade aparente de 8,72 Pa.s (a uma velocidade de deformação de $2,3 \text{ s}^{-1}$), um comportamento viscoelástico $G' > G''$, com um tamanho de gota de $6,12 \mu\text{m}$ e um potencial Zeta de -98 mV.

Foi elaborado um protocolo para o desenvolvimento de formulações à base de FucoPol com ácido L-ascórbico (5,0%, 8,0%, 1,0% e 15% (*m/m*)) usando azeite ou óleo de amêndoa como fase dispersa. A concentração de ácido L-ascórbico para cada formulação foi escolhida considerando os resultados obtidos para azeite (8,0% de ácido L-ascórbico com $\eta=2,71 \text{ Pa.s}$, a uma velocidade de deformação

de $2,30 \text{ s}^{-1}$) e óleo de amêndoa (15% ácido L-ascórbico com $\eta=5,15 \text{ Pa.s}$, a uma velocidade de deformação $2,30 \text{ s}^{-1}$) considerando o valor da viscosidade aparente como fator de decisão. A adição de ácido L-ascórbico desestabilizou as formulações, através da diminuição da viscosidade aparente, firmeza, coesividade e adesividade das emulsões, bem como alteração do comportamento viscoelástico ($G'' > G'$).

A validação de uma formulação à base de FucoPol foi realizada com sucesso. A formulação final mostrou-se adequada para uso tópico de acordo com a avaliação reológica e estabilidade ao longo do período de estudo (2 meses). Resultados *in vitro* revelaram a ausência de citotoxicidade, presença de capacidade de regeneração celular e propriedades intrínsecas de fotoproteção, no entanto provou ser um promotor de fotoproteção por efeito sinérgico. Os resultados obtidos demonstraram um compromisso entre a estabilidade, proteção contra a radiação ultravioleta, eficácia e cosmetividade.

Palavras-chave: exopolisacáridos, FucoPol, extração de biopolímeros, metodologia de superfície de resposta (MSR), emulsões O/A, formulações cosméticas, aplicação tópica.

CONTENTS

AGRADECIMENTOS	IX
ABSTRACT	XV
RESUMO.....	XVII
LIST OF FIGURES.....	XXV
LIST OF TABLES.....	XXXI
ACRONYMS.....	XXXV
SYMBOLS	XXXVII
AIMS AND THESIS ORGANIZATION	XXXIX
1. GENERAL INTRODUCTION.....	1
Bacterial Polysaccharides in Cosmetic Industry	1
1.1.1 Background	3
1.1.2 Bacterial Polysaccharides.....	4
1.1.2.1 Main Properties	4
1.1.2.2 Biotechnological importance in Cosmetic Industry	7
1.1.3 FucoPol.....	9
1.1.3.1 Main properties.....	10
1.1.4 Skin care.....	11
1.1.4.1 Skin structure.....	11
1.1.4.2 Cosmetic Products.....	13
1.1.4.2.1 Definition and Categories of cosmetics products	13
1.1.4.2.2 Cosmetic Formulation	14
1.1.5 Cosmetic emulsions.....	16
1.1.6 Conclusions	20
2. FUCOPOL EXTRACTION AND CHARACTERIZATION	21
CHAPTER 1. Optimization of FucoPol Extraction by Membrane-based Methods.....	23
Summary	25
2.1.1 Introduction	25
2.1.2 Materials and Methods	27
2.1.2.1 FucoPol Production	27
2.1.2.2 FucoPol Extraction and Purification	27

2.1.2.3	FucoPol Characterization	29
2.1.2.3.1	Chemical Composition	29
2.1.2.3.2	Elemental Analysis	29
2.1.2.3.3	Inorganic Salts Content	29
2.1.2.3.4	Molecular Mass Distribution	29
2.1.2.3.5	Fourier Transform Infrared (FT-IR) Spectroscopy	30
2.1.2.3.6	Thermogravimetric Analysis (TGA)	30
2.1.2.4	Apparent viscosity and viscoelastic properties	30
2.1.2.5	Emulsion Forming and Stabilizing Capacity	30
2.1.3	Results	31
2.1.3.1	Optimizing FucoPol Purification by Diafiltration and/or Ultrafiltration Procedures	31
2.1.3.2	Physical and Chemical Characterization of the Extracted FucoPol Samples	33
2.1.3.2.1	Composition	33
2.1.3.2.2	Molecular Mass Distribution	34
2.1.3.2.3	FT-IR Spectroscopy	34
2.1.3.2.4	Thermogravimetric Analysis	34
2.1.3.3	Rheological Properties of the Extracted FucoPol Samples in Aqueous Medium	36
2.1.3.4	Emulsion Forming and Stabilizing Capacity	38
2.1.4	Discussion	40
2.1.5	Conclusions	42
CHAPTER 2. FucoPol Deacetylation and Desuccinylation		43
Summary		45
2.2.1	Introduction	45
2.2.2	Materials and Methods	47
2.2.2.1	FucoPol production and extraction	47
2.2.2.2	Chemical deacylation/depyruvylation of FucoPol	47
2.2.2.3	Physical and chemical characterization	47
2.2.2.3.1	Composition	47
2.2.2.3.2	Fourier Transform Infrared analysis	47
2.2.2.3.3	Molecular mass distribution	47
2.2.2.3.4	Intrinsic viscosity	48
2.2.2.3.5	Thermal properties	48
2.2.2.4	Apparent viscosity and viscoelastic properties	48
2.2.2.5	Emulsion forming and stabilizing capacity	48
2.2.2.6	Characterization of the Emulsions	49

2.2.2.6.1	Type of emulsion.....	49
2.2.2.6.2	Microscopic observation	49
2.2.2.7	Film-forming capacity	49
2.2.2.7.1	Film preparation	49
2.2.2.7.2	Morphological characterization.....	49
2.2.2.8	Mechanical properties	50
2.2.3	Results and Discussion.....	51
2.2.3.1	Optimization of the chemical deacylation/ depyruvylation conditions.....	51
2.2.3.2	Physical and chemical characterization of the deacetylated/desuuccinylated FucoPol	52
2.2.3.2.1	Sugar composition.....	52
2.2.3.2.2	Structural analysis	52
2.2.3.2.3	Molecular mass distribution	53
2.2.3.2.4	Thermal properties.....	53
2.2.3.2.5	Intrinsic viscosity.....	54
2.2.3.3	Apparent viscosity and viscoelastic properties of the d-FucoPol solutions	54
2.2.3.3.1	Apparent viscosity	54
2.2.3.3.2	Effect of ionic strength.....	56
2.2.3.3.3	Effect of pH.....	56
2.2.3.3.4	Effect of temperature.....	58
2.2.3.4	Emulsion forming and stabilizing capacity	59
2.2.3.5	Film-forming capacity	62
2.2.3.5.1	Morphological Characterization.....	62
2.2.3.5.2	Mechanical Properties	62
2.2.4	Conclusions	64
3.	DEVELOPMENT AND CHARACTERIZATION OF FUCOPOL COSMETIC FORMULATIONS.....	65
CHAPTER 1.	Assessment of FucoPol Emulsifying Capacity using different Natural Oils	67
Summary	69
3.1.1	Introduction	69
3.1.2	Materials and Methods	71
3.1.2.1	Materials.....	71
3.1.2.2	Determination of surface-active properties	71
3.1.2.3	Emulsions' preparation.....	71
3.1.2.4	Factorial design of experiments.....	72
3.1.2.5	Characterization of the emulsions	72
3.1.2.5.1	Type of emulsion and microscopic observation.....	72

3.1.2.5.2	Apparent viscosity and viscoelastic properties.....	73
3.1.2.5.3	Texture analysis.....	73
3.1.3	Results and Discussion.....	74
3.1.3.1	Polymer characterization.....	74
3.1.3.2	Emulsion forming and stabilizing capacity of FucoPol.....	74
3.1.3.2.1	Preparation of FucoPol-stabilized emulsions with different oils.....	74
3.1.3.2.2	Evaluation of emulsions' stability.....	76
3.1.3.2.3	Assaying α -tocopherol as an additive to the FucoPol-stabilized emulsions.....	78
3.1.3.2.4	Comparison with Sepigel® 305.....	79
3.1.3.3	Emulsification Optimization by Response Surface Methodology.....	80
3.1.3.3.1	Response Analysis.....	80
3.1.3.3.2	RSM modelling.....	80
3.1.3.4	Characterization of the FucoPol-stabilized emulsions.....	83
3.1.3.4.1	Type of emulsion.....	83
3.1.3.4.2	Apparent viscosity and viscoelastic properties.....	84
3.1.3.5	Textural assessment.....	86
3.1.3.6	Comparative analysis of the FucoPol-stabilized emulsions.....	86
3.1.4	Conclusions.....	87
CHAPTER 2.	Development of Olive Oil and α -tocopherol containing Formulations.....	89
Summary	91
3.2.1	Introduction.....	91
3.2.2	Materials and Methods.....	93
3.2.2.1	Materials.....	93
3.2.2.2	Factorial design of experiments.....	93
3.2.2.3	Preparation of FucoPol-based emulsion formulations.....	94
3.2.2.4	Formulations' characterization.....	94
3.2.2.4.1	Physicochemical properties.....	94
3.2.2.4.2	Apparent viscosity and viscoelastic properties.....	95
3.2.2.4.3	Texture analysis.....	95
3.2.3	Results and Discussion.....	96
3.2.3.1	Selection of O/W emulsions' ingredients.....	96
3.2.3.2	O/W emulsions' optimization.....	96
3.2.3.3	Preparation of the emulsified formulations.....	98
3.2.3.4	Characterization of the emulsified formulations.....	99
3.2.3.4.1	Physicochemical characterization.....	99

3.2.3.4.2	Apparent viscosity and viscoelastic properties.....	103
3.2.3.4.3	Textural Assessment.....	105
3.2.3.5	Comparison of FucoPol-based formulation with commercial cosmetic cream.....	106
3.2.4	Conclusions	108
CHAPTER 3. Development of cosmetic formulations with L- ascorbic acid stabilized by FucoPol		109
Summary		111
3.3.1	Introduction	111
3.3.2	Materials and methods.....	113
3.3.2.1	Materials.....	113
3.3.2.2	Preparation of FucoPol-based emulsions	113
3.3.2.3	Preparation of FucoPol-based emulsion formulations.....	113
3.3.2.4	Formulations' characterization.....	114
3.3.3	Results and discussion.....	115
3.3.3.1	Defining L-ascorbic acid concentration in the emulsions' continuous phase	115
3.3.3.2	Preparation of the emulsified formulations with L-ascorbic acid	117
3.3.3.3	Characterization of FucoPol-based emulsified formulations	118
3.3.3.3.1	Organoleptic characteristics and physical stability	118
3.3.3.3.2	Emulsion type.....	118
3.3.3.3.3	pH and conductivity	120
3.3.3.3.4	Droplet size and Zeta-potential	120
3.3.3.3.5	Apparent viscosity and viscoelastic properties.....	122
3.3.3.3.6	Textural Assessment.....	124
3.3.3.3.7	Formulations accelerated stability	125
3.3.4	Conclusions	128
4. VALIDATION OF THE FUCOPOL-BASED CREAM: BIOACTIVE PROPERTIES AND SENSORIAL EVALUATION		129
Summary		131
4.1.1	Introduction	131
4.1.2	Materials and methods.....	133
4.1.2.1	Materials.....	133
4.1.2.2	Human Repeated Insult Patch Test of FucoPol.....	133
4.1.2.3	Preparation of the FucoPol-based cream.....	133
4.1.2.4	Physicochemical characterization of the FucoPol-based cream.....	134

4.1.2.5	Antioxidant activity	134
4.1.2.5.1	Tris(2-pyridyl)-s-triazine (TPTZ) antioxidant assay	134
4.1.2.5.2	Determination of Hill non-specific binding.....	134
4.1.2.6	Biological assays	135
4.1.2.6.1	Cell culture and media.....	135
4.1.2.6.2	Cytotoxicity	135
4.1.2.6.3	Wound healing	135
4.1.2.6.4	<i>In vitro</i> photoprotection assay	136
4.1.2.7	Sensorial evaluation	136
4.1.2.8	Optical microscopy image collection	137
4.1.3	Results	138
4.1.3.1	FucoPol’s safety	138
4.1.3.2	Characterization of the FucoPol-based cream.....	138
4.1.3.2.1	Physicochemical characterization.....	138
4.1.3.2.2	Apparent viscosity and viscoelastic properties.....	141
4.1.3.3	Textural assessment.....	143
4.1.3.4	Comparison of FucoPol-based cream with Bioderm® Prototype™ cream anti-wrinkles	144
4.1.3.5	Antioxidant activity	145
4.1.3.6	Cytotoxicity evaluation	146
4.1.3.7	Wound healing assay.....	147
4.1.3.8	Photoprotective activity.....	149
4.1.3.9	Sensorial analysis	151
4.1.4	Conclusion.....	153
5.	CONCLUDING REMARKS AND FUTURE WORK	155
	REFERENCES	161
	APPENDIX	193

LIST OF FIGURES

Figure 1.1.1. Tentative structure of FucoPol's repeating unit (deacetylated/desuccinylated form) (reproduced with permission from [49]).	10
Figure 1.1.2. Structure of the human skin (epidermis, dermis, and hypodermis) and epidermis layers (<i>Stratum Corneum</i> , <i>Stratum Lucidum</i> , <i>Stratum Granulosum</i> , <i>Stratum Spinosum</i> , <i>Stratum Basale</i>).	12
Figure 1.1.3. Possible transport pathways through the <i>stratum corneum</i> (adapted from [68,71]).	13
Figure 1.1.4. Moisture balance of the skin in the first generation of skin care. NMF - natural moisturizing factors (adapted from [83]).	15
Figure 1.1.5. Base cream recommended ingredients in cosmetic formulations.	16
Figure 1.1.6. Schematic representation of emulsion types (adapted from [102]): (a) oil-in-water (O/W), (b) water-in-oil (W/O), (c) water-in-oil-in-water (W/O/W), (d) oil-in-water-in-oil (O/W/O).	18
Figure 1.1.7. Schematic representation of oil-in-water (O/W) emulsification process.	18
Figure 1.1.8. Schematic representation of physicochemical instability mechanisms in O/W emulsion system (adapted from [99,101–104]).	18
Figure 2.1.1 Schematic representation of the set-up used for the diafiltration/ultrafiltration experiments (PI-pressure gauge).	28
Figure 2.1.2 - Retentate (full lines) and permeate (dashed lines) volumes, retentate conductivity (circles), and inlet pressure (italic), over time, for experiments F-1 ₁₀₀ (a), F-1 ₃₀ (b), F-2 ₁₀₀ (c), F-2 ₃₀ (d), F-3 ₁₀₀ (e) and F-3 ₃₀ (f).	32
Figure 2.1.3 - Polymer recovery (bars) and samples content in protein (closed circles) and inorganic salts (open circles) for the experiments performed with Methods 1, 2 and 3, with the 100 kDa and the 30 kDa membranes.	32
Figure 2.1.4. Comparative FT-IR spectra of the FucoPol samples extracted with Method 1 (F-1 ₁₀₀ ; F-1 ₃₀), Method 2 (F-2 ₁₀₀ ; F-2 ₃₀) and Method 3 (F-3 ₁₀₀ ; F-3 ₃₀).	35
Figure 2.1.5. Thermal analysis curves for the FucoPol samples obtained by the different tested methods: (A) Method 1, (B) Method 2, (C) Method 3; F-i ₁₀₀ , full blue line; F-i ₃₀ , dotted orange line).	35
Figure 2.1.6. Flow curves of FucoPol aqueous solutions (1.0 wt%): (A) Method 1, (B) Method 2, (C) Method 3; samples F-i ₁₀₀ (triangle) and F-i ₃₀ (circle); Dotted lines represent the Cross model; (n = 3).	36
Figure 2.1.7. Mechanical spectrum of FucoPol aqueous solutions (1.0 wt.%), G' (closed square) and G'' (open square): (A) Method 1, (B) Method 2, (C) Method 3; F-i ₁₀₀ , blue; F-i ₃₀ , orange. Data are shown as the average ± standard deviation (SD) (n = 3).	37
Figure 2.1.8. Olive oil/FucoPol (1.0 wt.%) emulsions (2:3 O/W ratio) after 24 h for the extracted samples. Method 1 (F-1 ₁₀₀ , A; F-1 ₃₀ , B); Method 2 (F-2 ₁₀₀ , C; F-2 ₃₀ , D); Method 3 (F-3 ₁₀₀ , E; F-3 ₃₀ , F); W-blank sample, oil:water.	38

- Figure 2.1.9. Flow curves for the prepared olive oil/FucoPol (1.0 wt.%) emulsions (2:3, O/W ratio): (A) Method 1, (B) Method 2, (C) Method 3; samples F-1₁₀₀ (triangle) and Fi₃₀ (circle). Dotted lines represent the Cross model. (n = 3). 39
- Figure 2.2.1. FT-IR spectra of FucoPol (green line) and d-FucoPol (gray line). 53
- Figure 2.2.2. Thermogravimetric curves of FucoPol (green line) and d-FucoPol (gray line). 54
- Figure 2.2.3. Flow curves of d-FucoPol (green) and FucoPol (gray) aqueous solutions: 0.75 wt.% (triangles), 1.0 wt.% (asterisk) 1.5 wt.% (diamonds), and 3.0 wt.% (circles). 55
- Figure 2.2.4. Flow curves of d-FucoPol aqueous solutions. (a) Effect of ionic strength: 0.1 M (dashed line), 0.5 M (circles), 1.0 M (diamonds), 2.0 M (triangles), and 3.0 M (squares). (b) Effect of pH: 3.6 (triangles), 4.8 (squares), 6.2 (circles), 8.5 (diamonds), and 11.5 (dashed line). (c) Effect of temperature: 10 °C (squares), 25 °C (circles), 45 °C (diamonds), 65 °C (triangles), and 80 °C (dashed line). 58
- Figure 2.2.5. Mechanical spectra for d-FucoPol. A: ionic strength (NaCl) effect : (a) 3.0 M, (b) 2.0 M, (c) 1.0 M, (d) 0.1 M, (e) 0.5 M; B: pH: (a) 3.6, (b) 4.8, (c) 6.2, (d) 8.5, (e) 11.5; C: temperature effect: (a) 10 °C, (b) 25 °C, (c) 45 °C, (d) 65 °C, (e) 80 °C. Elastic G' (close) and viscous G'' (open) moduli. 58
- Figure 2.2.6. (a) Optical microscopic (40x) images of olive oil/d-FucoPol emulsion (E) (O/W weight ratio of 2:3); contrast phase and fluorescence after Nile Blue A staining (A, B, respectively). (b) Filter paper wetting test for emulsion type determination. (W)-blank sample, oil/water; and film obtained with deacylated form of FucoPol. 60
- Figure 2.2.7. Rheological profile analysis of olive oil/d-FucoPol emulsion (green) and olive oil/FucoPol emulsion (gray) (O/W weight ratio of 2:3): (a) Flow curves; (b) Mechanical spectra: Elastic G' (closed) and viscous G'' (open) moduli. 61
- Figure 2.2.8. Film prepared with d-FucoPol (a) and its observation by SEM: surface (b) and cross-section (c) images. 62
- Figure 3.1.1. Surface tension of FucoPol solutions at concentrations ranging from 0.1 to 20 g/L. 74
- Figure 3.1.2. Emulsions prepared with FucoPol (0.5 or 1.0 wt.%) with castor oil, paraffin oil, almond oil and olive oil, at O/W weight ratios of 2:3 and 3:2. 76
- Figure 3.1.3. Emulsification index (EI%) overtime for emulsions prepared with FucoPol and different hydrophobic compounds: Castor oil (a.1,2), paraffin oil (b.1,2), almond oil (c.1,2) and olive oil (d.1,2), for FucoPol concentrations of 0.5wt% (gray) and 1.0wt% (orange), for O/W weight ratios of 2:3 (left) and 3:2 (right). Red dashed line represents EI (%) =50. (n = 3). 77
- Figure 3.1.4. Emulsification index (EI, %) over time for the FucoPol-stabilized emulsions with olive oil and α -tocopherol, at the 3:2 ratio: FucoPol (0.5 wt.% (a); 1.0 wt.% (b)); α -tocopherol: 0.0 wt.%, gray; 2.0 wt.%, green; 5.0 wt.%, blue. Red dashed line represents EI=50%. (n = 3). 79
- Figure 3.1.5. Three-dimensional response surface plot showing the interactive effects of different components on the O/W emulsion. (a) FucoPol and Olive oil (wt.%) with α -tocopherol fixed

- at 2.5 wt.%, **(b)** FucoPol and α -tocopherol (wt.%) with olive oil fixed at 30 wt.%, **(c)** Olive oil and α -tocopherol (wt.%) with FucoPol fixed at 0.8 wt.% 83
- Figure 3.1.6. **(a)** Optical microscopic (100x) images of FA **(A)** and FB **(B)** emulsions; contrast phase and fluorescence after Nile Blue A staining **(A1, B1, respectively)**. **(b)** Emulsion determination test by filter paper wetting..... 84
- Figure 3.1.7. Rheological profile analysis of FucoPol formulations FA(circles) and FB(triangles): **(a)** Viscosity curves as a function of the shear rate, flow curves fitted with Cross model ($n=3$); **(b)** Mechanical spectra: elastic G' (closed) and viscous G'' (open) moduli in the function of frequency..... 85
- Figure 3.2.1. Three-dimensional response **(A: E24; B: η)** surface plot showing the interactive effects of different ingredients on the O/W emulsion. **(a)** FucoPol and cetyl alcohol (wt.%) with glycerine fixed at 2.0 wt.%, **(b)** FucoPol and glycerine (wt.%) with cetyl alcohol fixed at 0.75 wt.%, **(c)** cetyl alcohol and glycerine (wt.%) with FucoPol fixed at 0.75 wt.% 98
- Figure 3.2.2. Formulations A, B, C, D, E, F: **(a)** freshly prepared formulations ($t=0$); **(b)** after 1 day; **(c)** after 60 days; centrifugation test for 1 day of storage **(d)** and for 60 days of storage **(e)**. .. 99
- Figure 3.2.3. **(a)** pH (circles) and conductivity (bars) and **(b)** droplet size (bars), Zeta-potential (blue circles), and PI (orange circles) for formulations A-F during the storage period ($t=1, 3, 7, 30, 60$ days). 102
- Figure 3.2.4. Formulations (A, B, C, D, E, F) after 1 day of preparation: **(a)** Emulsion determination test by filter paper wetting; **(b)** fluorescence optical microscopic (40x) images of formulations after Nile Blue A staining..... 102
- Figure 3.2.5. Flow curves for the prepared formulations: A **(a)**, B **(b)**, C **(c)**, D **(d)**, E **(e)**, and F **(f)** during the storage time; $t=1$ day (circles), $t=3$ days (squares), $t=7$ days (triangles), $t=30$ days (diamonds), and $t=60$ days (asterisk). 104
- Figure 3.2.6. Mechanical spectrum for formulations A **(a)**, B **(b)**, C **(c)**, D **(d)**, E **(e)**, and F **(f)**, at 1 day (orange) and 60 days (gray) of storage: G' (closed triangle) and G'' (open triangle)..... 105
- Figure 3.3.1. FucoPol-based emulsions prepared with *Olea europaea* fruit oil and *Prunus amygdalus dulcis* oil, supplemented with different L-ascorbic acid concentrations: **(a)**, 5.0 wt.%; **(b)**, 8.0 wt.%; **(c)**, 10 wt.%; **(d)**, 15 wt.%..... 115
- Figure 3.3.2. Flow curves for the FucoPol-based emulsions (analysed after 24 hours of preparation) with **(a)** *Olea europaea* fruit oil, **(b)** *Prunus amygdalus dulcis* oil, supplemented with L-ascorbic acid at concentrations of: 5.0 wt.% (triangles), 8.0 wt.% (diamonds), 10 wt.% (circles), and 15 wt.% (squares). 117
- Figure 3.3.3. Formulations C1 and C2 **(a)**; Emulsion determination test by filter paper wetting **(b)**; Optical microscopic (100x) observation under contrast phase **(c)** and fluorescence after Nile Blue A staining **(d)**..... 119
- Figure 3.3.4. **(a)** Emulsification index over storage period ($t=1, 3, 7, 45$ days); **(b)** Centrifugation test over storage period ($t=1, 3, 7, 45$ days)..... 119

- Figure 3.3.5. **(a)** pH and conductivity and **(b)** droplet size (blue bars), Zeta-potential (orange circles), and PI (blue circles) for formulations C1 and C2 during the storage period (t=1, 3, 7, 45 days). 121
- Figure 3.3.6. Flow curves for C1 **(a)** and C2 **(b)** formulations during the storage times: t=1 (circles), t=3 (squares), t=7 (triangles), and t=45 (asterisk). 122
- Figure 3.3.7. Mechanical spectrum for formulations C1 **(a)** and C2 **(b)** during the storage time: t=1 (orange), t=3 (blue), t=7 (green), and t=45 (gray). G' (closed triangle) and G'' (open triangle). 124
- Figure 3.3.8. **(a)** Emulsification index over storage temperature after 45 days **(b)** Centrifugation test over storage temperature after 45 days. 126
- Figure 3.3.9. Rheological profile analysis of formulations C1 **(a.1 and b.1)** and C2 **(a.2 and b.2)**: **(a)** viscosity curves as a function of the shear rate; **(b)** mechanical spectra: elastic G' (closed triangle) and viscous G'' (open triangle) moduli in the function of frequency. 4 °C (orange), 20 °C (blue), 30 °C (gray). 127
- Figure 4.1.1. FucoPol-based cream (F-cream) after 24 hours at different temperatures: **(a)** F-cream appearance, **(b)** phase contrast and **(c)** fluorescence optical microscopic (100x) images of the samples after Nile Blue A staining. 139
- Figure 4.1.2. **(A)** Emulsification index over storage period of **(a)** t=1, **(b)** t=3, **(c)** t=7, **(d)** t=60 days, and **(B)** samples submitted to the centrifugation test. 139
- Figure 4.1.3. **(a)** pH (open circles) and conductivity (blue bars) and **(b)** droplet size (blue bars), Zeta-potential (open circles), and PI (closed circles) for F-cream during the storage period (t=1, 3, 7, 60 days) at different temperatures (4 °C, 20 °C and 30 °C). 141
- Figure 4.1.4. Flow curves for FucoPol-based cream during the storage time (days) at different temperatures (°C): **(a)** t=1, **(b)** t=3, **(c)** t=7. **(d)** t=60; 4 °C (orange circles), 20 °C (blue circles), and 30 °C (grey circles). 142
- Figure 4.1.5. Mechanical spectrum for the FucoPol-based cream during the storage time (days) at different temperatures (°C): **(a)** t=1, **(b)** t=3, **(c)** t=7. **(d)** t=60; 4 °C (orange), 20 °C (blue), and 30 °C (grey). G' (closed triangle) and G'' (open triangle). 143
- Figure 4.1.6. Ferric-reducing antioxidant potential of FucoPol-based cream (orange), in comparison with Trolox (black): **(a)** Antioxidant potential follows a dose-dependent linear response, as reported by 595 nm absorption (Trolox: $y=1.182 \times 10^{-3}x-0.031$, $R^2=0.9905$ | F-cream: $y=1.235 \times 10^{-3}x+0.023$, $R^2=0.9864$). **(b)** Hill binding model reveals an increased slope in FucoPol-based cream antioxidant power, suggestive of synergistic effects. The x-axis is presented in log-scale. 145
- Figure 4.1.7. Cell viability of HaCaT cells after exposure to aqueous suspensions of the F-cream (gray bars) and Prototype™ Bioderm® (blue bars) during 48 h. C-, negative control (DMEM High); C+, positive control (DMEM High + 10% DMSO). 147

Figure 4.1.8. Microscope images of the wound healing assessment for HFFF2 cells post scratch (0 h) and after being exposed to DMEM (Control) and to DMEM supplemented with five different concentrations of F3 formulation (2.5, 5 and 10 mg/mL) for 16 h and 24 h..... 148

Figure 4.1.9. Microscope images of the wound healing assessment for HaCaT cells post scratch (0 h) and after being exposed to DMEM High (Control) and to DMEM High supplemented with five different concentrations of F-cream formulation (2.5, 5.0 and 10 mg/mL) for 16 h and 24 h..... 149

Figure 4.1.10. Metabolic viability of Vero cells exposed to Boderm® Prototype™ and F-cream aqueous suspensions (1:5 dilution), under 254 nm irradiation or no irradiation. Percentual data shown above bars is relative to the non-irradiated DMEM control condition..... 150

Figure 4.1.11. Morphological appearance of Vero cells in the *in vitro* photoprotection assay with Boderm® Prototype™ and F-cream aqueous suspensions (1:5 dilution): (a) non-irradiated cells, (b) Irradiated at 254-nm irradiation, for 30 min. DMEM is shown as control medium. 151

Figure 4.1.12. Sensorial analysis (immediate sensation)..... 152

This page was intentionally left blank

LIST OF TABLES

Table 1.1.1. Bacterial polysaccharides properties and their cosmetic applications.....	6
Table 1.1.2. Bacterial polysaccharides current applications in cosmetics.....	7
Table 1.1.3. Substances used in cosmetic formulation.....	15
Table 2.1.1. Recovery of FucoPol from the cell-free supernatant using Method 1 (diafiltration-ultrafiltration), Method 2 (ultrafiltration) and Method 3 (ultrafiltration-diafiltration-ultrafiltration) with 100 or 30 kDa MWCO membranes. Data are shown as the average \pm standard deviation (SD) ($n = 3$).....	31
Table 2.1.2. Physical-chemical characterization of FucoPol samples (Fuc: fucose; Gal: galactose; Glc: glucose; GlcA: glucuronic acid; Pyr: pyruvyl; Succ: succinyl; Acet: acetyl; Mw: molecular weight; PI: polydispersity index).	33
Table 2.1.3. Cross model parameters estimated for FucoPol samples (1.0 wt.%) recovered from the cultivation broth by the different tested different methods. η_0 –apparent viscosity of the second Newtonian plateau (Pa.s); τ –relaxation time (s); m –dimensionless constant. Data are shown as the average \pm standard deviation (SD) ($n = 3$).....	37
Table 2.1.4. Emulsification index (E24) and zero shear viscosity (η_0) for the emulsions prepared with the extracted FucoPol samples and olive oil, at an oil/water (O/W) ratio of 2:3. Data are shown as the average \pm standard deviation (SD) ($n = 3$).....	38
Table 2.1.5. Overall performance of the developed optimized procedure comprising ultrafiltration with a 30 kDa membrane, comparing to the previously used method (diafiltration-ultrafiltration with a 100 kDa membrane).	40
Table 2.2.1. Acyl groups (succinyl, acetyl and pyruvyl) contents of FucoPol sample subjected to alkaline treatment.....	52
Table 2.2.2. Cross model parameters estimated for d-FucoPol concentration (wt.%). η_0 –apparent viscosity of the first Newtonian plateau (Pa.s); τ –relaxation time (s); m –dimensionless constant. Data are shown as the average \pm standard deviation (SD) ($n = 3$). *Cross model is not appropriate to describe experimental data.....	56
Table 2.2.3. Cross model parameters estimated for d-FucoPol aqueous solutions (3.0 wt.%) tested at different ionic strength, pH, and temperatures. η_0 –apparent viscosity of the first Newtonian plateau; τ –relaxation time; m –dimensionless constant. Data are shown as the average \pm standard deviation (SD) ($n = 3$). Viscoelastic parameters estimated for d-FucoPol (3.0 wt.%). G' –storage/elastic modulus and G'' – loss/viscous modulus at $f=0.1$ Hz.	57
Table 2.2.4. Emulsification index (E24) and Cross model parameters estimated for the emulsions prepared with the deacylated FucoPol and olive oil, at an oil/water (O/W) weight ratio of 3:2: η_0 –apparent viscosity of the first Newtonian plateau (Pa. s); τ –relaxation time (s); m –dimensionless constant.....	60

Table 2.2.5. Mechanical parameters, and transparency of the films prepared with d-FucoPol and FucoPol, and other biopolymers. Data are shown as the average \pm standard deviation (SD) (n = 4).....	63
Table 3.1.1. Independent variables and their levels used in the response surface design.	72
Table 3.1.2. Emulsification activity measured at 24 h (E24) and emulsions' stability (ES) for the emulsions stabilized with FucoPol. Data is shown as the average \pm standard deviation (SD) (n = 3).....	75
Table 3.1.3. Emulsification activity at 24 hours (E24) and emulsions' stability over a period of 720 h, for the emulsion prepared with FucoPol, olive oil and α -tocopherol, at 3:2 (w/w) ratio. Data is shown as the average \pm standard deviation (SD) (n = 3).	79
Table 3.1.4. Central composite design (CCD) with studied variables (A: FucoPol, B: Olive oil, C: α -tocopherol), experiment and theoretically predicted values E24.	81
Table 3.1.5. ANOVA for response surface quadratic model. (SS)- Sum of Squares shows the variance of values; (MS)- Mean Square is the arithmetic mean of the squared differences; P-value < 0.05 indicate model terms are significant.....	82
Table 3.1.6. Cross model parameters estimated for formulations samples: η_0 -apparent viscosity of the first Newtonian plateau (Pa.s); τ -relaxation time (s); m -dimensionless constant; Data are shown as the average \pm standard deviation (SD) (n = 3); and textural parameters.	85
Table 3.2.1. Independent variables and their coded levels used in the RSM.	93
Table 3.2.2. Cosmetic formulation composition (wt.%). q.s.- quantity sufficient	94
Table 3.2.3. Central composite design (CCD) with studied variables (A: FucoPol, B: Cetyl alcohol, C: Glycerine), experimental values E24 and η (apparent viscosity measured at a shear rate of 0.1 s ⁻¹). Organoleptic characteristics and physical stability (centrifugation test) of experiments. SCV- (Smooth, creamy, viscous) OS- Olive smell, YW- yellowish white. ...	97
Table 3.2.4. Apparent viscosity (η , measured at 2.30 s ⁻¹) and viscoelastic parameters (G' , G'') at room temperature (~20 °C) for the emulsified formulations (A, B, C, D, E, F), for different storage times. G' -storage/elastic modulus and G'' - loss/viscous modulus at $f=0.1$ Hz.....	104
Table 3.2.5. Numerical values of the textural parameters for formulations tested of t=1 and t=60 at room temperature.....	106
Table 3.2.6. Rheological parameters and textural parameters of commercial products tested. Apparent viscosity (η , measured at 2.30 s ⁻¹) and viscoelastic parameters (G' , G'') measured at room temperature (~20 °C). G' -storage/elastic modulus and G'' - loss/viscous modulus, at $f=0.1$ Hz.	107
Table 3.3.1. Cosmetic formulation composition (wt.%). q.s- quantity sufficient	114
Table 3.3.2. pH, conductivity, E24, and apparent viscosity (η , measured at 2.30 s ⁻¹) for the emulsified emulsions with different L-ascorbic acid concentrations. *Data obtained under the same manufacturing and scale conditions.	116

Table 3.3.3. Numerical values of the textural parameters for formulations C1 and C2 during the storage period at room temperature. *Data obtained under the same manufacturing and scale conditions.	125
Table 3.3.4. Physicochemical characterization of formulation C1 and C2 during forty-five day-storage at 4 °C, and 30 °C. η at 2.30 s ⁻¹	126
Table 4.1.1. Cosmetic formulation composition. q.s- quantity sufficient	134
Table 4.1.2. Textural parameters for F-cream during the storage period (days) at different temperatures (°C).....	144
Table 4.1.3. Rheological parameters and textural parameters of the F-cream stored for 60 days at room temperature (20 °C) and Bioderm® Prototype™. Apparent viscosity (η , measured at 2.30 s ⁻¹) and viscoelastic parameters (G' , G'') at room temperature (20 °C). G' -storage/elastic modulus and G'' - loss/viscous moduli at $f=0.1$ Hz.	144
Table 4.1.4. Linear regression and Hill model parameters determined for Trolox and FucoPol-based Cream	146
Table 4.1.5. Cell migration of HFFF2 and HaCaT cell after exposure to F-cream aqueous suspensions, for 16 and 24 h after application of a scratch in the cells' monolayer. Results expressed in percentage of wound closure relatively to time 0 h.....	149

This page was intentionally left blank

ACRONYMS

A_{min}	Minimum absorbance
A_{max}	Maximum absorbance
ANOVA	Analysis of variance
BC	Bacterial Celulose
CAGR	Compound Annual Growth Rate
CCD	Central Composite Design
CMC	Critical Micelle Concentration
CPS	Capsular Polysaccharides
DLS	Dynamic Light Scattering
DMEM	Dulbecco's modified Eagle's medium
E24	Emulsification index after 24 h
EA	Emulsification Activity
EC ₅₀	Half maximal effective concentration
EI	Emulsification Index
EPS	Exopolysaccharides
ES	Emulsification Stability
FBS	Fetal Bovine Serum
FRAP	Ferric Reducing Antioxidant Potential
FT-IR	Fourier Transform Infrared Spectroscopy
GC	Gas Chromatography
HA	Hyaluronic Acid
HLB	Hydrophile-Lipophile Balance
HRIPT	Human Repeated Insult Patch Test
ICDRG	International Contact Dermatitis Research Group
INCI	International Nomenclature Cosmetic Ingredient
IR	Infrared
LPS	Lipopolysaccharides
LVE	Linear Viscoelastic limit
MALS	Multiangle Light Scattering
Mn	Molecular number
Mw	Average Molecular weight
MWCO	Molecular Weight Cut-Off
NMR	Nuclear Magnetic Resonance
O/W	Oil-in-Water
O/W/O	Oil-in-Water-in-Oil
PBS	Phosphate Buffered Saline
PI	Polydispersity Index
RH	Relative Humidity

ROS	Reactive Oxygen Species
RSM	Response Surface Methodology
SC	<i>Stratum Corneum</i>
SEC	Size Exclusion Chromatography
SEM	Scanning Electron Microscopy
TCD	Thermal Conductivity Detector
TEA	Triethanolamine
TFA	Trifluoroacetic Acid
TGA	Thermogravimetric Analysis
TMP	Transmembrane Pressure
TPTZ	2,4,6-Tris(2-pyridyl)-s-triazine
UV	Ultraviolet
UVA	Ultraviolet radiation A
UVB	Ultraviolet radiation B
UVR	Ultraviolet radiation R
WFRAP	Working Ferric Reducing Antioxidant Potential
W/O	Water-in-Oil
W/O/W	Water-in-Oil-in-Water
WTA	Cell-Wall Teichoic Acids

SYMBOLS

η	Apparent viscosity
η_0	Viscosity at zero shear rate
τ	Relaxation time
m	Dimensionless constant
$\dot{\gamma}$	Shear rate
$[\eta]$	Intrinsic viscosity
G'	Storage modulus
G''	Loss modulus
P_{in}	Inlet Pressure
P_{out}	Outlet Pressure

This page was intentionally left blank

AIMS AND THESIS ORGANIZATION

The scientific research work of this thesis integrated the utilization of the patented FucoPol polymer as a safe and effective cosmetic ingredient to develop FucoPol-based formulations. It was especially oriented to meet the commercial needs of the Biotechnology Portuguese company 73100, Lda. All the research and scientific work results from a partnership between 73100, Lda. and the NOVA School of Sciences and Technology at NOVA University of Lisbon (FCT NOVA), Portugal. The research project was financed by 73100, Lda. and by national funds from FCT—Fundação para a Ciência e a Tecnologia, I.P., in the scope of the projects UIDP/04378/2020 and UIDB/04378/2020 of the Research Unit on Applied Molecular Biosciences—UCIBIO and the project LA/P/0140/2020 of the Associate Laboratory Institute for Health and Bioeconomy—i4HB. The experimental work that supports this thesis was performed at the Biochemical Engineering Group of the Chemistry Department at FCT NOVA.

Considering the expansion of the complexity and competitiveness of the cosmetic market, it is of high importance for all cosmetic companies to hunt the development of innovative cosmetic formulations and applications, guaranteeing product quality and reinforcing their market positioning. 73100, Lda. searches for new commercially valuable applications using their patented polymers. Since the cosmetic industry is always searching for new ingredients, it is in the company's interest to explore the use of polymers in cosmetic and pharmaceutical formulations.

Water scarcity is a worldwide problem, and the polysaccharide purification process has a high-water demand to achieve superior purity levels. In this sense, it was of relevance to develop an optimized method to reduce water, time, and energy consumption, while maintaining or improving the product yield and properties. Consumers' utilization of cosmetic products is driven by three main factors: specific function, efficiency, and self-comfort. Therefore, the development and production of cosmetic applications has exponentially increased, leading to the market availability of a wide range of cosmetic ingredients. More recently, consumers' concern over safety and environmental issues has led the cosmetic industry to invest in raw material selection and natural product commercialization, with minimum transformation and requiring fewer chemical reagents. Accordingly, the utilization of polysaccharides in cosmetic products has received widespread attention, acting as improved carrier systems with a desired effect on the skin. Given their ease of application and appealing skin-feel, emulsions are the predominant form of skincare products.

Thus, this thesis was focused on the development and characterization of FucoPol-based emulsified formulations for topical application. During the development step, emulsions were required to be physically stable with minimal presence of additional ingredients. Safety assessment of FucoPol was performed by *in vivo* studies, and the biological effect of FucoPol-based emulsified formulations was assessed by *in vitro* studies, to achieve a final product that was both safe and efficient.

The work performed during this thesis resulted in one book chapter, two scientific papers published in international peer review journals, and three manuscripts submitted for publication. Furthermore, an additional manuscript is under preparation.

The thesis is organized into four sections, formatted as research papers, that have been either published or submitted for publication. The methodology applied in each section is either detailed within its context or is specified in previous sections (in these cases a hyperlink is available). For organization purposes, the Figures caption follow a section.chapter.image number logic, which means that, as an example, Figure 2.2.1 is the first figure of chapter 2 from the section 2. The Table nomenclature follows the same pattern.

Therefore, this thesis is organized as follows:

Section 1 consists of a literature review about the main properties of polysaccharides and main functions of the skin, focusing on the *stratum corneum*, which is the main barrier for the percutaneous absorption, and the principal diffusion routes through the skin. This chapter also provides a brief overview of the structural and chemical background of FucoPol, and the main properties with potential use in the pharmaceutical and cosmetic fields. Finally, the types of emulsions vehicles for dermal delivery are summarized, specifying their role and effect on the cosmetic product performance.

Section 2 describes both the production and extraction/purification process for FucoPol, characterizing the obtained biopolymer. This section is divided into two Chapters:

Chapter 1 describes the extraction procedure optimization aiming at reducing the total water consumption and extraction time, while keeping a high product recovery, thus making the downstream procedure more sustainable and cost-effective. Biopolymer physicochemical characterization was performed and FucoPol's properties in aqueous solution and its emulsifying behaviour were studied.

Chapter 2 describes the deacetylation and desuccinylation of FucoPol by an alkaline treatment, aiming at assessing the physicochemical and functional properties of the deacylated biopolymer (d-FucoPol) compared to the original FucoPol.

Section 3 describes the development of FucoPol-based emulsified cosmetic formulations. This section is divided into three Chapters:

Chapter 1 describes a preliminary study of the emulsion forming and stabilizing capacity of FucoPol using four different oils. A RSM approach was applied to optimize the FucoPol-based emulsions composition. The resulting emulsions were characterized in terms of morphology, rheological behaviour, and textural parameters.

Chapter 2 describes the development of O/W cosmetic emulsions stabilized by FucoPol and containing α -tocopherol. Formula composition was designed using RSM to determine the contents of FucoPol, cetyl alcohol, and glycerine that resulted in high emulsification index and high apparent viscosity. Formulations' stability studies, rheological and textural evaluation during the storage were presented. A comparison of the obtained emulsions with commercial cosmetic products was also detailed.

Chapter 3 describes the development of FucoPol-based cosmetic emulsions containing both α -tocopherol and L-ascorbic acid. The replacement of olive oil by almond oil in the formulation was also

evaluated. Optimized FucoPol-based cosmetic formulations were prepared and characterized in terms of physical and accelerated stability, rheological behaviour, and textural properties during the storage.

Section 4 describes the validation of the optimized FucoPol-based emulsified formulation (F-cream). The physicochemical, rheological and texture properties were evaluated over time at different conditions. In addition, the cream's cytotoxicity, antioxidant, *in vitro* photoprotection and *in vitro* wound healing capacity were also evaluated, as well as an *in vivo* by sensorial evaluation.

Section 5 highlights the overall main results of the thesis and their impact in the cosmetic industry, specifically in the development of new formulations with FucoPol as a functional and bioactive compound. Future work and perspectives are also described in this section.

This page was intentionally left blank

1. GENERAL INTRODUCTION

Bacterial Polysaccharides in Cosmetic Industry

This chapter was adapted from the following published book chapter:

Baptista, S.; Freitas, F. Bacterial Polysaccharides: Cosmetic Applications. In Polysaccharides of Microbial Origin; Oliveira, J., Radhouani, H., Reis, R.L., Eds.; Springer Nature AG: Cham, Switzerland, 2021, pp.1-42; doi.org/10.1007/978-3-030-35734-4_45-1.

This page was intentionally left blank

1.1.1 Background

Despite being among the most important structures in Nature, polysaccharides were often overlooked in the past. However, due to the recent global demand for a sustainable economy, the previous paradigm has shifted [1]. These natural polymers have particular physical and chemical properties and can be found in a wide range of life forms, from microorganisms to animals and plants, being essential for several biological functions [1–3]. In fact, polysaccharides are known to be decisive for cell adhesion, to serve as reservoirs in the cytoplasm, to be part of the cell membrane or cell wall, and to be a component of the defence, regulation, and information systems of the cell. Bacterial polysaccharides are extensively used in cosmetic products, especially given their diverse properties and functionalities [4]. Cosmetics can be defined as composite multiphase arrangements, with every single different component possessing a specific function on the final product [4]. Polysaccharides can be used as natural cosmetic components due to their unique physical and chemical properties, given the fact that they are biocompatible and biodegradable biopolymers [4,5].

Functional polysaccharides are claimed based on their functionality in cosmetics' formulation technology, such as film formers, gelling agents, thickeners, suspending agents, conditioners, and emulsifiers, that mainly rely on the physicochemical properties of the biopolymer. On the other hand, cosmetic active polysaccharides promote water loss reduction, protecting the skin's barrier function, and promoting a good sensorial attribute [6]. In this context, polysaccharides are of great interest in cosmetics for the development of stable functional formulations.

The continuous development of the cosmetics' industry technology and the understanding of skin's biology allowed the emergence of several novel active ingredients used in topical formulations. Still, cosmetic ingredients research is of utmost importance to further increase the stability, safety, and efficacy of cosmetic formulations. Natural ingredients are widely present in this industry because consumers have an interest in the benefits originated by these natural-based products. Sustainability has received, in recent years, increased interest from several important players from the cosmetic industry: consumers, companies, and academics. These entities share common concerns about cosmetics safety, and both its environmental and social impacts (resulting from unfair trade). The selection of raw materials from renewable and biological sources can withstand higher sustainability levels in the cosmetic industry. However, these alternative ingredients can be challenging due to underperformance, instability, and other limitations (aesthetic). Nevertheless, there are several bio-based ingredients with high potential as alternatives to commonly used raw materials [7,8]. In this sense, polysaccharides present several interesting applications, due to their capability of creating gel structures in aqueous environments (through the hydration of the sugar building blocks), stabilizing emulsions and forming films, acting as binders, viscosity-increasing promoters, and rheology modifiers, as well as suspending agents [4,6]. Polysaccharides interact, as active substances, with other ingredients of a cosmetic formulation, which grants them great benefits to be used, for example, as vehicles of dermatological formulations. This application is possible due to the non-reactive nature of polysaccharides when contacting the human skin. Moreover, these molecules can be metabolized and eliminated from the body using normal metabolic pathways [4,9].

1.1.2 Bacterial Polysaccharides

In recent years, microbial polysaccharides have emerged as viable substitutes to animal and plant-based ingredients in many different applications, ranging from the food and agricultural industries to the pharmaceutical, medical, and cosmetic industries. This diversity in applications derives from polysaccharides' fundamental and practical properties, granting them functions as stabilizers, emulsifiers, viscosifiers, and thickeners [1,5,10]. Therefore, the previously mentioned properties of bacterial polysaccharides contribute to their application in cosmetic formulations, with xanthan and gellan gum being widely used as cosmetic additives to control the viscosity, and as physicosensorial agents. Hyaluronic acid, bacterial cellulose, and levan are also relevant cosmetic ingredients, considering their application as bioactive components for skin regeneration/defence [4,5].

Being high molecular weight polymers that may share components with other cellular macromolecules and having fundamental intricacy and variety, bacterial polysaccharides can be classified in several groups: capsular polysaccharides (CPS) and exopolysaccharides (EPS), which are observed in all types of bacteria; lipopolysaccharides (LPS) and cell-wall teichoic acids (WTA), which are reported, respectively, in gram-negative and gram-positive bacteria [1,2,5].

CPS are extracellular polysaccharides that are important in bacteria pathogenicity due to their ability to encase microorganisms and promote adhesion and penetration of the host cell. They also act as virulence promoters by screening the immune response, to avoid antibody reactions (an interesting feature in the advancement of vaccines [2,10]).

EPS are high molecular weight (10-1000 kDa) extracellular polysaccharides secreted by many prokaryotes (both eubacteria and archaeobacteria) and eukaryotes (phytoplankton, fungi, and algae), which present a diverse chemical structure and composition, ranging from homopolymers to heteropolymers [5,11,12]. This diversity renders EPS auspicious in terms of commercial applications, in several sectors, such as paper manufacturing, pharmaceuticals, cosmetics, and food. For instance, since xanthan and gellan were allowed as food additives in Europe and the US, these two EPS gained great interest and are currently widely used [12,13]. However, the global polymer market fraction related to bacterial EPS is still small, mainly due to production costs, in terms of substrates and bioreactors used for microbial growth, and purification procedures [5,13].

1.1.2.1 Main Properties

Microbial polysaccharides present hydrophilic behaviour, a feature that renders them major interest for commercial purposes, due to their capacity to attract and hold water molecules, as well as to change basic properties of aqueous systems [14,15]. Moreover, microbial polysaccharides possess several relevant characteristics such as high viscosity at low concentrations (1), they also have gelling properties (2) that enables them to act as thickening and stabilizing agents (3) presenting compatibility with high salt concentrations (4) and stability against temperature changes and high shear pH (5); they have high water solubility and anti-freeze behaviour (6), presenting polyelectrolyte and ion exchange potential (7), having a surface-active, dispersing and flocculating capacity (8); they also present versatile

Section 1. General Introduction

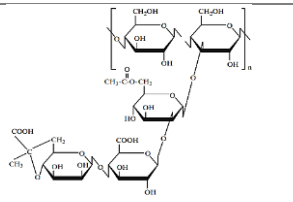
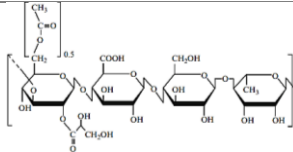
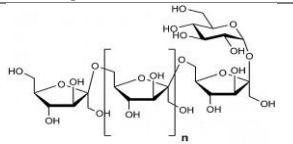
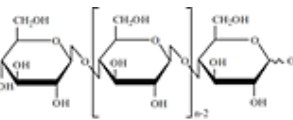
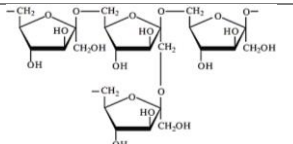
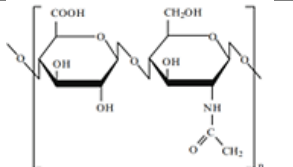
adhesive and film-forming properties (9), displaying capacity and selectivity for metal ions, proteins, lipids (10), with specific biodegradability (11) [14–17].

Polysaccharides can adapt their molecular structure and rigidity by changing the intra and inter-molecular interactions, which grants them unique rheological characteristics. In the cosmetics' industry, polysaccharides' capacity to present high viscosity at low concentrations is very important to allow a specific texture (of increased viscosity) to the formulation and to decrease elasticity-driven creaming of the droplets and other components of the emulsion. This ability derives from the polysaccharides' inflated molecular structure in aqueous solution, with a high effective volume fraction at low concentrations [15,16].

The main bacterial polysaccharides used in the cosmetic industry (Table 1.1.1) are xanthan gum, bacterial cellulose, levan, hyaluronic acid, gellan gum, and dextran due their ability as film formers, emulsion stabilizers, binders, and viscosity increasing and skin conditioning agents [4,5,18].

Section 1. General Introduction

Table 1.1.1. Bacterial polysaccharides properties and their cosmetic applications

Polysaccharide	Origin	Monomers	Mw	Chemical structure	Properties	Cosmetic application	Reference
Xanthan gum	<i>Xanthomonas</i> spp	Glucose Mannose Glucuronic acid	$(2.0-50) \times 10^6$		High viscosity Hydrocolloid	Thickener Emulsifier Rheology modifier Stabilizer	[1,19,20]
Gellan gum	<i>Sphingomonas paucimobilis</i>	Glucose Rhamnose Glucuronic acid	5.0×10^5		Gelling capacity Hydrocolloid Water soluble Film form capacity	Stabilizer Gelling agent	[4,20]
Dextran	<i>Leuconostoc mesenteroides</i> , <i>Streptococcus</i> , <i>Weissella</i> , <i>Pediococcus</i> and <i>Lactobacillus</i>	Glucose	$10^6 - 10^8$		Good stability (over wide temperature and pH ranges) Newtonian fluid behaviour	Moisturizer Thickener	[1,2,20]
Bacterial cellulose	<i>Gluconacetobacter xylinum</i> , <i>Agrobacterium</i> , <i>Alcaligenes</i> , <i>Rhizobium</i> , <i>Pseudomonas</i>	glucopyranose	$\sim 10^6$		Insoluble in water and in most solvents High crystallinity High water-holding capacity High tensile strength moldability	Thickener Emulsifier Viscosity controller Absorbent Skin regeneration Skin moisturizer Wound healing	[5,19–22]
Levan	<i>Acetobacter</i> , <i>Bacillus</i> , <i>Brenneria</i> , <i>Geobacillus</i> , <i>Halomonas</i> , <i>Lactobacillus</i>	Fructose	3.0×10^6		High water solubility Low viscosity Stabilizer Film form capacity	Cell-proliferating Skin moisturizing Skin irritation–alleviating effects Blending	[2,21]
Hyaluronic acid	<i>Streptococcus</i> sp.	Acetylglucosamine, glucuronic acid	2.0×10^6		Water soluble Highly viscous hydrocolloid Viscoelastic High swelling capacity	Humectant Moisturizer Softening agent Antiaging affect Immunostimulant Angiogenic	[4,19–21]

1.1.2.2 Biotechnological importance in Cosmetic Industry

Their eco-friendly nature is highly marketable to consumers, and there are many examples of applications acting as modifiers and stabilizers in make-up, skin care and hair care products [23]. The aforementioned features of polysaccharides (hydrophilicity, high molecular weight, and changeable molecular structure) allow their utilization in several applications, mainly related to their behaviour in aqueous media, in high-value markets [12,14]. The global hydrocolloids market, in which most polysaccharides are included, was estimated at USD 9 Billion in 2020 and to be at USD 11.7 Billion by 2027, with an expected compound annual growth rate (CAGR) of 3.7% (www.researchandmarkets.com). The cosmetics and Personal Care Products segment currently accounts for a 20.8% share of the global Hydrocolloids market (www.researchandmarkets.com). Even though this market is dominated by plant and algal polysaccharides, xanthan gum's market value, for instance, was estimated as USD 987.7 Million in 2020 and, expected to grow at a CAGR of 5.1% until the end of the year 2024 (www.researchandmarkets.com).

According to their role in the product, polysaccharides applied in cosmetics (Table 1.1.2) can be classified as functional or active polysaccharides [4]. Functional polysaccharides are usually classified based on their electrochemical charge in the product's structure and are commonly integrated into cosmetic products to act as gelling agents, viscosity adjusters, thickeners, and emulsifiers (according to their polymerized network ability to hold water) [6] and include xanthan gum, gellan gum and dextran. Polysaccharides are also frequently used in cosmetic applications as active ingredients and include bacterial cellulose (BC), levan and hyaluronic acid (HA) [4].

Table 1.1.2. Bacterial polysaccharides current applications in cosmetics

Polysaccharide	Current applications in cosmetics	References
Bacterial cellulose	Skin care, hair care, lipstick, eyeliner, moisturizing products, masks, hair dyes and colours, bath preparation, shampoos, toothpaste, antiperspirant.	[19,22,24]
Levan	Skin care, hair care products, whitener products.	[25]
Hyaluronic acid	Skin care, hair care, moisturizing and hydrating products, protective products, pre/after sun lotions, sunscreen.	[19,26,27]
Xanthan gum	Skin care, hair care, conditioners and shampoos, aftershave, shower gel and cream, body lotion, moisturizing products, sunscreen, toothpaste.	[6,19]
Gellan gum	Skin care, hair care, lotions and creams, makeup products, face masks and packs, toothpaste, suntans and sunscreens, toothpaste.	[28]
Dextran	Skin care, protective cosmetics, moisturizing products.	[6,18]

Section 1. General Introduction

Bacterial cellulose (BC) presents a porous network structure constituted by nanofibrous with high strength and low density, rendering it effective for membrane development for cosmetic products [4]. The Hainan Guangyu Biotechnology Co. Ltd. is a major BC producer and promoter for BC applications in the cosmetic industry. Indeed, reports show the use of BC in cosmetic formulations to produce stable oil-in-water emulsions which are non-irritating on the skin. Moreover, these emulsions can penetrate the skin and supply good hydration without the requirement of any surfactants [22,29]. By presenting good water holding capacity and gas permeability, BC was also reported as an acceptable carrier in cosmetic active ingredients such as moisturizers, whitening ingredients, anti-wrinkling agents, growth factors, enzymes, or a combination thereof [29].

Levan is an adhesive amphiphilic polymer. Its solubility in oil, low viscosity, and the ability to generate films are valorised in hair-fixing products [30]. Moreover, levan can be used in discoloration products because it reduces tyrosinase activity, reducing melanin production. It can also co-create a solid polymer matrix that dissipates at skin contact [30]. Additionally, levan has high compatibility with salts and surfactants, is heat stable, has water retention capacity, and is non-toxic [31]. Levan can also be used as an encapsulation agent, due to its ability to create nanoparticles in water. The polymers' biological activity (cell proliferation, skin repairing, and moisturizing) contributes to its use as part of three-dimensional artificial skin models, acting also as a protective agent against irritation. Furthermore, levan diminishes skin water loss, keeping it moisturized [4,5].

Hyaluronic acid (HA), also known as hyaluronan, plays several roles in biological processes regulation, like skin repair, cancer diagnosis, wound healing, tissue regeneration, anti-inflammatory, and immunomodulation [27,32,33]. HA activity is highly conditioned by its size but there are several specific applications for different molecular weight fractions, for use in medicine and cosmetics [4,26,27]. The differences in percutaneous absorption of different molecular weight HA across the *stratum corneum* show that the anti-wrinkle effect efficiency depends on the molecular weight of the used biopolymer [32]. In fact, research and development of HA and its related products have been abundant, with reports showing its effectiveness as dermal fillers, anti-wrinkle agents, and tissue regeneration agents [33,34]. HA cosmetic effects are mainly related to its performance as a soft tissue generator, a skin hydration improver, a collagen stimulator, and face rejuvenation inducer [32]. Apart from the topical application, scientific research has reported the benefits of HA-based treatments, such as the intradermal injection of HA (as fillers, gels, and implants) in treating facial wrinkles and promoting skin rejuvenation. Moreover, the safety, tolerability, and patient satisfaction have contributed to the diffuse utilization of HA in cosmetics [32]. There are already several FDA-approved dermal HA fillers in the market, commercialized by Restylane® (Medicis, USA), Prevelle Silk® (Mentor Corp., USA), Anika® (Anika Therapeutics, Inc., MA), and Juvéderm™ (Allergan, USA) [4].

Xanthan gum applications include the utilization as a thickener and dispersing agent, and emulsion stabilizer [35]. Xanthan gum is a hydrocolloid with the ability to dissolve in water at room temperature [36], acting as a non-gelling biopolymer and providing high viscosity at low concentrations [35] because of the semi-rigid conformation conferred by its side chains containing mannose and glucuronic acid [37]. In emulsions, xanthan presents similar rheological properties: high viscosity at low shear rates,

a strong non-thixotropic shear-thinning character, and a viscoelastic behaviour [37]. In pharmaceutical cream formulations, as in barium sulfate preparations, the suspension stability provided by xanthan is of utmost importance. In toothpaste, this feature is also an advantage, improving ingredients' suspension, due to high viscosity, and facilitating brushing onto and off the teeth. The uniform dispersal of pigments, long-term stability (in terms of pH, salinity, and temperature) and its ability to thicken, grants xanthan an extensive application as shampoo base [2]. Xanthan is produced and commercialized by major companies like CP Kelco, Merck, Pfizer, Rhone Poulenc, Sanofi-Elf, and Jungbunzlauer [4,21].

Gellan gum is mainly used in cosmetic formulations to increase viscosity and to stabilize emulsions, at low concentrations in dermal products (0.3-0.5%) and even lower in eye and hair products (0.0004%) [4]. Also, it forms gels at low concentrations (0.1%) which are available in the low acyl form (creating hard, brittle gels) and in the high acyl form (soft, elastic gels) [4,35]. Gellan provides suspensions with low viscosity because it has significant yield stress for low viscosity ranges. Gellan meets the requirements of the EC Cosmetics Regulation 1223/2009 [35] and is available with the trading names Gelrite™ and Kelcogel™ [38].

Dextran and its derivatives have several applications in cosmetics as moisturizers and thickeners, specifically cationic dextran because of its capacity to form complex salts with anionic or amphoteric surfactants, which can adsorb to hair/skin producing moisturizing effects, making it a useful conditioning agent. Dextran sulfate is another dextran derivative used in cosmetics as an anti-aging and anti-wrinkle product. Due to its moisture retention and increased lipase activity, it presents a smooth, fresh, and non-sticky feeling which results in supple skin with reduced weight [18].

In general, bio-polysaccharides have several properties that can be explored in the cosmetic industry, acting as alternative polymers produced in a sustainable and renewable way. The research and development of new bacterial polysaccharides can further establish the presence of these polymers in cosmetic formulations, through the discovery of new properties and applications.

1.1.3 FucoPol

Produced by *Enterobacter* A47 (DSM 23139), FucoPol is a high molecular weight (1.7×10^6 - 5.8×10^6 Da) fucose-rich EPS that was firstly reported by Alves et al. [39]. Patented by the Portuguese biotechnology company 73100, Lda. (WO2011073874) [40], FucoPol bioreactor production conditions have been developed and optimized using glycerol as carbon source [41–48]. The bioprocess, performed at controlled pH (7.0 ± 0.05), temperature (30 ± 0.1 °C), and dissolved oxygen concentration (10%), includes an initial batch phase, for cell growth, followed by a fed-batch phase under growth limiting conditions (nitrogen limitation) for improved polysaccharide synthesis [48].

FucoPol is a hexamer composed of fucose, galactose, glucose, and glucuronic acid (2.0:1.9:0.9:0.5 M ratio), with a main chain composed of $\alpha \rightarrow 4$ - α -L-Fucp-(1 \rightarrow 4)- α -L-Fucp-(1 \rightarrow 3)- β -D-Glcp(1 \rightarrow trimer repeating unit (Figure 1.1.1). At the first fucose C-3, a α -D-4,6-pyruvyl-Galp-(1 \rightarrow 4)- β -D-GlcAp-(1 \rightarrow 3)- α -D-Galp(1 \rightarrow trimer branch is present, with a pyruvate group at C-4 and C-6 of the terminal galactose [49]. This biopolymer also contains organic acyl substituents, comprising 3.5-6.8

wt.% acetyl, 0.6-3.0 wt.% succinyl and 3.7-14 wt.% pyruvyl [39,41,42,44,47,50–53]. Glucuronic acid, succinyl, and pyruvyl presence conferred anionic properties to the biopolymer [41].

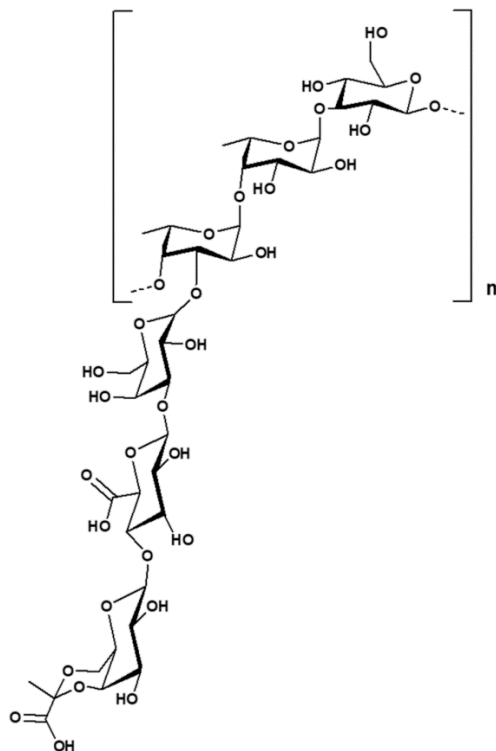


Figure 1.1.1. Tentative structure of FucoPol's repeating unit (deacetylated/desuccinylated form) (reproduced with permission from [49]).

1.1.3.1 Main properties

Many studies have reported interesting FucoPol properties which may be applied to the cosmetic field. Freitas et al.[41], Cruz et al.[54], and Torres et al.[50] reported the formation of viscous FucoPol aqueous solutions that presented a shear-thinning behaviour at different polymer concentrations (0.2-1.2 wt.%), anticipating FucoPol's potential utilization as a thickening agent and bioemulsifier. Freitas et al. [41,44] and Antunes [55] have proven FucoPol's ability to form and stabilize emulsions with different hydrophobic compounds. Freitas et al. [44] reported the biopolymer's capacity to form emulsions (0.5 wt.% FucoPol) with sunflower oil, corn oil and rice brand oil (3:2, (v/v) ratio), achieving emulsification index values after 24 hours (E24) of 60, 64 and 80%, respectively. Using the same FucoPol concentration, Antunes [55] further showed the biopolymer's emulsification ability with olive and soybean oils (3:2 (v/v) ratio), reporting E24 values of 70% and 96%, respectively; at a 2:3 (v/v) ratio for cedarwood and paraffin oils, FucoPol-driven emulsions reached E24 values of 81% and 64%, respectively. Freitas et al. [44] and Ferreira et al. [56] demonstrated FucoPol's ability to form biodegradable and hydrophilic films, highly permeable to water vapour (1.01×10^{-11} mol/m s Pa), and impermeable to

oxygen and carbon dioxide (0.7×10^{-16} mol m/m² s Pa and 42.7×10^{-16} mol m/m² s Pa, respectively), possessing promising mechanical properties such as high elongation at break (54.9 %) and low tension at break (3.1 MPa) and elastic modulus (2.8 MPa). Lourenço et al. [53] used FucoPol to encapsulate gallic acid and oregano essential oil. The authors reported that after encapsulation in FucoPol particles, both bioactive compounds retained their antioxidant activity. Concórdio-Reis et al. [52] studied FucoPol and FucoPol/AgNP biocomposite as potential bioactive materials for wound dressings applications, reporting that both were biocompatible and promoted *in vitro* keratinocytes migration, suggesting an enhancement of skin repair mechanisms; FucoPol/AgNP also presented antimicrobial activity, a significant feature in potential skin wound healing applications. Guerreiro et al. [57] performed *in vitro* cryopreservation assays of Vero, Saos-2, HFFF2 and C2C12 cell lines using a non-cytotoxic biopolymer concentration (2.5 mg/mL) and reported the cryoprotective potential of FucoPol, which may be important in future cryopreservation formulations. Guerreiro et al. [58] tested the biopolymer as a photostable agent and reported the protection of Vero epithelial and PM1 keratinocytic cells from UVA and UVB radiation at FucoPol concentrations of 0.02–2.0 % (w/v) and 0.2–2.0 % (w/v), respectively, revealing a 94% overall photostability up to 1.5 h of irradiation time; the antioxidant ability of FucoPol was shown in the protection of Vero cells against H₂O₂-induced acute exposure: a 0.25% (w/v) FucoPol concentration resulted in the attenuation of metabolic viability decay, accentuated the post-stress proliferation capacity and preserved cell morphology [49]. Fialho et al. [59] developed polymeric structures by cation-mediated gelation of FucoPol and demonstrated its potential to form hydrogel beads in the presence of iron(III) and copper(II). Vásquez-González et al. [60] used FucoPol in the formation of stable electrospun fibers: FucoPol's low water solubility and lack of molecular entanglements prevented fibers production with the biopolymer, whilst FucoPol:Polyethylene Oxide (1:3 w/w) blends formed non-agglomerated and homogeneous nanofibers with cylindrical morphology.

1.1.4 Skin care

1.1.4.1 Skin structure

The skin is an integrated and dynamic organ, which accounts for 10 to 15% of our body mass, making it the largest organ of the human body. Besides serving as a barrier to the external environment, protecting our body from physical damage and pathogens, the skin is also important in maintaining the body's homeostasis by preventing water loss and due to its role in the immune-neuroendocrine system [61–64]. Free radicals (endogenous and exogenous) can interact with the skin, producing negative effects that may result in skin-based diseases, such as psoriasis, eczema and urticaria, and skin cancer [62]. Therefore, the skin has a unique defence mechanism based on endogenous (derived from melanin) and exogenous (orally and topically administrated) antioxidants, in order to avoid these adverse effects of free radicals [65]. The skin defence mechanism inhibits microbial attacks, chemical, UV, and particulate matter damage by providing several protective barriers: physical, immunological, and metabolic [66]. This defence mechanism is intrinsically linked to the structure and function of skin layers elements

[65]. Basically, the human skin is constituted by three layers (from top to bottom): epidermis, dermis, and hypodermis (Figure 1.1.2).

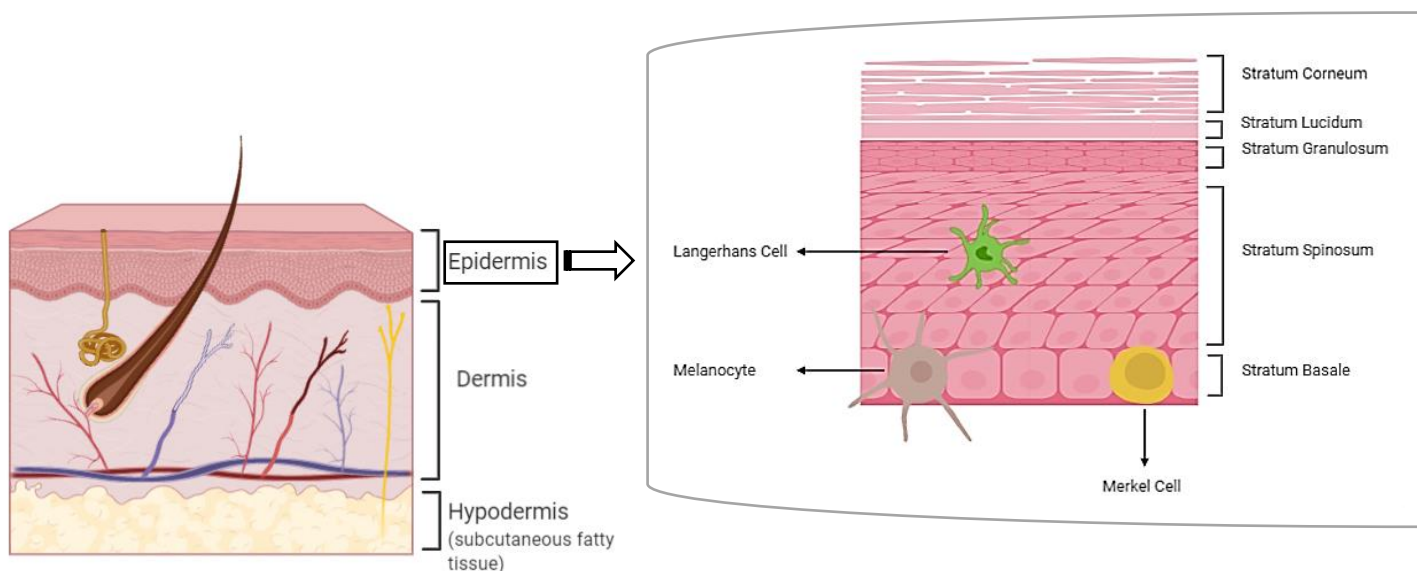


Figure 1.1.2. Structure of the human skin (epidermis, dermis, and hypodermis) and epidermis layers (*Stratum Corneum*, *Stratum Lucidum*, *Stratum Granulosum*, *Stratum Spinosum*, *Stratum Basale*).

The epidermis is mainly composed of keratinocyte cells (95%), which are the producers of the protein keratin, while the remaining 5% are melanocytes, Langerhans cells, and Merkel cells [61,62,67]. Since this skin layer does not include blood vessels, the nutrient delivery and waste disposal are dependent on the second layer (dermis) through the basement membrane [67]. Depending on keratinocyte differentiation, the epidermis is usually divided into four layers [62,67]: *stratum corneum*, *stratum granulosum*, *stratum spinosum*, and *stratum germinativum/basale* (Figure 1.1.2) [62,63,65,67]. The *stratum lucidum* is a fifth layer found in thick skin, such as the palms of the hands, the soles of the feet, and the digits [63,67]. Keratinocyte differentiation promotes several structural changes resulting in the formation of corneocytes (squamous cells with high physical and chemical resistance). Corneocytes constitute the upper epidermis layer, also known as *stratum corneum* (SC), controlling skin absorption which is important in the delivery of topical formulations ingredients [66,68,69]. In fact, diffusion through the SC is the rate limiting step for a substance permeating across the skin [66,68]. Moreover, the SC acts as the main barrier for skin water loss [66]. SC lipids specific content and composition and the structural arrangement of intercellular lipid matrix are responsible for the barrier features [70]. The intercellular lipids (ceramides, cholesterol, cholesteryl esters, fatty acids, and a small fraction of cholesterol sulfate) form bilayers surrounding the corneocytes acting as an adhesive between skin cells, forming an obstacle against exogenous agents [68,69].

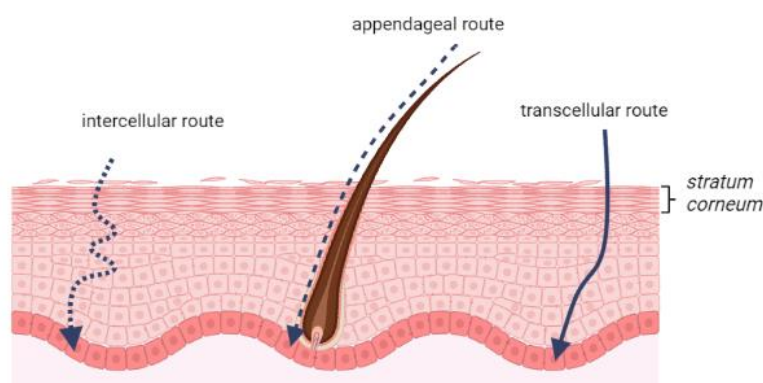


Figure 1.1.3. Possible transport pathways through the *stratum corneum* (adapted from [68,71]).

Molecule penetration in the skin (Figure 1.1.3) can occur through intercellular and transcellular routes (intact epidermis) or through appendageal routes. Molecule penetration via appendageal routes can be considered insignificant because skin appendages, formed by hair follicles and sweat glands, occupy only 0.1% of the total human skin surface [68]. Transcellular route occurs with cross-cell molecule penetration, whilst in intercellular route the molecules pass by the intercellular spaces, being the predominant pathway [68,72,73]. Permeant diffusion through the intercellular lipid matrix is required for both routes of intact epidermis [68,74].

The dermis, composed of fibroblasts, collagen, elastin, and hyaluronic acid [65] and containing blood vessels, nerves, glands, and hair follicles [9,63]. The major functions of this layer are the maintenance of skin characteristics and serving as a water reservoir for the skin [65].

The hypodermis, which is the deepest skin layer, provides the main structural support for the skin, consisting of adipose tissue that serves as a thermal barrier to the skin. This skin layer contains collagen and extracellular matrix and is interlaced with blood vessels and nerves [65,67].

1.1.4.2 Cosmetic Products

Cosmetic and personal care products represent a massive market, providing an extensive range of properties and benefits to the consumer, with millions of consumers using cosmetics and their ingredients daily [75,76]. In fact, cosmetic products global market was valued at USD 532.43 billion in 2017, and, through an expected annual growth rate of 7.14%, it can register USD 805.61 billion by 2023 [77].

1.1.4.2.1 Definition and Categories of cosmetics products

The European Union Council regulations define cosmetic products as “*any substance or mixture intended to be placed in contact with the external parts of the human body (epidermis, hair system, nails, lips, and external genital organs) or with the teeth and the mucous membranes of the oral cavity with a view exclusively or mainly to cleaning them, perfuming them, changing their appearance, protecting them, keeping them in good condition, or correcting body odors*” ([78], article 2.1). In general, a cosmetic product is applied for the direct treatment of the surface of the human body to maintain its

good condition (1), to change the body appearance (2), to protect the body (3) or to correct the body odour (4) [79]. These four functions must not affect the normal body functions or structure [5,29]

Cosmeceuticals, also known as active cosmetics, which were created in the 1980s, are cosmetic products containing biologically active ingredients with medicinal or drug-like benefits, aimed to satisfy the customer's health and beauty needs [80,81]. In fact, cosmeceuticals can act as skin protectors, deodorants, whitening, tanning and anti-wrinkling (or anti-aging) agents, and also possessing functions in nail and hair care products [82]. In consonance with their field of applications and functions, cosmetic products can be divided into seven categories, as follows. Cosmetics for personal cleansing (1) (soaps, deodorants, shampoos); cosmetics for the skin, hair, and integument care (2) (toothpaste, products for external intimate care); cosmetics for embellishment (3) (perfumes, lip colours); protective cosmetics (4) (solar products, anti-wrinkle products); corrective cosmetics (5) (beauty masks, hair dyes); maintenance cosmetics (6) (shaving cream, moisturizing creams); and active cosmetics (7) (fluoridated toothpaste, antiseptics) [79].

1.1.4.2.2 Cosmetic Formulation

The abundant advances in studying and understanding the physicochemical properties formulation systems (and their ingredients) have contributed to the development of biologically stable products. The first generation of skincare products emphasized the relevance of free amino acids in skin hydration. In fact, water, oily substances, and humectants combinations can be efficient to keep the epidermis biological homeostasis, acting upon the physicochemical condition of the SC, since the barrier function of the skin is maintained by moisture, lipids, and natural moisturizing factors (Figure 1.1.4) [83]. Any cosmetic formulation includes in its formulation base substances, active agents, and additives (Table 1.1.3) with different functions on the final product. Base substances are natural skin components; active agents are substances with specific functions such as protection, preservation, and/or improvement of the skin's natural condition; and additives are substances used to improve the product's stability, providing protection against microorganisms, temperature shifts, oxygen, and light related degradation, which improves the product's shelf life [4,84]. For example, the ingredients required for moisturising creams include solvents, emollients (10-40%), humectants (1-5%), emulsifiers (1-6%), thickening agents (0.1-2%), active ingredients (1-10%), neutralisers (0.01-0.055%), and preservatives (0.11-0.5%) (Figure 1.1.5) [85]. In addition, fragrances, chelating agents (prevent salt deposits, e.g., Mg^{2+} and Ca^{2+}), and antioxidants (prevent formulation oxidation) can also be added to the formulation [86].

Section 1. General Introduction

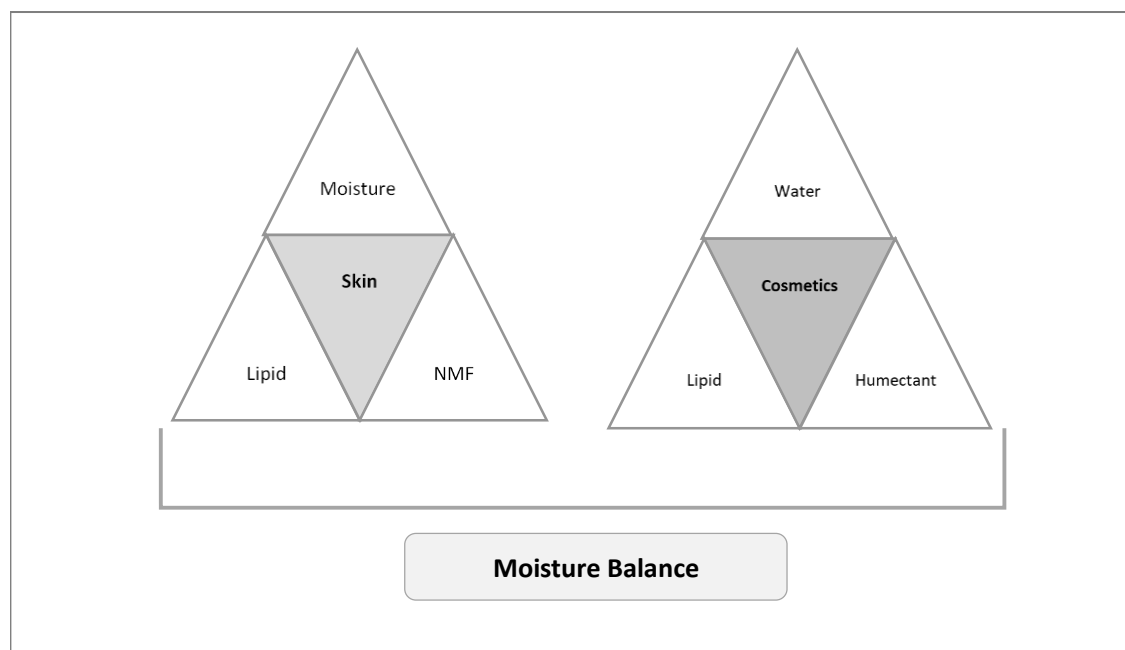


Figure 1.1.4. Moisture balance of the skin in the first generation of skin care. NMF - natural moisturizing factors (adapted from [83]).

Table 1.1.3. Substances used in cosmetic formulation

Substances	Ingredients	References
Base substances	Fatty acids Mineral oil products Triglycerides Wax esters	[4,84]
Active substances	Hyaluronic acid L-Fucose Valproic acid Vitamins (A, B3, C, E) Botanical extracts (Hesperidin, tea plant, ginseng, Resveratrol) Algal extract (<i>Botryococcus braunii</i>) Coenzyme Q10	[4,73,87–90]
Additives	Antioxidants Dyes and pigments Emulsifiers Perfumes Preservatives (Parabens, organic acids) Thickening agents (Types: lipid, naturally derived, mineral and synthetic) UV filters	[4,89,91,92]

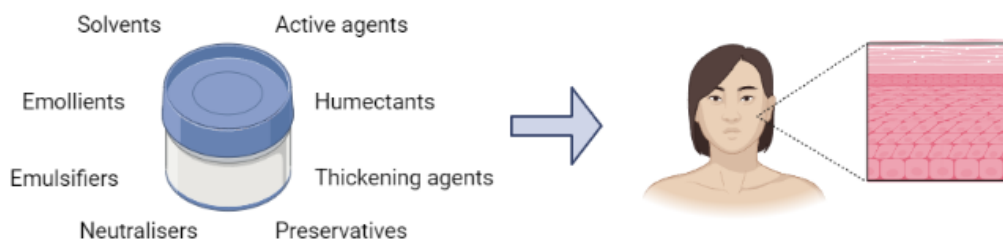


Figure 1.1.5. Base cream recommended ingredients in cosmetic formulations.

The active ingredients for cosmetics represent a large worldwide commercial market, projected to grow to US\$1.6 Billion by the year 2025 (www.prnewswire.com). These ingredients are named by the International Nomenclature Cosmetic Ingredient (INCI) standards and are listed according to their weight ratio in decreasing order. However, aromatic principles (fragrances) are only declared as perfumes or essences [84]. The modification of cosmetic products is a result of the overexposure to atmospheric oxygen, or due to the presence of microorganisms. Subsequently, antimicrobial and antioxidant preservatives can be added to cosmetic formulations to, respectively, inhibit microbial growth and suppress the formation of free radicals through oxidation [79]. Generally, the used additives in cosmetic formulations surpass the INCI listed base substances or active agents. Except for UV filters and consistency control substances, these additives should be averted due to their prowess to cause allergies [4,84]. Given their ability to protect consumers from UV radiation, UV filters are important additives in cosmetic formulations that are controlled by international safety regulations, which are strictly evaluated before the marketing of these products. Other additives, like TiO_2 and ZnO , were also analysed due to consumers' concerns and shown to be non-toxic and non-invasive, posing zero risk to human health [75]. The active ingredients used can be naturally synthesized (peptides, ceramides, most vitamins), purified from natural sources (botanicals, herbal extracts), obtained by cell culture fermentation (enzymes and cofactors, polysaccharides, and proteins), or extracted from animal sources. Still, the latter reduced greatly after the bovine spongiform encephalopathy related issues [93]. The specifications for any cosmetic ingredient are required to combine its chemical identification, in terms of structural formula, the raw material origins, the used extraction method; its physical arrangement, whether it is a powder, paste, gel or liquid; its molecular weight; its purity, with mandatory impurity characterization; its solubility in water and other relevant organic solvents; and additional specifications, like its organoleptic properties, flash point, melting/boiling point [4].

1.1.5 Cosmetic emulsions

Emulsions are the prevailing form of skincare products given their appealing feeling on the skin and ease of application when compared to waterless oils and lipids [94,95]. An emulsion is constituted by two or more immiscible materials forming a system where one material is suspended/dispersed

throughout another material, resulting in the dispersion of microscopic particles, forming colloids [19,96,97]. Given the characteristics of this biphasic system, constituted by lipophilic and hydrophilic components, an emulsion may be considered, in a straightforward way, analogous to human skin [97]. However, each formulation has specific intrinsic factors such as the systems nature and ingredients equilibrium; moreover, the emulsion phase proportion is decisive for the formulation behaviour. The outcome of the different aspects of the emulsions determines important parameters as its viscosity and macroscopic appearance [96].

The type of continuous and discontinuous phase used influences the nature of each emulsion system (Figure 1.1.6). Emulsions can be classified into four categories. Macroemulsions (1) are simple emulsions that can be oil-in-water (O/W) or water-in-oil (W/O) like lotions and creams, with droplet size range between 0.1 and 100 μm ; whilst nanoemulsions (2) are simple emulsions (O/W or W/O) with droplet size range between 20 and 200 nm. Thirdly, there are multiple emulsions (3) which are complex systems like oil-in-water-in-oil (O/W/O) or water-in-oil-in-water (W/O/W) with droplet sizes similar to macroemulsions; and microemulsions (4) which are water, oil, and surfactant/co-surfactant systems, constituting a single optically isotropic thermodynamically stable liquid solution, with droplet size range from 10 to 100 nm [19,95,97,98]). By allowing the penetration of hydrophilic substances through the skin's SC, O/W emulsions (Figure 1.1.7) are considered the most appropriate for topical application. The thermodynamic instability of O/W systems prevents their spontaneous production, being usually prepared by mechanical stirring to homogenize two heterogeneous phases. After mixing, interphase tension causes phase separation in O/W emulsions, which can lead to the degradation of its characteristics over time, during the storage period [96–98]. There are several types of interphase tension interactions (Figure 1.1.8): flocculation, occurs with stable particle collisions; coalescence, results from the predominant attraction force between droplets; phase separation develops due to prevalent repulsion forces, meaning a repel between colliding particles, preventing particle aggregation [97]; the upward movement of the dispersed phase, with lower density than the continuous phase, creates a thick separated layer, a process known as creaming [99,100]. Briefly, emulsion systems have a colloid behaviour, and their droplet interactions can lead to flocculation, coalescence, or phase separation. In addition, to occur phase separation by coalescence, it is required a preliminary accentuated decrease in the structural integrity of the emulsion [101].

There are several strategies to maintain emulsion stability overtime, such as electrostatic, steric, or solid particle stabilization [96,97]. Notwithstanding, the addition of emulsifiers are responsible for the stability of most cosmetic emulsions. Surface-active emulsifiers can be anionic, cationic, amphoteric, non-ionic, hydrophobic, lipophilic, ethoxylated, and non-ethyloxylated [95,97]. Depending on the desired application and formulation, different emulsifier agents (or surfactants) possess distinctive characteristics which will affect the emulsified mixture and type of emulsion obtained [97,98]. To ensure the formation of a macroscopically homogeneous and microscopically heterogeneous phase, the addition of one or more surface-active emulsifiers may be required [97].

Section 1. General Introduction

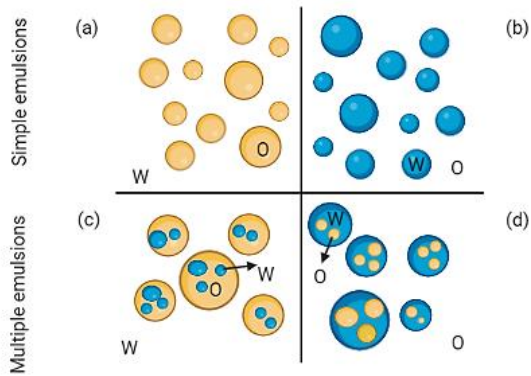


Figure 1.1.6. Schematic representation of emulsion types (adapted from [102]): (a) oil-in-water (O/W), (b) water-in-oil (W/O), (c) water-in-oil-in-water (W/O/W), (d) oil-in-water-in-oil (O/W/O).

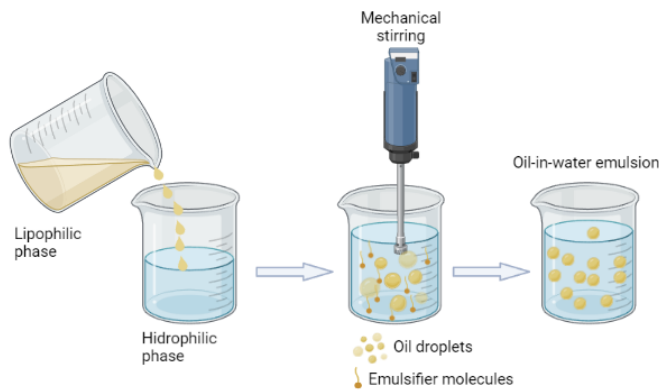


Figure 1.1.7. Schematic representation of oil-in-water (O/W) emulsification process.

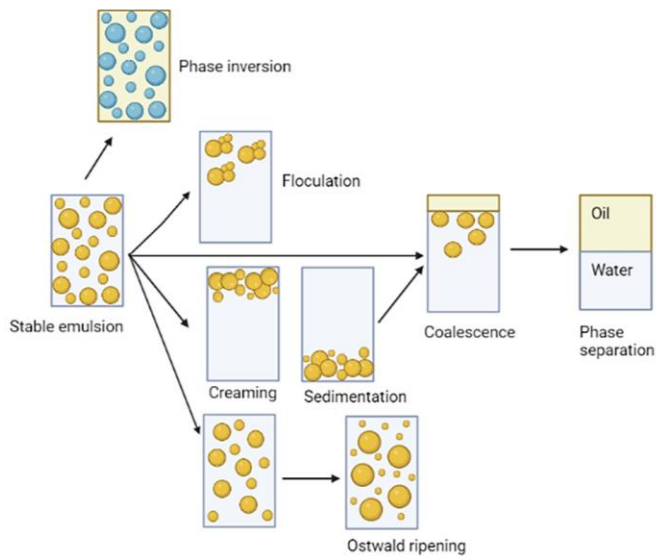


Figure 1.1.8. Schematic representation of physicochemical instability mechanisms in O/W emulsion system (adapted from [99,101–104]).

Section 1. General Introduction

Additionally, there are several other components used in cosmetic emulsions like emollients (sensory properties increasers) such as silicon oil and isopropyl myristate; moisturizers and humectants like glycerine and urea; active substances such as UV sunscreens and vitamins; antimicrobial agents; perfumes and colouring agents; and viscosity-increasing agents [4].

Even though most polysaccharides are not surface-active, they increase aqueous phase viscosity and inhibit droplet movement, contributing to the stabilization of emulsions. Nevertheless, emulsifiers based on high molecular weight polysaccharides have already been demonstrated to effectively form and stabilize O/W nanoemulsions. As previously mentioned, xanthan gum is a widely used polysaccharide ingredient in cosmetic industries, acting as a thickener and stabilizer in many applications [105]. In fact, xanthan gum is a beneficial hydrocolloid due to its solubility in hot/cold solutions, binding water promptly and productively [105]. Xanthan gum improves the emulsification of W/O emulsions by suspending insoluble ingredients, due to its high viscosity, and can be combined with other substances to enhance texture, flow behaviour, stability, and appearance of preparations [105]. In fact, 1.0% (w/v) of xanthan gum is enough to largely increase a liquids' viscosity, with many applications using as little as 0.1% (w/v) xanthan gum in their formulations [106]. Gellan gum is also used to stabilize emulsions, protecting them against temperature fluctuations, improving quality in transit and shelf-time [28]. In addition to xanthan gum and gellan gum, bacterial cellulose and hyaluronic acid have also been applied in emulsions [4,107].

1.1.6 Conclusions

A growing trend towards more sophisticated cosmetics and personal care products is observed due to the desire of formulators to obtain a competitive advantage to meet consumers' expectations for product improvements and enhancements. The literature review revealed the positive effects of polysaccharide-based formulations on human skin, namely the improvement of the skin barrier function and hydration. Moreover, polysaccharides rheological properties can increase formulation stability and enhance sensorial properties, which are important aspects of formulation technology. Accordingly, polysaccharides have been extensively used in cosmetic formulations. For example, hyaluronic acid is used as a bioactive ingredient, and in cosmetic vehicles; xanthan gum is used in cosmetic products due to its high viscosity-enhancing ability at low concentrations. Additionally, FucoPol is a promising bacterial polysaccharide, being presently studied as an ingredient in cosmetic formulations. Finally, polysaccharide-based formulations are important to maintain physiological skin conditions and to prevent and treat skin disorders related to barrier function alterations.

2. FUCOPOL EXTRACTION AND CHARACTERIZATION

This page was intentionally left blank

Optimization of FucoPol Extraction by Membrane-based Methods

The results presented in this chapter are part of the following published paper:

Baptista, S.; Torres, C.A.V.; Sevrin, C.; Grandfils, C.; Reis, M.A.M.; Freitas, F. Extraction of the Bacterial Extracellular Polysaccharide FucoPol by Membrane-Based Methods: Efficiency and Impact on Biopolymer Properties. *Polymers* 2022, 14, 390.

This page was intentionally left blank

Summary

In this chapter, membrane-based methods were evaluated for the recovery of FucoPol, the fucose-rich EPS secreted by the bacterium *Enterobacter A47*, aiming at reducing the total water consumption and extraction time, while keeping a high product recovery, thus making the downstream procedure more sustainable and cost-effective. The optimized method involved ultrafiltration of the cell-free supernatant using a 30 kDa molecular weight cut-off (MWCO) membrane that allowed for a 37% reduction of the total water consumption and a 55% reduction of the extraction time, compared to the previously used method (diafiltration-ultrafiltration with a 100 kDa MWCO membrane). This change in the downstream procedure improved the product's recovery (around 10% increase) and its purity, evidenced by the lower protein (8.2 wt.%) and inorganic salts (4.0 wt.%) contents of the samples (compared to 9.3 and 8.6 wt.%, respectively, for the previously used method), without impacting FucoPol's sugar and acyl groups composition, molecular mass distribution or thermal degradation profile. The biopolymer's emulsion-forming and stabilizing capacity was also not affected (emulsification activity (EA) with olive oil, at a 2:3 ratio, of $98 \pm 0\%$ for all samples), while the rheological properties were improved (the zero-shear viscosity increased from 8.89 ± 0.62 Pa.s to 17.40 ± 0.04 Pa.s), which can be assigned to the higher purity degree of the extracted samples. These findings demonstrate a significant improvement in the downstream procedure raising FucoPol's recovery, while reducing water consumption and operation time, key criteria in terms of process economic and environmental sustainability. Moreover, those changes improved the biopolymer's rheological properties, known to significantly impact FucoPol's utilization in cosmetic, pharmaceutical or food products.

2.1.1 Introduction

EPS are carbohydrate biopolymers secreted by the cells of many microorganisms that are released to the surroundings of the cells, remaining only loosely attached to them [108]. Many microbial EPS (e.g., xanthan and gellan gums, hyaluronic acid [109], and pullulan [4]) are utilized in high-value applications such as pharmaceutical, food, and cosmetic products [109–111] due to their biodegradable, biocompatible, and usually nontoxic nature [4,112].

Given their extracellular nature, EPS recovery from the culture broth involves rather simple downstream procedures that usually consist of cell removal, followed by biopolymer precipitation from the cell-free supernatant by addition of a precipitating agent (e.g., methanol, ethanol, isopropanol, acetone) and drying [108,113–116]. Although solvent precipitation with ethanol or acetone is the prevalent technique for EPS extraction, it usually yields rather impure polymers with high salts and/or protein contents [117]. Furthermore, this technique is expensive and impacts the environment due to the large volumes of used solvents and their handling/disposal [118]. Additional steps can be included in the downstream procedure, such as, for example, dilution of the broth for viscosity reduction or applying a heat treatment to kill bacteria and inactivate enzymes that could degrade the biopolymer during the process [52,118,119]. However, for high-value applications, in which a higher purity degree is often a prerequisite, specific

procedures must be used to reach high-purity products. Such procedures include, for example, reprecipitating the EPS from dilute aqueous solutions, deproteinization by chemical or enzymatic methods, and membrane processes, such as dialysis, ultrafiltration and diafiltration [118,120,121]. Pressure-driven membrane processes, like diafiltration and ultrafiltration, can achieve high separation yields, while having a low environmental impact [122]. Nevertheless, the EPS rheological properties often cause membrane fouling, which reduces flux performance and increases operation times and, consequently, the processes' operational costs [115,116,123,124]. Process optimization should therefore at least maximize the following criteria: recovery, highest purity, polymer performances adopting simple, rapid, and green procedures [108,115,116,124].

FucoPol is a fucose-rich EPS secreted by the bacterium *Enterobacter* A47 (DSM 23139) [41,42,59]. It is composed of neutral sugars, namely, fucose (32–36 mol%), galactose (25–26 mol%) and glucose (28–34 mol%), and the acidic sugar glucuronic acid (9–10 mol%). It also contains acyl groups: acetate (3–5 wt.%), pyruvate (13–14 wt.%), and succinate (3 wt.%) [50]. FucoPol's molecular weight was reported to range between 1.7×10^6 and 5.8×10^6 Da [41,59]. The presence of glucuronic acid, together with pyruvate and succinate, confers the biopolymer an anionic nature that promotes its interaction with cations and charged macromolecules [50,53]. FucoPol has proven valuable properties that include its thickening [53], filmogenic [44,56,125] and gelling capacity [59], as well as the ability to form and stabilize emulsions [41,44,55]. FucoPol recovery from the culture broth involves dilution with water for viscosity reduction, centrifugation for cell removal, heat treatment for enzyme inactivation and, finally, diafiltration and ultrafiltration of the cell-free supernatant with a 100 kDa (MWCO) membrane [126]. Given the high viscosity of FucoPol aqueous media [39], the broth is usually diluted by 1:2 to 1:10 (v/v) [42,47,52,118,127], thus generating very large volumes for processing. Moreover, during the downstream procedures, product losses occur which decrease the process efficiency.

This study focused on optimizing the downstream procedure for FucoPol recovery from *Enterobacter* A47 cultivation broth. Three methods were designed and tested, using membranes of two different MWCO, namely, 100 kDa, which had been utilized in previous studies [52,128], and 30 kDa. The performance of each method was evaluated in terms of operating time, water consumption, and polymer recovery. The impact of the different purification methods on FucoPol's physical-chemical properties, as well as on the biopolymer's rheological properties and emulsifying behaviour, were also evaluated.

2.1.2 Materials and Methods

2.1.2.1 FucoPol Production

Enterobacter A47 (DSM 23139) was previously cryopreserved at -80°C , using glycerol (20% (v/v)) as a cryoprotective agent. The cryopreserved vial is inoculated, using the plating technique, into four 500 mL shake flasks with 200 mL of liquid Luria Bertani (LB) medium in each flask (10.0 g/L peptone; 5.0 g/L yeast extract; 10.0 g/L NaCl; pH 6.8-7.0). Incubation is performed at 30°C for 16 h, using an orbital shaker at 200 rpm. At the end of incubation period, it was obtained 800 mL of inoculum.

FucoPol production [42] was achieved by inoculating 0,8 L (10% (v/v)) of *Enterobacter* A47 in 7.2 L (90% (v/v)) of Medium E*(5.8 g/L K_2HPO_4 ; 3.7 g/L KH_2PO_4 ; 3.3 g/L $(\text{NH}_4)_2\text{HPO}_4$; pH 7.0), supplemented with 40 g/L glycerol, operating the 10 L bioreactor (BioStat B-Plus, Sartorius, Göttingen, Germany), in batch mode during 8 h. After 8h, the bioreactor is operated in fed-batch mode for 88h, using Medium E* supplemented with 1000 g/L of glycerol as feeding solution at a constant rate of 5 mL/h. Automatic addition of HCl (2 M) or NaOH (5 M) was performed to control pH at 7.00 ± 0.05 . Temperature was maintained at $30.0 \pm 0.1^{\circ}\text{C}$ and the aeration rate was constant at 1.6 standard litres per minute of compressed air. Dissolved oxygen concentration was constant at 10% of air saturation by stirring rate automatic adjustment (300-800 rpm). Antifoam addition was also controlled to prevent foam formation.

The cultivation broth was collected and utilized for the extraction and purification experiments.

2.1.2.2 FucoPol Extraction and Purification

The culture broth (240 mL) was diluted with deionized water to a final volume of 2400 mL, and centrifuged ($13,000\times g$, 45 min) for cell removal. The cell pellet was discarded, and the cell-free supernatant was subjected to a thermal treatment (70°C , for 1 h) for enzyme inactivation [118]. The remaining cells and denatured proteins were removed by centrifugation ($13,000\times g$, 45 min) and the resulting treated cell-free supernatant was used for the purification experiments that comprised three different methods, as described below. The set-up (Figure 2.1.1) included a crossflow module (Sartocon Slide Holder, Sartorius, Göttingen, Germany), using either a 100 kDa or a 30 kDa MWCO (Hydrosart, Sartorius, Göttingen, Germany), with a surface area of 0.1 m^2 . All experiments were performed at room temperature ($\sim 23^{\circ}\text{C}$).

Method 1 comprised a diafiltration step followed by an ultrafiltration step (Figure 2.1.1), as described by Meireles et al. [118] and was used as a reference method. Briefly, the procedure consisted in operating the module in a diafiltration mode, in which deionized water was continuously added to the supernatant vessel, in view to keep a volume constant in the retentate's vessel ($\sim 2400\text{ mL}$). When the retentate's conductivity reached a value below $200\ \mu\text{S}/\text{cm}$, water addition to the vessel was suspended and the solution was concentrated to a volume of $\sim 240\text{ mL}$ by operating the module in an ultrafiltration mode.

Method 2 consisted in operating the crossflow module entirely in the ultrafiltration. The treated supernatant in the retentate vessel (2400 mL) was concentrated to a volume of $\sim 240\text{ mL}$. Afterwards,

the retentate was diluted with deionized water to the initial solution's volume and the ultrafiltration step was repeated. This procedure (ultrafiltration/dilution) was carried out until the retentate reached a conductivity below 200 $\mu\text{S}/\text{cm}$.

Method 3 was identical to Method 1, exception made that the supernatant in the retentate vessel was first concentrated to 50% of its initial volume (~ 1200 mL). Then, during the diafiltration mode, deionized water was added to the retentate vessel to keep the volume at ~ 1200 mL, until the conductivity reached a value below 200 $\mu\text{S}/\text{cm}$. Finally, the ultrafiltration mode was implemented to concentrate the retentate to a final volume of ~ 240 mL.

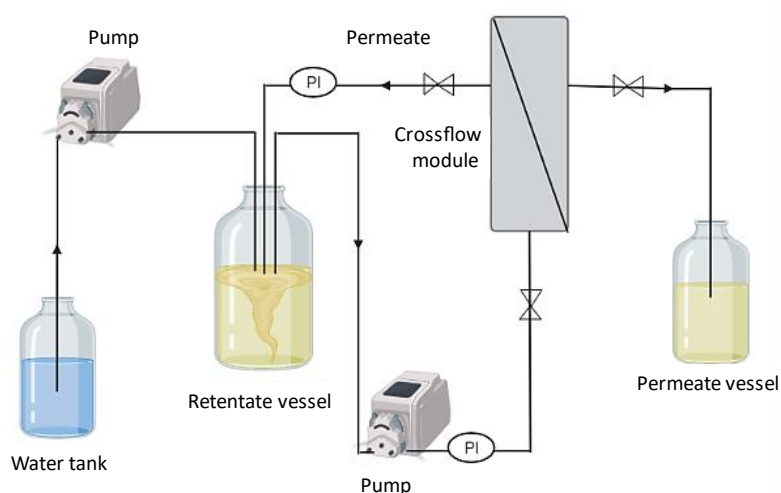


Figure 2.1.1 Schematic representation of the set-up used for the diafiltration/ultrafiltration experiments (PI-pressure gauge).

At the end of the purification procedures, the concentrated retentate was freeze-dried (ScanVac CoolSafeTM, LaboGene, Allerød, Denmark) at -110 °C for 48 h, for product quantification. The samples obtained with the 100 kDa and 30 kDa membranes were identified as F- i_{100} and F- i_{30} , respectively (i = method 1, 2 or 3).

The inlet (P_{in} , bar) and outlet (P_{out} , bar) pressures, as well as the time (min) and the overall volume of water (L) required to reach a conductivity value below 200 $\mu\text{S}/\text{cm}$, were registered. The transmembrane pressure (TMP, bar) was determined using the following equation [129]:

$$\text{TMP} = \frac{(P_{in} + P_{out})}{2} \quad (2.1.1)$$

2.1.2.3 FucoPol Characterization

2.1.2.3.1 Chemical Composition

Freeze-dried FucoPol samples (5 mg) were dissolved in deionized water (5 mL) and hydrolyzed with 0.1 mL 99% trifluoroacetic acid (TFA) at 100 °C for 4 h, as described by Freitas et al. [44]. The monosaccharide contents in the hydrolysate were identified and quantified by liquid chromatography, using a CarboPac PA10 column (Thermo Scientific™ Dionex™, Sunnyvale, CA, USA), equipped with an amperometric detector. The analysis was performed at 30 °C with sodium hydroxide (NaOH 4 mM) as eluent, at a flow rate of 0.9 mL/min. Fucose, glucose, galactose, and glucuronic acid at a concentration between 5 and 100 ppm were used as standards. The acyl substituents groups, namely, acetate, succinate and pyruvate, were quantified by liquid chromatography, using a Aminex HPX-87H 300×7.8 mm column (Biorad, Hercules, CA, USA), connected to an infrared (IR) detector, using sulfuric acid 0.01 N as eluent, at a flow rate of 0.6 mL/min, at 30 °C. Acetic, succinic and pyruvic acid were used as standard at a concentration between 25 and 500 ppm.

2.1.2.3.2 Elemental Analysis

Elemental analysis was performed in an Elemental Analyzer Thermo Finnigan-CE Instruments (Wigan, UK), model Flash EA 1112 CHNS, equipped with a gas chromatography (GC) and a thermal conductivity detector (TCD).

2.1.2.3.3 Inorganic Salts Content

The total inorganic salts content of the samples was determined gravimetrically by incinerating 50 mg of dried polymer samples at 550 °C for 12 h.

2.1.2.3.4 Molecular Mass Distribution

Molecular number (M_n), average molecular weights (M_w), and polydispersity index ($PI = M_w/M_n$) of FucoPol samples were obtained by size exclusion chromatography coupled with multiangle light scattering (SEC-MALS), as described by Torres et al. [43]. FucoPol solutions (2 mg/mL) were dissolved in 0.1 M Tris-HCl + 0.2 M NaCl, pH 8.09 buffer, which was also the SEC mobile phase. These solutions were warmed for 1 h at 80 °C under lateral agitation in a water bath. Dissolution of the polymer was continued for 24 h under a rocking roller at room temperature. The SEC columns (PL Aquagel-OH mixed 8 μ m; 300 × 7.5 mm) protected by a guard column (Polymer Laboratory, Berkshire, UK; 50 × 7.5 mm, part no. 1149–1840) were equilibrated overnight before running the analysis at a flow rate of 1 mL/min at room temperature. Each analysis was conducted in duplicate. The purity and molecular mass distribution of the polysaccharide were monitored with MALS and IR detectors. These data were analyzed with Astra software (CA, US) (V 4.73.04). A dn/dc of 0.190 mL/g was adopted to calculate the M_w .

2.1.2.3.5 Fourier Transform Infrared (FT-IR) Spectroscopy

FT-IR spectroscopy with Diamond ATR (Attenuated Total Reflectance) was used to collect the spectra of the samples with a Perkin Elmer Spectrum Two (Perkin Elmer Inc., Waltham, MA, US), equipped with a lithium tantalate (LiTaO₃) detector with an SNR (signal to noise ratio) of 14,500:1. The resolution was 0.5 cm⁻¹ and the number of scans was eight. The samples were placed in the absorbance chamber and corrected by applying the ATR-correction function of Perkin Elmer Spectrum (Waltham, MA, US) software at the region of 4500–500 cm⁻¹.

2.1.2.3.6 Thermogravimetric Analysis (TGA)

TGA was performed using a Thermogravimetric Analyzer Labsys EVO (Setaram, France). The samples (10 mg) were placed in aluminum crucibles and heated from room temperature to 550 °C, with a heating rate of 10 °C/min, in air. The thermal degradation temperature (T_{deg}, °C) corresponds to the temperature value obtained for the maximum decreasing peak of the sample mass.

2.1.2.4 Apparent viscosity and viscoelastic properties

The rheological properties of FucoPol aqueous solutions (1.0 wt%) were studied using a MCR 92 modular compact rheometer (Anton Paar, Madrid, Spain), equipped with a PP50/S parallel plate geometry (diameter 50 mm). The temperature was kept constant at 25 °C using a P-PTD 200/AIR Peltier plate (Anton Paar, Madrid, Spain). The flow curves were determined using a steady-state flow ramp in a shear rate range of 0.01 to 1000 s⁻¹. The flow curves obtained were fitted to the equation based on Cross model [39] described as follows:

$$\eta = \frac{\eta_0}{1+(\tau\dot{\gamma})^m} \quad (2.1.2)$$

where η is the apparent viscosity (Pa.s), η_0 (Pa.s) is the viscosity at zero shear rate, τ (s) is the relaxation time, and m is a dimensionless constant, related to the exponent of power-law (n) by $m= 1- n$ [24,27]. Frequency sweep tests were performed with frequency ranging from 0.01 to 100 rad/s with a constant strain of 0.5% that was well within the linear viscoelastic limit (LVE), which was evaluated through preliminary amplitude sweep tests. All tests were performed in triplicate.

2.1.2.5 Emulsion Forming and Stabilizing Capacity

The ability of the extracted FucoPol samples to stabilize emulsions was assessed by mixing 3 mL FucoPol (1.0 wt.%) aqueous solution with 2 mL olive oil (purchased from a local market) to give a 2:3 (w/w) emulsion ratio. The mixtures were manually agitated for 40 s and left standing for 24 h, at room temperature. The emulsification index E24 (%) was determined using the following equation [44]:

$$E24 = \frac{h_e}{h_T} \times 100 \quad (2.1.3)$$

where h_e (mm) is the height of the emulsion layer and h_T (mm) is the overall height of the mixture. The rheological behaviour of the different emulsions was evaluated as described above. All tests were performed in triplicate.

2.1.3 Results

2.1.3.1 Optimizing FucoPol Purification by Diafiltration and/or Ultrafiltration Procedures

At the end of the cultivation run, the culture broth had an apparent viscosity higher than 11 Pa.s (at a shear rate of 0.008 s^{-1}). The broth was diluted with deionized water (1:10, v/v), for viscosity reduction, thus allowing for cell removal by centrifugation. The resultant cell-free supernatant was subjected to a thermal treatment to inactivate bacterial enzymes [41,118], and the treated cell-free supernatant was used for testing FucoPol recovery using membranes of two different MWCO, namely, 100 kDa and 30 kDa. Three methods were evaluated for each membrane (Table 2.1.1). The retentate's conductivity was used to evaluate the purification progress: a value below $200 \mu\text{S/cm}$ was targeted as indicative of the elimination of most low Mw compounds from the sample (the treated cell-free supernatant had an initial conductivity value of $2800 \pm 300 \mu\text{S/cm}$). The extraction time was defined as the time required to reach the target for the retentate's conductivity, followed by its concentration to the initial broth volume (~240 mL).

Table 2.1.1. Recovery of FucoPol from the cell-free supernatant using Method 1 (diafiltration-ultrafiltration), Method 2 (ultrafiltration) and Method 3 (ultrafiltration-diafiltration-ultrafiltration) with 100 or 30 kDa MWCO membranes. Data are shown as the average \pm standard deviation (SD) ($n = 3$).

Method	Membrane (kDa)	Sample	Average TMP (bar)	Extraction Time (min)	Water Consumption (L)	Polymer Recovery (g)
1	100	F-1 ₁₀₀	0.63 ± 0.13	105 ± 6	9.6 ± 0.0	1.20 ± 0.11
	30	F-1 ₃₀	0.62 ± 0.16	130 ± 6	9.6 ± 0.0	1.38 ± 0.04
2	100	F-2 ₁₀₀	0.73 ± 0.05	77 ± 8	4.3 ± 0.0	1.22 ± 0.04
	30	F-2 ₃₀	0.67 ± 0.20	66 ± 6	4.3 ± 0.0	1.31 ± 0.05
3	100	F-3 ₁₀₀	0.76 ± 0.11	81 ± 4	6.0 ± 0.0	1.06 ± 0.09
	30	F-3 ₃₀	0.71 ± 0.14	85 ± 1	6.0 ± 0.0	1.50 ± 0.04

The results summarized in Table 2.1.1 and Figure 2.1.2a-b highlight that Method 1 (diafiltration-ultrafiltration) with either membrane involved the largest water consumption (9.6 L) and took the longest time (105–130 min) to reach the envisaged conductivity value (Table 2.1.1 and Figure 2.1.2a-b). Although the similar TMP (0.63 ± 0.13 and 0.62 ± 0.16 bar) was applied for both membranes, the extraction time with the 30 kDa membrane was higher due to the lower cut-off. The retentate's conductivity decreased significantly during the initial 23–28 min, continuing to decrease afterwards until the target conductivity value was achieved (Figure 2.1.2a-b). The sample obtained after concentration of the

retentate had a slightly higher conductivity as a concentration effect of the final ultrafiltration step. Compared to sample F-1₁₀₀ (1.20 ± 0.11 g), a higher polymer recovery was noticed for sample F-1₃₀ (1.38 ± 0.04 g). Interestingly, sample F-1₃₀ had lower protein and inorganic salts contents, thus showing its higher purity (Figure 2.1.3).

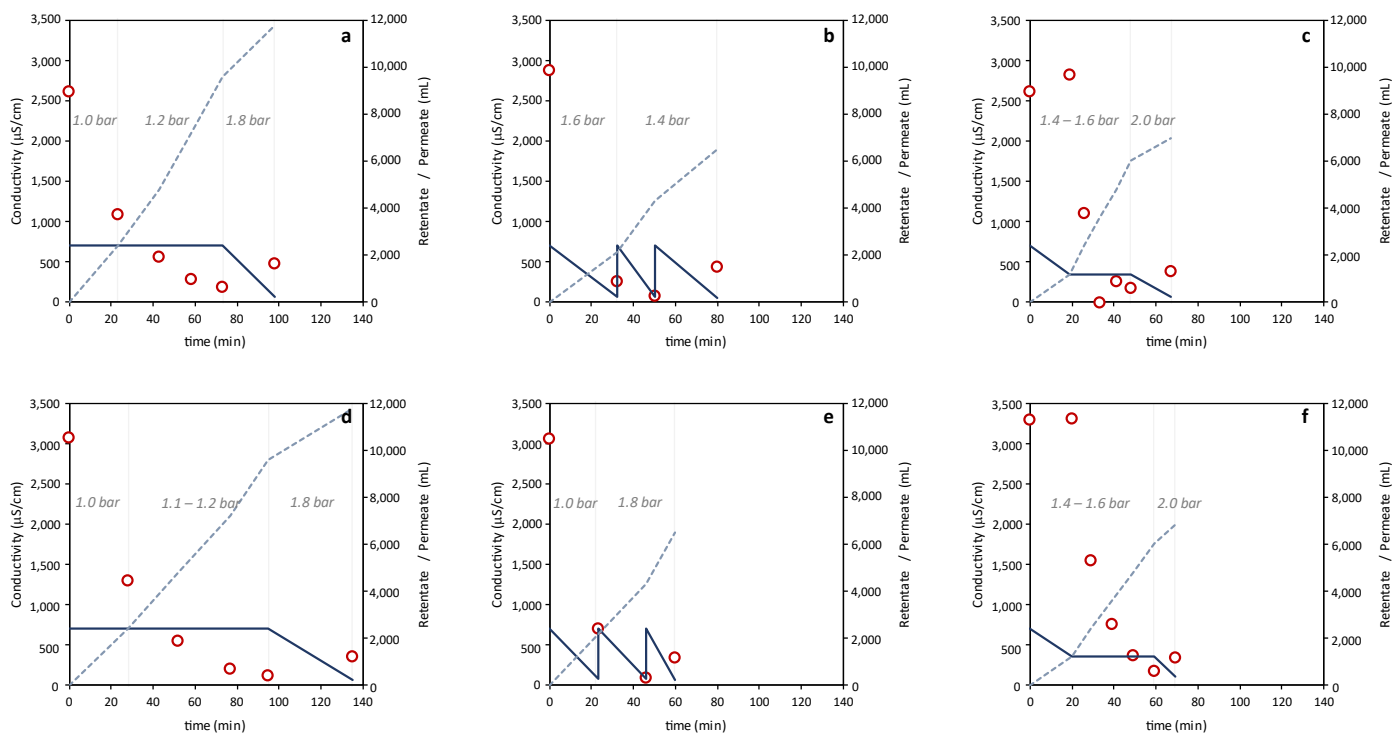


Figure 2.1.2 - Retentate (full lines) and permeate (dashed lines) volumes, retentate conductivity (circles), and inlet pressure (italic), over time, for experiments F-1₁₀₀ (a), F-1₃₀ (b), F-2₁₀₀ (c), F-2₃₀ (d), F-3₁₀₀ (e) and F-3₃₀ (f).

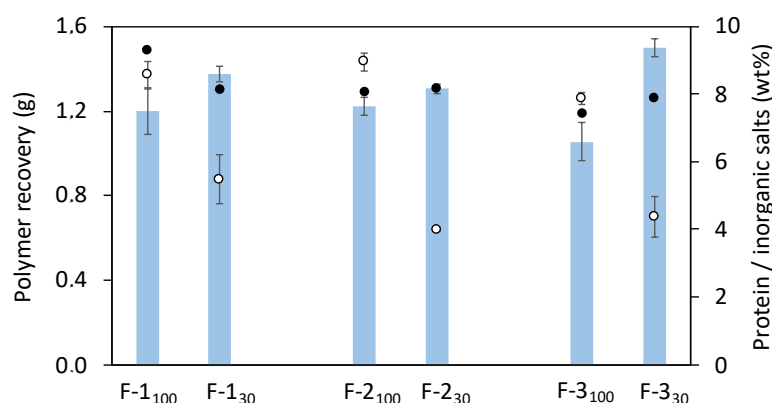


Figure 2.1.3 - Polymer recovery (bars) and samples content in protein (closed circles) and inorganic salts (open circles) for the experiments performed with Methods 1, 2 and 3, with the 100 kDa and the 30 kDa membranes.

A considerable reduction in water consumption (from 9.6 L to 4.3 and 6.0 L) was observed for Methods 2 (ultrafiltration) and 3 (ultrafiltration-diafiltration-concentration), together with a reduction of the overall extraction time (66–77 and 81–85 min, respectively) (Table 2.1.1, Figure 2.1.2). The

sharpest drop in conductivity was observed for Method 2, where after the first ultrafiltration step (that took 30 min) it dropped down below 1000 $\mu\text{S}/\text{cm}$ (Figure 2.1.2c-d).

Similarly to Method 1, for Methods 2 and 3 the 30 kDa membrane gave rise to higher polymer recovery: 1.31 ± 0.05 and 1.50 ± 0.04 g, respectively, compared to the 100 kDa one (1.22 ± 0.04 and 1.06 ± 0.09 g, respectively) (Table 2.1.1). Interestingly, identical protein removal was achieved with both membranes in either method, as shown by the similar protein content in the samples (7.4–8.2 wt.%). In contrast, salt removal from the supernatant was more efficient for the 30 kDa membrane (4.0–4.4 wt.%, compared to 7.9–8.2 wt.% for the 100 kDa membrane) (Figure 2.1.3).

2.1.3.2 Physical and Chemical Characterization of the Extracted FucoPol Samples

2.1.3.2.1 Composition

The extracted FucoPol samples were characterized in terms of their sugar and acyl groups composition to assess the impact of the tested extraction and purification methods. As shown in Table 2.1.2, all samples had identical sugar composition, namely, fucose, galactose, glucose, and glucuronic acid contents of 38–41 mol%, 24 mol%, 27–29 mol% and 6–7 mol%, respectively. This sugar monomer composition is similar to former data reported for glycerol-derived FucoPol [4,41,43,52,54,58] despite a slightly higher fucose content and a lower glucuronic acid content (Table 2.1.2). The higher fucose content renders the biopolymer more advantageous due to the biological activity reported for fucose-containing polysaccharides, namely, the reduction of allergic reactions, wound healing, antiaging [87,130], anti-inflammatory, and anticancer activities [131,132]. Regarding the acyl groups content, all samples had similar composition (5.1–5.4 wt.% pyruvyl, 1.0–1.1 wt.% succinyl and 4.4–5.4 wt.% acetyl), in the ranges of previously reported values [41–44] (Table 2.1.2).

Table 2.1.2. Physical-chemical characterization of FucoPol samples (Fuc: fucose; Gal: galactose; Glc: glucose; GlcA: glucuronic acid; Pyr: pyruvyl; Succ: succinyl; Acet: acetyl; Mw: molecular weight; PI: polydispersity index).

Sample	Sugar Monomers (mol%)				Acyl Groups (wt.%)			Mw ($\times 10^6$) (Da)	PI	T _{deg} (°C)
	Fuc	Gal	Glc	GlcA	Pyr	Succ	Acet			
FucoPol(*)	32–36	25–26	28–34	9–10	3.7–14.0	0.6–3.0	3.5–6.8	1.7–5.8	1.3–1.9	268
F-1 ₁₀₀	38	24	28	7	5.4	1.1	5.4	1.6	1.36	262
F-1 ₃₀	40	24	29	6	5.2	1.0	4.4	1.7	1.74	261
F-2 ₁₀₀	40	24	29	7	5.2	1.0	5.4	1.4	1.51	261
F-2 ₃₀	40	24	29	7	5.2	1.1	4.6	1.6	1.48	262
F-3 ₁₀₀	41	24	27	7	5.1	1.0	4.2	1.7	1.70	263
F-3 ₃₀	40	24	29	7	5.3	1.1	5.3	2.0	1.71	262

(*) [39,41–44,47,52,53].

2.1.3.2.2 Molecular Mass Distribution

The extracted samples had similar average Mw that ranged from 1.4×10^6 Da to 2.0×10^6 Da, with PI values of 1.36–1.74 (Table 2.1.2). These values are comparable to those reported in previous studies for FucoPol (Mw = 1.7×10^6 – 5.8×10^6 Da and PI = 1.3–1.9) [41,47,54,59], thus confirming that the applied extraction and purification methods had no significant impact on FucoPol's molecular mass distribution. All samples contained polydisperse macromolecules, as expected for carbohydrate polymers, but given their low PI values, their size distribution was rather narrow, indicating homogeneous FucoPol samples were produced by all tested procedures.

2.1.3.2.3 FT-IR Spectroscopy

The FT-IR spectra of the extracted FucoPol samples (Figure 2.1.4) are identical to those reported in the literature for FucoPol [41,52]. Common to all polysaccharides, two bands are observed around the 3280–2930 cm^{-1} region (Figure 2.1.4, green): the strong broadband appearing at 3282 cm^{-1} represents the O-H stretching of hydroxyls' vibrations, and the weak signal at 2923 cm^{-1} is due to the C-H stretching peak of CH_2 groups [52,133]. In addition, the IR absorption bands around 970–1145 cm^{-1} (Figure 2.1.4, blue) are mainly due to C-C and C-O stretching in the pyranoid ring and C-O-C stretching of glycosidic bonds [134–136]. The bands observed at 1725 cm^{-1} (Figure 2.1.4, yellow) and at 1248 cm^{-1} may be attributed to the acyl substituents present in FucoPol's structure, namely, the C=O stretching vibrations of carbonyls and the C-O-C vibrations, respectively [41,135]. The peak around 1603 cm^{-1} and the peaks in the region between 1400 and 1370 cm^{-1} (Figure 2.1.4, yellow and orange) may be assigned to the asymmetric and symmetric stretching of carboxylates from glucuronic acid [41,52,54]. The presence of bound water might be indicated by the bending vibration of O-H associated with a peak around 1603 cm^{-1} (Figure 2.1.4, yellow) [134–136].

2.1.3.2.4 Thermogravimetric Analysis

All extracted FucoPol samples displayed similar TGA curves, with two main degradation steps (Figure 2.1.5). The first degradation step, corresponding to weight losses of 8–12%, occurred between around 36 and 137 °C and is related to the elimination of water molecules physically entrapped or/and adsorbed to the polysaccharide through hydrogen bonding [137,138]. Samples F-1₁₀₀ and F-1₃₀ had the lowest weight loss values at this temperature range (10 and 8%, respectively), suggesting they had lower contents of adsorbed water compared to the samples obtained by Methods 2 and 3 that displayed the same weight loss (12%). The second and more significant weight loss, similar to all samples (41–43%), occurring between 203 and 344 °C, is the degradation of FucoPol's saccharide chain, namely, the depolymerization and the dehydration of saccharide rings [139]. The T_{deg} of the samples was determined to be in the range 261–263 °C, thus showing no significant differences among the samples extracted by each of the tested methods. As the temperature further increases, there is the formation of polynuclear aromatic and graphitic carbon structures, resulting in the formation of a char that accounted for 33–40% of the samples' mass. Interestingly, Methods 2 and 3 yielded FucoPol samples with lower char yield

(33–35%) compared to those obtained with Method 1 (36–40%), which may be related to the samples' lower content in inorganic salts (Figure 2.1.3).

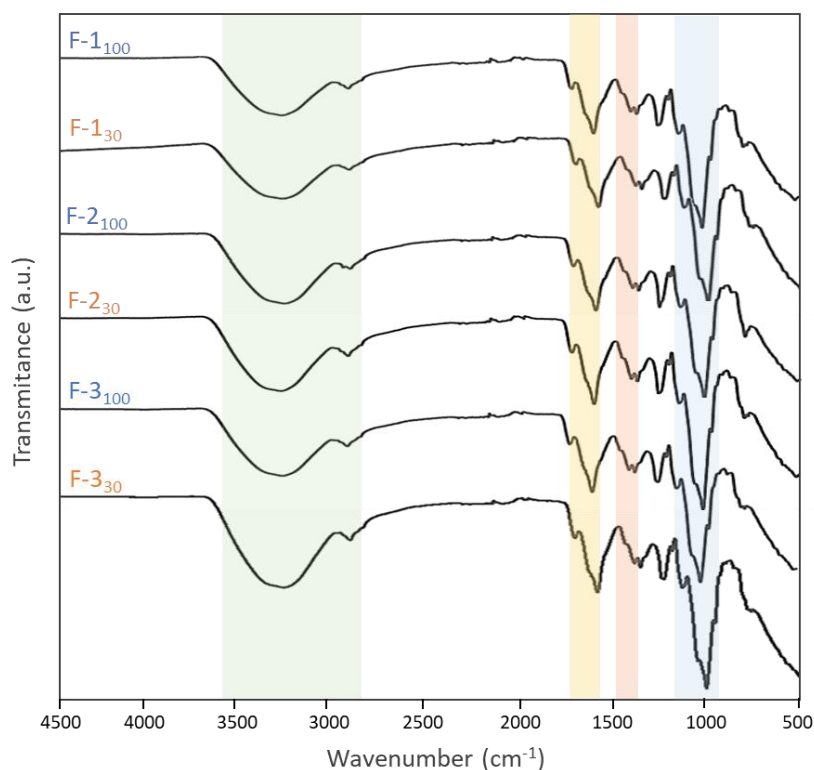


Figure 2.1.4. Comparative FT-IR spectra of the FucoPol samples extracted with Method 1 (F-1₁₀₀; F-1₃₀), Method 2 (F-2₁₀₀; F-2₃₀) and Method 3 (F-3₁₀₀; F-3₃₀).

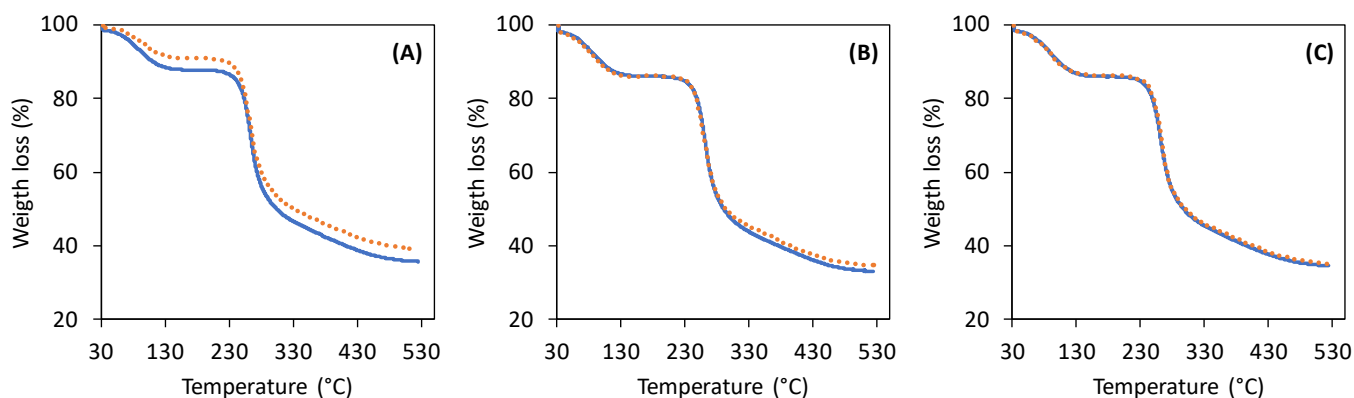


Figure 2.1.5. Thermal analysis curves for the FucoPol samples obtained by the different tested methods: (A) Method 1, (B) Method 2, (C) Method 3; F-i₁₀₀, full blue line; F-i₃₀, dotted orange line).

2.1.3.3 Rheological Properties of the Extracted FucoPol Samples in Aqueous Medium

As shown in Figure 2.1.6, the aqueous solutions of all FucoPol samples displayed a shear-thinning fluid behaviour, typical of high molecular weight polysaccharides [140] that agrees with previous studies [44,50,54,118]. Nevertheless, slight differences are noticed among the samples, namely, a lower apparent viscosity for the samples obtained with Method 1 (Figure 2.1.6A) compared to those of Methods 2 and 3 (Figure 2.1.6B-C). Moreover, the samples recovered with the 30 kDa MWCO membrane had a slightly higher viscosity for all methods. These findings can be explained by the lower inorganic salts content of samples F-2₃₀ and F3₃₀ (Figure 2.1.3). Xue et al. [141] reported that the presence of inorganic salts typically decreases the viscosity of polysaccharides (e.g., welan) solutions due to the electrostatic interaction established with the polysaccharide chain.

A non-Newtonian mathematical model, the Cross model, was fitted from the experimental results (Figure 2.1.6) with the resulting parameters given on Table 2.1.3. Samples F-1₁₀₀ and F-1₃₀, recovered from the cultivation broth by Method 1 (diafiltration-ultrafiltration), had the lowest η_0 values (8.89 ± 0.04 and 10.40 ± 0.84 Pa.s, respectively), as well as the lowest τ (1.26 ± 0.07 and 1.58 ± 0.08 s, respectively), thus confirming the lowest apparent viscosity of their aqueous solutions. The highest η_0 values were observed for FucoPol samples F-2₃₀ and F-3₃₀ (17.40 ± 0.04 Pa.s and 16.30 ± 0.04 , respectively), both recovered with the 30 kDa membrane, but with different methods. The m constant values are similar for all samples and agree with those reported for FucoPol (0.645 ± 0.024) [44,50] in close agreement with former data published by Morris [142] for polysaccharides ($m = 0.76$).

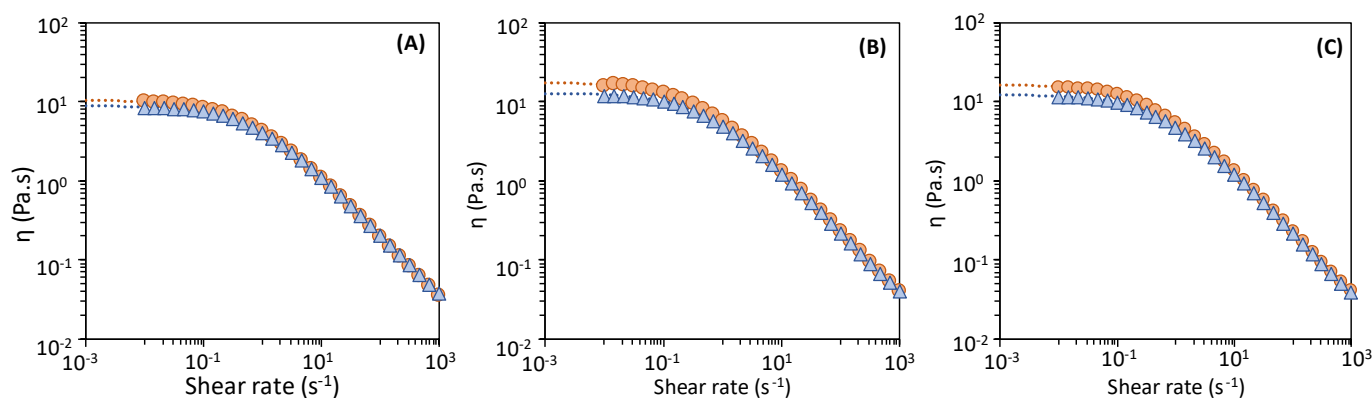


Figure 2.1.6. Flow curves of FucoPol aqueous solutions (1.0 wt.%): (A) Method 1, (B) Method 2, (C) Method 3; samples F-1₁₀₀ (triangle) and F1₃₀ (circle); Dotted lines represent the Cross model; ($n = 3$).

Table 2.1.3. Cross model parameters estimated for FucoPol samples (1.0 wt.%) recovered from the cultivation broth by the different tested different methods. η_0 —apparent viscosity of the first Newtonian plateau (Pa.s); τ —relaxation time (s); m —dimensionless constant. Data are shown as the average \pm standard deviation (SD) ($n = 3$).

Method	Membrane Cut-Off (kDa)	Sample	Cross model		
			η_0 (Pa.s)	τ (s)	m
1	100	F-1 ₁₀₀	8.89 \pm 0.62	1.26 \pm 0.07	0.78 \pm 0.00
	30	F-1 ₃₀	10.40 \pm 0.84	1.58 \pm 0.08	0.78 \pm 0.00
2	100	F-2 ₁₀₀	12.80 \pm 0.58	1.89 \pm 0.11	0.77 \pm 0.00
	30	F-2 ₃₀	17.40 \pm 0.04	1.68 \pm 0.21	0.78 \pm 0.00
3	100	F-3 ₁₀₀	12.30 \pm 1.16	1.77 \pm 0.03	0.78 \pm 0.00
	30	F-3 ₃₀	16.30 \pm 0.04	2.23 \pm 0.03	0.78 \pm 0.00

$$RE = \sum_{i=1}^n (|x_{exp,i} - x_{calc,i}| / x_{exp,i}) / n \text{ is between } 0.011 \text{ and } 0.019$$

The mechanical spectra (Figure 2.1.7) of the six FucoPol samples in aqueous media showed that the loss modulus (G'') is higher than the storage modulus (G'), indicating a liquidlike behaviour [41,54]. The mechanical spectra for all samples are quite similar, with G' increasing at a higher rate than G'' at the given frequency, with the crossover of dynamic moduli being perceived at similar frequencies. Nevertheless, for samples F-1₁₀₀ and F-1₃₀, the crossover occurred at a slightly higher frequency (0.6 Hz) (Figure 2.1.7A) than for the remaining samples (0.5 Hz for samples F-2₁₀₀ and F-3₁₀₀, and 0.4 Hz for samples F-2₃₀ and F-3₃₀) (Figure 2.1.7B,C). The higher the viscosity the lowest will be the energy necessary to store energy and observe a $G' = G''$ crossover, i.e., the crossover will occur at lower frequencies [54]. In previous studies, FucoPol aqueous solutions of similar concentration (1.0–1.2 wt.%) were reported to have dynamic crossover values occurring at higher frequencies (2.8–10 Hz) [44,50,54,143]. Such discrepancies might be related to the extraction method used in previous studies (dialysis with 10–12 kDa membranes) [41,44].

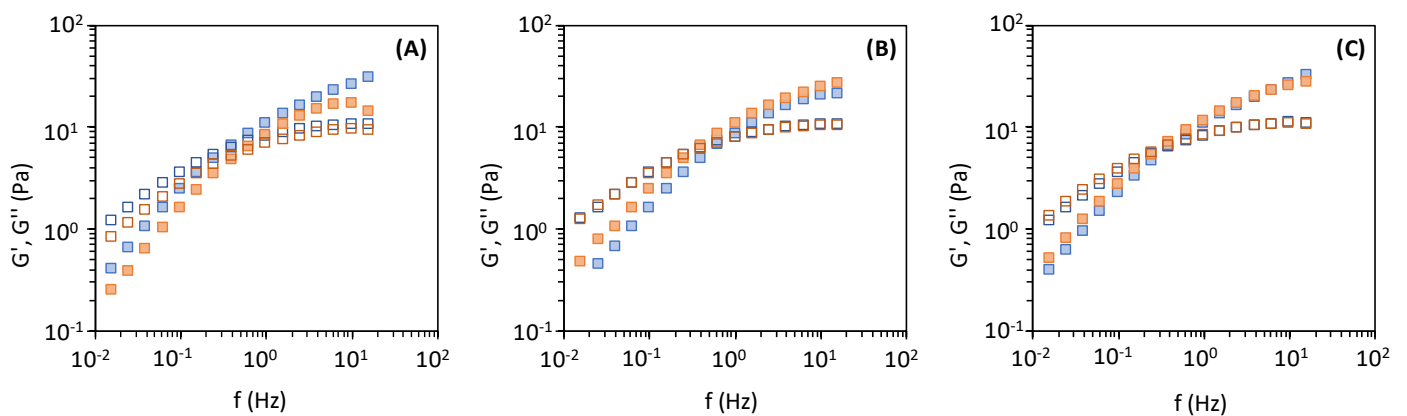


Figure 2.1.7. Mechanical spectrum of FucoPol aqueous solutions (1.0 wt.%), G' (closed square) and G'' (open square): (A) Method 1, (B) Method 2, (C) Method 3; F-i₁₀₀, blue; F-i₃₀, orange. Data are shown as the average \pm standard deviation (SD) ($n = 3$).

2.1.3.4 Emulsion Forming and Stabilizing Capacity

The ability of FucoPol to form and stabilize emulsions was assayed for all extracted samples by preparing emulsions using olive oil as the test hydrophobic compound. The assays consisted in mixing each FucoPol sample, at a concentration of 1.0 wt.%, with olive oil, at a 2:3 (v/v) ratio (Figure 2.1.8). The results show that all samples efficiently emulsified olive oil ($E_{24} = 98\%$) (Table 2.1.4). According to Willumsen and Karlson [144], a good emulsifier has E_{24} values equal to or above 50%. FucoPol's ability to form and stabilize emulsions with different hydrophobic compounds (e.g., cedarwood oil, sunflower oil, corn oil and, rice bran oil), at different O/W ratios (e.g., 1:4, 2:3, 3:2, 4:1), was previously demonstrated with reported E_{24} values ranging from 41 to 80% [41,44,55].

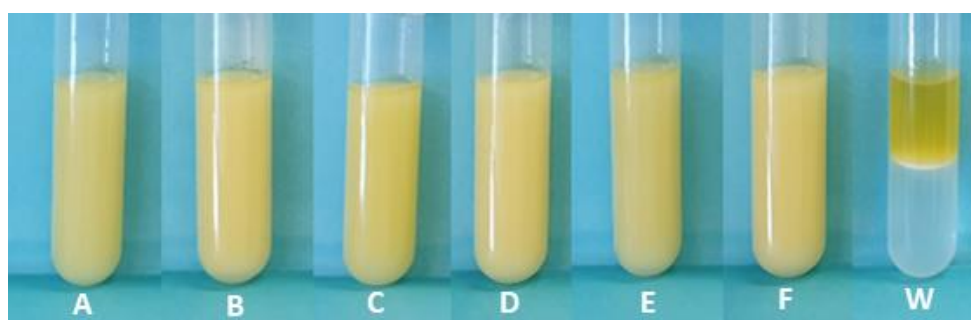


Figure 2.1.8. Olive oil/FucoPol (1.0 wt.%) emulsions (2:3 O/W ratio) after 24 h for the extracted samples. Method 1 (F-1₁₀₀, **A**; F-1₃₀, **B**); Method 2 (F-2₁₀₀, **C**; F-2₃₀, **D**); Method 3 (F-3₁₀₀, **E**; F-3₃₀, **F**); **W**-blank sample, oil:water.

Table 2.1.4. Emulsification index (E_{24}) and zero shear viscosity (η_0) for the emulsions prepared with the extracted FucoPol samples and olive oil, at an oil/water (O/W) ratio of 2:3. Data are shown as the average \pm standard deviation (SD) ($n = 3$).

Method	Membrane Cut-Off (kDa)	Sample	E_{24} (%)	η_0 (Pa.s)
1	100	F-1 ₁₀₀	98 \pm 0	46.5 \pm 5.3
	30	F-1 ₃₀	98 \pm 0	41.3 \pm 19.1
2	100	F-2 ₁₀₀	98 \pm 0	81.5 \pm 10.5
	30	F-2 ₃₀	98 \pm 0	90.2 \pm 4.4
3	100	F-3 ₁₀₀	98 \pm 0	66.9 \pm 3.8
	30	F-3 ₃₀	98 \pm 0	63.9 \pm 6.3

As shown in Figure 2.1.9, the olive oil/FucoPol emulsions exhibited shear-thinning flow behaviour. Moreover, the η_0 of the emulsions was considerably higher (Table 2.1.4) compared to the corresponding aqueous solutions (Table 2.1.3). As reported by Calero et al. [145], the increase of the apparent viscosity of the resulting emulsions relatively to the polymer aqueous solutions is typically explained by an increase of polymer chain entanglements within the aqueous layer surrounding the oil droplets, leading to

a higher resistance to flow under steady shear. The lowest η_0 was observed for the emulsions prepared with samples F-1₁₀₀ (46.5 ± 5.3 Pa.s) and F-1₃₀ (41.3 ± 19.1 Pa.s), which were also those displaying the lowest viscosity in aqueous solution (8.89 ± 0.62 and 10.40 ± 0.84 Pa.s, respectively). The highest η_0 value was noticed for the emulsion prepared with sample F-2₃₀ whose aqueous solutions also displayed the highest η_0 (17.40 ± 0.04 Pa.s) (Table 2.2.3).

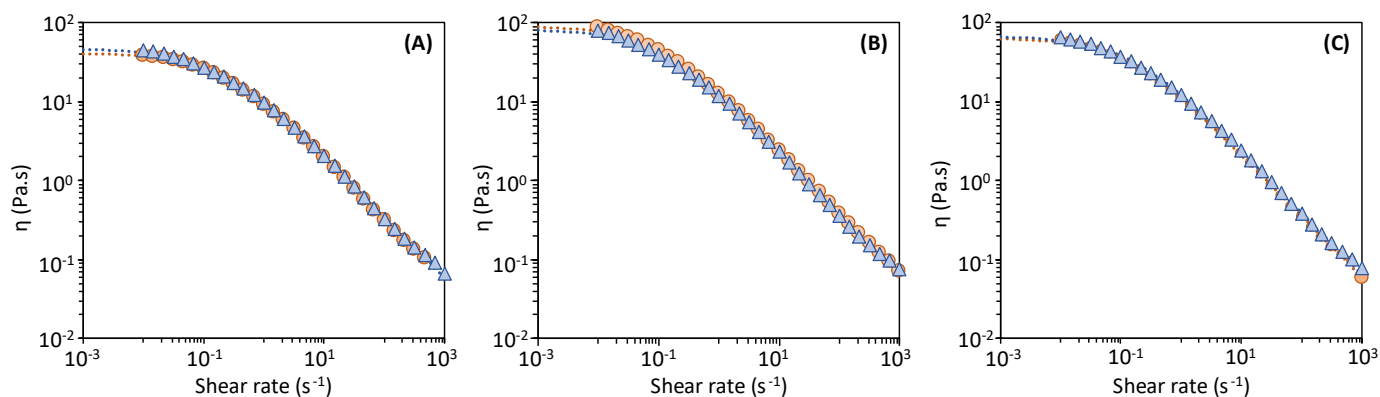


Figure 2.1.9. Flow curves for the prepared olive oil/FucoPol (1.0 wt.%) emulsions (2:3, o:w ratio): (A) Method 1, (B) Method 2, (C) Method 3; samples F-1₁₀₀ (triangle) and F-1₃₀ (circle). Dotted lines represent the Cross model. ($n = 3$).

2.1.4 Discussion

The results obtained in this study show that Method 2 (ultrafiltration with the 30 kDa membrane-sample F-2₃₀) reached the best performance in terms of operation time and water consumption, together with good FucoPol recovery (Table 2.1.5). Compared to Method 1 (diafiltration-ultrafiltration with a 100 kDa membrane-sample F-1₁₀₀) that was used in previous studies [52,126,128], there was a reduction of the extraction time from 105 ± 6 min to 66 ± 6 min and a reduction of the water consumption by 55%. This is translated in terms of energy, water, and time savings for the overall FucoPol production process that are of special relevance for the process scale up. Thus, the optimized downstream procedure contributes to render the process more sustainable from an economic and environmental point of view.

Table 2.1.5. Overall performance of the developed optimized procedure comprising ultrafiltration with a 30 kDa membrane, comparing to the previously used method (diafiltration-ultrafiltration with a 100 kDa membrane).

Parameter	Ultrafiltration 30 kDa Membrane
Process	
Water consumption	↓ 55%
Extraction time	↓ 37%
Product recovery	↑ 10%
FucoPol composition	Similar (↑ fucose content)
Contaminants	
Protein content	↓ 12%
Inorganic salts content	↓ 53%
Molecular mass distribution	
Mw	Unchanged
PI	Similar
Thermal properties	
Apparent viscosity	↑ 96%
Emulsion forming capacity	
E24	Unchanged (98%)
Emulsion viscosity	↑ 100%

On the other hand, the optimized procedure also yielded FucoPol with a higher purity degree, as shown by its lower protein and inorganic salts that were reduced by 12 and 53%, respectively (Table 2.1.5), compared to the previously used procedure (Method 1). Of special relevance is the fact that FucoPol molecular structure was not apparently affected by the conditions, as shown by its similar sugar and acyl groups composition, identical FT-IR spectrum, and similar molecular mass distribution. There was also no significant impact on FucoPol's thermal degradation profile, despite the slightly lower adsorbed water content and char yield.

Interestingly, the aqueous solutions prepared with FucoPol recovered by the optimized method displayed a higher apparent viscosity (Table 2.1.5). The ultrafiltration process may originate shearing stress which can enhance dissociation of polysaccharide aggregates, increasing the fraction of polymer chains truly dissolved in solution, resulting in viscosity augmentation [118,142]. For Methods 2 and 3, the module was operated solely/mostly in the ultrafiltration mode. This difference could explain the highest viscosity of samples F-2_i and F-3_i aqueous solutions compared to those recovered by Method 1. The highest TMP experienced in Method 2 (0.73 ± 0.05 and 0.67 ± 0.20 bar) and Method 3 (0.76 ± 0.11 and 0.71 ± 0.14 bar) compared to Method 1 (0.63 ± 0.13 and 0.62 ± 0.16 bar) (Table 2.1.1) might have promoted shearing stress experienced by the polysaccharide chains, thus contributing to their disentanglement. The ability of FucoPol to form emulsion with olive oil was not affected, with the emulsions prepared with the sample recovered with the optimized procedure displaying the same E24 value (98%). Moreover, the resulting emulsions were characterized by a significantly higher apparent viscosity, a feature of relevance for FucoPol's utilization in cosmetic, pharmaceutical or food products [108,109,111,113,114,146].

2.1.5 Conclusions

This study reports the optimized extraction procedure for recovery of FucoPol from the cultivation broth of *Enterobacter A47*, using an ultrafiltration method with a 30 kDa membrane in contrast to a diafiltration-ultrafiltration procedure with a 100 kDa membrane made from the same material chemistry. Compared to methods reported earlier, the optimized downstream procedure allowed water and time savings, concomitant with improved FucoPol recovery and purity. There was no significant impact on the biopolymer's physical-chemical performances, still improving the rheological properties of the purified biopolymer. The olive oil emulsions stabilized with the extracted FucoPol also disclosed higher viscosity, a characteristic of relevance for FucoPol's development into pharmaceutical and cosmetic applications.

These findings are also relevant for process implementation at large scale, considering the benefits in terms of energy, water and time saving, all factors contributing to making FucoPol production more cost-effective and environmentally sustainable. Additionally, the developed downstream procedure might be applied for the extraction of other EPS.

FucoPol Deacetylation and Desuccinylation

The results presented in this chapter are part of the following submitted paper:

Baptista, S.; Araújo, D.; Concórdio-Reis, P.; Marques, A.C.; Fortunato, E. Alves, V.D.; Freitas, F. Deacetylation and desuccinylation of the fucose-rich polysaccharide FucoPol: Impact on Biopolymer physical and chemical properties. Submitted to *Molecules*.

This page was intentionally left blank

Summary

FucoPol is an acylated polysaccharide with demonstrated valuable functional properties that include shear-thinning fluid behaviour, film-forming capacity, and emulsion forming and stabilizing capacity. In this study, different conditions (concentration, temperature, and time) for alkaline treatment were investigated to deacylate FucoPol. Complete deacetylation and desuccinylation was achieved with 0.02 M NaOH, at 60 °C for 15 minutes, with no significant impact on the biopolymer's sugar composition, pyruvate content and molecular mass distribution. FucoPol depyruvylation by acid hydrolysis was attempted, but it resulted in very low polymer recovery. The effect of ionic strength, pH, and temperature on the deacetylated/desuccinylated polysaccharide, d-FucoPol, was evaluated, as well as its emulsion and film-forming capacity. d-FucoPol aqueous solutions maintained the shear-thinning behaviour characteristic of FucoPol, but the apparent viscosity decreased significantly. Moreover, contrary to FucoPol, whose solutions were not affected by the media's ionic strength, d-FucoPol solutions had significantly higher apparent viscosity for higher ionic strength. On the other hand, d-FucoPol solutions were not affected by the pH in the range 3.6–11.5, while FucoPol had decreased viscosity for acidic pH values and for pH above 10.5. Although d-FucoPol displayed an EA for olive oil similar to that of FucoPol ($98 \pm 0\%$) for an oil-to-water ratio of 2:3, the emulsions were less viscous. d-FucoPol films were transparent and flexible, with higher Young's modulus (798 ± 152 MPa), stress at break (22.5 ± 2.5 MPa) and elongation at break ($9.3 \pm 0.7\%$) than FucoPol (458 ± 32 MPa, 15.5 ± 0.3 MPa and $8.1 \pm 1.0\%$, respectively). Given these findings, d-FucoPol arises as a promising novel polysaccharide, with distinctive properties that may render it useful for utilization as suspending or emulsifier agent, and as a barrier in coatings and packaging films.

2.2.1 Introduction

FucoPol is a water-soluble anionic heteropolysaccharide secreted by the Gram-negative bacterium *Enterobacter* A47 (DSM 23139) composed of fucose, glucose, galactose, glucuronic acid (2.0:1.9:0.9:0.5 molar ratio) with an intrinsic viscosity value of 8.9 dL/g [41,48,53]. Structurally, it comprises a main chain composed of a $\rightarrow 4$ - α -L-Fucp-(1 \rightarrow 4)- α -L-Fucp-(1 \rightarrow 3)- β -D-Glcp(1 \rightarrow trimer repeating unit, and a trimer branch α -D-4,6-pyruvyl-Galp-(1 \rightarrow 4)- β -D-GlcAp-(1 \rightarrow 3)- α -D-Galp(1 \rightarrow in the C-3 of the first fucose [49]. Glucuronic acid, pyruvate, and succinate confer FucoPol an anionic nature that promotes its interaction with charged molecules [50,53,147]. FucoPol's aqueous solutions present a shear-thinning behaviour, with viscoelastic properties comparable to those of guar gum and fucogel [41].

Interchain and/or intrachain interactions between polysaccharide molecules are greatly affected by their degree of substitution and the type of substituent groups [148,149]. The presence of organic acyl groups, such as acetyl, pyruvyl, succinyl, among others, are important for the polysaccharides' functional properties, including their viscoelastic properties, gelling ability, and bioactivity [148]. Moreover, acyl groups concentration influences polysaccharides' hydrophobicity affecting their structure in

solution. In fact, several studies have previously demonstrated the improvements achieved by of deacetylation of polysaccharides on several properties such as wound healing and antimicrobial activity [150]; rheological properties [151]; gelation properties [152]; and film forming [153]. Chemical removal of charged substituents causes the stabilisation of the helical structure, resulting in polymer stiffening [154]. Well studied deacylated polysaccharides include gellan and xanthan gums. For gellan gum, deacetylation induces the formation of harder gels with higher thermal stability [155] than acetylated biopolymer. It also improves the capacity to form hydrogels when mixed with cationic surfactants [148], and promotes cation-induced gelation in presence of Ca^{2+} in a physiological environment [156]. For xanthan gum, deacetylation increases the gel strength and viscoelasticity [157,158], as well as the formation of films with a higher water absorption behaviour when compared to the acetylated form [159]. Ridout et al. [154] studied the removal of succinyl and acetyl in succinoglycan polysaccharide. Succinyl removal improved pseudoplasticity of the aqueous solutions, while the increasing the biopolymer's order-disorder transition cooperativity. When acetyl removal was performed the order-disorder transition temperature decreased, whereas succinyl removal increased this physical property [154].

Deacetylation and desuccinylation can be achieved using chemical (e.g., alkaline treatments at high temperature and/or high pressure [160]), enzymatic [161] or physical (e.g., ultrasound) treatments [162]. Guetta et al. [163] obtained deacetylated Fucogel by alkaline conditions using 0.1 M NaOH for 30 min at 80 °C. For chitin deacetylation, Kjartansson et al. [162] used 12.5 M NaOH treatment for 4 h at 100 °C. Pinto et al. [164] used NaOH and KOH 0.01 M at 25 °C for 3 hours to obtain deacetylated xanthan gum.

This study focused on the development of a procedure for the removal of acetyl, succinyl and pyruvyl substituent groups from the FucoPol macromolecule. The removal of these substituent groups from FucoPol was not studied so far. Alkaline treatments with NaOH were designed and tested for FucoPol's deacetylation/desuccinylation, while acid treatment with hydrochloric and oxalic acids were attempted for pyruvate removal. The impact of the applied treatments on the polysaccharides' physical-chemical properties were evaluated, including the rheological properties, emulsifying behaviour, and film-forming capacity.

2.2.2 Materials and Methods

2.2.2.1 FucoPol production and extraction

FucoPol was produced and extracted from the cell-free supernatant by ultrafiltration procedure as previously described in Section 2, Chapter 1 (2.1.2.1 and 2.1.2.2).

2.2.2.2 Chemical deacylation/depyruvylation of FucoPol

FucoPol deacetylation and desuccinylation studies under alkaline conditions were based on the procedures described by Pinto et al. [164] and Lima et al. [165], by subjecting the polysaccharide to different NaOH concentrations (0.005, 0.01, 0.02 and 0.05 M), temperatures (40 and 60 °C) and reaction times (15, 30 and 60 minutes). Briefly, FucoPol samples (5 mg) were dissolving in deionized water (5 mL) and contacted with NaOH, under controlled temperature. After the treatment, the samples were cooled to room temperature and extensively dialysed using a 12 kDa MWCO membrane (ZelluTrans/Roth) against deionized water to eliminate the low molecular weight compounds resulting from the hydrolysis procedure and salts. Finally, the samples were freeze-dried (ScanVac CoolSafe™, LaboGene, Lillerød, Denmark), at -110 °C for 48 h.

Depyruvylation studies were undertaken on the deacetylated/desuccinylated FucoPol by its hydrolysis with hydrochloric or oxalic acids, following the procedures described by Pinto et al. [164] and Herasimenka et al. [166], respectively. Hydrolysis was achieved using FucoPol solution (1.0 wt.%) in hydrochloric acid (2.0 M) at 80 °C for 16 hours. The hydrolysis with oxalic acid (0.5 M) was performed using FucoPol solution (0.1 wt.%) at 100 °C for 2h. The samples were dialysed and freeze-dried as described above.

All assays were performed in duplicate.

2.2.2.3 Physical and chemical characterization

2.2.2.3.1 Composition

The monosaccharides profiles and acyl substituents groups of the deacetylated/desuccinylated FucoPol (herein named d-FucoPol), as well as the native FucoPol were determined as previously described in Section 2, Chapter 1 (2.1.2.3.1).

2.2.2.3.2 Fourier Transform Infrared analysis

Fourier Transform Infrared (FT-IR) spectroscopy was assessed as previously described in previous in Section 2, Chapter 1 (2.1.2.3.5).

2.2.2.3.3 Molecular mass distribution

The average molecular weight (M_w), molecular number (M_n), and polydispersity index ($PI = M_w/M_n$) were determined by Size Exclusion Chromatography (SEC). The samples were dissolved in deionized water (2–4 mg/mL) and injected in a size exclusion-high performance liquid chromatography

(SEC-HPLC) system (Knauer, Smartline system 1000, Germany) equipped with a Phenomenex Phenogel Linear LC Column (300 mm x 7.8 mm, Knauer) coupled to a refractive index detector (RI detector, Knauer Smartline 2300). The analysis was performed at 25 °C with LiNO₃ 0.1 M as eluent, at a flow rate of 0.6 mL/min and injection volume of 50 µL. The Mw was estimated after universal calibration with pullulans (≤ 600 kDa) [167].

2.2.2.3.4 Intrinsic viscosity

The intrinsic viscosity $[\eta]$ was determined by double extrapolation to zero concentration of the Huggins and Kraemer equations, as described by Freitas et al. [41]. Capillary viscosity measurements were performed on an automatic viscosity measuring unit AVS 450 (Schott-Gerate, Germany), with an Ubbelohde capillary viscometer (Ref. 53013/Ic, Schott-Gerate, Germany) immersed in a water bath at constant temperature (25 ± 0.5 °C).

2.2.2.3.5 Thermal properties

Thermogravimetric Analysis (TGA) was performed as described in Section 2, Chapter 1 (2.1.2.3.6).

2.2.2.4 Apparent viscosity and viscoelastic properties

Aqueous d-FucoPol solutions (0.75, 1.5, and 3.0 wt.%) were prepared in 0.1 M NaCl. For the 3.0 wt.% d-FucoPol solution, different pH values (3.6, 4.8, 6.2, 8.5, 11.5), temperatures (10, 25, 45, 65, and 80 °C), and ionic strength values (0.1, 0.5, 1.0, 2.0, and 3.0 M NaCl) were tested. The solutions' pH was adjusted by the addition of 0.01 M HCl or 0.01 M NaOH.

The apparent viscosity of the d-FucoPol aqueous solutions was determined at 25 °C (except for those meant for evaluating the effect of temperature), using a controlled stress rheometer (Haake Mars III–Thermo Scientific, Karlsruhe, Germany), with a UTC–Peltier system to control temperature, and a cone-plate sensor system (angle 2°, diameter 35 mm) and the shearing geometry covered with paraffin oil to prevent water loss [39]. The Cross-model equation was used to fit the flow curves obtained was determined as previously described in Section 2, Chapter 1 (2.1.2.4). Frequency sweep tests were performed with frequency ranging from 0.01 to 100 Hz with a constant strain of 1% that was well within the LVE, which was evaluated through preliminary amplitude sweep tests.

2.2.2.5 Emulsion forming and stabilizing capacity

The ability of d-FucoPol to stabilize emulsions was assessed by mixing 3 mL of a polymer aqueous solution (1.0 wt.%) with 2 mL olive oil (purchased from a local market) to provide a 2:3 (w/w). The emulsification method and the emulsification index after 24 hours (E24, %) were performed as described in Section 2, Chapter 1 (2.1.2.5). The rheological properties of the emulsion were determined as described above (section 2.2.2.4).

2.2.2.6 Characterization of the Emulsions

2.2.2.6.1 Type of emulsion

The method described by Kavitate et al. [168] was used to determine the type of emulsion. A droplet of the test emulsion was placed onto Whatman™ filter paper (0.2 μm, GE Healthcare Life Sciences, Munich, Germany) and its ability to disperse on the surface was evaluated.

2.2.2.6.2 Microscopic observation

The emulsions were stained with Nile Blue (a lipophilic dye), as adapted by Martins et al. [169]. Briefly, 10 μL of the emulsion were stained with 1% (v/v) Nile Blue A (Sigma-Aldrich, Darmstadt, Germany) and observed in a Zeiss Imager D2 epifluorescence microscope (Carl Zeiss, Oberkochen, Germany), with a magnification of 40x through ZEN lite software (Carl Zeiss, Oberkochen, Germany).

2.2.2.7 Film-forming capacity

2.2.2.7.1 Film preparation

d-FucoPol films were prepared following the procedure described by Freitas et al. [44]. Briefly, d-FucoPol solutions (1.5 wt.%) were prepared by dissolving the polymer in deionized water, under stirring for 12 hours, at room temperature. Then, glycerol (86–88 wt.%, Scharlau) was added as plasticizer (30 wt.%, on a dry basis). After removing air bubbles under vacuum, the solution was transferred to plastic Petri dishes (diameter of 6.5 cm) and dried at a temperature of 30 °C. The formed films were peeled from the dishes' surface and conditioned at a controlled relative humidity (RH) of 58%, at 22 °C, during 48 h.

2.2.2.7.2 Morphological characterization

The films' thickness was measured at three different points using a digital micrometer (Mitutoyo, UK). The films' morphology was observed by Scanning Electron Microscopy (SEM) using a SEM Hitachi TM 3030Plus Tabletop (Krefeld, Germany). The dry film was fixed on SEM stubs and coated with a thin layer of 15 nm Au/Pd. Samples observation was performed, in a secondary electron's observation mode, at their surface and cross-section with an acceleration voltage of 15 kV. The films' transparency was determined by measuring their transmittance at 600 nm (T₆₀₀), using a UV-Vis spectrophotometer (CamSpec M509T, Leeds, UK), and calculated using the equation [126]:

$$\text{Transparency} = \frac{-\log T_{600}}{X} \quad (2.2.1)$$

where X corresponds to the film's thickness (mm).

2.2.2.8 Mechanical properties

The mechanical properties of the films were assessed under tensile tests using a texture analyser TMS-Pro (Food Technology Corporation, Kent, UK) equipped with a 250 N load cell. The films were cut into rectangular-shaped strips (30 mm x 15 mm), attached to tensile grips A/TG, and stretched with a crosshead speed of 0.5 mm/s in tensile mode, until breaking. The films' stiffness was determined by the Young's modulus (MPa), calculated as the slope of the linear initial section of the stress-strain curve. The tensile strength at break was determined as the ratio of the maximum force to the films' initial cross-sectional area. The elongation at break (MPa) was determined as the ratio of the sample extension upon rupture by the initial gage length. Four replicas were analysed.

2.2.3 Results and Discussion

2.2.3.1 Optimization of the chemical deacylation/ depyruvylation conditions

FucoPol deacetylation and desuccinylation studies under alkaline conditions were performed using several NaOH concentrations, temperatures, and reaction times (Table 2.2.1) to define the ones leading to complete acetyl and succinyl groups' removal. The original FucoPol sample had succinyl and acetyl contents of 1.1 wt.% and 5.8 wt.%, respectively, which are within the values reported in previous studies (0.6–3.0 wt% and 3.5–6.8 wt%, respectively). As shown in Table 2.2.1, acetyl was more easily removed from the polymer's molecule as milder conditions achieved its complete removal. No acetate was detected in the samples treated with an alkali concentration of only 0.01 M, under 60 °C for 60 min, and at a lower temperature (40 °C) and shorter reaction time (15 min) for NaOH 0.02 M. As reported by Due et al. [152], the hydroxyl group performs a nucleophile attack in the electron-deficient carbonyl carbon of the acetyl group, resulting in the substitution of the acetyl group by a hydroxyl group. On the other hand, harsher conditions were required for complete succinyl removal, namely, higher NaOH concentration (0.02 M) and longer reaction time (≥ 30 min). Succinyl and pyruvyl have been reported to form strong intra-molecular hydrogen bonds, conferring higher stability to their ester linkages compared to acetyl groups [170], which might explain the faster removal of acetyl groups from FucoPol.

FucoPol depyruvylation was attempted by acid hydrolysis with oxalic acid and hydrochloride acid, following procedures described in the literature for pyruvate removal from xanthan gum [164,166]. However, all treatments in acidic media were accompanied by very low polymer recovery, which is probably inherent to the pyruvate branching position (2,3 linkage instead of 4,6 position which is more often encountered) [57,164].

Given these results, treatment with NaOH 0.02 M at 60 °C for 15 minutes was selected as the most suitable to reach complete deacetylation and desuccinylation, while saving on alkali usage and reaction time. The deacetylated and desuccinylated FucoPol was named d-FucoPol.

Table 2.2.1. Acyl groups (succinyl, acetyl and pyruvyl) contents of FucoPol sample subjected to alkaline treatment.

Acyls groups (wt.%)	NaOH (M)	40 °C			60 °C		
		15 (min)	30 (min)	60 (min)	15 (min)	30 (min)	60 (min)
Succinyl	0.005	0.70±0.02	0.67±0.02	0.62±0.01	0.65±0.08	0.64±0.02	0.47±0.01
	0.01	0.35±0.02	0.26±0.04	0.27±0.04	0.34±0.02	0.29±0.00	0.22±0.04
	0.02	0.19±0.00	-	-	-	-	-
	0.05	-	-	-	-	-	-
Acetyl	0.005	3.15±0.22	3.02±0.07	2.55±0.10	2.90±0.38	2.87±0.08	1.85±0.01
	0.01	1.41±0.15	1.16±0.06	0.61±0.10	1.05±0.17	0.44±0.05	-
	0.02	-	-	-	-	-	-
	0.05	-	-	-	-	-	-
Pyruvyl	0.005	3.61±0.35	3.58±0.04	3.580±0.5	3.96±0.27	4.05±0.29	4.01±0.27
	0.01	3.68±0.30	3.52±0.11	3.77±0.53	3.63±0.47	3.68±0.29	4.03±0.62
	0.02	3.63±0.05	3.30±0.00	3.50±0.22	3.54±0.21	4.00±0.12	3.99±0.55
	0.05	3.65±0.64	3.45±0.50	3.90±0.14	3.73±0.09	3.89±0.24	3.88±0.45

2.2.3.2 Physical and chemical characterization of the deacetylated/desuccinylated FucoPol

2.2.3.2.1 Sugar composition

The compositional analysis of d-FucoPol showed the alkaline deacetylation/desuccinylation treatment had no significant impact on the polysaccharide's monosaccharide structure, which remained identical to that of the original FucoPol sample. Fucose and galactose contents (37 and 27 mol%, respectively) remained essentially the same (36 and 28 mol%, respectively), while a slight increase of the glucose content was noticed for d-FucoPol (29 mol%, compared to 26 mol% for FucoPol). There was also a reduction of the content in glucuronic acid from 10 to 7 mol%. Deacetylation leads to the removal of acetyl protecting groups in glucuronic acid and to the formation of β -D-glucosiduronic acid, which could explain the slightly decrease of content of glucuronic acid detected after this chemical reaction [171]. The analysis showed a sugar content increase of approximately 8% from the polymer's dry weight, which is in agreement with the removal of the substituents (acetate and succinate).

2.2.3.2.2 Structural analysis

As shown in Figure 2.2.1, the FT-IR spectrum of d-FucoPol is similar to that reported in the literature for FucoPol [41,52,147], displaying peaks around 3283–2925 cm^{-1} attributed to O-H stretching of hydroxyls' vibrations and C-H stretching peak of CH_2 groups, around 970–1145 cm^{-1} related C-C and C-O stretching in the pyranoid ring and C-O-C stretching of glycosidic bonds, and at 1603 cm^{-1} associated with the bending vibration of O-H indicating bound water [147]. The main difference noticed for d-FucoPol is the absence of the peak at 1720 cm^{-1} (corresponding to the C=O stretching vibrations of carbonyls), and a noticeable peak intensity decrease at 1261 cm^{-1} (C-O-C vibrations) which are probably related to the removal of the acetyl e succinyl groups from the macromolecule [150,152,153,172].

Additionally, the peak appearing at 1403 cm^{-1} , which may be assigned to the asymmetric and symmetric stretching of carboxylates from glucuronic acid [147], had a decreased intensity compared to FucoPol spectrum that might be correlated with the observed decrease of the polymer's glucuronic content (from 10 to 7mol%).

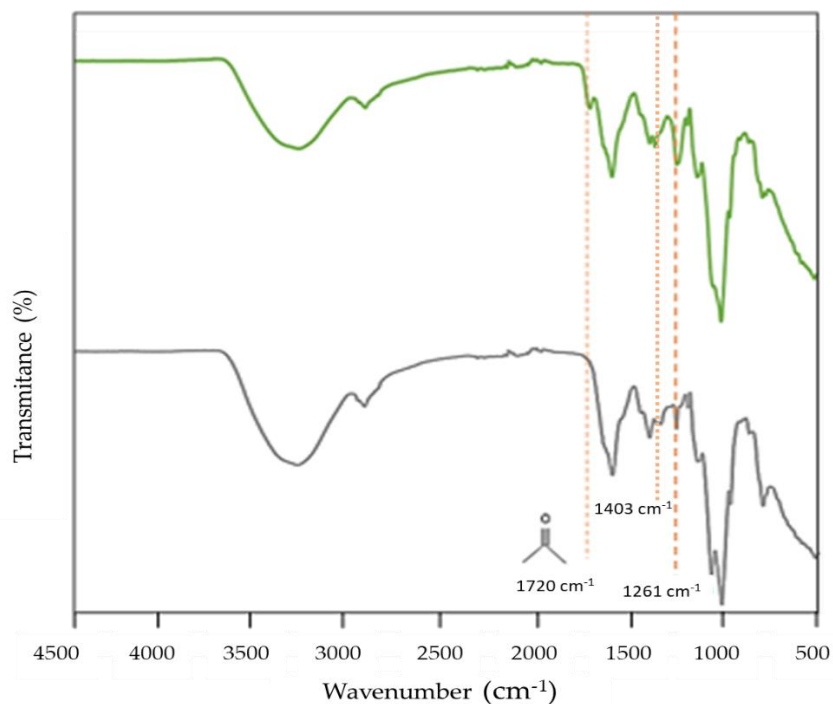


Figure 2.2.1. FT-IR spectra of FucoPol (green line) and d-FucoPol (gray line).

2.2.3.2.3 Molecular mass distribution

d-FucoPol showed an average M_w of 2.7×10^6 Da and a PI of 1.7, which are within the ranges reported in previous studies ($M_w = 1.7 \times 10^6 - 5.8 \times 10^6$ Da; PI = 1.3–1.9) [41,52,54,59,147]. Contrary to the results obtained by Wang et al. [173], where the deacetylation reduced the molecular weight of native xanthan gum (from 1.1×10^6 to 1.0×10^6 Da). The same was reported for succinoglycan where the removal process of acetyl and succinyl groups decrease the molecular weight from 1.2×10^6 to 1.1×10^6 Da [154]. These findings confirm that the applied alkaline treatments had no significant impact on the biopolymer's molecular mass distribution.

2.2.3.2.4 Thermal properties

FucoPol and d-FucoPol displayed similar TGA curves, with two degradation steps (Figure 2.2.2) [59,147]. In the first degradation step, occurring between 40 and around 150–160 °C, corresponded to similar weight losses were found for both samples (11–13%), which corresponded to the loss of water adsorbed to the polysaccharides due to their hygroscopic nature [147]. The second and main degradation step occurred between 196 and 320 °C, with weight losses of around 41% for both samples,

which can be attributed to the thermal depolymerization of the polysaccharides' chains and the dehydration of the saccharide rings [139]. The T_{deg} value was similar for both FucoPol (259 °C) and d-FucoPol (256 °C), thus confirming no significant differences between them. For higher temperatures, there was a gradual reduction of the samples' weight, resulting in char yields of 31–36% at 500 °C.

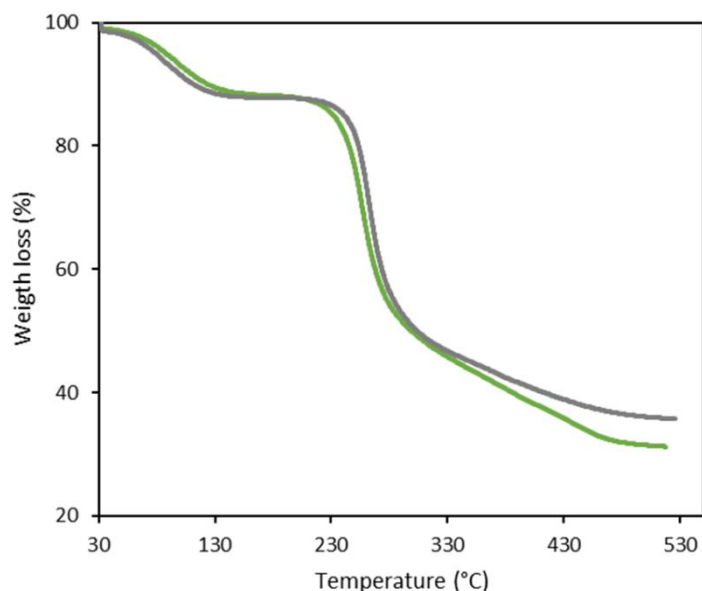


Figure 2.2.2. Thermogravimetric curves of FucoPol (green line) and d-FucoPol (gray line).

2.2.3.2.5 Intrinsic viscosity

The intrinsic viscosity, $[\eta]$, of d-FucoPol was 2.45 ± 0.33 dL/g. This value is lower than that previously reported for FucoPol (11.0 dL/g) [54]. This fact can be correlated to a considerable difference in their chain stiffness. Deacylated FucoPol may have a weaker chain stiffness than FucoPol, decreasing the hydrodynamic volume occupied by the polymer chains, resulting in a lower $[\eta]$ [174]. In addition, the removal of succinyl groups leads to a lower number on negative charges on the polyelectrolyte d-Fucopol chains, decreasing the intra-chain charge repulsion, with a positive effect on the decrease of chains hydrodynamic volume. Similar effect was reported by Wang et al. [173] for deacetylated xanthan that displayed an intrinsic viscosity of 43.3 dL/g, corresponding to a 42% decrease compared to native xanthan gum. A lower intrinsic viscosity can be an advantage if the intended application is conducive to absorption and diffusion *in vivo*, thus allowing enhanced biological activity [175].

2.2.3.3 Apparent viscosity and viscoelastic properties of the d-FucoPol solutions

2.2.3.3.1 Apparent viscosity

d-FucoPol's aqueous solutions displayed a shear-thinning behaviour (Figure 2.2.3), similar to that of FucoPol and typical of high molecular weight polysaccharides [140,147], for all three tested polymer concentrations (0.75, 1.5, and 3.0 wt.%). A clear increase of the apparent viscosity is observed

when increasing the polymer concentration tested. However, the thickening capacity of d-Fucopol was considerably lower than that of FucoPol (Figure 2.2.3). Indeed, the 1.5 wt.% d-FucoPol solution displayed a zero-shear viscosity of 1.61 ± 0.01 Pa.s, which is considerably lower than the value (17.40 ± 0.04 Pa.s) found for a 1.0 wt.% [147] and for 1.5 wt.% (64.78 ± 0.31 Pa.s) FucoPol solution (Table 2.2.2). These results suggest that the acetyl and/or succinyl groups were probably responsible for promoting intermolecular interactions in FucoPol solutions, contributing to its higher apparent viscosity [148], thus, their removal resulted in the observed lower viscosity. For both polymer types, higher η_0 values are associated with higher estimated t values, representing higher relaxation times. The highest η_0 value was observed for the 3.0 wt.% d-FucoPol solution (29.5 ± 0.09 Pa.s) (Table 2.2.2), which was chosen for the subsequent tests for evaluating the effect of the ionic strength, pH, and temperature on d-FucoPol's viscoelastic properties.

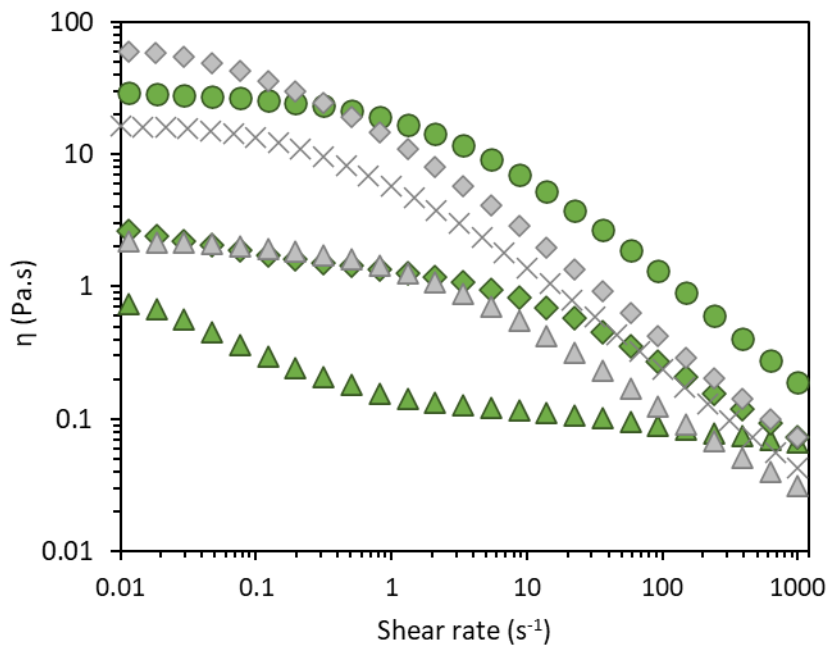


Figure 2.2.3. Flow curves of d-FucoPol (green) and FucoPol (gray) aqueous solutions: 0.75 wt.% (triangles), 1.0 wt.% (asterisk) 1.5 wt.% (diamonds), and 3.0 wt.% (circles).

Table 2.2.2. Cross model parameters estimated for d-FucoPol concentration (wt.%). η_0 —apparent viscosity of the first Newtonian plateau (Pa.s); τ —relaxation time (s); m —dimensionless constant. Data are shown as the average \pm standard deviation (SD) ($n = 3$). *Cross model is not appropriate to describe experimental data.

Sample	Concentration (wt.%)	Cross model parameters			Reference
		η_0 (Pa.s)	τ (s)	m	
	0.75	-*	-*	-*	
d-FucoPol	1.5	1.61 \pm 0.01	0.11 \pm 0.00	0.67 \pm 0.01	This study
	3.0	29.5 \pm 0.09	0.55 \pm 0.01	0.75 \pm 0.01	
FucoPol	0.75	2.20 \pm 0.01	0.51 \pm 0.00	0.72 \pm 0.00	This study
	1.0	17.40 \pm 0.04	1.68 \pm 0.21	0.78 \pm 0.00	[147]
	1.5	64.78 \pm 0.31	5.66 \pm 0.15	0.83 \pm 0.02	This study

2.2.3.3.2 Effect of ionic strength

As shown in Figure 2.2.4a, although the d-FucoPol solutions kept a shear-thinning behaviour for all tested ionic strength values (0.1, 0.5, 1.0, 2.0 and 3.0 M NaCl), increasing the NaCl concentration resulted in higher η_0 , which increased from 26.1 \pm 0.27 Pa.s for the 0.1 M solution to 86.9 \pm 0.80 Pa.s for the 3.0 M solution, concomitant with higher τ (from 0.62 \pm 0.02 to 1.01 \pm 0.04 s) and m (from 0.72 \pm 0.01 to 0.76 \pm 0.01). These results show that the d-FucoPol solutions' viscosity was highly impacted by the ionic strength. This behaviour may result from polymer aggregation probably induced by the higher salinity of the solution [176]. This behaviour of d-FucoPol contrasts with that of native FucoPol whose viscosity was practically unaffected by the solution's ionic strength within the range from 0.05 to 0.50 M NaCl [50].

For all tested ionic strength values, at low frequencies, the loss modulus (G'') was higher than the storage modulus (G') (Figure 2.2.5A), denoting a liquid-like behaviour for the biopolymer solution [147], with a crossover occurring at 1.0 Hz, except for the 3.0 M solution, in which a slight decrease was noticed (0.6 Hz) (Table 2.2.3). Both G' and G'' values increased for higher ionic strength (Table 2.2.3), with also increasing gaps between the moduli envisage stronger intermolecular interactions occurring for higher ionic strength values, being responsible for the reinforcement of the entangled polymer system [177].

2.2.3.3.3 Effect of pH

In contrast with FucoPol solutions, for which the apparent viscosity was reduced for high (pH \geq 10.5) and low pH (pH \leq 3) values [50], d-FucoPol solutions' viscosity was not impacted by the solution's pH within the tested range (3.6–11.5) (Figure 2.2.4b), with all solutions presenting similar η_0 (40.1–44.7 Pa.s), τ (0.71–0.80s) and m (0.73–0.78) values (Table 2.2.3). Possibly due to succinyl group elimination, the polymer chains became less susceptible to pH changes, presenting an interesting opposite behaviour to that of FucoPol whose solutions had decreased viscosity upon increasing the pH [50].

For all pH values tested, at low frequencies, the loss modulus (G'') was higher than the storage modulus (G') (Figure 2.2.5B), implying a liquid-like behaviour for the biopolymer solution [147], but

the values of both moduli and their crossover (1.0 Hz) remained unchanged for the entire range of pH values tested (Table 2.2.3). The deacetylation apparently confers pH resistance to FucoPol aqueous solutions, which can be advantageous for some applications, such as, for example, drug delivery [178,179].

Table 2.2.3. Cross model parameters estimated for d-FucoPol aqueous solutions (3.0 wt.%) tested at different ionic strength, pH, and temperatures. η_0 —apparent viscosity of the first Newtonian plateau; τ —relaxation time; m —dimensionless constant. Data are shown as the average \pm standard deviation (SD) ($n = 3$). Viscoelastic parameters estimated for d-FucoPol (3.0 wt.%). G' —storage/elastic modulus and G'' —loss/viscous modulus at $f=0.1$ Hz.

Parameter	Cross model			Viscoelastic Parameters		
	η_0 (Pa.s)	τ (s)	m	G' (Pa)	G'' (Pa)	Crossover (Hz)
Ionic strength (M) (pH=6.2, 25 °C)						
0.1	36.2 \pm 0.12	0.54 \pm 0.01	0.74 \pm 0.00	4.05	11.3	1.0
0.5	40.1 \pm 0.16	0.51 \pm 0.01	0.78 \pm 0.01	5.40	14.3	1.0
1.0	47.9 \pm 0.93	0.91 \pm 0.06	0.73 \pm 0.01	7.40	18.1	1.0
2.0	65.6 \pm 0.56	0.92 \pm 0.03	0.75 \pm 0.01	10.9	23.7	1.0
3.0	86.9 \pm 0.80	1.01 \pm 0.04	0.76 \pm 0.01	15.5	29.5	0.6
pH (0.1 M, 25 °C)						
3.6	40.4 \pm 0.44	0.71 \pm 0.03	0.74 \pm 0.01	7.15	16.6	1.0
4.8	44.7 \pm 0.47	0.80 \pm 0.03	0.73 \pm 0.01	7.65	17.8	1.0
6.2	40.1 \pm 0.16	0.71 \pm 0.01	0.78 \pm 0.00	5.40	14.3	1.0
8.5	41.0 \pm 0.45	0.75 \pm 0.03	0.75 \pm 0.03	6.98	17.4	1.0
11.5	40.6 \pm 0.33	0.74 \pm 0.02	0.74 \pm 0.01	6.70	17.1	1.0
Temperature (°C) (0.1 M, pH=6.2)						
10	79.1 \pm 0.46	1.26 \pm 0.02	0.76 \pm 0.01	13.5	25.1	0.6
25	36.2 \pm 0.12	0.54 \pm 0.01	0.77 \pm 0.00	4.05	11.3	1.0
45	13.0 \pm 0.05	0.21 \pm 0.06	0.76 \pm 0.01	1.31	6.31	3.2
65	5.83 \pm 0.05	0.11 \pm 0.01	0.69 \pm 0.02	0.22	2.42	10
80	2.66 \pm 0.04	0.06 \pm 0.01	0.67 \pm 0.04	0.12	1.39	10

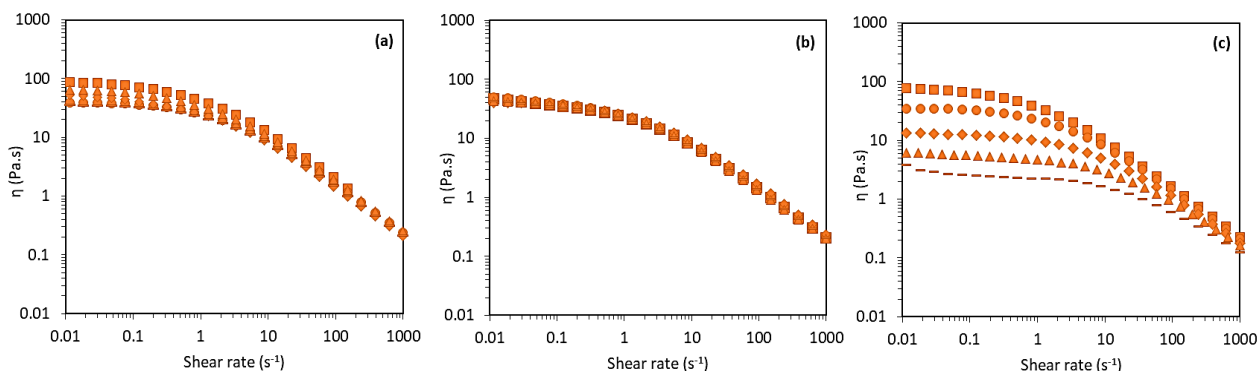


Figure 2.2.4. Flow curves of d-FucoPol aqueous solutions. (a) Effect of ionic strength: 0.1 M (dashed line), 0.5 M (circles), 1.0 M (diamonds), 2.0 M (triangles), and 3.0 M (squares). (b) Effect of pH: 3.6 (triangles), 4.8 (squares), 6.2 (circles), 8.5 (diamonds), and 11.5 (dashed line). (c) Effect of temperature: 10 °C (squares), 25 °C (circles), 45 °C (diamonds), 65 °C (triangles), and 80 °C (dashed line).

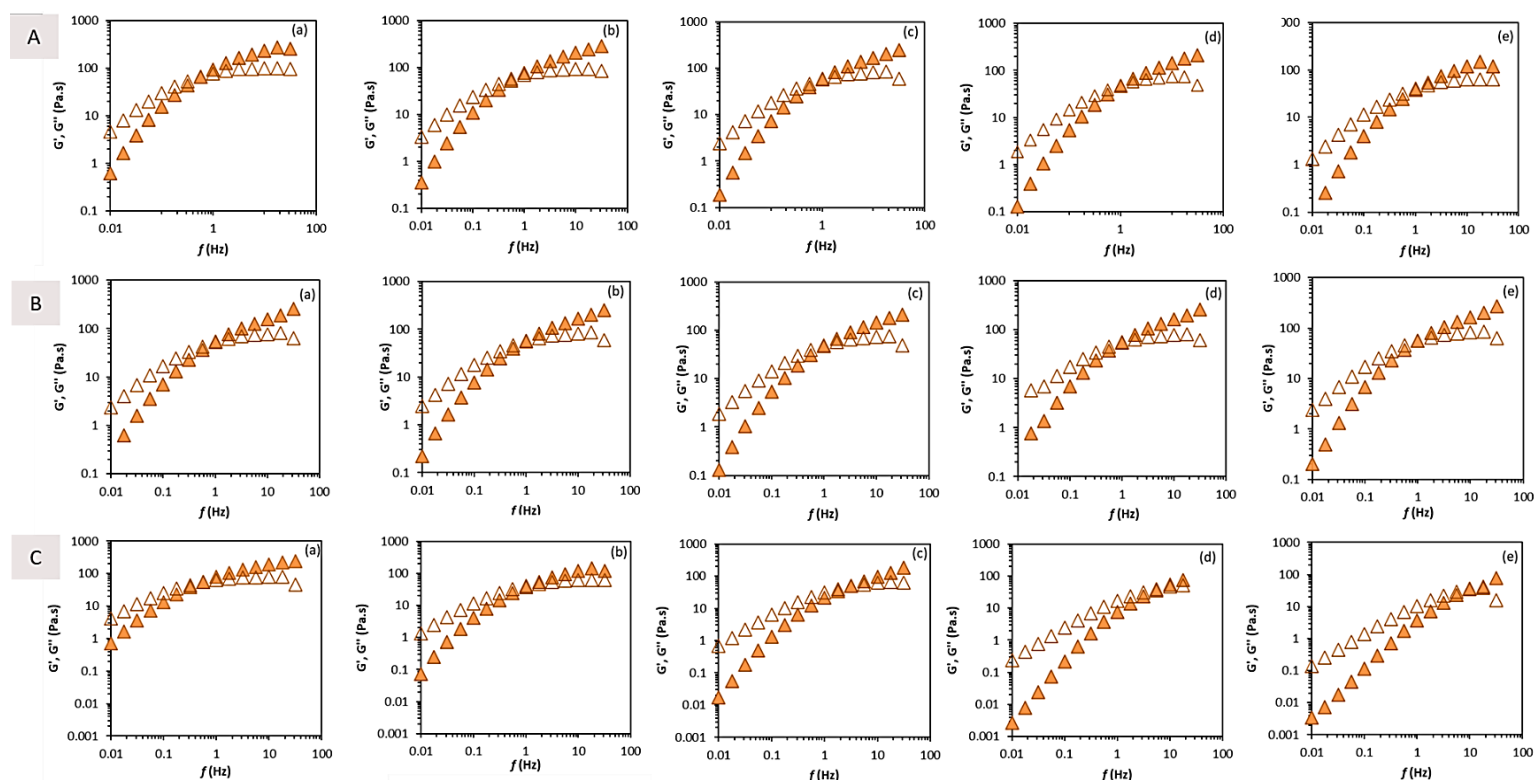


Figure 2.2.5. Mechanical spectra for d-FucoPol. **A**: ionic strength (NaCl) effect : (a) 3.0 M, (b) 2.0 M, (c) 1.0 M, (d) 0.1 M, (e) 0.5 M; **B**: pH: (a) 3.6, (b) 4.8, (c) 6.2, (d) 8.5, (e) 11.5; **C**: temperature effect: (a) 10 °C, (b) 25 °C, (c) 45 °C, (d) 65 °C, (e) 80 °C. Elastic G' (close) and viscous G'' (open) moduli.

2.2.3.3.4 Effect of temperature

Similarly to FucoPol [54], increasing the temperature lead to the reduction of d-FucoPol's solutions apparent viscosity, despite maintaining their shear-thinning behaviour (Figure 2.2.4c). As shown

on Table 2.2.3, the η_0 decreased from 79.1 ± 0.46 to 2.66 ± 0.04 Pa.s, as the temperature increased from 10 to 80 °C. This effect was previously described by several authors, showing that high temperatures do not promote interactions between polymer molecules, which lowered the reported viscosity values [180–182]. In fact, temperature increase enhances molecular motion and reduces the intermolecular entanglements, thus, resulting in a reduction of the solution's apparent viscosity [181]. It is notorious in Figure 2.2.4c that the shear rate corresponding to the transition from Newtonian to shear-thinning behaviour moves to higher values as the temperature increases, which means that for higher temperatures the formation of new interactions is faster. As expected, η_0 and τ decreased with increasing temperatures. The relaxation time (τ) decreased from 1.26 ± 0.02 to 0.06 ± 0.01 as the temperature increased from 10 to 80 °C. This fact indicates that less time is needed to form new interactions between polymer molecules at higher temperatures. Consequently, the transition from the Newtonian plateau to the shear-thinning regime is less evident and moves to higher shear rate values [54].

As expected, the $G'' > G'$ at low frequencies, indicating a liquid-like behaviour (Table 2.2.3; Figure 2.2.5C). Moreover, the dynamic crossover, after which the elastic contribution is predominant, occurs at increasingly higher values as the temperature increases. At low temperatures (10 and 25 °C), the crossover occurred at lower frequencies (0.6-1.0 Hz), indicating a more entangled system storing most of the energy received [50,54]. However, at higher temperatures (65 and 80 °C) the crossover was perceived at 10 Hz (Table 2.2.3; Figure 2.2.5-C(d-e)), showing a much lower number of polymer interactions needing a higher frequency energy input to notice a larger amount of energy stored compared to that dissipated [177].

2.2.3.4 Emulsion forming and stabilizing capacity

The ability of d-FucoPol to form and stabilize emulsions was assessed and compared with that of FucoPol which has been reported as a good emulsifier against several oils [41,44,147]. Emulsions were prepared by mixing d-FucoPol aqueous solution (1.0 wt.%) with olive oil as the test hydrophobic compound, at an O/W weight ratio of 2:3. The results (Table 2.2.4) show that d-FucoPol had identical emulsifying ability (E24 = 98%) as FucoPol (E24 = 81–98%) [147,183], under similar conditions. The microscopic observation (Figure 2.2.6a) of the emulsion displayed dispersed oil droplets in the aqueous phase, a characteristic of oil-in-water (O/W) emulsions [184,185]. Additionally, the emulsions' droplets rapidly dispersed in the filter paper (Figure 2.2.6b) wetting test, thus confirming its O/W nature [168,186,187].

Section 2. Chapter 2. FucoPol Deacetylation and Desuccinylation

Table 2.2.4. Emulsification index (E24) and Cross model parameters estimated for the emulsions prepared with the deacetylated FucoPol and olive oil, at an oil/water (O/W) weight ratio of 3:2: η_0 —apparent viscosity of the first Newtonian plateau (Pa. s); τ —relaxation time (s); m —dimensionless constant.

Sample	E24 (%)	Cross model parameters			Reference
		η_0 (Pa.s)	τ (s)	m	
d-FucoPol	98±0	13.9±2.4	1.64±0.13	0.74±0.00	This study
FucoPol (*)	81-98	46.5±5.3	-	-	[147,183]

$$RE = \sum_{i=1}^n (|x_{eI-,i} - x_{calc,i}|/x_{exp})/n \text{ is between } 0.011 \text{ and } 0.019.$$

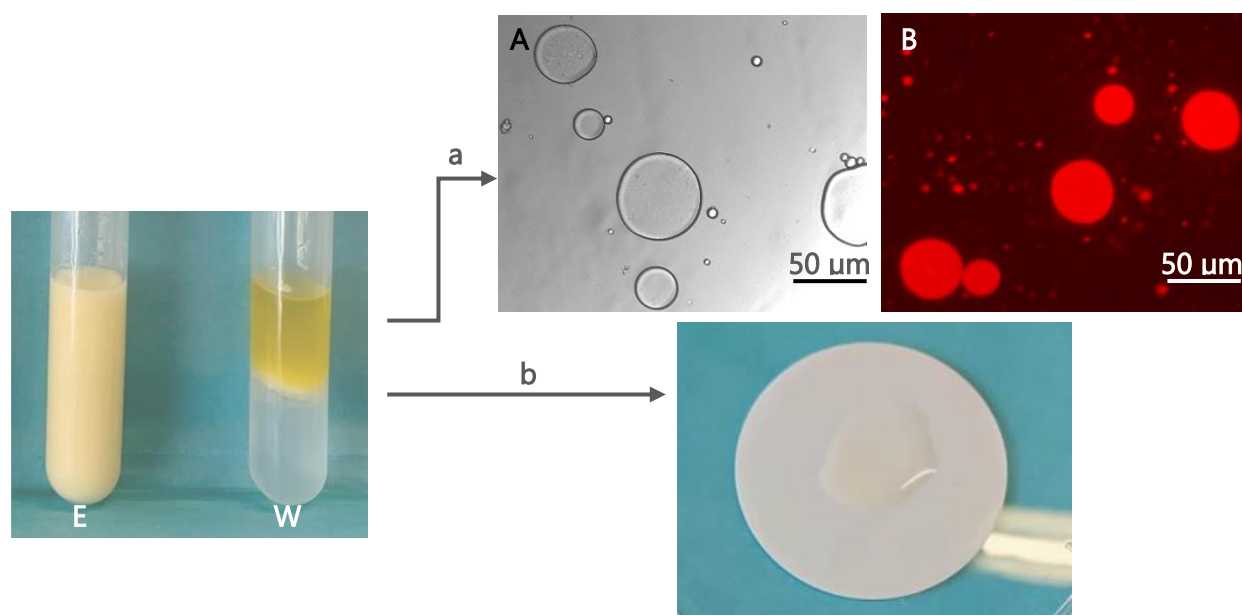


Figure 2.2.6. (a) Optical microscopic (40x) images of olive oil/d-FucoPol emulsion (E) (O/W weight ratio of 2:3); contrast phase and fluorescence after Nile Blue A staining (A, B, respectively). (b) Filter paper wetting test for emulsion type determination. (W)-blank sample, oil/water; and film obtained with deacetylated form of FucoPol.

As shown in Figure 2.2.7a, the emulsion stabilized by d-FucoPol exhibited shear-thinning flow behaviour characteristic of oil/FucoPol emulsions [50,147,183]. This flow behaviour is a common attribute of emulsions, in which the individual droplets and/or aggregated droplet clusters are deformed and disturbed by imposed forces at higher shear rates, leading to a reduction in both flow resistance and viscosity [188]. The experimental results were fitted to the Cross model and the resulting parameters are given in Table 2.2.4. The η_0 value observed for d-FucoPol emulsion (13.92 ± 2.36 Pa.s) was lower than that of FucoPol emulsion (46.5 ± 5.3 Pa.s) (Table 2.2.4), thus suggesting that the FucoPol's acetyl and succinyl substituents are relevant for the emulsion to maintain a high apparent viscosity, as previously reported for chitin and for the polysaccharide from *Millettia speciosa* Champ [151,189]. In fact, the

presence of acetyl groups is known to contribute to the reduction of interfacial tension and the increase of the rate of molecules' adsorption onto the interface, which leads to the expeditious formation of smaller droplets [188]. This alteration in the viscosity of the interdroplet aqueous solution may be the main cause of variation in the emulsion's viscosity [190].

Nevertheless, the d-FucoPol (1.0 wt.%) stabilized emulsion still displayed a significantly higher viscosity (13.92 ± 2.36 Pa.s) than the 1.5 wt.% polymer's aqueous solution (1.61 ± 0.01 Pa.s) (Table 2.2.3). This fact is frequently caused by the formation of a network composed of polymer chains and oil droplets, leading to a higher resistance to flow under steady shear [145]. The same was observed for emulsions stabilized with the native FucoPol [147].

Interestingly, the d-FucoPol stabilized emulsion presented G' higher than G'' across the whole frequency range (0.01–10 Hz) (Figure 7b) and did not display any crossover, meaning that the oil/deacetylated polymer emulsions displayed a distinct gel-like behaviour [191,192]. Gel-like emulsions have been shown to be suitable for cosmetic applications because this elastic mechanical property favours the emulsion stability over long storage periods. Moreover, this structure was demonstrated to improve moisturizing properties in emulsions with shear-thinning behaviour [193]. This observation can be related to the formation of a three-dimensional network, supported by the development of an entangled network between absorbed and non-absorbed biopolymer molecules which impacts the hydrocolloid properties of the emulsion [191,192,194]. This behaviour was not observed for the emulsions prepared with FucoPol in its native form [183] that presented a liquid-like behaviour, where $G'' > G'$, for frequencies of 0.02–0.6 Hz (Figure 2.2.7b).

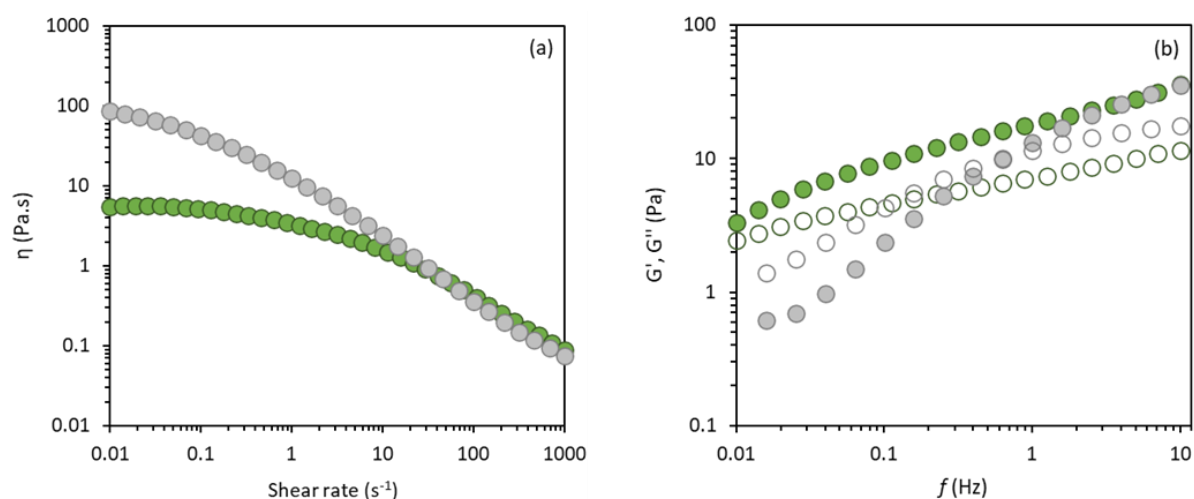


Figure 2.2.7. Rheological profile analysis of olive oil/d-FucoPol emulsion (green) and olive oil/FucoPol emulsion (gray) (O/W weight ratio of 2:3): (a) Flow curves; (b) Mechanical spectra: Elastic G' (closed) and viscous G'' (open) moduli.

2.2.3.5 Film-forming capacity

2.2.3.5.1 Morphological Characterization

d-FucoPol formed slightly opaque flexible films with a brownish tone (Figure 2.2.8a) and a thickness of $45 \pm 12 \mu\text{m}$ (Figure 2.2.8c). The films' transparency was 5.16 ± 1.09 (Table 2.2.5), a value higher than that reported for native FucoPol films (3.67) [126], thus indicating that the deacetylation and desuccinylation of the polysaccharide slightly increased its film opacity [195]. Transparency is important in packaging applications, providing see through properties and preventing light transmission [196,197], and in wound dressings to accurately monitor wound healing [198]. The films' complete solubilization when placed in water indicated the inexistence of cross-linking reactions [126]. As shown by the SEM images, the films were compact (Figure 2.2.8c), with a smooth surface (Figure 2.2.8b). Regarding FucoPol morphology, the study of Ferreira et al. [125] revealed that FucoPol was constituted by dense and irregular structure.

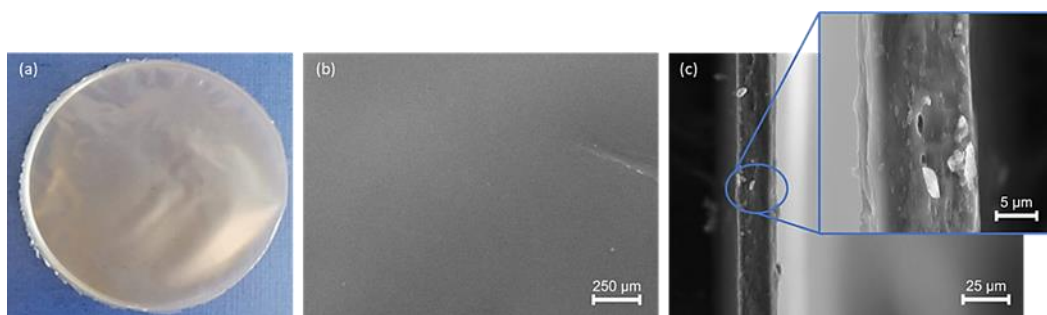


Figure 2.2.8. Film prepared with d-FucoPol (a) and its observation by SEM: surface (b) and cross-section (c) images.

2.2.3.5.2 Mechanical Properties

d-FucoPol films showed a higher mechanical resistance (Table 2.2.5) compared to the film prepared with the native FucoPol, illustrated by the higher Young's modulus ($798 \pm 152 \text{ MPa}$), concomitant with a higher stress at break ($22.46 \pm 2.54 \text{ MPa}$) and higher elongation at break ($9.27 \pm 0.66\%$) [44]. According to Jin et al. [199], deacylation promotes film's strength and cohesiveness, which gives an indication of film's stiffness. In terms of polysaccharide films' mechanical properties, these are heavily determined by three factors: the intrinsic characteristics of the chosen biopolymer; the presence of additives (plasticizers, cross-linking agents, film formation promoters); and the polymeric matrix water content present during the mechanical measurements [126,200]. For these reasons, the comparison of the films' mechanical properties obtained in different investigations is challenging due to the subjective nature of reported results which are usually obtained under specific conditions.

Section 2. Chapter 2. FucoPol Deacetylation and Desuccinylation

Table 2.2.5. Mechanical parameters, and transparency of the films prepared with d-FucoPol and FucoPol, and other biopolymers. Data are shown as the average \pm standard deviation (SD) (n = 4).

Sample	Mechanical parameters			Transparency	References
	Young modulus (MPa)	Stress at break (MPa)	Elongation at break (%)		
d-FucoPol	798 \pm 152	22.5 \pm 2.5	9.3 \pm 0.7	5.16 \pm 1.09	This study
FucoPol	458 \pm 32	15.5 \pm 0.3	8.1 \pm 1.0	3.67 \pm 0.57	[44,126]
GalactoPol	1738 \pm 114	51.0 \pm 3.0	9.5 \pm 3.9	-	[201]
Chitosan	21.8 \pm 4.06	8.90 \pm 1.6	38.5 \pm 5.2	-	[202]

2.2.4 Conclusions

Acetyl and succinyl substituent groups were removed from FucoPol's molecule by an alkaline treatment under mild conditions of temperature and alkali concentration. Although the deacetylated/desuccinyated polysaccharide, d-FucoPol, maintained the same sugar composition and molecular mass distribution as the native FucoPol, there was a significant reduction of d-FucoPol aqueous solutions' apparent viscosity, which was also significantly affected by the ionic strength of the solution and the temperature. Nevertheless, the solutions' viscosity was not impacted by the pH, contrarily to native FucoPol solutions. d-FucoPol kept the ability to form and stabilize emulsions, although the resulting emulsions had lower apparent viscosity. Additionally, the film-forming capacity of the FucoPol was also kept, with higher mechanical resistance. Given these features, d-FucoPol presents itself as a promising FucoPol derivative with distinctive properties that render it value for several applications, including packaging, cosmetics, and in other areas as suspending, thickening or emulsifier agent.

3. DEVELOPMENT AND CHARACTERIZATION OF FUCOPOL COSMETIC FORMULATIONS

This page was intentionally left blank

CHAPTER 1

Assessment of FucoPol Emulsifying Capacity using different Natural Oils

The results presented in this chapter are part of the following published paper:

Baptista, S.; Pereira, J.R.; Gil, C.; Torres, C.A.V.; Reis, M.A.M.; Freitas, F. Development of Olive Oil and α -Tocopherol Containing Emulsions Stabilized by FucoPol: Rheological and Textural Analyses. *Polymers* (Basel) 2022, 14, 1–17.

This page was intentionally left blank

Summary

Biobased raw materials like natural polysaccharides are increasingly sought by the cosmetic industry for their valuable properties. Such biodegradable and usually non-cytotoxic biopolymers are commonly used in skin-care products as rheological modifiers, bioemulsifiers and/or bioactive ingredients. FucoPol is a natural polysaccharide with reported biocompatibility, emulsion-forming and stabilizing capacity, shear-thinning behaviour, and bioactivity (e.g., antioxidant capacity, wound healing ability) that potentiate its utilization in skin-care products. In this chapter, olive oil and α -tocopherol containing emulsions were stabilized with FucoPol. Although the presence of α -tocopherol negatively impacted the emulsions' stability, it increased their emulsification index (EI). Moreover, FucoPol outperformed the commercial emulsifier Sepigel® 305, under the tested conditions, with higher EI and higher stability under storage for 30 days. The formulation of FucoPol-based emulsions with olive oil and α -tocopherol was studied by Response Surface Methodology (RSM) that allowed the definition of the ingredients' content to attain high emulsification. The RSM model established that α -tocopherol concentration had no significant impact on the EI within the tested ranges, with optimal emulsification for FucoPol concentration in the range 0.8–1.3 wt.% and olive oil contents of 20–30 wt.%. Formulations with 25 wt.% olive oil and either 0.5 or 2.0 wt.% α -tocopherol were emulsified with 1.0 wt.% or 0.7 wt.% FucoPol, respectively, resulting in oil-in-water (O/W) emulsions. The emulsions had similar shear-thinning behaviour, but the formulation with higher FucoPol content displayed higher apparent viscosity, higher consistency, as well as higher firmness, adhesiveness, and cohesiveness, but lower spreadability. These findings show FucoPol's high performance as an emulsifier for olive oil/ α -tocopherol, which are supported by an effective impact on the physicochemical and structural characteristics of the emulsions. Hence, this natural polysaccharide is a potential alternative to other emulsifiers.

3.1.1 Introduction

The cosmetics industry's interest in moving towards sustainability has significantly increased the incorporation of natural polymers into cosmetic formulations. Among those, many polysaccharides have properties similar to non-biodegradable synthetic polymers, which makes them environmentally friendly alternative raw materials [203,204]. Specifically, bacterial polysaccharides can be used in formulations as moisturizing agents, thickeners, stabilizers, and texturizers, acting as a biocompatible and biodegradable component that protect and maintain the skin and improves the formulations efficacy [109,204]. Emulsions, usually used in the cosmetic, pharmaceutical, and food industries, are the most common type of skincare products due to their appealing feeling on the skin and ease of application [109,205]. Oil in water (O/W) emulsions are usually used in personal care products, which rely on the utilization of hydrophilic polymers as thickeners, rheology modifiers, emulsion stabilizers, emulsifiers, and moisturizers [205–207].

FucoPol properties have been widely reported and include the ability to form viscous solutions with shear-thinning fluid behaviour [50], emulsion forming and stabilizing capacity [41,147], and

bioactivity (antioxidant capacity [49] , wound healing ability [52] and photoprotection [58]), which make it a very interesting polysaccharide for biotechnological applications in the field of cosmetics [4,109].

The design process of cosmetic products encompasses the characterization of the biotechnological properties, the compatibility evaluation, and adequate utilization ratios of new raw materials, which require reproducible, simple, and fast instrumental methods to compare results with benchmark products in the market [204,205]. For instance, rheology and texture analysis has been demonstrated to be suitable tools for the screening procedure of raw materials to predict their contribution in the final formulation [203].

Response surface methodology (RSM) is a statistical method suitable to study the interactions between several factors that might influence the desired product. The RSM approach is based on modelling the relationship between input parameters and their response, providing the desirable conditions [208] to optimize complex processes. Compared to other methods, RSM has been reported to allow a more efficient and easier arrangement and interpretation of experiments [209,210]. By applying an RSM technique the number of experimental investigations required to assess multiple variables and their interactions is significantly reduced. Generally, an empirical central composite design (CCD) is used as a subgroup of surface response methods, consisting of three groups of design points (factorial, axial, and centre points) to fit a second-order polynomial model by a least-squares technique [208,211,212].

The objective of this study was to develop emulsions using the bacterial heteropolysaccharide FucoPol as an emulsifying agent, assessing the emulsions' rheological and textural properties. For that purpose, a preliminary assessment of the emulsion forming and stabilizing capacity of FucoPol for four hydrophobic compounds, at different oil/water (O/W) weight ratios, was conducted. Then, the selected hydrophobic compound (olive oil) was used to prepare emulsions with α -tocopherol. RSM was used to define the optimal concentration ranges for FucoPol, olive oil, and α -tocopherol. The optimized FucoPol-based emulsions were characterized in terms of their rheological and textural properties.

3.1.2 Materials and Methods

3.1.2.1 Materials

Castor, paraffin, almond, and olive oils were purchased from a local market. Sepigel® 305 was obtained from SEPPIC (Courbevoie, France). α -tocopherol (vitamin E) was acquired from Sigma-Aldrich (Munich, Germany). FucoPol was produced by the bioreactor cultivation and extracted from the broth by ultrafiltration according to the procedure previously described in Section 2, Chapter 1 (2.1.2.1 and 2.1.2.2). FucoPol was composed of fucose (36 mol%), glucose (33 mol%), galactose (26 mol%), and glucuronic acid (5 mol%), with a total acyl groups content of 11.1 wt.%. The sample had protein and inorganic salts contents of 13 wt.% and 7.2 wt.%, respectively.

3.1.2.2 Determination of surface-active properties

FucoPol was dissolved in MilliQ water at concentrations ranging from 0.1 to 20 g/L, and the surface tension of the solutions was determined by the drop pendant method [21] using a Tensiometer (Kruss, Advance, Hamburg, Germany), at room temperature. The critical micelle concentration (CMC) was determined by plotting the surface tension as a function of FucoPol concentration and extrapolating the point where the slope of the curve abruptly changes. The results were expressed as the mean of three solution drops \pm standard deviation.

3.1.2.3 Emulsions' preparation

The emulsions were prepared as described in Section 2, Chapter 1 (2.1.2.5), using castor oil, paraffin oil, almond oil, olive oil as the oil phases, and a FucoPol solution (1.0 or 0.5 wt.%) as the aqueous phase, at O/W weight ratios of 3:2 and 2:3. The emulsification index (EI, %) and the emulsification stability (ES, %) were determined by the following equations [168]:

$$EI = \frac{h_e}{h_T} \times 100 \quad (3.1.1)$$

$$ES = \frac{\text{Final EI}}{\text{Initial EI}} \times 100 \quad (3.1.2)$$

where h_e (mm) is the height of the emulsion layer and h_T (mm) is the overall height of the mixture after emulsification. Initial and final EI are the values measured at 24 h and after 720 hours (30 days), respectively.

Emulsions with olive oil (O/W weight ratio of 3:2) were also prepared with Sepigel® 305, a commercial emulsifier, at concentrations of 0.5 and 1.0 wt.%. An active ingredient, α -tocopherol, was added to the oil phase at different concentrations (0.0, 2.0, and 5.0 wt.%) and emulsions stabilized with FucoPol or Sepigel® (1.0 and 0.5 wt.%) were prepared with olive oil at an O/W weight ratio of 3:2.

3.1.2.4 Factorial design of experiments

Response surface methodology (RSM) [213] was applied to determine the best formulation to prepare olive oil and α -tocopherol emulsions stabilized with FucoPol. A five-level three-variable central composite design (CCD) was applied, consisting of seventeen runs, with eight factorial points, six axial points, and three central points (Table 3.1.1).

Table 3.1.1. Independent variables and their levels used in the response surface design.

Independent variables	Coded variable	Factor level				
		$-\alpha$	-1	0	1	α
FucoPol (wt.%)	A	-0.00	0.30	0.80	1.30	1.64
Olive oil (wt.%)	B	13.18	20.00	30.00	40.00	46.82
α -tocopherol (wt.%)	C	-0.00	1.00	2.50	4.00	5.02

The central points are used to determine the experimental error and the reproducibility of the data. The independent variables are coded to have low and high levels of -1 and $+1$, respectively. The axial points $-\alpha$ and $+\alpha$ were fixed at 1.682 from the centre point and make the design rotatable. The mathematical relationship between the independent variables can be approximated by the second-order polynomial model equation:

$$Y = \beta_0 + \sum_{i=1}^n \beta_i x_i + \sum_{i=1}^n \sum_{j=1}^n \beta_{ij} x_i x_j + \sum_{i=1}^n \beta_{ii} x_i^2 \quad (3.1.3)$$

where Y is the predicted response; x_i are the independent variables ($n=3$). The parameter β_0 is the model constant; β_i are the linear coefficients; β_{ii} are the quadratic coefficients and β_{ij} are the cross-product coefficients [214]. A full factorial design of experiments was drawn up using the Design-Expert (Design-Expert® software package from Stat-Ease Inc.). The validated model was plotted in a three-dimensional graph and a surface response that corresponds to the best emulsification was generated. Analysis of variance (ANOVA) was used to determine the regression coefficients of individual linear, quadratic, and interaction terms.

3.1.2.5 Characterization of the emulsions

3.1.2.5.1 Type of emulsion and microscopic observation

The Type of emulsion and microscopic observation were achieved as described in Section 2, Chapter 2 (2.2.2.6).

3.1.2.5.2 Apparent viscosity and viscoelastic properties

The emulsions' rheological properties were studied using an MCR 92 modular compact rheometer (Anton Paar, Graz, Austria), equipped with a PP50/S parallel plate geometry (diameter 50 mm) and a P-PTD 200/AIR Peltier plate to keep the measurement temperature constant at 25 °C. A steady-state flow ramp was used to determine flow curves for shear rates between 0.01 and 1000 s⁻¹. The flow curves were fitted to the Cross model as previously described in Section 2, Chapter 1 (2.1.2.4). Frequency sweep tests were performed with frequency ranging from 0.01 to 16 Hz for a constant strain of 0.5% that was well within the LVE evaluated through preliminary amplitude sweep tests.

3.1.2.5.3 Texture analysis

Texture analysis was performed as described by Tafuro et al. [203]. The firmness, consistency, cohesiveness, and adhesivity of the attained formulations were determined using a texture analyser (TMS-Pro, Food Technology Corporation, Sterling, USA) equipped with a 50 N load cell (Mecmesin, Sterling, USA). The sample was placed in a female conic holder and was compressed 10 mm of depth (which represented a deformation of the sample of about 70%); this procedure was done twice by a male conic probe at a speed of 2 mm/s. The samples' mechanical parameters were determined from the force-displacement curve: the firmness corresponded to the highest force value attained by the sample during the first compression; the consistency was calculated by the area under the curve of the first compression; the cohesiveness was determined through the ratio of the areas under the curve from the first and the second compressions; and the adhesiveness was determined from the area under the curve from the negative peak attained after the first compression [203,204].

3.1.3 Results and Discussion

3.1.3.1 Polymer characterization

Figure 3.1.1 shows the equilibrium surface tension as a function of FucoPol concentration. Two distinct regions can be identified: up to around 11.5 g/L, there is a reduction of the surface tension with increasing FucoPol concentration, while above such value the surface tension remains constant irrespective of the biopolymer's concentration. FucoPol's critical micelle concentration (CMC) was determined to be approximately 11.5 g/L, corresponding to the point of intersection between the horizontal and angular lines [215,216]. This value is considerably higher than those reported for commercial polysaccharides like xanthan and guar gum (approximately 0.15 g/L and 5 g/L, respectively) [217], suggesting a lower thermodynamic stability of the particles system [218]. Nevertheless, FucoPol reduced the surface tension of water from 72 mN/m to 54.6 mN/m at the CMC, a value that is within the range reported for other microbial biosurfactants (34-69 mN/m) [219–221]. Moreover, polymeric biosurfactants, despite not significantly lowering the water's surface tension, are generally more effective in the formation and stabilization of emulsions [219,222].

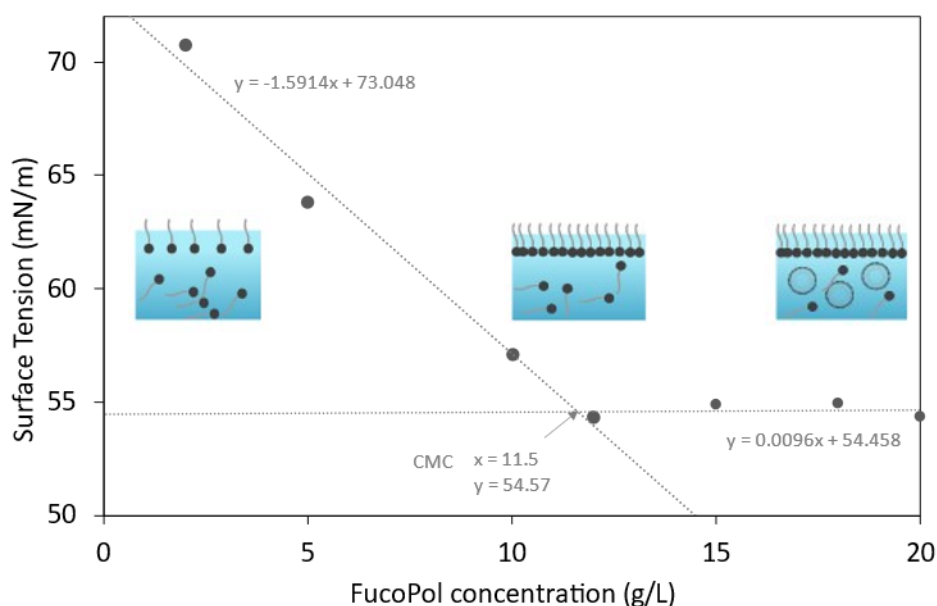


Figure 3.1.1. Surface tension of FucoPol solutions at concentrations ranging from 0.1 to 20 g/L.

3.1.3.2 Emulsion forming and stabilizing capacity of FucoPol

3.1.3.2.1 Preparation of FucoPol-stabilized emulsions with different oils

FucoPol was used to prepare emulsions with four different oils commonly used in cosmetic products' formulations, namely, castor oil [223–226], paraffin oil [227–229], almond oil [230,231] and olive oil [232–236]. Castor oil is a natural oil, acting as an antimicrobial, anti-inflammatory, antioxidant, wound healing, vasoconstrictive [237] and UV-protective agent [238]. Paraffin oil is a petroleum-based derivative that enables the regulation of viscosity in formulations, possessing protective and lubricating

properties which prevent skin dehydration [239]. Almond oil is an abundant macro and micronutrients source utilized in cosmetics due to its moisturizing and restructuring properties [230]. Olive oil, composed of squalene, phytosterol, tocopherol, vitamins A and E, and fatty acids (oleic and linoleic acids), is indicated for skin applications due to its acidity and soothing effect [147,227,240].

The assays consisted of mixing the biopolymer, at a concentration of 0.5 or 1.0 wt.%, with each oil, at 2:3 or 3:2 weight ratios. As shown in Figure 3.1.2, FucoPol efficiently emulsified all the tested hydrophobic compounds, with EI at 24 h (E24) values above 50% (Table 3.1.2), which is the criterium for a good emulsifier [144]. For the 2:3 weight ratio, increasing the concentration of the polymer from 0.5 wt.% to 1.0 wt.% resulted in increased E24 for all the tested oils (Table 3.1.2). For the 3:2 weight ratio, on the other hand, this was not observed. In fact, for all tested oils, the E24 value decreased except for castor oil (E24 increased from 53 to 100%). All other oils presented negligible emulsification (Figure 3.1.2; Table 3.1.2). For 0.5 wt.% of FucoPol, increasing the oil ratio from 2:3 to 3:2 resulted in higher E24, except for castor oil.

Table 3.1.2. Emulsification activity measured at 24 h (E24) and emulsions' stability (ES) for the emulsions stabilized with FucoPol. Data is shown as the average \pm standard deviation (SD) (n = 3).

Oil	FucoPol	E24 (%)		ES (%)	
		2:3	3:2	2:3	3:2
Castor oil	0.5%	70 \pm 3	53 \pm 4	81 \pm 3	77 \pm 4
	1.0%	100 \pm 0	100 \pm 0	20 \pm 0	11 \pm 0
Paraffin oil	0.5%	58 \pm 2	80 \pm 4	87 \pm 5	68 \pm 6
	1.0%	85 \pm 2	6 \pm 0	54 \pm 1	78 \pm 0
Almond oil	0.5%	84 \pm 4	93 \pm 6	50 \pm 3	47 \pm 6
	1.0%	89 \pm 0	0 \pm 0	31 \pm 6	0 \pm 0
Olive oil	0.5%	58 \pm 0	76 \pm 0	85 \pm 2	97 \pm 0
	1.0%	81 \pm 1	56 \pm 0	56 \pm 1	100 \pm 0

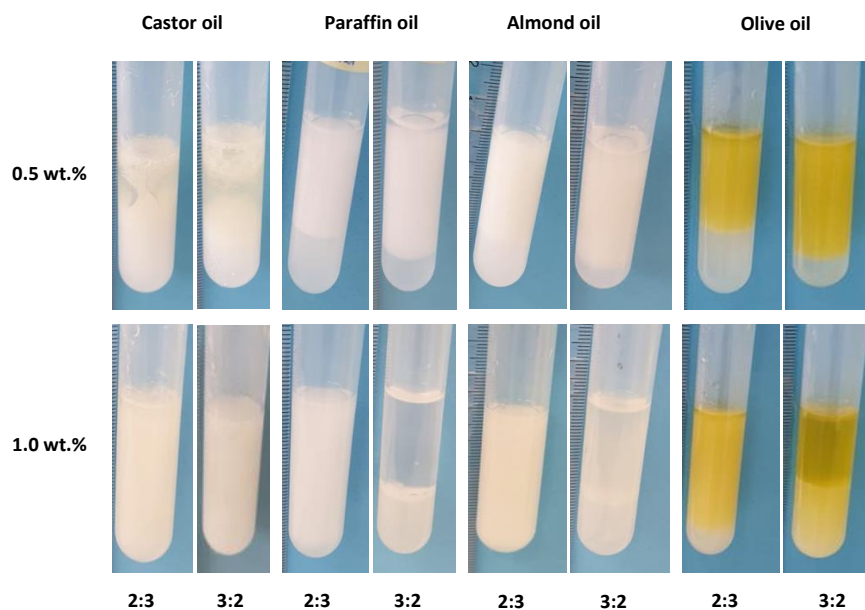


Figure 3.1.2. Emulsions prepared with FucoPol (0.5 or 1.0 wt.%) with castor oil, paraffin oil, almond oil and olive oil, at O/W weight ratios of 2:3 and 3:2.

3.1.3.2.2 Evaluation of emulsions' stability

Cosmetic applications require that the emulsions have adequate shelf-life, usually up to six months [235,241–243]. The stability of the emulsions prepared with FucoPol was evaluated at room temperature, by measuring their EI over a period of 720 h (30 days). As shown in Figure 3.1.3, FucoPol emulsion stabilizing capacity depended on the O/W weight ratio, as well as on the tested oil. All FucoPol-stabilized emulsions had no detectable changes in odour or colour during the storage period.

The least stable sample was the emulsion prepared with castor oil at an O/W weight ratio of 3:2 and a FucoPol concentration of 1.0 wt.% (Figure 3.1.3(a.2)). This sample's EI dropped from 100% at 24 h to 18% at 7 days, with an overall ES of 11% (Table 3.1.2). Nevertheless, the emulsions prepared with castor oil with 0.5 wt.% FucoPol (Figure 3.1.3(a.1-2)) were stable for both O/W weight ratios, presenting ES values of $81 \pm 3\%$ and $77 \pm 4\%$, respectively (Table 3.1.2).

Most of the emulsions prepared with paraffin oil and almond oil also showed a significant decrease of their EI during the 720 hours shelf-life test (Figure 3.1.3b-c) with ES values of 0 to 54% (Table 3.1.2). Despite the lower E₂₄ values (56–76%), the olive oil/FucoPol emulsions, for both O/W weight ratios tested, showed higher stability (Figure 3.1.3(d.1-2)), corresponding to ES values of 85–100% (Table 3.1.2). Antunes et al. [42] obtained olive oil/FucoPol emulsions in 2:3 and 3:2 (v/v) ratios that maintained at least 50% of the initial EI for 9 weeks, which agrees with the results reported on this study.

Section 3. Chapter 1. Assessment of FucoPol Emulsifying Capacity using different Natural Oils

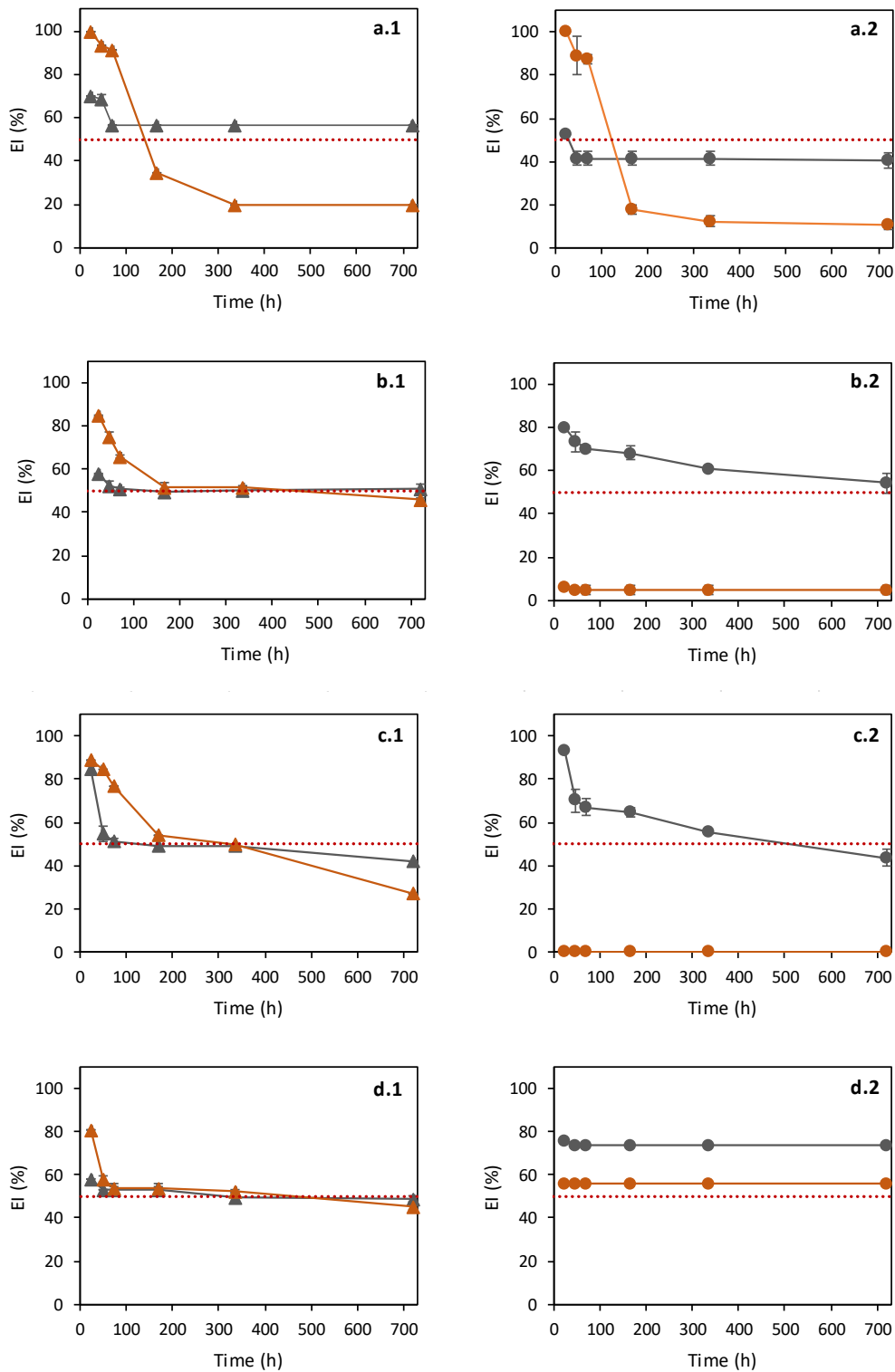


Figure 3.1.3. Emulsification index (EI,%) overtime for emulsions prepared with FucoPol and different hydrophobic compounds: Castor oil (a.1,2), paraffin oil (b.1,2), almond oil (c.1,2) and olive oil (d.1,2), for FucoPol concentrations of 0.5 wt% (gray) and 1.0wt% (orange), for o:w weight ratios of 2:3 (left) and 3:2 (right). Red dashed line represents EI (%) =50. (n = 3).

The results obtained in this study demonstrate that FucoPol is a promising stabilizer for emulsions with any of the tested oils, provided the adequate O/W weight ratio and FucoPol concentration are utilized. Castor oil (at the 2:3 weight ratio, 0.5 wt.% FucoPol), paraffin oil (at the 3:2 weight ratio, 0.5 wt.% FucoPol) and olive oil (at the 3:2 weight ratio, 0.5 wt.% FucoPol, and at the 2:3 ratio for either 0.5 or 1.0 wt.% FucoPol) presented high EI and were stable over the 720 h storage period. Given the good results obtained for olive oil and its known biological properties [147,227,240], this oil was chosen for the subsequent studies.

3.1.3.2.3 Assaying α -tocopherol as an additive to the FucoPol-stabilized emulsions

The effect of α -tocopherol, an antioxidant commonly used in cosmetic formulations [244,245], on FucoPol/olive oil emulsions was evaluated by testing different concentrations of this additive on the EI and on the emulsions' stability. According to the risk profile of tocopherols [246], the maximum concentration of α -tocopherol allowed in cosmetic products is 5.0 wt.%. Nonetheless, the α -tocopherol concentration in the skin care cosmetics below 0.2% is sufficient to protect lipids against peroxidation [247]. Therefore, α -tocopherol at concentrations of 2.0 and 5.0 wt.% were selected for testing as additive in FucoPol/olive oil emulsions.

As shown in Table 3.1.3, the addition of α -tocopherol led to an increase of the E24 values for both FucoPol concentrations tested. Compared to the samples with no α -tocopherol that had E24 values of 76% and 56%, for FucoPol concentrations of 0.5 and 1.0 wt.%, respectively (Table 3.1.3), the addition of α -tocopherol resulted in higher E24 (80–86% and 61%, respectively). However, the resulting emulsions were less stable, especially for those prepared with 1.0 wt.% FucoPol that had ES of 53 % (2.0 wt.% α -tocopherol) and 63 % (5.0 wt.% α -tocopherol), compared to 96% for the sample with no α -tocopherol (Figure 3.1.4, Table 3.1.3). For the emulsions prepared with 0.5 wt.% FucoPol, the ES was 82% and 90%, for 2.0 and 5.0 wt.% α -tocopherol, respectively (Table 3.1.3). Despite the observed ES reduction, the sample containing 5.0 wt.% α -tocopherol had an ES of 90% at 720 hours, identical to the sample with no additive (Table 3.1.3).

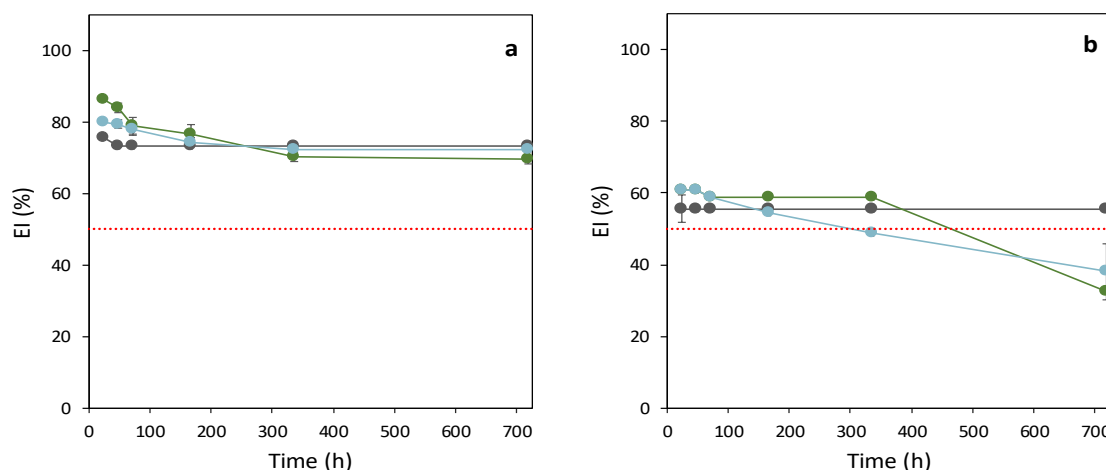


Figure 3.1.4. Emulsification index (EI, %) over time for the FucoPol-stabilized emulsions with olive oil and α -tocopherol, at the 3:2 ratio: FucoPol (0.5 wt.% (a); 1.0 wt.% (b)); α -tocopherol: 0.0 wt.%, gray; 2.0 wt.%, green; 5.0 wt.%, blue. Red dashed line represents EI=50%. ($n = 3$).

Table 3.1.3. Emulsification activity at 24 hours (E24) and emulsions' stability over a period of 720 h, for the emulsion prepared with FucoPol, olive oil and a-tocopherol, at 3:2 (w/w) ratio. Data is shown as the average \pm standard deviation (SD) ($n = 3$).

Emulsifier	α -tocopherol (wt.%)	0.5 wt.% emulsifier		1.0 wt.% emulsifier	
		E24 (%)	ES (%)	E24 (%)	ES (%)
FucoPol	0	76 \pm 0	87 \pm 3	56 \pm 0	96 \pm 0
	2.0	86 \pm 1	82 \pm 1	61 \pm 0	53 \pm 5
	5.0	80 \pm 1	90 \pm 1	61 \pm 0	63 \pm 12
Sepigel® 305	0	0 \pm 0	-	49 \pm 0	100 \pm 0
	2.0	0 \pm 0	-	0 \pm 0	-
	5.0	0 \pm 0	-	0 \pm 0	-

3.1.3.2.4 Comparison with Sepigel® 305

The commercial emulsifier agent Sepigel® 305 (also known as Farcosgel polyacrylamide, C13-14/isoparaffin and laureth-7) was used to prepare emulsions with olive oil (O/W weight ratio of 3:2), with and without α -tocopherol, and the results were compared to those of FucoPol's emulsions (Table 3.1.3). Sepigel® 305 is a synthetic hydrophilic polymer used in cosmetics to provide increased viscosity and stability to the formulation [61]. Sepigel® 305 is composed by a blend of polyacrylamide (10–20%), C13–14 Isoparaffin (1–5%), and Laureth-7 (1–5%). In its composition, each compound presents a specific function: the pre-neutralized polyacrylamide polymer is contained within an emulsion, where isoparaffin forms an oily phase and laureth-7 acts as a surfactant [61–63]. The comparison between

Sepigel® 305 and FucoPol aims to discuss the possibility to replace a widely used chemical agent with a naturally produced polymer in cosmetic formulations. Interestingly, no emulsification was observed for the 0.5 wt.% Sepigel® samples and an EI of $49 \pm 0\%$ was obtained for 1.0 wt.%, which was, nevertheless, stable for the 720 h shelf-life periods assay. The addition of α -tocopherol had a negative impact, and no emulsification was observed for any additive concentration. According to Anchisi et al [243], Sepigel® 305 at concentrations of 1.5–7%, with an oil phase consisting mainly of a fluid oil, resulted in good emulsification for O/W skin creams. Other studies have reported the development of stable emulsions containing this polymer at concentrations higher than 2.0 wt.% [248–251]. At lower concentrations (< 1.5 wt.%), the synthetic hydrophilic polymer was able to stabilize O/W formulations only with the addition of different emulsifying ingredients and emulsion stabilizers [252,253]. These results showed the ability of the natural polymer FucoPol to emulsify without the addition of other agents at low concentrations, which becomes an advantage compared to the synthetic polymer Sepigel® 305.

3.1.3.3 Emulsification Optimization by Response Surface Methodology

3.1.3.3.1 Response Analysis

Table 3.1.4 shows the data for the 17 runs of the CCD. Results show that the emulsification after 24 h ranged from 0.0 to 97.8%. Good emulsification index ($E_{24} > 95\%$) was obtained in runs 1, 5, 11, 12, 14, 16 and 17, for which FucoPol concentration was 0.8–1.3 wt.%, and the olive oil content was 20–30 wt.%, irrespective of the α -tocopherol content that varied from 0.0–5.0 wt.%. These results suggest that α -tocopherol concentration has little effect on the E_{24} . Outside those FucoPol and olive oil concentration ranges, E_{24} of 30.4–78.3% were attained. As expected, no emulsification was obtained in run 15 due to the absence of the bioemulsifier. Moreover, there was also no emulsification for runs 2, 6 and 10.

3.1.3.3.2 RSM modelling

RSM methodology was used to evaluate the effect of each ingredient (FucoPol, olive oil and α -tocopherol) on the E_{24} of the emulsions, as well as the combined effect of the variables. ANOVA was used to define the working ranges for each variable resulting in the highest E_{24} values. The statistical analysis (Table 3.1.5) shows that the proposed model was adequate [254]. The quadratic model was found to be significant (f -value = 18.51 and p -value = 0.001) and it was supported by an insignificant lack-of-fit ($p = 0.634$) toward the response (E_{24}). There is only a 0.10% chance that a “Model F-Value” could occur due to noise, meaning that the greater f -value from unity explains adequately the variation of the data around its mean, in addition the estimated factor effects are real [255,256]. The R^2 (0.965) was in reasonable agreement with the adjusted R^2 (0.913). The adjusted coefficient of determination indicated that the 91.31% of the variability in the response could be explained by the model. Hence, the quadratic model is an accurate representation of the actual relationships between the response and the variables. The observed precision of 12.19 indicates an adequate signal (ratio > 4 is desirable). The

statistical analysis indicates that the proposed model was adequate to predict the ingredients' concentrations to obtain stable emulsions ($E_{24} > 50\%$) [144].

Table 3.1.4. Central composite design (CCD) with studied variables (A: FucoPol, B: Olive oil, C: α -tocopherol), experiment and theoretically predicted values E_{24} .

Run	A: FucoPol (wt.%)	B: Olive oil (wt.%)	C: α -tocopherol (wt.%)	E24 (%)	
				Actual Value	Predicted value
1	0.8	30	2.5	97.8	97.1
2	1.6	30	2.5	0.0	3.0
3	0.3	20	4.0	30.4	26.8
4	0.8	46.8	2.5	78.3	57.3
5	0.8	30	0.0	95.7	100
6	1.3	40	4.0	0.0	19.5
7	0.3	20	1.0	76.1	56.6
8	0.3	40	4.0	69.6	72.7
9	0.8	13.2	2.5	73.9	95.0
10	1.3	40	1.0	0.0	3.6
11	0.8	30	5.0	95.7	90.0
12	0.8	30	2.5	97.7	97.1
13	0.3	40	1.0	69.6	78.7
14	0.8	30	2.5	97.6	97.1
15	0.0	30	2.5	0.0	15.3
16	1.3	20	4.0	95.6	87.0
17	1.3	20	1.0	97.8	94.6

E_{24} predicted value= $97.07 - 3.82A - 11.24B - 3.5C - 28.26AB + 5.43AC + 5.98BC - 34.31A^2 - 7.41B^2 - 0.4880C^2$

The response of the RSM was shown as three-dimensional surface graphs (Figure 3.1.5), and contour plots resulted in an infinite number of combinations of the FucoPol, olive oil, and α -tocopherol. The result suggests that FucoPol concentration between 0.8–1.3 wt.% and olive oil concentration between 20–30 wt.% reach E_{24} values above 95.6%. Moreover, α -tocopherol does not appear to influence the E_{24} value (Figure 3.1.5). Figure 3.1.5a shows an inversely proportional interaction between FucoPol and olive oil, whereby E_{24} value increases with the increase in FucoPol concentration and decrease in olive oil concentration. Figure 3.1.5b corroborates the observed inverse proportionality between FucoPol and olive oil concentrations. Lastly, Figure 3.1.5c shows higher E_{24} values for olive oil between 25–30 wt.%.

Table 3.1.5. ANOVA for response surface quadratic model. (SS)- Sum of Squares shows the variance of values; (MS)- Mean Square is the arithmetic mean of the squared differences; P-value < 0.05 indicate model terms are significant.

Source	SS	MS	<i>f</i> -value	<i>p</i> -value	Significance
Model	24439.63	2715.51	18.51	0.001	Significant
A: FucoPol	199.37	199.37	1.360	0.287	
B: Olive oil	2854.49	2854.49	19.46	0.004	
C: α -tocopherol	167.58	167.58	1.140	0.326	
AB	6390.15	6390.15	43.56	0.001	
AC	236.31	236.31	1.610	0.251	
BC	286.08	286.08	1.950	0.212	
A ²	14317.43	14317.43	97.60	0.0001	
B ²	0.0002	0.0002	1.4x10 ⁻⁶	0.999	
C ²	72.96	72.96	0.497	0.507	
Lack of Fit	582.37	145.59	0.766	0.634	Not significant
R ²			0.965		
R ² adjusted			0.913		
R ² predicted			0.622		
Adequate precision			12.19		

Based on Figure 3.1.5, increasing the concentration of FucoPol resulted in emulsions more stable against coalescence, avoiding emulsion phase separation [70]. This is due to FucoPol's ability to allow a specific texture (of increased viscosity) to the formulation and to decrease elasticity-driven creaming of the droplets [3]. FucoPol concentration and olive oil concentration have inversely proportional effects, as shown by the *p*-value < 0.05 (Table 3.1.5). In this case, linear (B), interaction (AB) and quadratic (A²) are significant model terms on E24 including a positive linear effect (*p* = 0.004) of olive oil and a quadratic effect (*p* = 0.0001) of FucoPol, interacting with himself on the response [67]. This result agrees with results obtained for bacterial cellulose, in which emulsions became more stable as the concentration increased, reaching 1.0 wt.% [71]. In contrast, for xanthan gum concentrations of 0.12% and 0.2%, emulsions became more stable with 50 wt.% of oil [72–74].

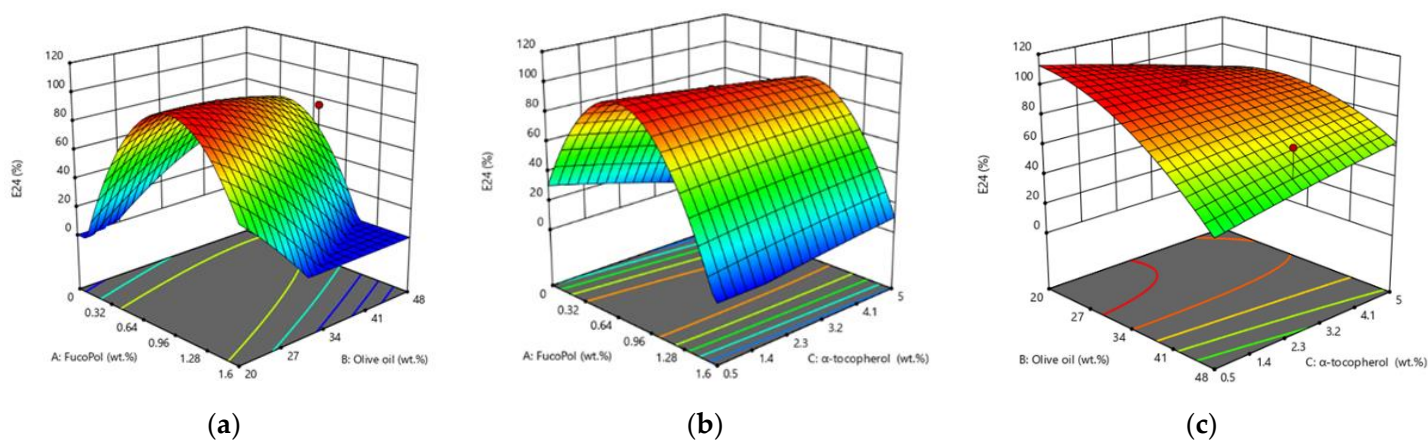


Figure 3.1.5. Three-dimensional response surface plot showing the interactive effects of different components on the O/W emulsion. (a) FucoPol and Olive oil (wt.%) with α -tocopherol fixed at 2.5 wt.%, (b) FucoPol and α -tocopherol (wt.%) with olive oil fixed at 30 wt.%, (c) Olive oil and α -tocopherol (wt.%) with FucoPol fixed at 0.8 wt.%.

Based on the results obtained in the CCD, two FucoPol-stabilized emulsions were prepared (5g): FA that comprised 1.0 wt.% FucoPol, 25 wt.% olive oil, 0.5 wt.% α -tocopherol and water (q.s.); and FB that comprised 0.7 wt.% FucoPol, 25 wt.% olive oil, 2.0 wt.% α -tocopherol and water (q.s.). FA and FB yielded E24 values of $98.0 \pm 0.40\%$ and $84.7 \pm 0 \%$, respectively.

3.1.3.4 Characterization of the FucoPol-stabilized emulsions

3.1.3.4.1 Type of emulsion

The microscopic observation (Figure 3.1.6a) of the emulsions showed compartmentalized structures characteristic of O/W emulsions, consisting of dispersed oil droplets in the aqueous phase [184,185]. Furthermore, in the emulsion determination test (Figure 3.1.6b), the emulsions' droplets rapidly dispersed on the filter paper, thus confirming their O/W nature [168,186,187]. O/W emulsions represent nearly 65% of the total emulsified products available in the cosmetic industry market due to their sensorial properties [257,258] and are present in several products such as creams and lotions [258,259]. W/O emulsions are commonly used in waterproof products by providing higher hydration to emulsions [258]. However, these emulsions usually are responsible for an oily sensation on the skin, which enhances the consumer preference for O/W emulsified products [260].

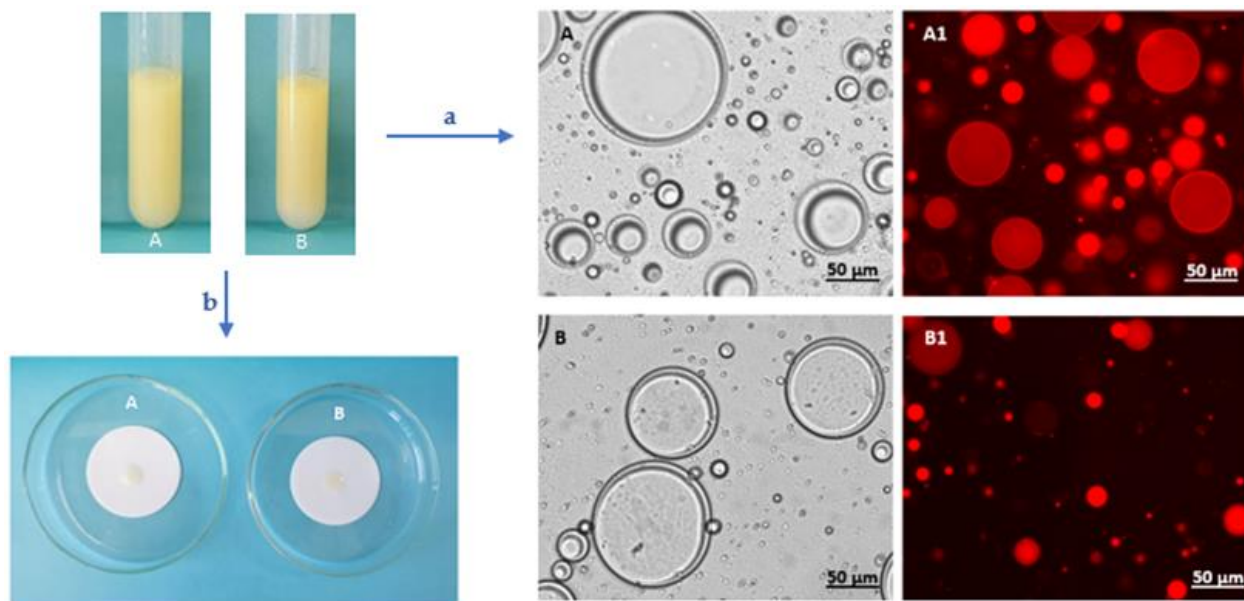


Figure 3.1.6. (a) Optical microscopic (100x) images of FA (A) and FB (B) emulsions; contrast phase and fluorescence after Nile Blue A staining (A1, B1, respectively). (b) Emulsion determination test by filter paper wetting.

3.1.3.4.2 Apparent viscosity and viscoelastic properties

As shown in Figure 3.1.7a, both samples presented a shear-thinning behaviour, as the viscosity progressively decreased under increasing shear rates, in agreement with previous studies that reported the same behaviour for FucoPol/olive oil emulsions [147] in Section 2, Chapter 1 and 2. This effect is observed when spherical shape is detangled by polymer chains and the droplets begin to deform, forming an ellipsoidal shape. Moreover, layer formation, due to aggregate breaking into elemental constituents, is concurring to the shear plane, decreasing the overall flow resistance [203,204,261,262]. This shear-thinning behaviour was observed for emulsions stabilized by other polysaccharides, such as xanthan gum and guar gum [261,263]. Nevertheless, slight differences are noticed between samples, namely, a lower apparent viscosity for the emulsion FB (Figure 3.1.7a, triangles) compared to emulsion FA (Figure 3.1.7a, circles), which was probably due to the lower polymer concentration in FB. FucoPol increased viscosity in water phase leads to decreased droplets' mobility and collision numbers, which can explain the observed behaviour [264].

A non-Newtonian mathematical model, the Cross model, was fitted to the experimental results (Figure 3.1.7a) with the resulting parameters given on Table 3.1.6. The highest η_0 value was observed for emulsion FA (13.92 ± 2.36 Pa.s) but the τ fitting parameter was similar for both emulsions. The emulsions had identical degree of shear-thinning as shown by the similar values of m (0.74 ± 0.00 and 0.68 ± 0.01) [265].

The mechanical spectra (Figure 3.1.7-b) of the two FucoPol-stabilized emulsions showed higher loss modulus (G'') than storage modulus (G'), indicating a liquid-like behaviour [16], with FucoPol viscosity being the dominant property influencing the emulsions' stability [241,266]. The mechanical spectra for two emulsions are quite similar, with G'' increasing at a higher rate than G' , with the crossover of dynamic moduli being perceived at lower frequency (0.6 Hz) for emulsion FA than for emulsion FB (1.6 Hz). This indicates that for emulsion FA, higher viscosity translates into lower energy storage threshold, featuring a $G' = G''$ crossover at a lower frequency [54,147]. After the crossover point, increasing the frequency displays a solid-like behaviour (weakly structured gel) for both emulsions ($G' > G''$) [241,267].

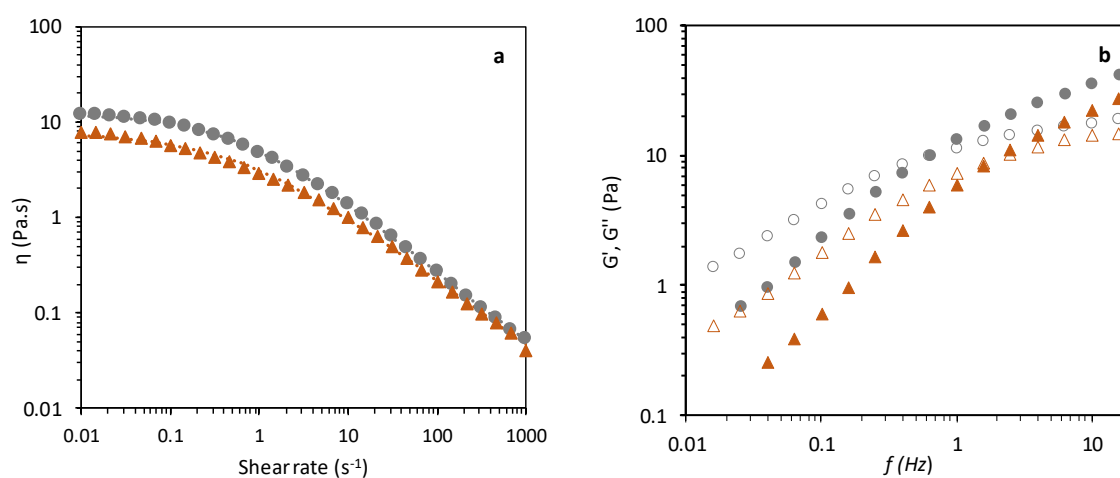


Figure 3.1.7. Rheological profile analysis of FucoPol formulations FA(circles) and FB(triangles): (a) Viscosity curves as a function of the shear rate, flow curves fitted with Cross model ($n=3$); (b) Mechanical spectra: elastic G' (closed) and viscous G'' (open) moduli in the function of frequency.

Table 3.1.6. Cross model parameters estimated for formulations samples: η_0 —apparent viscosity of the first Newtonian plateau (Pa.s); τ —relaxation time (s); m —dimensionless constant; Data are shown as the average \pm standard deviation (SD) ($n = 3$); and textural parameters.

Emulsion	Cross model parameters			Textural parameters			
	η_0 (Pa.s)	τ (s)	m	Firmness (N)	Consistency (mJ)	Adhesiveness (mJ)	Cohesiveness (N)
FA	13.92±2.36	1.64±0.13	0.74±0.00	0.074	0.088	0.156	0.748
FB	7.59±0.04	1.72±0.04	0.68±0.01	0.074	0.055	0.129	0.688

$$RE = \sum_{i=1}^n (|x_{e,i} - x_{c,i}| / x_{e,i}) / n \text{ is between } 0.011 \text{ and } 0.019.$$

3.1.3.5 Textural assessment

As shown in Table 3.1.6, the FucoPol-stabilized emulsions FA and FB had the same firmness (0.074 N) when perforated 11 mm with a conic probe. The consistency of emulsion FA was 0.088 mJ, while that of sample FB was 0.055 mJ. Studies showed that the firmness and energy required to deform a sample are related to the sample's spreadability: high firmness and consistency values indicate a less spreadable sample, whilst lower consistency and firmness values indicate a more spreadable sample [203,204]. Hence, these results show that both samples are very spreadable, presenting low firmness and consistency values. Moreover, emulsion FB was more spreadable than sample FA (Table 3.1.6). The spreadability (skin cover capacity overtime) is crucial in cosmetic emulsions development being a decisive factor for consumer's approval of products [268]. While both samples showed some adhesivity, emulsion FA (0.156 mJ) seemed to be more adhesive than FB (0.129 mJ). When a formulation is spread, verifying the material uniform scattering throughout the applied surface is pivotal to avoid the active substance's accumulation or dissipation and to insure the correct utilization of the formulation [203,204]. Therefore, the cohesiveness was also an important parameter to be observed. Given this, emulsion FA (0.748 N) is slightly more cohesive than emulsion FB (0.688 N), which concludes that sample FA has higher firmness, adhesiveness, cohesiveness but is less spreadable than sample FB. These results are concordant with η_0 (Pa.s) values (Table 3.1.6), where emulsion FA exhibited higher apparent viscosity (13.92 ± 2.36 Pa.s) than FB (7.59 ± 0.04 Pa.s).

3.1.3.6 Comparative analysis of the FucoPol-stabilized emulsions

FB emulsion had a slightly higher spreadability value [268], a feature of interest for cosmetic and pharmaceutical applications. Furthermore, at high shear rates (e.g., 1000 s^{-1} , which is representative of a skin spreading process [268]), both FA and FB emulsions displayed analogous viscosity (0.05 Pa.s and 0.04 Pa.s, respectively). Such characteristics are found in lotions or light creams [258,260], thus confirming the potential of FucoPol for the development of skin care cosmetic products.

3.1.4 Conclusions

The overall pressure and interest for sustainability and eco-friendly choices have driven the cosmetic industries to research alternative formula ingredients. Specifically, several synthetic polymers are facing possible restrictions due to their non-biodegradable nature. Polysaccharide's addition may be viable alternatives for use in cosmetics as stabilizers and rheological modifiers.

This study demonstrated the ability of the bacterial polysaccharide FucoPol to emulsify olive oil and α -tocopherol, outperforming the commercial emulsifier Sepigel®. The resulting O/W emulsions had good viscosity and spreadability, which substantiates its relevance in the development of cosmetic applications. The emulsion textural properties can be modulated by using different FucoPol and α -tocopherol contents, thus yielding formulations suitable for use in different skin-care products. The intrinsic antioxidant capacity of FucoPol adds to that of α -tocopherol, which, together with FucoPol's wound-healing ability, render this natural polysaccharide as a valuable biomaterial for cosmetic formulations' development.

This page was intentionally left blank

CHAPTER 2

Development of Olive Oil and α -tocopherol containing Formulations

The results presented in this chapter are part of the following submitted paper:

Baptista, S.; Freitas, F. FucoPol-based cosmetic creams: Formulation design, stability evaluation, rheological and texture assessment. Submitted to *Molecules*.

This page was intentionally left blank

Summary

Driven by the costumers' growing awareness for environmental issues, production of topical formulations based on sustainable ingredients is receiving widespread attention from researchers and industry. Although numerous sustainable ingredients (natural, organic, or green chemistry-derived compounds) have been investigated, there is a lack of comparative studies between conventional ingredients and sustainable alternatives. In this chapter, olive oil (30 wt.%) and α -tocopherol (2.5 wt.%) containing oil-in-water (O/W) emulsions stabilized with the bacterial fucose-rich polysaccharide FucoPol were formulated envisaging their validation as cosmetic creams. Formula composition was designed using Response Surface Methodology (RSM) to determine the contents of FucoPol (1.5 wt.%), cetyl alcohol (1.5 wt.%) and glycerine (3.0 wt.%) that resulted in high emulsification index after 24 hours ($E_{24} \geq 98\%$), concomitant with an apparent viscosity of 8.72 Pa.s. The optimized FucoPol emulsion was formulated with 1.5 wt.% FucoPol, 1.5 wt.% cetyl alcohol, and 3.0 wt.% glycerine, having an apparent viscosity of 8.72 Pa.s (measured at a shear rate 2.3 s^{-1}) and droplet size and Zeta-potential values of $6.12 \mu\text{m}$ and -98 mV , respectively. After comparison with several available commercial products, the optimized formulation displayed the desired criterium of thin emulsion system, possessing the physicochemical properties and stability suitable for use in cosmeceutical applications.

3.2.1 Introduction

The global market demand for products based on innovative ingredients and technologies has compelled the cosmetic industry to rapidly increase the research and development of natural, organic, and eco-friendly formulations [109,191,269]. One of the most notorious examples of this growing interest is the incremental utilization of natural polysaccharides in cosmetic formulations. These biopolymers are composed of carbohydrates with several hydroxyl groups that, given their chemical composition, strongly interact with water [109,269]. There are many functional polysaccharides, able to act as film formers, gelling agents, thickeners, suspending agents, conditioners, and emulsifiers. These features derive from the biopolymers' physical and chemical properties and are critical for polysaccharide-based cosmetics' formulation technologies [109]. Examples of natural polysaccharides with consolidated utilization in commercial skin-care products include xanthan gum and cellulose, which are used as thickeners and stabilizing agents, and hyaluronic acid that is applied as a moisturizing and bioactive ingredient [4,109,111,269,270].

Emulsions are extensively used in cosmetic products to stabilize active substances, bioavailability, and sensory properties [271]. Being complex multiphase systems, emulsions' stabilization with polysaccharides is obtained by increasing the viscosity of the aqueous phase, thereby inhibiting droplet movement [271,272]. The high molecular weight and presence of hydrophilic groups often provides polysaccharides with thickening ability and water-holding properties, two attributes of interest for their application in cosmetic formulations [272]. Classical O/W emulsions comprise a continuous phase, in which oil is present as a dispersed phase, and emulsifiers to stabilize oil droplets dispersion [109,271].

Emulsions' rheological properties are essential physical attributes of these systems [183]. From the customer point of view, the cosmetics functional properties are critical: the product cannot be overly fluid (no structure, low viscosity) nor extremely dense (highly structured, high viscosity) [273]. Moreover, the product's viscosity can influence the mixing, pumping, and packing process [273,274]. Finding the optimum formulation and process conditions is essential during the development of new emulsions systems considering the final product stability, which influences its shelf life [191,273].

FucoPol is a high molecular weight ($1.7 \times 10^6 - 5.8 \times 10^6$ Da) bacterial fucose-rich polysaccharide, with a fucose content of 32–40 mol% and nearly equimolar contents of glucose (28–34 mol%) and galactose (24–26 mol%). Its structure also comprises glucuronic acid (7–10 mol%), and acyl groups: acetate (3.5–6.8 wt.%), pyruvate (3.7–14 wt.%), and succinate (0.6–3.0 wt.%) [147]. The development of emulsions based on FucoPol has been widely studied [41,44,55,147,183]. For instance, in previous chapter (Section 3, Chapter 1) was developed an innovative O/W emulsion, composed of olive oil and α -tocopherol as oil phase; FucoPol was used in the aqueous phase and presented a stabilizing effect which translated into appropriate rheological and textural behaviour of the emulsion. In addition, FucoPol has bioactive properties that further sustain its potential for use in the cosmetic field, such as wound healing ability [52], photoprotection [58], and antioxidant effect [49].

In this study, the main objective was the development of O/W emulsions using FucoPol as a substitute for synthetic emulsifying agent commonly used in cosmetic products. RSM was used to define the optimal concentration ranges for FucoPol, cetyl alcohol, and glycerine. FucoPol-based cosmetic formulations were prepared and characterized in terms of physical stability, rheological, and textural properties, and compared with cosmetic emulsion-based products available on the market.

3.2.2 Materials and Methods

3.2.2.1 Materials

Olea europaea (olive) fruit oil was purchased from a local market. Sepigel® 305 was obtained from SEPPIC (Courbevoie, France). α -tocopherol (vitamin E), methyl paraben, cetyl alcohol, and stearic acid were acquired from Sigma-Aldrich (Munich, Germany). Triethanolamine (TEA) was acquired from Acros Organics B.V.B.A. (Geel, Belgium), and glycerine was acquired from Honeywell (Seelze, Germany). FucoPol was produced and purified by ultrafiltration with a 30 kDa membrane according to the method previously described in Section 2, Chapter 1 (2.1.2.1 and 2.1.2.2). FucoPol was composed of 40 mol% fucose, 29 mol% glucose, 24 mol% galactose, and 7.0 mol% glucuronic acid, with a total acyl groups content of 11.6 wt.%. The sample had protein and inorganic salts contents of 8.2 wt.% and 4.0 wt.%, respectively.

3.2.2.2 Factorial design of experiments

Response surface methodology (RSM) [213] was applied to determine the best conditions for development of cosmetic formulations stabilized with FucoPol. A three-factor central composite design (CCD) analysed the effect of independent variables (Table 3.2.1): FucoPol (A: 0.0–1.5 wt.%); cetyl alcohol (B: 0.0–1.5 wt.%), and glycerine (C: 1.0–3.0 wt.%).

Table 3.2.1. Independent variables and their coded levels used in the RSM.

Independent variables	Coded variables	Factor level		
		-1	0	1
FucoPol (wt.%)	A	0.00	0.75	1.50
Cetyl alcohol (wt.%)	B	0.00	0.75	1.50
Glycerine (wt.%)	C	1.00	2.00	3.00

The mathematical relationship between the independent variables can be approximated by the second-order polynomial model equation:

$$Y = \beta_0 + \sum_{i=1}^n \beta_i x_i + \sum_{i=1}^n \sum_{j=1}^n \beta_{ij} x_i x_j + \sum_{i=1}^n \beta_{ii} x_i^2 \quad (3.2.1)$$

where Y is the predicted response; x_i are the independent variables ($n=3$). The parameter β_0 is the model constant; β_i are the linear coefficients; β_{ii} are the quadratic coefficients and β_{ij} are the cross-product coefficients [183]. A full factorial design of experiments was obtained using the Design-Expert (Design-Expert® software package from Stat-Ease Inc.). The validated model was plotted in a three-dimensional graph, generating a surface response that corresponds to the best emulsification index and apparent viscosity. Analysis of variance (ANOVA) was used to determine the regression coefficients of individual linear, quadratic, and interaction terms.

The emulsions were prepared by heating the oil phase (1.63 g) comprising olive oil (30 wt.%), cetyl alcohol (0.0–1.5 wt.%) and α -tocopherol (2.5 wt.%), and the aqueous phase (3.37 g) comprising FucoPol (0.0–1.5 wt.%), glycerine (1.0–3.0 wt.%), TEA (0.5 wt.%) and methyl paraben (0.02 wt.%) at 75 °C in a recirculated heated water bath Thermomix® ME (B.Braun, Melsungen, Germany). The mixtures were emulsified by manual agitation for 40 s, followed by vortex agitation for 10 s. The emulsification index (EI, %) was determined using the equation 3.1.1. described in Section 3, Chapter 1 (3.1.2.3).

3.2.2.3 Preparation of FucoPol-based emulsion formulations

Six formulations were prepared according to Table 3.2.2, including three formulations based on FucoPol as main emulsifier (formulations A, B and C) and three formulations based on stearic acid and/or Sepigel® 305 as emulsifier agents (formulations D, E and F). The oil phase (32.5 g) and the aqueous phase (67.5 g) were heated at 75 °C in a recirculated heated water bath Thermomix® ME (B.Braun, Melsungen, Germany). The emulsification was performed by slowly adding the oil phase to the aqueous phase and mixing with a shear rate of about 11,000 rpm (IKA T25 easy clean digital ULTRA TURRAX, Staufen, Germany), for 3 min, followed by manual continuous stirring until room temperature was attained [191]. All formulations were prepared in batches of 100 g.

Table 3.2.2. Cosmetic formulation composition (wt.%). q.s.- quantity sufficient

INCI name	Function	Concentration (wt.%)					
		A	B	C	D	E	F
Aqueous phase							
Water	Solvent	q.s.	q.s.	q.s.	q.s.	q.s.	q.s.
FucoPol	Emulsifier agent	1.5	1.5	1.5	-	-	-
Sepigel® 305	Emulsifier agent	-	-	-	-	1.5	-
Glycerine	Emollient/humectant	-	-	3	3	3	3
Methyl paraben	Preservative	0.02	0.02	0.02	0.02	0.02	0.02
TEA	pH regulator	0.5	0.5	0.5	0.5	0.5	0.5
Oil phase							
Cetyl alcohol	Co-emulsifier agent	-	1.5	1.5	1.5	-	1.5
Stearic acid	Emulsifier agent	-	-	-	5	1.5	1.5
<i>Olea europaea</i> (Olive) fruit oil	Oil, dispersed phase	30	30	30	30	30	30
α -tocopherol	Antioxidant	2.5	2.5	2.5	2.5	2.5	2.5

3.2.2.4 Formulations' characterization

3.2.2.4.1 Physicochemical properties

The organoleptic (colour, odour) and macroscopic appearance of each formulation were visually analysed. The EI was determined during the storage period (t=1, 3, 7, 30, 60 days) using equation 3.1.1, as described in Section 3, Chapter 1 (3.1.2.3).

The pH and the conductivity were determined by dispersing the formulation sample in deionized water (10%, w/w) [275–277]. The emulsion type and the microscopic observation were achieved as described

in Section 2, Chapter 2 (2.2.2.6). The physical stability was evaluated by centrifuging 1 g of the sample, at 4800 rpm, for 30 minutes [278].

Dynamic Light Scattering (DLS) was performed to determine the average particle size, the polydispersity index (PI) and the Zeta Potential, using a nanoPartica SZ-100V2 series (Horiba, Liege, Belgium) with a laser of 532 nm and controlling temperature with a Peltier system (25 °C). DLS measurements were performed by diluting the samples (1:10, *w/w*) in a disposable cell with a scattering angle equal to 90°. Cumulants statistics data analysis was performed to determine the hydrodynamic size and polydispersity. Zeta-potential measurements were performed in a graphite electrode cell with a 173° scattering angle [20].

3.2.2.4.2 Apparent viscosity and viscoelastic properties

The formulations' rheological properties were studied using an MCR 92 modular compact rheometer (Anton Paar, Graz, Austria), equipped with a CP35-2 cone-plate sensor system (angle 2°, diameter 35 mm) and a P-PTD 200/AIR Peltier plate to keep the measurement temperature constant at 25 °C. Dynamic viscosity measurements were performed at shear rates between 0.01 and 1000 s⁻¹. Frequency sweep analysis was performed at frequencies ranging from 0.01 to 10 Hz, for a constant strain of 0.1–1.0% that was well within the LVE evaluated through preliminary amplitude sweep tests [183].

3.2.2.4.3 Texture analysis

The firmness, consistency, cohesiveness, and adhesivity of the attained formulations were determined using a texture analyser (TMS-Pro, Food Technology Corporation, Sterling, VA, USA) equipped with a 10 N load cell (Mecmesin, Sterling, VA, USA) as previously described in Section 3, Chapter 1 (3.1.2.5.3).

3.2.3 Results and Discussion

3.2.3.1 Selection of O/W emulsions' ingredients

The objective of this study was to utilize FucoPol as the main emulsifier in novel cosmetic formulations given its previously demonstrated emulsion forming and stabilizing capacity [147,183]. Previous studies proved FucoPol at concentrations ranging from 0.8 to 1.3 wt.% efficiently emulsified *Olea europaea* (olive) fruit oil (20–30 wt.%) and α -tocopherol (1.0–5.0 wt.%), which substantiates its relevance in the development of cosmetic applications [183]. α -tocopherol is widely used as a cosmetic antioxidant ingredient, presenting an active role in anti-aging mechanisms, and acting as a coadjutant in atopic dermatitis and melanoma treatments [244,279]. *Olea europaea* (olive) fruit oil is an anti-aging ingredient indicated for dermatology applications due to its acidity, antioxidant activity, and soothing effect [183,280], preventing, for example, the appearance of stretch marks [236]. Hence, FucoPol-based emulsions containing olive oil and α -tocopherol were the basis of the present study.

Other ingredients that were selected for the emulsions' formulation were cetyl alcohol, glycerine, triethanolamine (TEA) and methyl paraben. Cetyl alcohol is a long-chain alcohol [271] commonly used in cosmetics at concentrations of 0.1–5.0 wt.% [281], with no toxic effects, as co-emulsifier [282], surfactant [283], thickener [284], and opacifying agent [285]. As co-emulsifier, a cetyl alcohol concentration higher than 2.0% should be avoided to prevent a soaping effect [260]. Glycerine, responsible for the improvement of skin's smoothness and moisture [286], is used as humectant in cosmetics at variable concentrations: 10% in face/neck products; 5.0% in body/hand products; 3.3% in moisturizing products [287]. TEA is used in cosmetics as a pH adjuster [288], and used in personal care products at concentrations between 0.0002% and 19% [260,288–291]. Methyl paraben, a safe preservative ingredient found in most cosmetics products [228], can be used singly or in combination to enhance the antimicrobial effect, at concentrations below 0.3% [292,293], being normally a non-irritating and non-sensitizing ingredient [292].

3.2.3.2 O/W emulsions' optimization

With the objective of defining the composition resulting into emulsions with high EI after 24 h (E24), concomitant with high apparent viscosity, different FucoPol, cetyl alcohol, and glycerine concentrations were tested. High E24 values ($\geq 95\%$) were obtained in most runs, except in runs 7, 8, 9, and 11 (Appendix 1), which were devoid of the FucoPol, irrespective of the cetyl alcohol and glycerine content that varied from 0.0–1.5 wt.%, and 1.0–3.0 wt.%, respectively. Higher FucoPol concentrations also conferred higher apparent viscosity to the emulsions, regardless of cetyl alcohol and glycerine concentrations. The emulsions presented a yellowish white colour, olive odour, and creamy/smooth texture, showing physical stability (as shown by the centrifugation test) for apparent viscosity values ≥ 90 Pa.s. Table 3.2.3 shows that the maximum apparent viscosity obtained values were 249 Pa.s (Run 4) and 244 Pa.s (Run 6), both containing a FucoPol concentration of 1.5 wt.%.

ANOVA was used to define the working ranges for each variable resulting in the highest E24 and η values. The coefficients of multiple determination (R^2) values of E24 and η were 0.974 and 0.995,

respectively. For η , the R^2 was in reasonable agreement with the adjusted R^2 (0.989) and the predicted R^2 (0.967). The adjusted coefficient of determination indicated that 98.9% of the variability in the response could be explained by the model. The quadratic model was significant (f -value = 169.92 and p -value < 0.0001), being supported by an insignificant lack-of-fit (p = 0.778) toward the response (η), meaning that the error predicted by the model was above the error of the replicas [50]. There is only 0.01% chance for a noise derived “Model F-Value”, which implies an adequate variation of the data around its mathematical mean; in addition, the estimated factor effects are real [183,256,294]. The statistical analysis indicates that the proposed model was adequate to predict the ingredients’ concentrations to obtain emulsions with higher viscosities. The same did not happen for E24, where the R^2 , adjusted R^2 , and predicted R^2 were 0.974, 0.941 and 0.718, correspondingly. The difference between the predicted R^2 and the adjusted R^2 was higher than 0.2, which may indicate a large block effect or a possible problem with the model and/or data.

The response of the RSM is shown in Figure 3.2.1A and 3.2.1B. The results suggest that cetyl alcohol and glycerine did not influence the E24 and η values. Moreover, FucoPol at 1.5 wt.% led to emulsions with η values above 206 Pa.s. Based on Figure 3.2.1, increasing the concentration of FucoPol resulted in more viscous emulsions, and more stable against coalescence, avoiding emulsions’ phase separation [183,295]. This is due to FucoPol’s ability to avoid droplets creaming and promote an increased viscosity of the formulation, as reported before (Chapter 1, Section 3). Based on these results, the ingredients concentrations that promoted higher η and E24 values were defined as: 1.5 wt.% FucoPol, 1.5 wt.% cetyl alcohol and 3.0 wt.% glycerine.

Table 3.2.3. Central composite design (CCD) with studied variables (A: FucoPol, B: Cetyl alcohol, C: Glycerine), experimental values E24 and η (apparent viscosity measured at a shear rate of 0.1 s^{-1}). Organoleptic characteristics and physical stability (centrifugation test) of experiments. SCV- (Smooth, creamy, viscous) OS- Olive smell, YW- yellowish white.

Run	FucoPol, A (wt.%)	Cetyl alcohol, B (wt.%)	Glycerin, C (wt.%)	E24 (%)	η (Pa.s)	Organoleptic Characteristics			Physical stability
						Colour	Apperance	Odour	
1	1.50	0.00	3.00	95	206	YW	SCV	OS	Yes
2	0.75	0.75	2.00	100	20	YW	SCV	OS	No
3	1.50	0.00	1.00	98	206	YW	SCV	OS	Yes
4	1.50	1.50	3.00	98	249	YW	SCV	OS	Yes
5	0.75	0.75	2.00	100	52	YW	SCV	OS	No
6	1.50	1.50	1.00	98	244	YW	SCV	OS	Yes
7	0.00	0.00	1.00	0.00	-	-	-	-	-
8	0.00	1.50	3.00	0.00	-	-	-	-	-
9	0.00	1.50	1.00	0.00	-	-	-	-	-
10	0.75	0.75	2.00	100	21	YW	SCV	OS	No
11	0.00	0.00	3.00	0.00	-	-	-	-	-

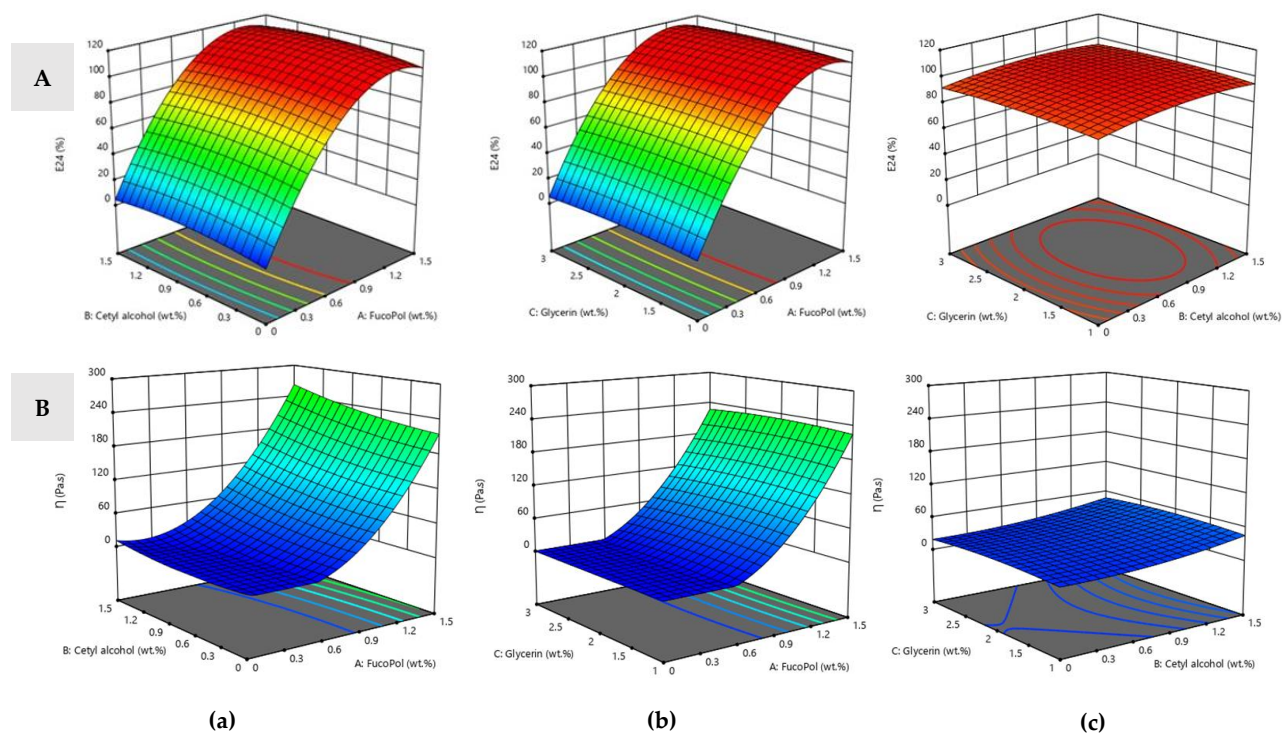


Figure 3.2.1. Three-dimensional response (A: E24; B: η) surface plot showing the interactive effects of different ingredients on the O/W emulsion. (a) FucoPol and cetyl alcohol (wt.%) with glycerine fixed at 2.0 wt.%, (b) FucoPol and glycerine (wt.%) with cetyl alcohol fixed at 0.75 wt.%, (c) cetyl alcohol and glycerine (wt.%) with FucoPol fixed at 0.75 wt.%.

3.2.3.3 Preparation of the emulsified formulations

To evaluate FucoPol's behaviour as an ingredient for cosmetic creams, three formulations were designed, all containing 1.5 wt.% FucoPol (formulations A, B and C) (Table 3.2.2). Formulation A was prepared with FucoPol as sole emulsifier, while formulation B additionally contained 1.5 wt.% cetyl alcohol as co-emulsifier. Formulation C was similar to formulation B but 3.0 wt.% glycerine was added to it as emollient (Table 3.2.2). Three other formulations were developed using synthetic emulsifying agents and compared with the FucoPol-based formulations. Formulations D and F were similar to formulation C, but FucoPol was replaced by stearic acid as main emulsifier at two concentrations, namely, 5.0 and 1.5 wt.%, respectively. Formulation E was similar to formulation F but the co-emulsifier cetyl alcohol was replaced by Sepigel® 305 (1.5 wt.%). Sepigel® 305 is a non-ionic synthetic hydrophilic polymer that provides increased viscosity and stability in cosmetic formulations [183,296]. Stearic acid, a solid saturated fatty acid [297] commonly present in cosmetic formulations (92–96% of products) [298,299] in concentrations between 1.0–25% for moisturizing skin care applications [300], was used as a non-ionic emulsifier. This emulsifier has been reported to induce increased cream viscosity, which results in hardening of the product during storage, especially when glycerine is added as humectant [301].

3.2.3.4 Characterization of the emulsified formulations

3.2.3.4.1 Physicochemical characterization

The freshly prepared formulations (Figure 3.2.2a) presented a yellowish white colour (except formulation A which was completely white) and had a slight olive oil odour. Macroscopic observation, throughout the 60-day storage period, showed the formulations maintained their homogeneous texture, with no visible oil/water phase separation, as confirmed by their EI that was kept unchanged (100%) (Figure 3.2.2b-c and Appendix 2). The formulations' physical stability (Figure 3.2.2d-e) was evaluated by the centrifugation test to check for the presence of phase separation [294], sedimentation, or creaming [302]. Formulations A and E remained stable for 60 days, showing no phase separation, while formulations B, C, D showed phase separation, and formulation F showed creaming after 30 days of storage (Appendix 3).

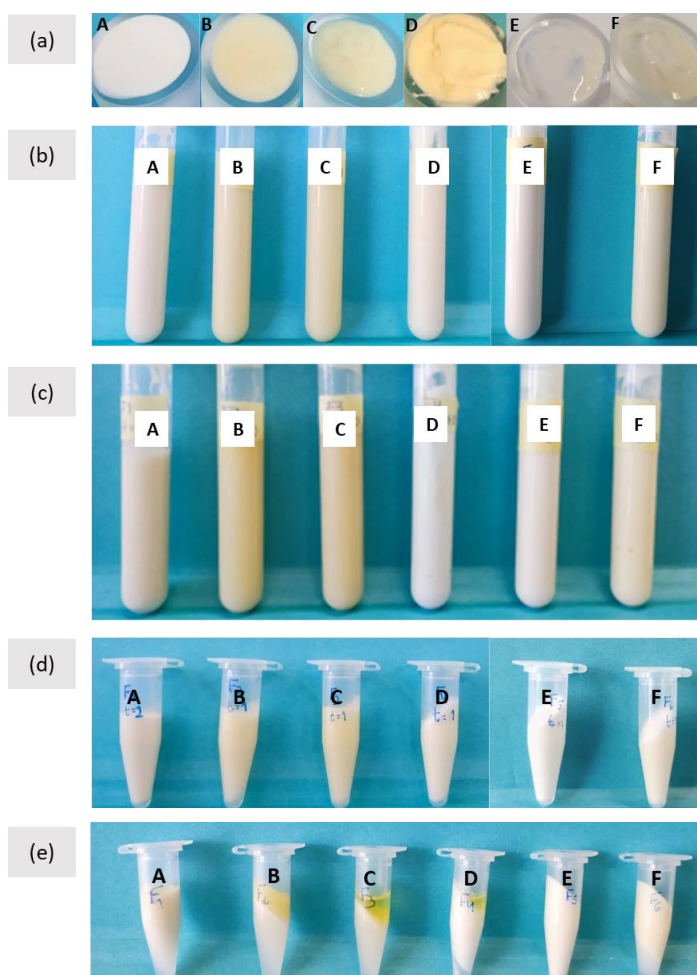


Figure 3.2.2. Formulations A, B, C, D, E, F: (a) freshly prepared formulations ($t=0$); (b) after 1 day; (c) after 60 days; centrifugation test for 1 day of storage (d) and for 60 days of storage (e).

As presented in Figure 3.2.3a, formulations B and C were slightly acidic with pH values in the range 6.3–6.9 throughout the storage period (60 days), whilst formulations A, D, E, and F had pH values above 7. Skin care products must not affect the acid-base balance of the skin's individual layers nor disrupt the *stratum corneum* barrier function [303]. Given the skin's surface pH (5.5), an acceptable

formulation should have a pH value ranging from 4.0 to 7.0 [294,304,305], to avoid skin irritation [242]. Interestingly, the pH value of formulation C (1.5 wt.% FucoPol, 1.5 wt.% cetyl alcohol, and 3.0 wt.% glycerine) was within the optimal range from 6.59 ± 0.01 to 6.30 ± 0.01 during the whole 60-day study period, supporting its suitability for use as a topical cream.

The conductivity value, which is indicative of the number of free ions and water present in the system [294], is used to detect physical modifications [306] and to assess if the formed emulsion is an O/W or a W/O system [276,305]. As observed in Figure 3.2.3a, formulation A showed a significant increase in the conductivity value (from 102 ± 0.6 to 283 ± 2.0 $\mu\text{S}/\text{cm}$) after 7 days of storage, while for formulations B and C the changes were less significant (from 106 ± 0.3 to 122 ± 0.2 $\mu\text{S}/\text{cm}$, and from 109 ± 0.9 to 107 ± 0.7 $\mu\text{S}/\text{cm}$). Conductivity stability over the 60-day storage period (Figure 3.2.3a) indicated an absence of physical changes for formulations C, D, and F. Formulations A, B, and C presented higher conductivity values (>100 $\mu\text{S}/\text{cm}$) corresponding to an O/W system, indicating that the aqueous phase is the continuous phase of the system, whereas the oil phase is nonconductive [276]. Formulations D, E, and F (<50 $\mu\text{S}/\text{cm}$) are considered W/O systems. This result corroborates the emulsion determination test (Figure 3.2.4a), and the microscopic observation (Figure 3.2.4b), where formulations A, B, and C droplets dispersed on the filter paper, thus confirming their O/W nature [168,183,187]; and showed compartmentalized structures characteristic of O/W systems, consisting of dispersed oil droplets in the aqueous phase [183,184]. Thus, these results confirm that FucoPol forms O/W emulsions, in contrast to Sepigel®305 and stearic acid under the same conditions. In addition to acting as an emulsifying agent, FucoPol appeared to have pH-lowering effect. As mentioned before, consumers prefer O/W emulsions due to their sensorial properties (easy to spread, non-greasy) [183,228,257] representing nearly 65% of the total emulsified products available in the cosmetic industry [307].

The formulations' physical stability was also assessed by measuring the droplet size during the storage period at room temperature (~ 20 °C). The distribution profile of oil droplets and their size influences the emulsion's stability, with smaller droplet sizes and lower PI values (<0.3) being responsible for higher stability [191,294,308–310]. As shown in Figure 3.2.3b, all formulations presented a droplet size characteristic of macroemulsions (>0.1 – 50 μm), experiencing a considerable increase in droplet size after 30 days of storage. This effect was less evident for formulation D (3.17 – 9.63 μm) that contained a higher concentration of stearic acid (5.0 wt.%) compared to formulation F (1.5 wt.% stearic acid), which suggests that higher emulsifier concentration allows a decrease of the droplet size and, consequently, an increased stability during storage [311]. At lower emulsifier concentrations, the droplet covering ability of the emulsion decreases, causing the coalescence of neighbour droplets that results on the formation of larger droplets [185]. Furthermore, non-ionic emulsifiers can reduce the droplet size of olive oil (triglycerides)-in-water emulsions [312]. For FucoPol containing formulations, the addition of cetyl alcohol and glycerine (formulation C, Figure 3.2.3b), allowed for a decrease of the droplet size (8.68 – 40.0 μm to 6.12 – 24.2 μm) and a slight increase of the stability during storage, when compared to formulation A. In general, the droplet size of an emulsion is determined by the homogenization technique applied, the environmental conditions, and ingredients used for its preparation [313]. Furthermore,

there are some technical issues to obtain small droplet size emulsions using polysaccharide-type emulsifiers [270]. The ideal monodisperse system should have a PI value lower than 0.3 [276,309], which was not verified in any of the formulations ($0.47 \leq \text{PI} \leq 5.02$ for $t=60$ days) indicating considerable polydisperse droplets sizes.

As shown in Figure 3.2.3b, the Zeta-potential of formulations A, B, C, E and F was -193 mV, -98.4 mV, -97.9 mV, -160 mV and -86.7 mV, respectively: with evident stability for formulation C during the storage period. The formulation is considered stable when the Zeta-potential value is more than $+25$ mV or lower than -25 mV [294]. However, some W/O emulsions are highly stable despite having low Zeta-potential values [314], such as formulation D that showed a rapid aggregation regardless of its absolute Zeta-potential value (0.0 mV) [315].

Section 3. Chapter 2. Development of Olive Oil and α -tocopherol containing Formulations

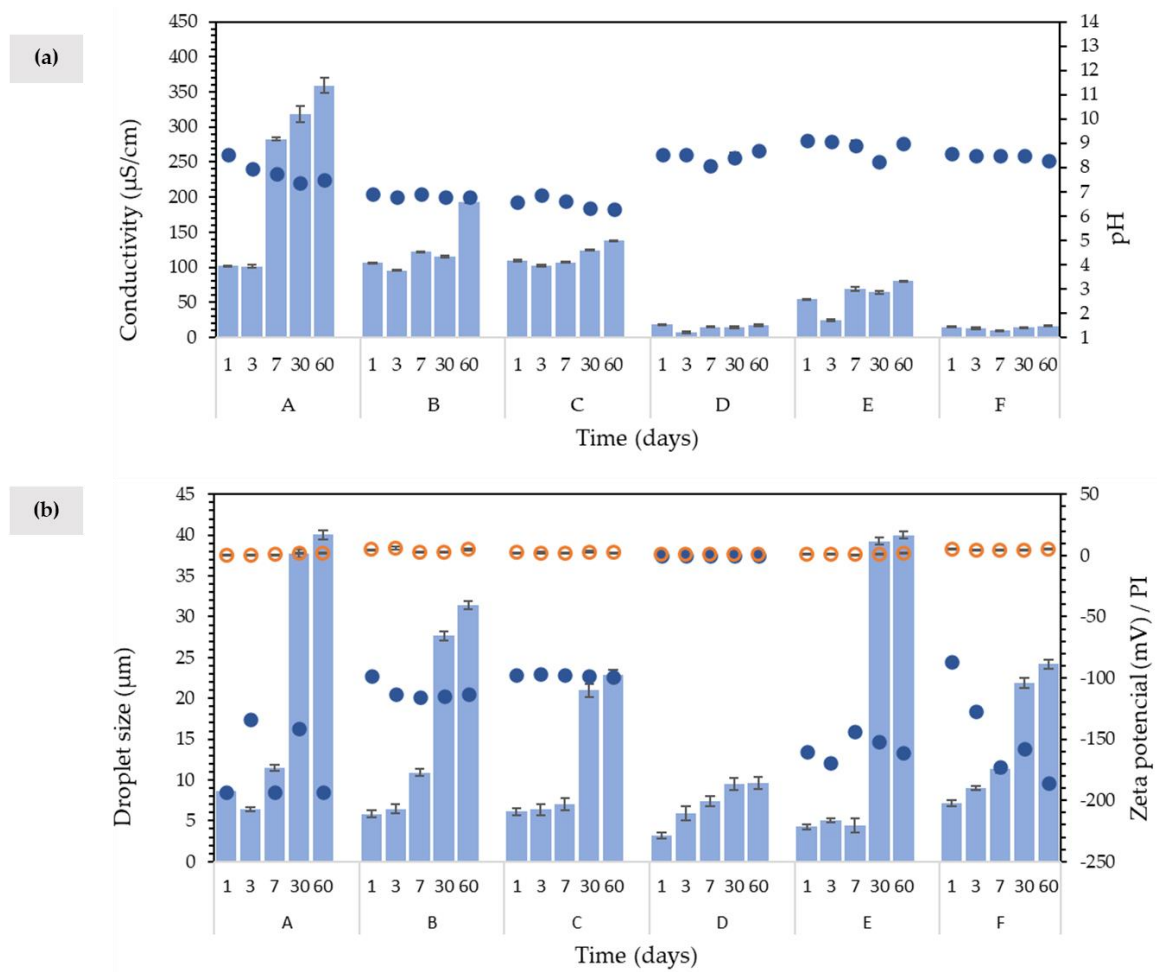


Figure 3.2.3. (a) pH (circles) and conductivity (bars) and (b) droplet size (bars), Zeta-potential (blue circles), and PI (orange circles) for formulations A-F during the storage period ($t=1, 3, 7, 30, 60$ days).

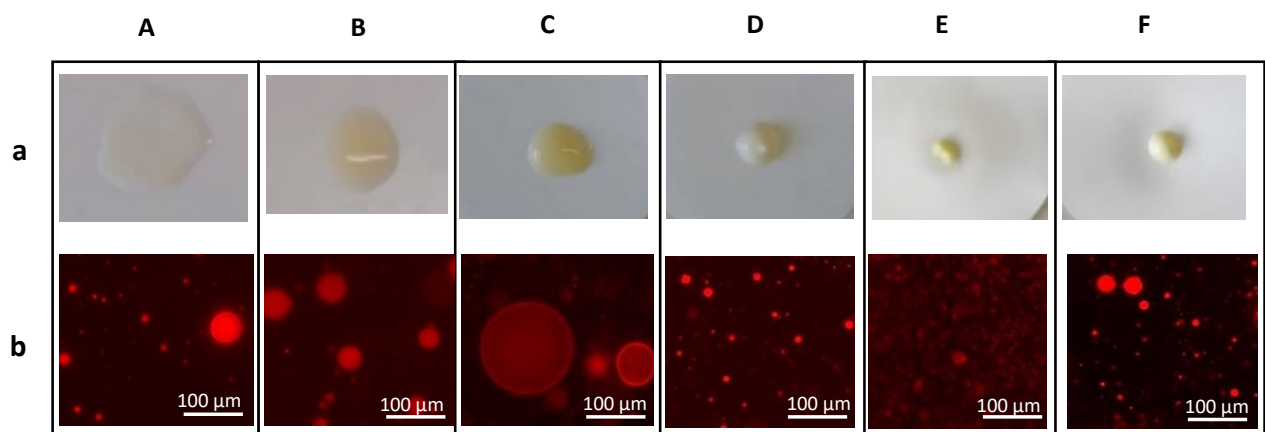


Figure 3.2.4. Formulations (A, B, C, D, E, F) after 1 day of preparation: (a) Emulsion determination test by filter paper wetting; (b) fluorescence optical microscopic (40x) images of formulations after Nile Blue A staining.

3.2.3.4.2 Apparent viscosity and viscoelastic properties

All formulations exhibited a similar shear-thinning behaviour to the torque response, as the viscosity gradually decreased under increasing shear rates (Figure 3.2.5). The viscosity decrease under a shear rate is attributed, in shear-thinning emulsions, to their semi-flexible molecular structure [235]. Except for Formulation E (Figure 3.2.5e), all formulations exhibited a slight decrease of viscosity during the storage time. As mentioned before, formulations containing stearic acid became hard during storage, corroborated by the increase in viscosity values over the storage time.

A cosmetic preparation stability over storage time is related to its tendency to exhibit changes in particle migration [303]. In fact, for the FucoPol-based formulations (Figure 3.2.5a-c, Table 3.2.4), compared to formulation A (8.7 Pa.s), there was an increase of the viscosity to 19.5 Pa.s in formulation B with the addition of 1.5 wt.% cetyl alcohol (Figure 3.2.5b); in formulation C (Figure 3.2.5c) the addition of both glycerine (3.0 wt.%) and cetyl alcohol (1.5 wt.%) further increased the viscosity to 34.3 Pa.s. This demonstrates that, contrary to the result obtained in section 2.2.3.2, glycerine and cetyl alcohol led to increased apparent viscosity. This may be due to the homogenization method applied (mechanical homogenization *vs* manual homogenization) or to the upscale, from 5 g to 100 g, which possibly changes the behaviour and efficiency of the ingredients [191]. Comparing formulations C (34.3 Pa.s) and F (6.2 Pa.s) (Table 3.2.4), it is possible to conclude that, for the same emulsifier concentration (1.5 wt.%), FucoPol conferred significantly higher apparent viscosity than stearic acid.

As shown in Table 3.2.4 and Appendix 4, all formulations showed solid-like behaviour, with the storage module higher than the loss module ($G' > G''$ at 0.1 Hz). This behaviour was more pronounced in formulations D, E, and F, meaning that these formulations present a strong network [235,273,316] with higher stability. Formulations A, B, and C showed a weak gel rheological pattern with an increasing difference between G' and G'' values as the frequency increases from 0.01 to 10 Hz. This behaviour indicated a dominance of the elastic components over the viscous components of the system, and that physical bonds between the macromolecules held the system's structure [204]. Figure 3.2.6 illustrates the structural stability for the first day and after 60 days of storage at room temperature. The formulations containing a synthetic emulsifier showed much higher values of G' and G'' than FucoPol. The G' and G'' modules of most formulations decreased with storage time, except for formulations E and F, suggesting more structured systems which can influence the spreading behaviour [191]. For formulations A and B, it was visible a crossover at 0.01 Hz at $t=1$ day, while for $t=60$ days the crossover occurs at higher frequencies (0.3 Hz for formulation A, and 0.03 Hz for formulation B). For formulation C, G' gradually became bigger than G'' during the whole frequency range investigated (0.01 - 10 Hz). Similar behaviour has been reported for bacterial cellulose emulsions [316].

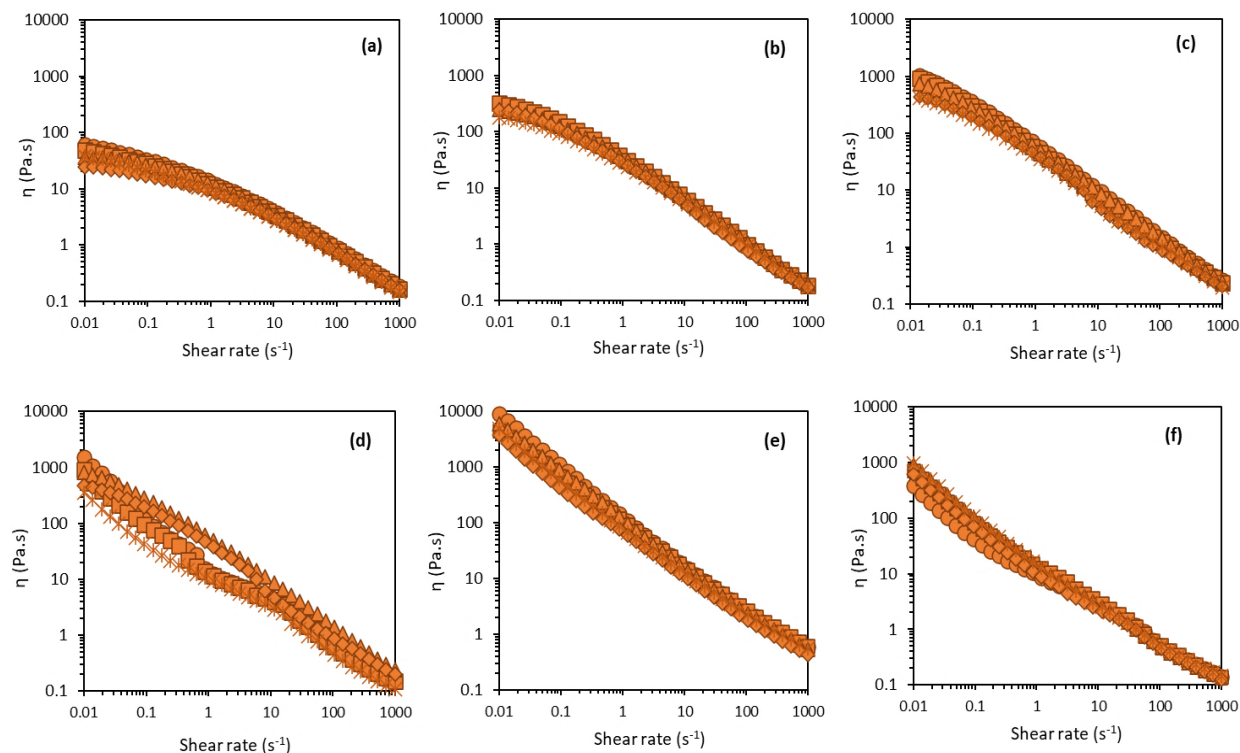


Figure 3.2.5. Flow curves for the prepared formulations: A (a), B (b), C (c), D (d), E (e), and F (f) during the storage time; $t=1$ day (circles), $t=3$ days (squares), $t=7$ days (triangles), $t=30$ days (diamonds), and $t=60$ days (asterisk).

Table 3.2.4. Apparent viscosity (η , measured at 2.30 s^{-1}) and viscoelastic parameters (G' , G'') at room temperature ($\sim 20^\circ \text{C}$) for the emulsified formulations (A, B, C, D, E, F), for different storage times. G' -storage/elastic modulus and G'' - loss/viscous modulus at $f=0.1 \text{ Hz}$.

Time (days)	A			B			C		
	η (Pa.s)	G' (Pa)	G'' (Pa)	η (Pa.s)	G' (Pa)	G'' (Pa)	η (Pa.s)	G' (Pa)	G'' (Pa)
1	8.72	64.8	36.6	19.5	94.6	55.7	34.3	137	58.8
3	7.91	41.8	29.8	19.7	53.2	38.0	27.2	87.1	43.4
7	7.97	23.8	22.8	19.6	78.8	48.5	30.6	151	59.2
30	6.42	21.1	19.3	16.0	58.2	36.5	23.7	82.5	40.1
60	6.10	11.8	14.9	15.5	35.1	28.2	22.4	56.2	35.2
Time (days)	D			E			F		
	η (Pa.s)	G' (Pa)	G'' (Pa)	η (Pa.s)	G' (Pa)	G'' (Pa)	η (Pa.s)	G' (Pa)	G'' (Pa)
1	8.75	949	249	59.6	1329	94.2	6.19	286	75.6
3	8.30	708	198	54.9	1219	84.7	8.72	267	72.7
7	8.97	573	146	54.0	1349	97.7	7.51	269	74.6
30	6.98	492	188	36.0	1217	98.9	5.83	284	92.4
60	6.57	483	125	38.8	1262	93.9	7.69	269	80.1

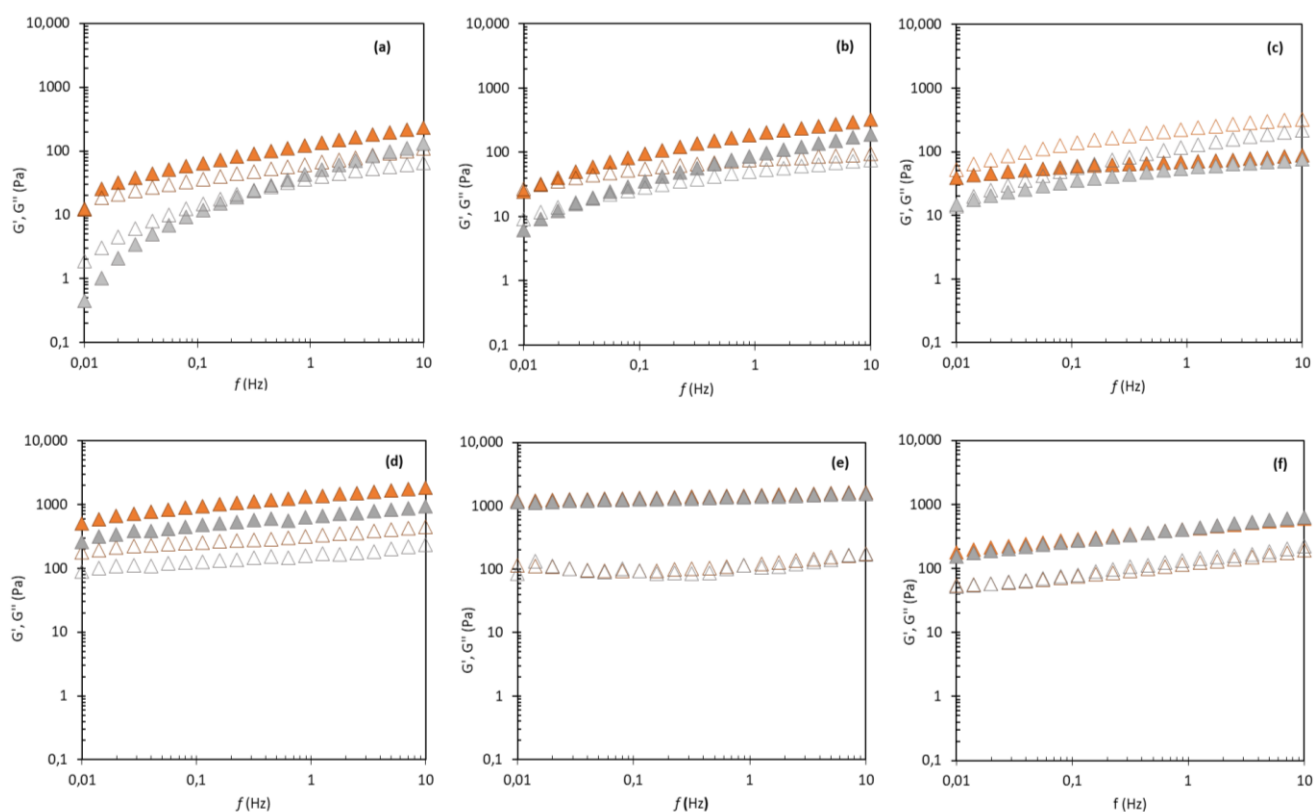


Figure 3.2.6. Mechanical spectrum for formulations A (a), B (b), C (c), D (d), E (e), and F (f), at 1 day (orange) and 60 days (gray) of storage: G' (closed triangle) and G'' (open triangle).

3.2.3.4.3 Textural Assessment

The textural parameter values (firmness, consistency, cohesiveness, and adhesiveness) of the prepared emulsified formulations are summarized in Table 3.2.5. In general, at the end of the storage time (60 days), a decrease of the firmness, consistency, and adhesiveness of the formulations was observed. However, there are some relevant considerations for the FucoPol-based formulations: the addition of glycerine and cetyl alcohol increased not only their apparent viscosity, but also their firmness and cohesiveness. In fact, the addition of cetyl alcohol increased the firmness from 0.064 N (formulation A) to 0.162 N (formulation B), while further adding glycerine (formulation C) resulted in increased firmness (0.194 N). These results are concordant with the η values (Table 3.2.4), where formulation A exhibited lower apparent viscosity (8.72 Pa.s) than formulation C (34.3 Pa.s).

Spreadability is an important texture parameter which infers on the product's contact with skin (i.e., how it feels on the touch) and ease of removal from packaging, which may affect utilization compliance [317,318]. This parameter is crucial in cosmetic emulsion development being a decisive factor for consumers' approval of products [183,268]. Formulation A at $t=1$ day showed lower firmness (0.064 N) and consistency (0.261 mJ) values, indicating a more spreadable cream sample [183]. On the other hand, formulations C and E showed lower spreadability than the other. Consistency, a textural parameter directly influenced by viscosity, determines the cosmetic formulation application on the skin (higher

consistency means higher difficulty of application and vice-versa) [303]. In terms of adhesiveness, formulations B (0.467 mJ), C (0.387 mJ) and E (0.499 mJ) seemed to be more adhesive than formulations A (0.244 mJ), D (0.338 mJ), and F (0.317 mJ). For FucoPol-based formulations, glycerine and cetyl alcohol positively impacted the physical characteristics. These results are consistent with the rheology assays.

Table 3.2.5. Numerical values of the textural parameters for formulations tested of t=1 and t=60 at room temperature.

Formulation	Time (days)	Textural parameters			
		Firmness (N)	Consistency (mJ)	Cohesiveness (N)	Adhesiveness (mJ)
A	1	0.064	0.261	0.741	0.244
	60	0.029	0.119	0.970	0.133
B	1	0.162	0.505	0.925	0.467
	60	0.088	0.198	0.921	0.266
C	1	0.194	0.387	1.034	0.387
	60	0.047	0.160	1.004	0.129
D	1	0.115	0.445	0.931	0.338
	60	0.067	0.225	0.891	0.169
E	1	0.136	0.504	0.852	0.499
	60	0.086	0.231	1.087	0.188
F	1	0.097	0.319	0.976	0.317
	60	0.049	0.273	0.844	0.126

3.2.3.5 Comparison of FucoPol-based formulation with commercial cosmetic cream

Formulation C (after 60 days of storage) was compared to several cosmetic products available in the market in terms of pH, conductivity, droplet size, physical stability (by centrifugation test), and rheological and textural parameters. In the centrifugation test to assess the physical stability, formulation C showed phase separation, while Sephora® hand cream showed sedimentation (Appendix 5). As shown in Table 3.2.6, Formulation C presented a pH value similar to Uriage® Xémose (face cream) (6.68) but lower than the other tested commercial products, such as Shiseido® primer (8.17) and Sephora® hand cream (8.18). These values are higher than the optimal pH range (between 4.0 and 7.0) compatible with human skin. Nonetheless, the droplet sizes of Shiseido® primer (22.0 μm) and Sephora® hand cream (27.9 μm) are very similar to that of Formulation C (24.2 μm). In terms of rheological parameters, Formulation C and Uriage® Xémose presented higher apparent viscosity values, 23.7 Pa.s and 25.9 Pa.s, respectively, and showed a similar viscoelastic profile to Shiseido® primer. Uriage® Xémose and Formulation C displayed very similar textural parameters, which suggests that Formulation C has adequate sensory characteristics for a face cream. In general, Formulation C seems to have suitable physical characteristics to be used in cosmetic products, being, in some cases, equal or superior to the tested commercial products.

Section 3. Chapter 2. Development of Olive Oil and α -tocopherol containing Formulations

Table 3.2.6. Rheological parameters and textural parameters of commercial products tested. Apparent viscosity (η , measured at 2.30 s^{-1}) and viscoelastic parameters (G' , G'') measured at room temperature ($\sim 20 \text{ }^\circ\text{C}$). G' -storage/elastic modulus and G'' - loss/viscous modulus, at $f=0.1 \text{ Hz}$.

Product	pH	Conductivity ($\mu\text{S/cm}$)	Droplet size (μm)	Rheological Parameters			Textural Parameters			
				η ($\text{Pa}\cdot\text{s}$)	G' (Pa)	G'' (Pa)	Firmness (N)	Consistency (mJ)	Cohesiveness (N)	Adhesiveness (mJ)
Cien® Body lotion	5.78	739	15.9	12.1	800	156	0.056	0.329	0.832	0.273
Uriage® Pruriced	7.95	727	13.5	14.2	25.1	9.27	0.062	0.224	0.980	0.245
Shiseido® Primer	8.17	257	22.0	6.93	207	57.6	0.068	0.198	0.897	0.193
Sephora® Hand cream	8.18	105	27.9	73.4	5575	625	0.190	0.699	0.931	0.471
Uriage® Xémore	6.68	510	19.0	25.9	25.1	9.27	0.130	0.543	1.049	0.449
Formulation C	6.30	138	24.2	23.7	203	68.7	0.047	0.117	0.943	0.192

3.2.4 Conclusions

This study demonstrates FucoPol's suitability for the development of emulsified formulations with good physical and chemical properties for their utilization as cosmetic creams. The fucose-rich biopolymer has shown to possess great potential to replace stearic acid as an emulsifier, resulting in emulsions with similar stability, viscosity, firmness, spreadability and droplet size, which were also shown to be comparable to commercial creams. However, there are still some challenges to overcome in the development process of a completely new cosmetic formulation containing FucoPol. For instance, adjusting ingredients concentration (increasing [FucoPol] and/or [stearic acid]; decrease in Olive Fruit Oil) could reduce the loss of physical stability after 30 days of storage displayed by Formulation C in this study. Increase in the homogenization time could also be decisive to increase the product stability overtime by lowering the droplet size. Preparing emulsions on a temperature-controlled environment can eliminate temperature variations that may have contributed to the disruption of the system. Accelerated stability tests can be applied to assess the formulation behaviour at different storage temperatures, inferring about the ideal packaging system and storage conditions. Although further tests must be done to fine tune the formulations, the results obtained substantiate the relevance of FucoPol in the development of topical formulations.

Development of cosmetic formulations with L- ascorbic acid stabilized by FucoPol

The results presented in this chapter are part of the following paper:

Baptista, S.; Baptista, F.; Freitas, F. Development of cosmetic formulations with L- ascorbic acid stabilized by FucoPol. In preparation

This page was intentionally left blank

Summary

The main function of vitamin C, as an antioxidant, is to combat free radicals and prevent premature aging, smoothing wrinkles, and expression lines. In addition, it acts directly on the depigmentation and prevention of blemishes on the skin. In this chapter, L-ascorbic acid was added to the FucoPol-based formulation developed in the previous chapter. The optimized formulations were obtained with L-ascorbic acid 8.0 wt.% for *Olea europaea* oil (Formulation C1) with a η value of 2.71 Pa.s (measured at shear rate of 2.3 s^{-1}) and $E_{24} = 96\%$, and 15 wt.% for *Prunus Amygdalus dulcis* (Formulation C2) with a η value of 5.15 Pa.s (at a shear rate of 2.3 s^{-1}) and $E_{24} = 99\%$. The stability of FucoPol-based creams containing L-ascorbic acid was investigated during 45 days at 4 °C, 20 °C and 30 °C. The results showed that all formulations maintained the organoleptic characteristics until 45 days, with minimal pH variations. However, the resulting Zeta-potential ($> -25 \text{ mV}$) indicated lower emulsion stability when compared to FucoPol-based formulation developed in the previous chapter (-98 mV). The accelerated stability tests proved the formulations' stability at 4 °C with $EI = 95\%$ for C1 and $EI = 100\%$ for C2. The rheological assessment demonstrated that the formulation presents a shear-thinning and liquid-like behaviour.

3.3.1 Introduction

Constituting 36% of the global cosmetic market, the skincare market is one of the leaders of the cosmetic industry. Product-wise, skin health enhancement and aging reduction demand by consumers have prompted the industry to include bioactive ingredients, such as vitamins (e.g., vitamin C), in their formulations [319]. The biologically active form of vitamin C, also known as ascorbic acid, possesses well-known positive effects on the skin [320–323], acting as an antioxidant to treat oxidative damage (photoaging). Ascorbic acid action as an antioxidant is based on its specificity to neutralize reactive oxygen species, such as free oxygen radicals, superoxide, and hydroxyl, preventing molecular processes that lead to the skin's photoaging [322,324]. It has also been reported as a cofactor in collagen synthesis which reduces wrinkles, and as a tyrosinase inhibitor helping to reduce hyperpigmentation [325,326]. For these reasons, this ingredient is widely used in pharmaceutical and cosmetic formulations [301,322,324].

Ascorbic acid is highly soluble in water, being easily oxidized and forming dehydroascorbic acid in its solubilized form [322,325]. Although ascorbic acid oxidation is an issue during storage, it depends on several factors such as temperature, light, pH and storage conditions and can happen in aerobic and anaerobic conditions [321–323,325,327]. Ascorbic acid oxidations occur at its highest rate under alkaline conditions and high temperatures ($> 50 \text{ °C}$) and its reaction with O_2 can be catalyzed by the presence of metal ions [328,329]. Ascorbic acid can be administered to skin cells by either topical or local routes [322]. However, being a hydrophilic molecule, ascorbic acid penetration in the lipophilic *stratum corneum* is deficient. L-ascorbic acid, the most used form of ascorbic acid in cosmetics, is an anionic molecule, further limiting skin penetration [322,326,330].

Ascorbic acid presents synergistic interactions with α -tocopherol, a lipid-soluble antioxidant in low-density lipoprotein and lipid membrane oxidation. In fact, ascorbic acid has been suggested as a regenerator of α -tocopherol from the formed α -tocopherol radicals by several studies which reported the increase of antioxidant effects of α -tocopherol in the presence of ascorbic acid [322,324,329–331]. Therefore, in skin care formulations, the combined utilization of both ingredients has been suggested [301,322]. Ascorbic acid is responsible for the protection of cellular aqueous compartments and α -tocopherol protects lipid structures by inhibiting lipid peroxyl radicals' propagation [332–334]. Additionally, protection against erythema and sunburn cell formation in topical application was reported [334]. The combination of L-ascorbic acid 15% and α -tocopherol 1.0% promoted, in comparison to stand alone formulations of each ingredient, greater protection against erythema and prevented the formation of thymine dimers formation, as reported by Yi et al. [331]. Regarding L-ascorbic acid instability in aqueous solution, several derivatives have been used by the cosmetic industry, such as ascorbyl 6-palmitate, tetra-isopalmitoyl ascorbate, magnesium ascorbyl phosphate, sodium ascorbyl phosphate, ascorbyl 2-glucoside, ascorbyl 2-phosphate-6-palmitate, and 3-O-ethyl ascorbate [322,335]. The necessary enzymatic conversion to free ascorbic acid in the skin assigns a relatively low topical efficiency for these derivatives [333–335].

Topical formulations pH is decisive for the bioavailability of their ingredients. Hence, the introduction of ascorbic acid in cosmetic and dermatological formulations, such as O/W microemulsions, O/W and W/O emulsions and W/O/W emulsions [323,334], results in slower degradation rates of ascorbic acid at higher pH values, comparing to aqueous solutions [332], which suggests a higher protection of ascorbic acid in emulsions. Natural oils, widely present in pharmaceutical formulations, are penetration enhancement agents, serving also as sources of several bioactive compounds [240,336,337]. Therefore, these natural agents present a valid alternative to synthetic materials, enabling the percutaneous absorption of topical formulation ingredients into the lower skin layers [338]. In fact, free fatty acids, present in natural oils, have been reported to fluidize and reversibly disintegrate *stratum corneum* lipids which modifies the skin barrier [336]. Moreover, carrier oils or fatty acid-containing natural oils have been reported to enhance transdermal penetration of hydrophilic and lipophilic compounds [339,340]. Olive oil [341–344] and almond oil [344,345] have been reported to have similar skin permeation effects.

The objective of the present study was to evaluate the effect of L-ascorbic acid concentration in a FucoPol-based cosmetic cream developed in the previous Chapter 2 (Section 3). The replacement of olive oil by almond oil in the formulation was also evaluated. FucoPol-based cosmetic formulations were prepared and characterized in terms of physical and accelerated stability, rheological, and textural properties.

3.3.2 Materials and methods

3.3.2.1 Materials

Olea europaea fruit oil and *Prunus amygdalus dulcis* oil were purchased from a local market. α -tocopherol, L-ascorbic acid, methyl paraben and cetyl alcohol were acquired from Sigma-Aldrich (Munich, Germany). Triethanolamine (TEA) was acquired from Acros Organics B.V.B.A. (Geel, Belgium), and glycerine was acquired from Honeywell (Seelze, Germany). FucoPol was produced and purified by ultrafiltration with a 30 kDa membrane according to the method previously described in Section 2, Chapter 1 (2.1.2.1 and 2.1.2.2). FucoPol was composed of 40 mol% fucose, 29 mol% glucose, 24 mol% galactose, and 7.0 mol% glucuronic acid, with a total acyl groups content of 11.6 wt.%. The sample had protein and inorganic salts contents of 8.2 wt.% and 4.0 wt.%, respectively.

3.3.2.2 Preparation of FucoPol-based emulsions

The emulsions were prepared by heating the oil phase (1.63 g) comprising either olive oil (30 wt.%) or almond oil (30 wt.%), cetyl alcohol (0.0–2.0 wt.%) and α -tocopherol (2.5 wt.%), and the aqueous phase (3.37 g) comprising FucoPol (1.5 wt.%), glycerine (1.0–3.0 wt.%), TEA (0.5 wt.%) and methyl paraben (0.02 wt.%) at 75 °C in a recirculated heated water bath Thermomix® ME (B.Braun, Melsungen, Germany). L-ascorbic acid (5.0, 8.0, 10 and 15 wt.%) was added to the aqueous phase. The aqueous phase involved an extra pH adjustment step (made with TEA) to achieve a pH close to 5.5. The mixtures were emulsified by manual agitation for 40 s, followed by vortex agitation for 10 s. The emulsification index (EI, %) after 24 hours (E24, %) was determined as previously described in Section 2, Chapter 1 (2.1.2.5).

3.3.2.3 Preparation of FucoPol-based emulsion formulations

Two FucoPol-based formulations (C1 and C2) were prepared according to Table 3.3.1. The FucoPol-based cream C developed in Section 3, Chapter 2, was supplemented with L-ascorbic acid (formulation C1). Formulation C2 was also based on formulation C but *Olea europaea* fruit oil was replaced by *Prunus amygdalus dulcis* oil. The formulations were prepared following the method previously described in Section 3, Chapter 2 (3.2.2.3). The aqueous phase involved an extra pH adjustment step (made with TEA) to achieve a pH close to 5.5. All formulations were prepared in batches of 100 g.

Table 3.3.1. Cosmetic formulation composition (wt.%). q.s- quantity sufficient

INCI name	Function	Concentration (wt.%)	
		C1	C2
Aqueous phase			
Water	Solvent	q.s. 100	q.s. 100
FucoPol	Emulsifier agent	1.5	1.5
L-ascorbic acid	Antioxidant	8.0	15
Glycerine	Emollient/humectant	3.0	3.0
Methyl paraben	Preservative	0.02	0.02
TEA	pH regulator	q.s.	q.s.
Oil phase			
Cetyl alcohol	Co-emulsifier agent	1.5	1.5
<i>Olea europaea</i> (Olive) fruit oil	Oil, dispersed phase	30	-
<i>Prunus amygdalus dulcis</i> (almond) oil	Oil, dispersed phase	-	30
α -tocopherol	Antioxidant	2.5	2.5

3.3.2.4 Formulations' characterization

The complete physicochemical characterization was performed according to the methods previously described in Section 3, Chapter 2 (3.2.2.4) during the storage period (t=1, 3, 7, and 45 days). Additionally, the accelerated stability tests were performed to investigate the effect of the temperature in cosmetic formulations stability after 45 days at 4 °C and 30 °C.

3.3.3 Results and discussion

3.3.3.1 Defining L-ascorbic acid concentration in the emulsions' continuous phase

The FucoPol-based emulsion formulation C (developed in Section 3, Chapter 2) was supplemented with different L-ascorbic acid concentrations (5.0, 8.0, 10 and 15 wt.%) to assess those that achieve high EI at 24 h (E24) concomitant with high apparent viscosity. Additionally, the same four concentrations of L-ascorbic acid were evaluated in another FucoPol-based emulsion formulation, similar to C, but in which *Olea europaea* fruit oil was replaced by *Prunus amygdalus dulcis*. *Prunus amygdalus dulcis* is a non-toxic, non-irritating, non-sensitising and non-comedogenic ingredient, being an easily emulsifiable and water insoluble oil with positive spreading coefficient and a high solubility effect in lipophilic cosmetic raw materials. These penetrating, moisturising, and restructuring properties are widely appreciated in the cosmetic industry, with this oil being present in several cosmetic products [230,231].

Figure 3.3.1 shows the emulsions' macroscopic appearance after 24 h of preparation. The *Olea europaea* fruit oil containing emulsions presented a yellow colour and a slight olive odour, whilst those containing *Prunus amygdalus dulcis* displayed a white colour and smooth almond scent. *Olea europaea* fruit oil emulsions presented high E24 values that ranged between 89-96% for all tested L-ascorbic acid concentrations, (Table 3.3.2.). This indicates a direct effect of L-ascorbic acid in the obtained emulsion, as increasing the L-ascorbic acid concentration translated into the increase of the emulsification capacity, supported by higher E24 values at higher L-ascorbic acid concentrations. In the same conditions, the addition of L-ascorbic acid decreases the E24 value by 2.0%, when compared to FucoPol-based emulsion formulation C (developed in Section 3, Chapter 2). For the emulsions with *Prunus amygdalus dulcis*, the E24 was similar for all L-ascorbic acid concentrations (98-99%), meaning that emulsion formation and maintenance was not affected by the presence of L-ascorbic acid at the tested concentrations.

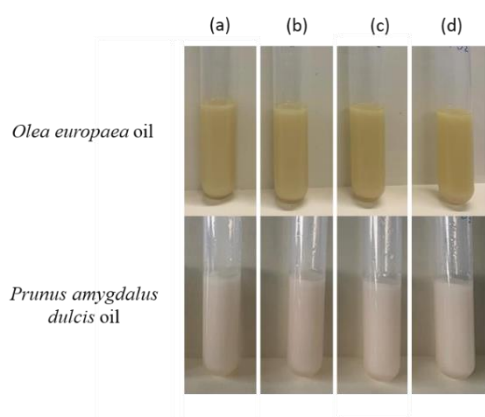


Figure 3.3.1. FucoPol-based emulsions prepared with *Olea europaea* fruit oil and *Prunus amygdalus dulcis* oil, supplemented with different L-ascorbic acid concentrations: (a), 5.0 wt.%; (b), 8.0 wt.%; (c), 10 wt.%; (d), 15 wt.%.

Table 3.3.2. pH, conductivity, E24, and apparent viscosity (η , measured at 2.30 s^{-1}) for the emulsified emulsions with different L-ascorbic acid concentrations. *Data obtained under the same manufacturing and scale conditions.

Natural oil	L-ascorbic acid (wt.%)	pH	Conductivity ($\mu\text{S/cm}$)	E24 (%)	η (Pa.s)
<i>Olea europaea</i>	5.0	5.54	1638 \pm 37	89 \pm 0.0	3.33
	8.0	5.51	1570 \pm 51	96 \pm 0.0	2.71
	10	5.60	1788 \pm 29	96 \pm 0.0	2.52
	15	5.52	2304 \pm 28	96 \pm 0.0	1.92
<i>Prunus Amygdalus dulcis</i>	5.0	5.53	910.3 \pm 19	98 \pm 0.0	3.23
	8.0	5.60	1316 \pm 21	98 \pm 0.0	3.82
	10	5.59	1624 \pm 22	98 \pm 0.0	4.59
	15	5.57	1845 \pm 31	99 \pm 0.0	5.15
Formulation C*	-	6.30	138	98 \pm 0.0	28.1

Due to the acid character of L-ascorbic acid [346], the preparation of the aqueous phase involved an extra pH adjustment step (made with TEA) to achieve a pH close to 5.5, the skin surface pH value [294], and within the range (4.0 to 7.0) reported for topical formulations [294,304]. All emulsions presented initial pH values of 5.6 ± 0.03 , which were kept after 24 h. The conductivity values (Table 3.3.2) indicate that the emulsions are O/W systems, due to the high conductivity values obtained (910.3–2304 $\mu\text{S/cm}$) [276,347]. Nevertheless, for *Prunus amygdalus dulcis* oil emulsions, the conductivity increased with increasing L-ascorbic acid concentration (from 910.3 $\mu\text{S/cm}$ to 1845 $\mu\text{S/cm}$), while the conductivity increase for *Olea europaea* oil emulsions was less significant (from 1638 $\mu\text{S/cm}$ to 2304 $\mu\text{S/cm}$).

In terms of rheological properties (Figure 3.3.2 and Appendix 6), all emulsions exhibited a shear thinning behaviour (Figure 3.3.2) to the torque response characteristic of FucoPol-based formulations (studied in previous chapter 2), as the viscosity gradually decreased under increasing shear rates [50]. The emulsions with *Olea europaea* oil (Table 3.3.2) displayed a slight decrease of the apparent viscosity (from 3.33 Pa.s to 1.92 Pa.s, measured at a shear rate of 2.30 s^{-1}) for increasing L-ascorbic acid concentrations (from 5.0 to 15 wt.%, respectively). Contrarily, for *Prunus amygdalus dulcis* oil (Table 3.2.2), the apparent viscosity of the emulsions gradually increased (from 3.23 Pa.s to 5.15 Pa.s, at 2.30 s^{-1} , with L-ascorbic acid concentration increasing from 5.0 to 15 wt.%, respectively). Comparing with FucoPol-based emulsion formulation C, the supplementation with L-ascorbic acid resulted in an abrupt decrease in apparent viscosity in the same conditions (Table 3.3.2). Olive oil and almond oil have different fatty acid compositions, with *Olea europaea* oil being composed mainly by 68–80% oleic (C18:1), 9.3-12.5% palmitic (C16:0), 4.6-12% linoleic (C18:2), and 0.42-1.91% linolenic (C18:3) acid [348–350], and *Prunus amygdalus dulcis* oil being mainly constituted mainly by 65–74% oleic (C18:1), 18–25%

linoleic (C18:2) and 6–7% palmitic acid (C16:0) [231]. The carbon content and structural differences of oils have been reported to be decisive factors determining an emulsion viscosity [351]. In addition, a higher amount of double bonds present in the molecular structure of an oil lead to lower apparent viscosity values [318]. The addition of L-ascorbic acid may interact with the oil constituents differently, leading to the formation of smaller droplets with almond oil thus increasing the viscosity; whilst the interaction between L-ascorbic acid and *Olea europaea* oil molecules leads to higher droplet size formation, which decreases the emulsion's viscosity. The observation of droplet size formed with both oils and its evolution with increasing L-ascorbic acid concentrations during the formulation preparation could confirm this assumption.

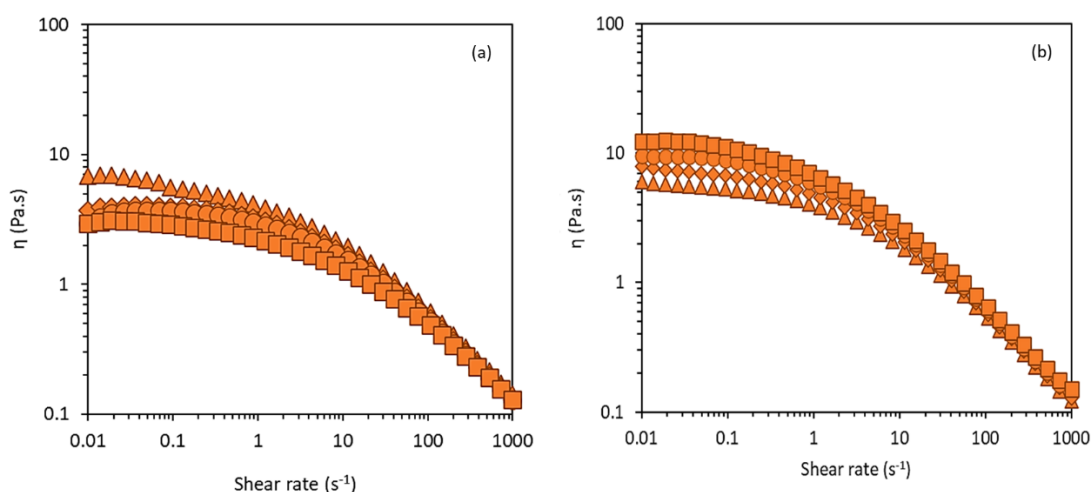


Figure 3.3.2. Flow curves for the FucoPol-based emulsions (analysed after 24 hours of preparation) with (a) *Olea europaea* fruit oil, (b) *Prunus amygdalus dulcis* oil, supplemented with L-ascorbic acid at concentrations of: 5.0 wt.% (triangles), 8.0 wt.% (diamonds), 10 wt.% (circles), and 15 wt.% (squares).

3.3.3.2 Preparation of the emulsified formulations with L-ascorbic acid

Two formulations (C1 and C2) were designed based on FucoPol-based cream developed in Section 3, Chapter 2. The L-ascorbic acid concentration for each formulation was chosen considering the results obtained for *Olea europaea* and *Prunus amygdalus dulcis* oils considering apparent viscosity value as a decision factor. Thus, the L-ascorbic acid concentration chosen for the *Olea europaea* oil was 8.0 wt.% with a η value of 2.71 Pa.s (measured at shear rate of 2.3 s^{-1}) and $E_{24} = 96\%$, and 15 wt.% for *Prunus Amygdalus dulcis* with a η value of 5.15 Pa.s (at a shear rate of 2.3 s^{-1}) and $E_{24} = 99\%$. For cosmetic formulations containing ascorbic acid, the optimal concentration to have a required effect must be higher than 5.0 wt.% [322,352], which was also a decision factor. Formulations were formed by mechanical homogenization.

3.3.3.3 Characterization of FucoPol-based emulsified formulations

3.3.3.3.1 Organoleptic characteristics and physical stability

Regarding the macroscopic observation of the freshly prepared formulations (Figure 3.3.3a), formulation C1 presented a yellowish white colour and a slight olive oil odour characteristic of the FucoPol-based cream C (formulated in Section 3, Chapter 2). Formulation C2 presented a bright white colour and slight marzipan odour due to the presence of almond oil. Throughout the 7-day storage period, the formulations maintained their homogeneous texture, with no visible oil/water phase separation, also confirmed by their unchanged EI (100%) (Figure 3.3.4a). After forty-five days of storage both formulations lost stability evidenced by decrease in the emulsification to 90% for formulation C1 and to 93% for formulation C2. The formulations also maintained the initial colour during the storage period, indicating no detectable L-ascorbic acid degradation has occurred [323,328,333]. Nevertheless, as shown by the centrifugation test (Figure 3.3.4b), both formulations had lower physical stability than formulation C (Section 3, Chapter 2), displaying creaming after 24 h of storage. This breaking mechanism, often observed in skin lotion emulsions [206], result from centrifugal external forces exceeding the Brownian motion of droplets, creating a concentration gradient with low density droplets shifting to the top [101,103]. These results indicate that the addition of L-ascorbic decreased the FucoPol-based emulsion physical stability, even using *Prunus amygdalus dulcis* oil instead of *Olea europaea* oil, compared to formulation C.

3.3.3.3.2 Emulsion type

The emulsions' droplets rapidly dispersed on the filter paper (Figure 3.3.3b), confirming their O/W nature [168,187], similar to that for FucoPol-based emulsion formulation C (Section 3, Chapter 2). Furthermore, upon microscopic observation (Figure 3.3.3c-d), compartmentalized structures characteristic of O/W emulsions, consisting of dispersed oil droplets in the aqueous phase [184,185] were observed, thus confirming the formulations' O/W nature.

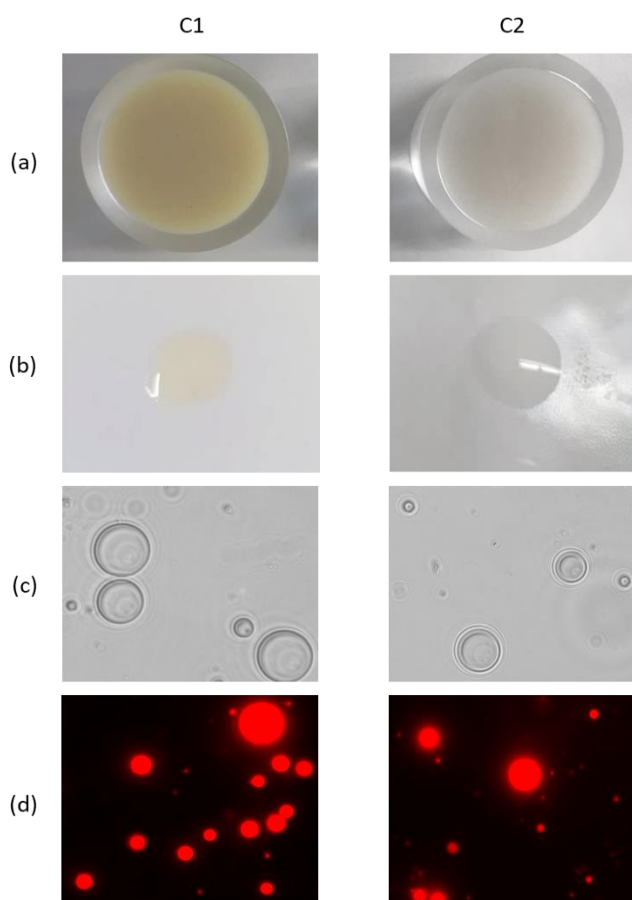


Figure 3.3.3. Formulations C1 and C2 (a); Emulsion determination test by filter paper wetting (b); Optical microscopic (100x) observation under contrast phase (c) and fluorescence after Nile Blue A staining (d).

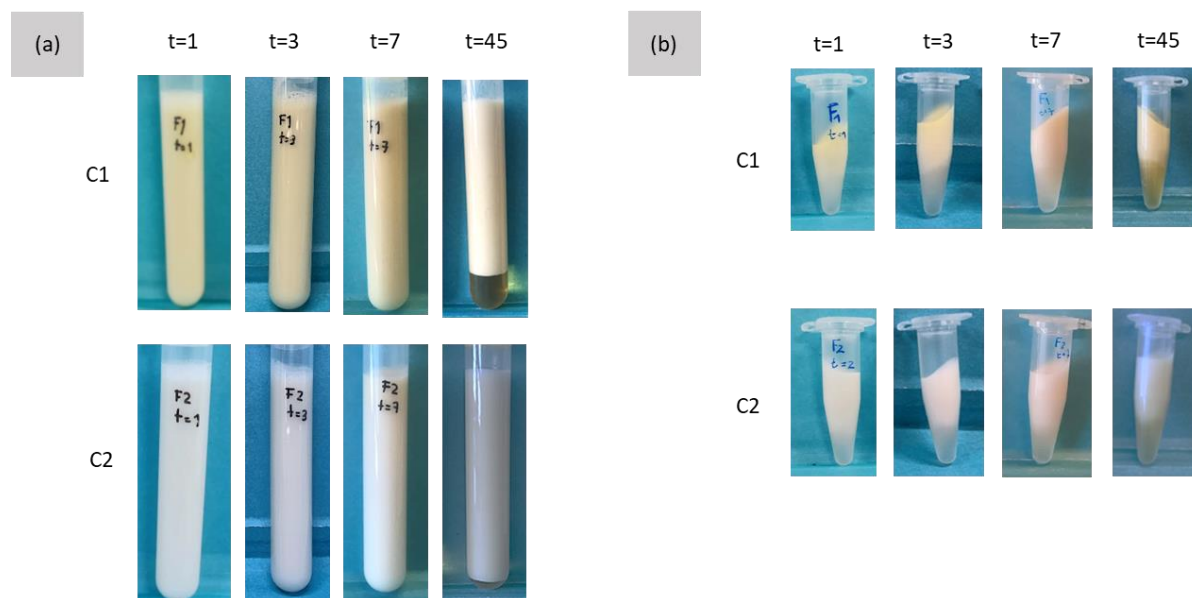


Figure 3.3.4. (a) Emulsification index over storage period (t=1, 3, 7, 45 days); (b) Centrifugation test over storage period (t=1, 3, 7, 45 days).

3.3.3.3.3 pH and conductivity

The pH and conductivity values over the storage period are represented in Figure 3.3.5a. The pH values for formulations C1 and C2 were slightly acidic (5.7 and 5.5, respectively) which were maintained during the 7-day storage period (Figure 3.3.5a). After forty-five days, the pH value increased for both formulations C1 and C2 (6.8 and 6.03, respectively). The pH value of both formulations was within the optimal range (4.0– 7.0) [294,304,305] reported to avoid skin irritation [242], thus supporting their suitability for topical use. Additionally, the pH stability during the storage period (45 days) indicated that both emulsified systems provided protection to ascorbic acid, because a significant increase in pH would be indicative of vitamin C degradation [332].

The conductivity value, which is indicative of the free ions and water content in the system [294], can be used to detect physical modifications [306] and to assess if the formed emulsion is an O/W or a W/O system [276,305]. Formulations C1 and C2 showed high conductivity values ($>1300 \mu\text{S}/\text{cm}$) characteristic of O/W systems [305] corroborating the results obtained by the emulsion determination test and the microscopic observation. As observed in Figure 3.3.5a, formulation C1 maintained the conductivity values during the 7-day storage period (1354–1360 $\mu\text{S}/\text{cm}$) increasing to 2728 $\mu\text{S}/\text{cm}$ after forty-five days, while formulation C2 showed a minor decrease in the conductivity value (from 2986 to 2714 $\mu\text{S}/\text{cm}$) during the 7-day storage period, and an increase to 3893 $\mu\text{S}/\text{cm}$ after forty-five days. The behaviour of formulation C1 was similar to formulation C, maintaining the conductivity values (110–138 $\mu\text{S}/\text{cm}$), despite the increase of free ions in the system caused by L-ascorbic acid addition. Conductivity instability over the 45-day storage period indicated a presence of physical changes. Conductivity differences are usually related to the increase of oil proportion in the upper part of the emulsion and water proportion increase in the lower part of emulsion, leading to emulsion creaming/sedimentation [305].

3.3.3.3.4 Droplet size and Zeta-potential

The C1 and C2 physical stability was also assessed by measuring the droplet size during the storage period at room temperature ($\sim 20^\circ\text{C}$). The distribution profile of oil droplets and their size influence the emulsion's stability, with smaller droplet sizes and lower PI values (< 0.3) being correlated with higher emulsions' stability [191,294,308–310]. As shown in Figure 3.3.5b, all formulations presented a droplet size characteristic for macroemulsions ($> 0.1\text{--}50 \mu\text{m}$) [353], experiencing a considerable increase in droplet size after 45 days of storage. For C1, droplet size increased from 0.8 μm to 17 μm , while for C2 droplet size increased from 0.8 to 37 μm . As mentioned before, the droplet size of an emulsion is determined by the homogenization technique applied, the environmental conditions, and ingredients used for its preparation [313]. Moreover, the movement of dispersed droplets through the continuous phase increments the probability of droplet collisions, resulting in higher droplet sizes [354]. Comparing C1 and C2 to the FucoPol based-emulsion formulation C, the addition of L-ascorbic acid leads to an 87% decrease in droplet size. Small droplet size usually improves the stability of emulsions by favouring Brownian motion over gravity, preventing creaming/sedimentation mechanisms regardless of storage period. Additionally, small droplet size contributes to flocculation and coalescence inhibition [355]. However, contrary to what was expected, formulation C1 and C2 showed creaming after 1-day

of storage while formulation C showed a breaking mechanism (phase separation) after 30-day of storage. The ideal monodisperse system should have a PI value lower than 0.3 [276,309], which was not verified for neither C1 nor C2 ($0.65 \leq PI \leq 5.2$ for $t=45$ days) indicating considerable polydisperse droplets sizes. However, while in C the PI remained constant during the storage (between 2.2–2.9), in C1 a significant decrease of the PI was noticed between the third and the forty-fifth days of storage (2.4 and 0.77, respectively), and for formulation C2 a significant increase was observed between the seventh and the forty-fifth days of storage (0.66 and 5.2, respectively).

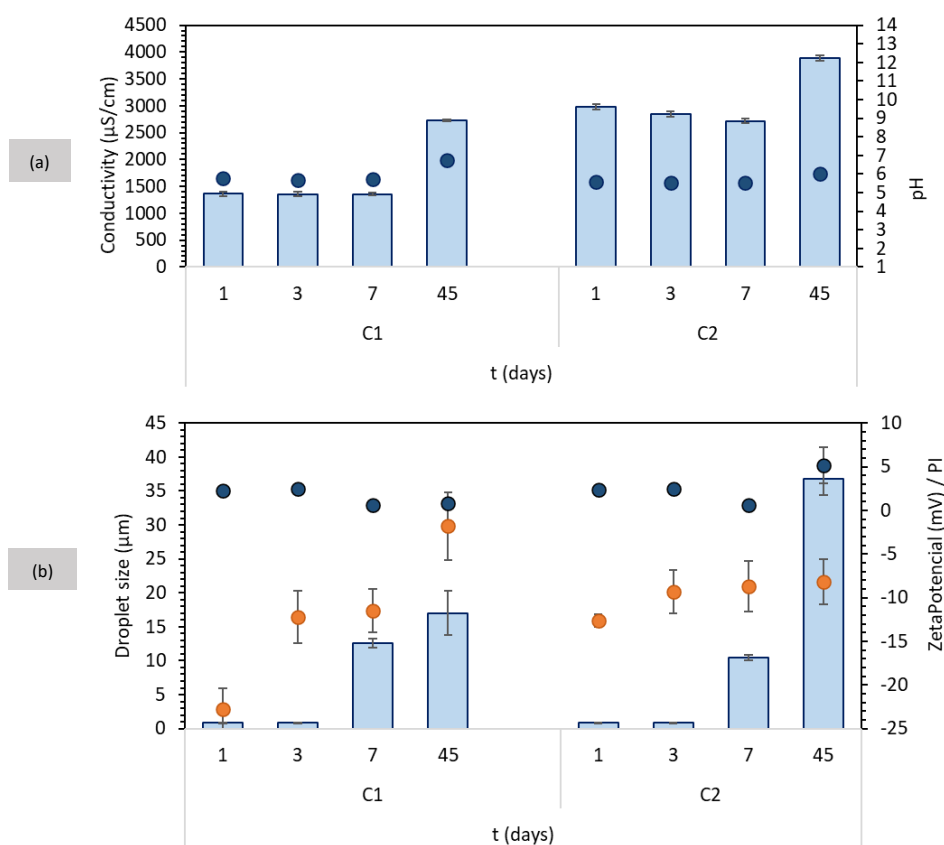


Figure 3.3.5. (a) pH and conductivity and (b) droplet size (blue bars), Zeta-potential (orange circles), and PI (blue circles) for formulations C1 and C2 during the storage period ($t=1, 3, 7, 45$ days).

As shown in Figure 3.3.5b, the Zeta-potential for formulations C1 and C2 was -22.0 mV and -12.6 mV, respectively. The formulation is considered stable when the Zeta-potential value is more than $+25$ mV or lower than -25 mV [294]. Although for C1 the Zeta-potential value was close to -25 mV, during the storage period, both C1 and C2 suffered a decrease of zeta-potential values, corroborating the observed instability parameters and the negative effect of L-ascorbic acid in a FucoPol-based cream. L-ascorbic acid has been reported to adsorb at the oil-water interface and promote droplet fusion, leading to their separation from the emulsion oil layer, causing instability of the entire system [356]. Formulation C presented higher absolute Zeta-potential value (-98 mV) and pH (6.3) values, with no need for

adjustment with TEA. L-ascorbic acid decrease the pH of formulation and was previously reported [357] that higher pH promotes a higher Zeta-potential, increasing interface's repulsive force. Considering the structure of an O/W system, with water being a high dielectric fluid and oil being a low dielectric fluid, the repulsive force between charged droplets from the interface promote the stabilization of the emulsion, due to the asymmetric distribution of counter-ions at the interface, originating a dipole normal to the fluid–fluid interface [358] Lower pH values cause the neutralization of the interface charges which promotes the gradual separation of surfactant from the O/W interface, leading to lower emulsion stability [357].

3.3.3.3.5 Apparent viscosity and viscoelastic properties

Formulations C1 and C2 presented a shear-thinning behaviour (Figure 3.3.6), as the viscosity progressively decreased under increasing shear rates, in agreement with previous results for FucoPol containing emulsions [147,183]. This pseudoplastic behaviour is ideal for cosmetic formulations by promoting the sliding of the formulation on the skin, creating a protective layer, and acting as a shear condensing fluid [318]. Up to third day, formulation C1 (Figure 3.3.6a) showed lower apparent viscosity than formulation C2 (Figure 3.3.6b). Considering that *Olea europaea* oil (83.5 Pa.s) has higher a viscosity than *Prunus amygdalus dulcis* oil (56.8 Pa.s) [359], the higher L-ascorbic acid concentration used in C2 (15 wt.%) may lead to a viscosity increase. L-ascorbic may increase water phase viscosity leading to a decreased droplets' mobility and collision numbers, which can explain the observed behaviour. Formulation C1 exhibited a slight increase of viscosity during the storage time, while formulation C2 exhibited a slight decrease. The C1 apparent viscosity at the first day of storage (24 h) presented similar results as the results reported in section 2.3.3.1. (2.5 Pa.s and 2.7 Pa.s, at shear rate 2.30 s^{-1}), indicating that upscale from 5g to 100g and the homogenization method applied (mechanical homogenization vs manual homogenization) did not influence the behaviour and efficiency of the ingredients [191]. On the other hand, for C2 the viscosity decreased to 5.1 Pa.s (section 2.3.3.1) to 3.4 Pa.s at shear rate of 2.30 s^{-1} .

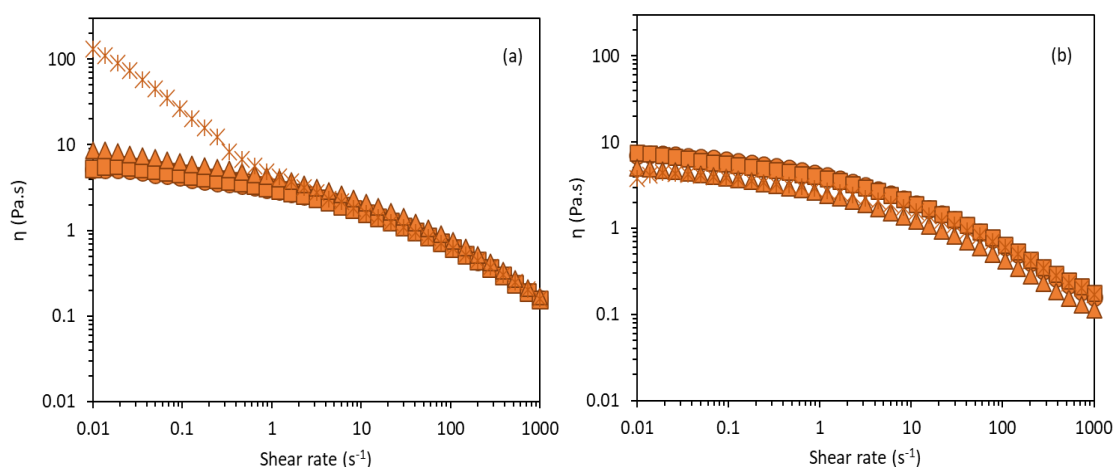


Figure 3.3.6. Flow curves for C1 (a) and C2 (b) formulations during the storage times: $t=1$ (circles), $t=3$ (squares), $t=7$ (triangles), and $t=45$ (asterisk).

The apparent viscosity at a given shear rate is also an important parameter to predict the behaviour of the cosmetic formulation in different physical operations: squeezing (0.1 s^{-1}), pouring (10 s^{-1}) and rubbing (100 s^{-1}) [318]. Hence, formulation C2 (6.9 Pa.s) seems to be more squeezable than formulation C1 (5.2 Pa.s). On the other hand, both formulations C1 and C2 have analogous values for pouring (1.65 Pa.s and 1.92 Pa.s, respectively), and rubbing out (0.62 Pa.s and 0.61 Pa.s, respectively).

The mechanical spectra of the FucoPol-based formulations are illustrated in Figure 3.3.7. Both formulations C1 and C2 showed liquid-like behaviour, with the loss module storage module higher than the storage module ($G'' > G'$ at 0.1 Hz) [147]. While for C1 the G'' and G' modules showed similar profiles during the storage period (Figure 3.3.7.a), for C2 the G'' and G' modules showed higher values at 1-day and decreased thereafter (Figure 3.3.7.b). This behaviour indicated the lower stability of this formulation, indicated the dominance of viscous components over the elastic components, and that the physical bonds between the macromolecules do not have the capacity to maintain the system's structure [204]. This behaviour contrasts with that of the FucoPol-based emulsion formulation C result (Section 3, Chapter 2), where the storage module was higher than the loss module ($G' > G''$ at 0.1 Hz) showing a solid-like behaviour characteristic of cosmetic formulations [191,235,316]. In both systems (Figure 3.3.7), it was possible to observe that G' and G'' increase with frequency increase, indicating that G' and G'' are functionally dependent on frequency, implying a less stable system, corroborated by the observed breaking mechanism (creaming) [357] after the centrifuge test (Figure 3.3.4b). Contrarily, formulation C (Section 3, Chapter 2) presented a G' and G'' almost constant, indicating a more stable system.

Crossover frequency is an indicator of a material's viscoelastic behaviour, in which lower crossover values translate into more elastic materials [360,361]. For formulation C1, the crossover was maintained at 2.5 Hz after 3-day storage and increased to 5.1 Hz after 7 days, disappearing after 45 days. For formulation C2 it was observed a shift of the crossover value (from 0.6 to 10 Hz) during the storage period. The initial crossover value for C2 indicated the formation of a more structured formulation, which declined over storage period. This observed shift of the crossover point towards higher frequencies overtime can be attributed to the ageing of formulation C2, yielding a wider plateau region arising from the increased biopolymer molecules' entanglement density and from a higher oil droplet packing [145]. This effect could be observed in the creaming mechanism from Figure 3.3.4b, which was more evident in formulation C2 than in C1. For formulation C1, the loss of structure was not so pronounced, displaying a crossover point at high frequency after 1 day of storage. The results obtained suggest that when an emulsion present a wider plateau relaxation zone after a short ageing time, it often translates into a longer physical stability [145]. In summary, formulation C2 was initially the most structured system and storage time affected (declined) this characteristic; formulation C1 started as the less structured system but its structure loss not as pronounced as in formulation C2.

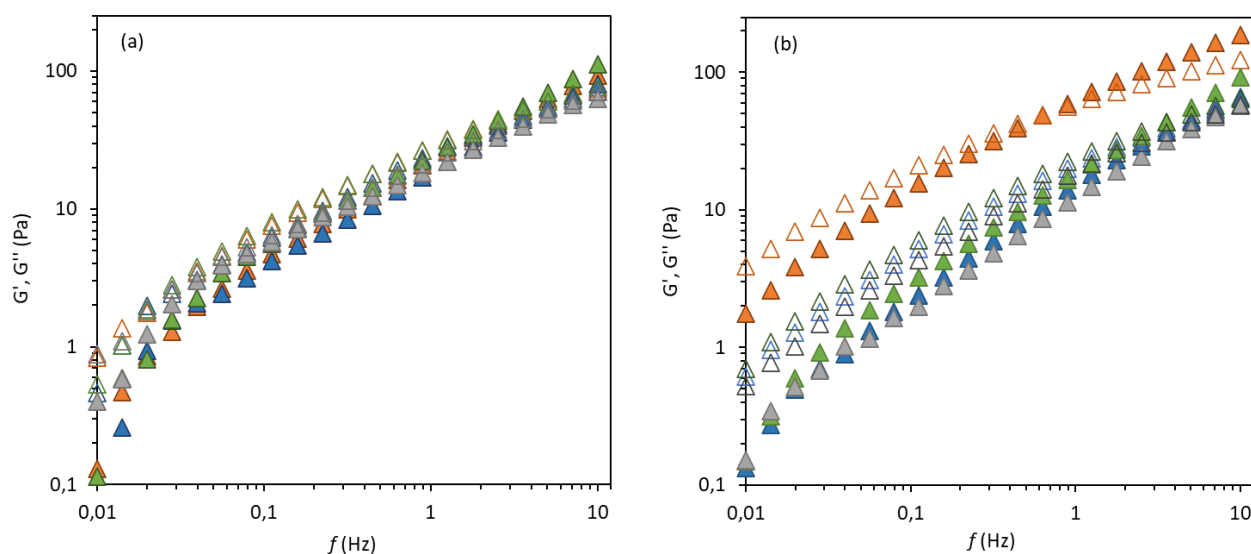


Figure 3.3.7. Mechanical spectrum for formulations C1 (a) and C2 (b) during the storage time: $t=1$ (orange), $t=3$ (blue), $t=7$ (green), and $t=45$ (gray). G' (closed triangle) and G'' (open triangle).

The pH value can also influence the emulsion's flow behaviour. The lower pH values of formulations C1 and C2 (5.7 and 5.5, respectively), compared to formulation C (pH=6.3), apparently decreased the values of G' and G'' , leading to a more viscous fluid (rather than elastic), which might explain the lower stability of emulsions C1 and C2 [357,362].

3.3.3.3.6 Textural Assessment

The textural parameter values (firmness, consistency, cohesiveness, and adhesiveness) of the prepared formulations are summarized in Table 3.3.3. In general, at the end of storage time ($t=45$ days), it was observed an increase in firmness and consistency of the formulations, indicating that C1 slightly less spreadability (usually attributed to higher firmness and consistency values) than C2. The spreadability, or the skin cover capacity over time, is crucial in cosmetic emulsion development being a decisive factor for consumers' approval of products [268]. Furthermore, at shear rates that represent the skin spreading process (1000 s^{-1}) [268], both C1 and C2 emulsions displayed similar viscosity ($0.16 \text{ Pa}\cdot\text{s}$). While both samples showed lower adhesivity, emulsion C1 (0.077 mJ) seemed to be more adhesive than C2 (0.073 mJ). Therefore, the cohesiveness was also an important parameter to be observed, and formulation C2 was slightly more cohesive than C1. These results once again prove the negative effect of the addition of L-ascorbic acid. Comparing to the FucoPol-based cream C, L-ascorbic acid induced a decrease of 80% in firmness, 83% in consistency and 80% in adhesiveness, after 1 day-storage.

Table 3.3.3. Numerical values of the textural parameters for formulations C1 and C2 during the storage period at room temperature. *Data obtained under the same manufacturing and scale conditions.

Formulation	Time (days)	Textural parameters			
		Firmness (N)	Consistency (mJ)	Cohesiveness (N)	Adhesiveness (mJ)
C1	1	0.039	0.065	1.027	0.077
	3	0.071	0.078	0.759	0.063
	7	0.064	0.177	0.817	0.075
	45	0.086	0.186	0.949	0.038
C2	1	0.039	0.053	1.069	0.073
	3	0.064	0.099	0.950	0.078
	7	0.064	0.129	1.377	0.079
	45	0.077	0.153	0.924	0.057
Formulation C*	1	0.194	0.385	1.035	0.387
	60	0.047	0.160	1.004	0.129

3.3.3.3.7 Formulations accelerated stability

The accelerated stability is an important parameter to assess the formulation behaviour during storage. The formulations were preserved during forty-four days at 4 °C and 30 °C. Concerning the macroscopic organoleptic characteristics (Figure 3.3.8a), the formulations C1 and C2 maintained the colour, odour, and texture regardless of storage temperature. Regarding EI values (Table 3.3.4.), formulations stored at 4 °C presented higher values (95% for C1 and 100% for C2) than those stored at 30 °C (81.3 % for C1 and 94% for C2) and at 20 °C (90% for C1 and 93% for C2). At 4 °C, the resistance to structural breakdown seemed to be higher, resulting in lower creamed emulsions (Figure 3.3.8b). These results were corroborated with higher zeta-potential values for formulation C1 (−21 mV) and C2 (−18mV), at 4°C. At 30 °C, C1 had −2.6 mV and C2 had −3.1 mV of zeta-potential, whilst C1 and C2 had, respectively, −1.8 mV and −8.2 mV, at 20°C. This variation on Zeta-potential values might be explained by chemical alterations (emulsifiers decomposition) or development of charged molecules [354]. Zeta-potential > +25 or < −25 provide a momentary stability of the emulsion, tending to droplet gathering (flocculation and coalescence effect) [354] during the storage.

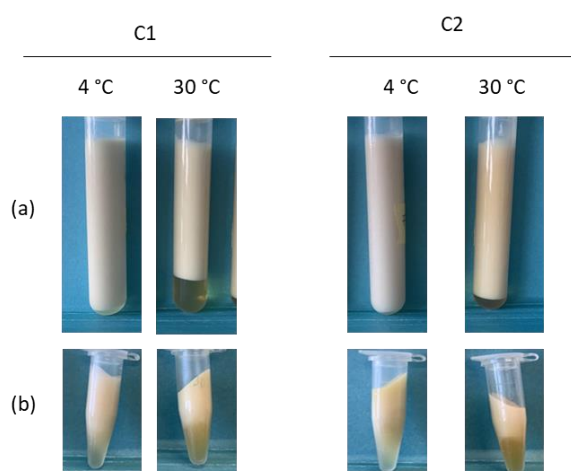


Figure 3.3.8. (a) Emulsification index over storage temperature after 45 days (b) Centrifugation test over storage temperature after 45 days.

Table 3.3.4. Physicochemical characterization of formulation C1 and C2 during forty-five day-storage at 4 °C, and 30 °C. η at 2.30 s⁻¹.

Temperature (°C)	Formulation	pH	Conductivity (μs/cm)	Droplet			Firmness (N)	Consistency (mJ)	Cohesiveness (N)	Adhesiveness (mJ)
				size (μm)	EI (%)	η (Pa.s)				
4	C1	6.6	1593±12	150±7.7	95.0	1.7	0.100	0.198	0.784	0.062
	C2	6.1	2561±45	11.8±0.5	100	2.8	0.065	0.205	0.914	0.083
30	C1	6.6	1596±7.1	90.5±3.2	81.3	2.2	0.099	0.200	0.979	0.043
	C2	6.4	2563±29	8.97±0.4	94.0	1.9	0.080	0.021	0.833	0.054
20	C1	6.8	2728±12	17.0±3.3	90.0	3.2	0.086	0.186	0.949	0.038
	C2	6.0	3893±51	36.8±2.4	93.0	2.4	0.077	0.153	0.924	0.057

The pH values for all temperatures remained similar (6.0–6.8) at the end of the storage period. At 4 °C there was a higher stability during the shelf life for both formulations C1 and C2, considering the minimal difference between conductivity values obtained after 24 hours and 45-days of storage (C1: 1360 to 1593 μs/cm; C2: 2986 to 2561 μs/cm). Regardless of temperature, all formulations presented non-Newtonian (shear-thinning) and liquid-like behaviour (Table 3.4.4. and Figure 3.3.9). Formulation C1 stored at room temperature (20 °C) presented higher apparent viscosity values (3.2 Pa.s, at 2.30 s⁻¹) compared to other temperatures. These fluctuations are possibly due to structural rearrangements [191]. The viscosity of cosmetic formulations containing polymers are susceptible to dry and/or humid storage conditions, influenced by temperature [35,206]. Furthermore, the increase of storage temperature promotes the decrease in viscosity, and vice-versa, resulting in a destabilization effect [354]. An emulsion viscosity can be influenced by the oil-phase crystallization, controlled by temperature and storage time,

which induces the emulsion droplets partial coalescence or results in conformational alterations on the biopolymer [354,363]. The temperature also appears to influence droplet size, being different for each type of formulation. Larger droplets were observed for formulation C1 at 4 °C and 30 °C (from 17 μm to 150 μm and 90.5 μm, respectively). The droplet size increase might be attributed to the coalescence of droplets [354]. On the other hand, for formulation C2, a decrease in the particle size was noted, when stored at 4 °C and 30°C (from 38.8 μm to 11.8 μm and 8.97 μm). Regarding the texture parameters, the most accentuated difference is the drastic decrease in consistency for Formulation C2 at 30 °C (0.021 mJ) compared to the value for 4 °C (0.205 mJ) and 20 °C (0.153 mJ). The decrease in cohesiveness for 4 °C (0.789 mJ) in the C1 formulation compared to the value for 30 °C (0.979 mJ) and 20°C (0.949 mJ), also denotes an effect of temperature on the formulation textural properties.

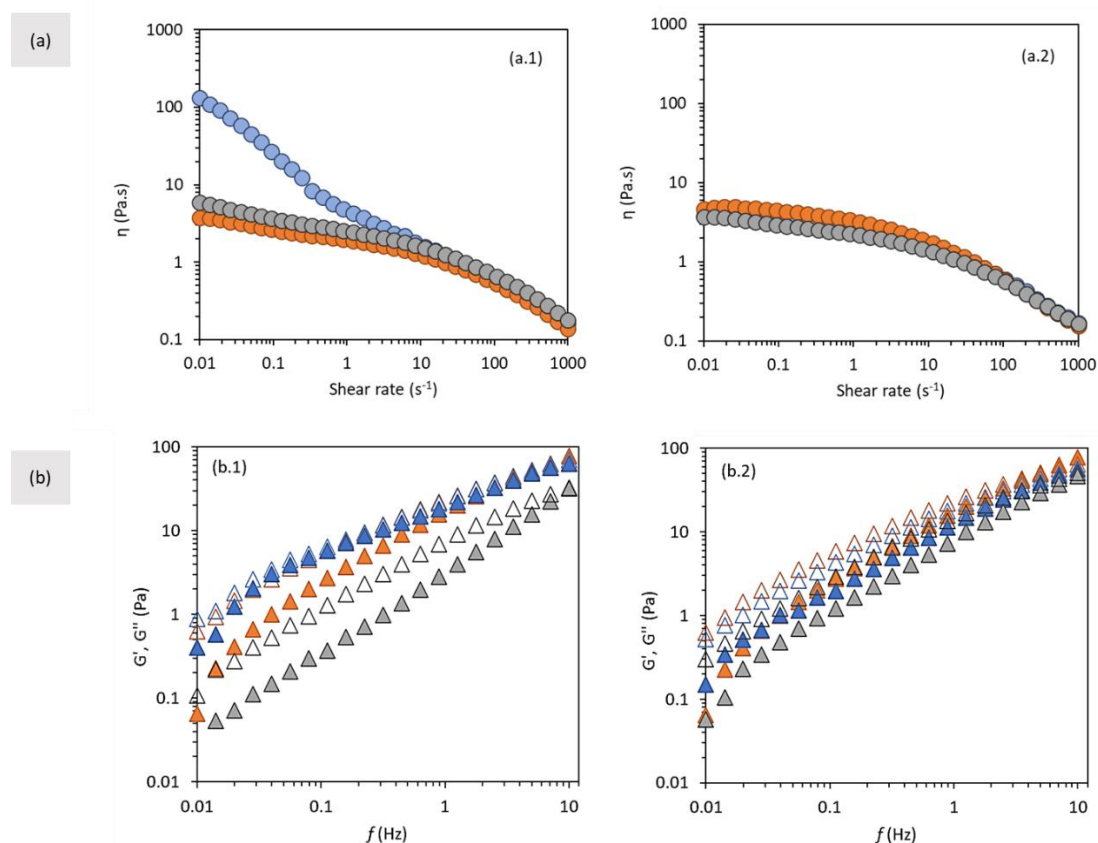


Figure 3.3.9. Rheological profile analysis of formulations C1 (**a.1** and **b.1**) and C2 (**a.2** and **b.2**): (a) viscosity curves as a function of the shear rate; (b) mechanical spectra: elastic G' (closed triangle) and viscous G'' (open triangle) moduli in the function of frequency. 4 °C (orange), 20 °C (blue), 30 °C (gray).

3.3.4 Conclusions

In this study, FucoPol-based creams containing either *Prunus amygdalus dulcis* oil or *Olea europaea* oil, supplemented with α -tocopherol (vitamin E) and L-ascorbic acid (vitamin C) as bioactive agents were studied. Vitamin C has been widely used in cosmetic and dermatological products due to its physiological effects on the skin. However, it presents handling issues, inherent to its high risk of oxidation in light, high temperatures and presence of water. In this study, the combination with α -tocopherol was beneficial because this vitamin acts synergistically with L-ascorbic to regenerate the oxidized molecules.

Although resulting in particle size reduction, the presence of L-ascorbic acid in the aqueous phase resulted in O/W systems with lower physical stability, as demonstrated by the decrease of the emulsions' apparent viscosity, firmness, cohesiveness and adhesivity, as well viscoelastic behaviour change. Macroscopic evaluation of formulations during the storage period showed no L-ascorbic acid degradation, supported by the maintenance of their colour and odour, attributed to α -tocopherol protection. Since the main objective of this study was to evaluate L-ascorbic acid effect on the FucoPol-based cream, which showed from the beginning to be an unstable formulation with adequate behaviour in the cosmetic industry, HPLC analysis of L-ascorbic acid was not performed. However, HPLC confirmation of L-ascorbic acid content during the storage period is required in stable formulations. Future work to improve the stability of the FucoPol-based creams containing L-ascorbic acid may include formulation tuning with higher FucoPol and/or cetyl alcohol contents, and the evaluating the possibility of L-ascorbic acid encapsulation with FucoPol prior to formulation.

4. VALIDATION OF THE FUCOPOL-BASED CREAM: BIOACTIVE PROPERTIES AND SENSORIAL EVALUATION

The results presented in this section are part of the following submitted paper:

Baptista, S., Pereira, J.P., Guerreiro, B.M., Baptista, F., Silva J.C., Freitas, F. Cosmetic emulsion based on the fucose-rich polysaccharide FucoPol: Bioactive properties and Sensorial evaluation. Submitted to *Colloids and Surfaces B*.

This page was intentionally left blank

Summary

The constant development of new technologies and the interest in the incorporation of novel sustainable ingredients has rendered the cosmetic industry as one of the fastest growing industrial sectors. Consumers' demand for the utilization of biodegradable ingredients has precipitated the utilization of natural polymers as stabilizers in newly developed emulsions. In this section, the physicochemical characteristics, bioactive properties, and sensorial evaluation of O/W a cosmetic formulation containing FucoPol were assessed. The FucoPol-based cream stability was investigated during 2 months at 4 °C, 20 °C and 30 °C. The results showed that formulation maintained the organoleptic characteristics, pH (5.88–6.19) and minimal variations on apparent viscosity. The accelerated stability tests proved the formulation stability at 4 °C and 30 °C without the occurrence of breaking mechanisms. The rheological assessment demonstrated that the formulation presents a shear-thinning and solid-liquid behaviour ideal for topical applications. The *in vitro* studies revealed that the formulation was non-cytotoxic for HaCaT cells at concentrations between 0.78–12.5 mg/mL; promoted HFFF2 cell migration (46–69.9 % of wound closure) at a concentration of 2.5 mg/mL and HaCaT cell migration at a concentration of 10 mg/mL (95–97.9 % of wound closure). On application over skin, the formulated cream provides a hydration and softness with desire spreadability without residues after application. After comparison with a commercial product, FucoPol showed potential to be applied as a functional and/or active polysaccharide in cosmetic formulations, forming a cream with appealing sensorial properties that can act as a moisturizer with photoprotection, antioxidant, and regeneration properties.

4.1.1 Introduction

The use of natural active ingredients in modern skincare products formulations is expanding. Many of them confer diverse therapeutic properties to cosmetics, including skin whitening, antioxidation, wound healing pro-collagen, and UV-protection [80,364–366]. Cosmeceuticals, i.e., cosmetic products with drug-like properties, have rapidly expanded in the last few years with the emergence of novel locally applied beneficial products and products for degenerative skin disease prevention [81,93,367]. These products are not only cosmetics, in the sense of the demand for desirable aesthetic properties but are also medical products requiring the approval within strict physicochemical standards to deliver their benefits without threatening the user's health [364]. For example, wrinkle reducing products can also enhance skin tone, texture, and radiance. In fact, anti-aging applications show the highest growth rates amongst skin-care products, with several examples of creams with: antiwrinkle and firming properties; moisturizing and lifting characteristics; and skin toning and whitening activities [80,93,364]. In addition to the growth of age symptoms correction products, the development of aging prevention products is demanded, for skin daily protection and to decrease the skin aging process [93,368].

Cosmetics for skin topical application are responsible for the restoration or maintenance of the skin's barrier properties, and can include moisturizers, antioxidants, anti-inflammatory agents, and/or UV-protection agents in their composition [369].

Tissue damages can be caused by several mechanisms but deterioration from free radicals, such as reactive oxygen species (ROS), is more prevalent [93]. ROS are generated by UVR radiation, comprising 95–98% of UVA and 2–5% UVB, which leads to skin damage [65]. This mechanism directly modifies the chemical composition of cellular DNA and lipids; alters the dermal matrix proteins, such as collagen produced by dermal fibroblasts; or damages the epidermis *stratum corneum* envelop (the skin's permeability and mechanical barrier) [330,369,370]. Exposure to UV radiation induces not only premature skin aging, or photoaging, but may also lead to erythema (sunburn), immunosuppression, and carcinogenesis [368,371–373].

Although photoaging prevention is primarily achieved by photoprotection, the utilization of exogenous compounds, like antioxidants, is also relevant [368]. Vitamins (B3 [374,375], C [375–377], and E [375,378]) with acceptable skin penetration, are the most used antioxidant substances to prevent antiaging [379]. Antioxidants scavenge ROS and convert them into stable radicals or non-radical species, thus preventing oxidation reactions and the effect of oxidative stress [380]. In cosmetic preparations, antioxidants have the dual role as active ingredients and as oxidation protectors of other ingredients present on the formulation, contributing to increase the product's shelf-life [369,375].

Cosmeceuticals also need to be attractive for the consumer, and fragrance is essential aspect of these products, being considered, from the consumer's perspective, an essential factor during product selection [381]. Moreover, fragrances mask the often-undesirable smells of other ingredients present in cosmetic formulations, such as fatty acids, oils, and surfactants. The utilization of essential oils, such as lemon oil, can implement a pleasant aroma in different products while also functioning as preservatives and active agents, being considered multi-purpose ingredients in cosmetic formulations which offer many skin-related benefits [382]. Specifically, lemon essential oil has antiseptic properties, important in skin and hair care products [383], presenting also antimicrobial properties, which could be further explored in new applications [382].

Given the previously demonstrated functional properties of FucoPol in Section 2 and 3, together with the biopolymer's bioactivity action as a photoprotector [58], antioxidant [49] and skin regenerator [52], the objective of the present study was the formulation and characterization of a stable FucoPol-based cream, which was compared to a cosmetic emulsion-based product available on the market. *In vivo* safety assessment of FucoPol by the Human Repeated Insult Patch Test (HRIPT) and evaluation of the FucoPol-based cream antioxidant capacity cytotoxicity, photoprotective and wound healing potential.

4.1.2 Materials and methods

4.1.2.1 Materials

Olea europaea and *Citrus limon* peel oil was purchased from a local market. α -tocopherol, methyl paraben and cetyl alcohol, sodium acetate, glacial acetic acid, (\pm)-6-Hydroxy-2,5,7,8-tetramethylchromane-2-carboxylic acid (Trolox) and 2,4,6-Tris(2-pyridyl)-s-triazine (TPTZ) were acquired from Sigma-Aldrich (Munich, Germany). Triethanolamine (TEA) was acquired from Acros Organics B.V.B.A. (Geel, Belgium), and glycerine was acquired from Honeywell (Seelze, Germany). D-Glucose, sodium pyruvate, TrypLE Express and penicillin–streptomycin (#15140122) were acquired from Thermo Fisher Scientific (Waltham, Massachusetts, USA).

FucoPol was produced and purified by ultrafiltration with a 30 kDa membrane according to the method previously described in Section 2, Chapter 1 (2.1.2.1 and 2.1.2.2).

4.1.2.2 Human Repeated Insult Patch Test of FucoPol

The *in vivo* study was performed according to the rules of Good Clinical Practices, under the standardized procedures and were submitted and approved by the Ethical Committee of PhD Trials®. A safety assessment was achieved using a Marzulli and Maibach Human Repeat Insult Patch Test (HRIPT) protocol [384]. A dermatologist evaluated, according to the International Contact Dermatitis Research Group (ICDRG) [385], the irritation and allergic reactions to the tested patches on a panel of 51 healthy volunteers (female and male; aged 18-65; phototype I-IV). The applications were repeated 9 times over a period of 3 consecutive weeks, period necessary for the possible induction of an allergy. After a 2-week rest period, with no product application, a single application of the product under occlusive patch, to the induction site and to a virgin site, for a defined time (48 h), enables to reveal a possible induced allergy. The results are mainly expressed as descriptive data and do not require a statistical treatment.

4.1.2.3 Preparation of the FucoPol-based cream

The emulsified formulation (F-cream) was prepared according to the composition presented in Table 4.1.1., following the method described in Section 3, Chapter 2 (3.2.2.3). The fragrance (*Citrus limon* peel oil) was then added to the formulation, at 30 °C. Formulations were prepared in 100 g batches.

Table 4.1.1. Cosmetic formulation composition. q.s- quantity sufficient

INCI name	Function	Concentration (wt.%)
Aqueous phase		
Water	Solvent	q.s.
FucoPol	Emulsifier	1.5
Glycerine	Emollient/humectant	3.0
Methyl paraben	Preservative	0.02
TEA	pH regulator	0.5
Oil phase		
Cetyl alcohol	Co-emulsifier	1.5
<i>Olea europaea</i> (Olive) fruit oil	Oil, dispersed phase	30
α -tocopherol	Antioxidant	2.5
Additive		
<i>Citrus limon</i> peel oil	Fragrance	0.2

4.1.2.4 Physicochemical characterization of the FucoPol-based cream

The physicochemical characterization during the storage period (t=1,3,7,60 days) was done according to the procedures described previously in Section 3, Chapter 2 (3.2.2.4.1), at different temperatures, namely, 4, 20 and 30 °C.

4.1.2.5 Antioxidant activity

4.1.2.5.1 Tris(2-pyridyl)-s-triazine (TPTZ) antioxidant assay

The ferric reducing antioxidant potential (FRAP) was determined with an adaptation of the original method [53]. A working FRAP solution (WFRAP) was prepared by mixing 250 mL of 0.3 M cold acetate buffer (prepared by mixing 1.6 g sodium acetate and 8 mL glacial acetic acid with 500 mL deionized water), 25 mL of 0.01 M cold Tris(2-pyridyl)-s-triazine TPTZ (dark storage) dissolved in 0.04 M HCl, and 25 mL of 0.02 M FeCl₃·6H₂O (freshly prepared, dark storage). After homogenization of the initial mix, 2.7 mL WFRAP were mixed with 270 μ L deionized water and 90 μ L test substance (control: 90 μ L deionized water). The mixture was quickly vortexed, incubated at 37 °C for 30 min, and the optical density at 595 nm was measured. Trolox (a water-soluble analogue of vitamin E) was assayed as positive control at concentrations of 300, 250, 200, 150, 100, and 50 μ M. F-cream samples were prepared at corresponding α -tocopherol concentrations of 37.8, 75.7, 151.5, 227, 250, 303, 378.8, 500, 757.5, 1000 and 1250 μ M.

4.1.2.5.2 Determination of Hill non-specific binding

The ferric reducing antioxidant power was fit to a non-specific Hill binding model, as previously described [49]. The effective concentration required to produce 50% of the total antioxidant response (EC_{50}) and the corresponding Hill binding coefficient (H) were estimated by the following equation [386].

$$y = A_{min} + \frac{A_{max} - A_{min}}{1 + \left(\frac{x}{EC_{50}}\right)^{-H}} \quad (4.1.1)$$

where A_{min} and A_{max} are the lowest and highest absorbance value, respectively, collected for the given concentration range.

4.1.2.6 Biological assays

4.1.2.6.1 Cell culture and media

Fibroblast cells (HFFF2, Human Caucasian Foetal Foreskin Fibroblasts from a 14- to 18-week-old human foetus, ECACC, UK) were cultured in Dulbecco's modified Eagle's medium (DMEM, #L0066, from Biowest, with 1.0 g/L glucose, stable glutamine, and sodium pyruvate) supplemented with penicillin (100 U/ml), streptomycin (100 µg/mL), 1% of Fugizone and 10% FBS (Fetal Bovine Serum, S. America origin, Biowest, #S1810).

Keratinocyte cells (HaCaT, *in vitro* spontaneously transformed keratinocytes from histologically normal skin, AddexBio, USA) were cultured in DMEM with high glucose content (4.5 g/L glucose, and sodium bicarbonate) supplemented with penicillin (100 U/mL), streptomycin (100 µg/mL), 1% of Fugizone and 10% FBS (Fetal Bovine Serum, S. America origin, Biowest, #S1810).

4.1.2.6.2 Cytotoxicity

HaCaT cells were cultivated in high-glucose DMEM in a 96-well microplate. HaCaT cells were seeded at a concentration of 25,000 cells/cm² and incubated during 24 h at 37 °C, 5% CO₂. For the cytotoxicity assessment, the cells were exposed to a concentration range of 0.7 - 100 mg/mL of the test sample, either F-cream or Bioderm® Prototype™ formulations, during 48 h. DMEM – high glucose + 10 % DMSO (dimethyl sulfoxide) was used as the positive control, while the negative control was DMEM – high glucose. After 48 h, the well volumes were discarded and 100 µL of a resazurin:DMEM – high glucose solution (50% resazurin dissolved at a concentration of 0.04 mg/mL in phosphate buffer saline (PBS) + 50% DMEM – high glucose) were added and incubated during 4 h at 37 °C, 5% CO₂. Cell viability was assessed by measuring the optical density at 570 and 600 nm.

4.1.2.6.3 Wound healing

HFFF2 and HaCaT cells were cultivated in low-glucose and high-glucose DMEM, respectively, in a 24-well plate. Cells were seeded at a concentration of 15,000 cells/cm² and incubated at 37 °C, 5% CO₂. After achieving a confluence of 80%, a wound was created with a pipette tip and each well was washed twice with PBS to remove non-adherent cells. For the wound healing assessment, cells were exposed for 24 h to a culture media supplemented with different concentrations of the F-cream formulation, namely 2.5, 5 and 10 mg/mL. For the controls, the cells were only exposed to culture media. The media was removed from the wells and the cells were washed twice with PBS. Photographs were collected at times 0, 16 and 24 h. Afterwards, the wells were replenished with the previously removed culture media. Images taken show the typical cell morphology and were used to evaluate the wound closure ability of the F-cream formulation in fibroblasts and keratinocytes. Image analysis was

performed using ImageJ 1.47v software (NIH, USA) [387] and wound area measured between borderlines. The wound closure (%) was determined by the following equation [388]:

$$\text{Wound Closure (\%)} = \frac{(\text{Initial Area} - \text{Final Area})}{\text{Initial Area}} \times 100 \quad (4.1.2)$$

where the *Initial Area* is the area measured between borderlines at time 0 h and *Final Area* is the area measured between borderlines after 16 h or 24 h. All the experiments were performed in quadruplicate.

4.1.2.6.4 *In vitro* photoprotection assay

Vero (monkey kidney epithelium, ATCC® CCL-81™) cells were cultured in 3-mL Petri dishes for a final concentration of 100,000 adhered cells/cm² and left to incubate at 37 °C for 24 h for successful cell adherence. After reaching 70% confluence, cells exposed to Dulbecco's modified Eagle's medium (low-glucose DMEM, #L0066, from Biowest, with 1.0 g/L glucose, stable glutamine and sodium pyruvate) supplemented with penicillin (100 U/ml), streptomycin (100 µg/mL), 1% of Fugizone and 10% FBS (Fetal Bovine Serum, S. America origin, Biowest, #S1810), F-cream and Bioderm® Prototype™ formulations were either irradiated for 30 min in a biological safety cabinet (ESCO Labculture, Singapore) with a 254 nm ultraviolet lamp or non-irradiated and left at room temperature for the same time interval. After irradiation, all Petri cultures were left to incubate at 37 °C for 24 h before assessing cell viability – to account for any signs of delayed radiation-induced cell death [389] – with the metabolic indicator resazurin [390], by adding a resazurin:DMEM solution (50% resazurin dissolved at a concentration of 0.04 mg/mL in PBS + 50% DMEM), incubating during 2 h at 37 °C, 5% CO₂ and measuring the optical density at 570 and 600 nm. The irradiance of the UVC lamp of the biological safety cabinet, measured with a Delta Ohm HD 2102.2 Luxmeter equipped with an LP471UVC probe, was 2.0 W/m².

4.1.2.7 Sensorial evaluation

The sensory analysis was conducted according to ISO 11136:2014, using a panel of 33 volunteers with no dermatological diseases (Appendix 7). The panel provided a sensory analysis of the formulation. Each volunteer answered 10 questions about the formulation's sensory attributes (fragrance, consistency, and stickiness), skin feel during application (spreadability and oiliness), and skin feel after application (vanishing, hydration, softness, and freshness). Responses were given in a scale from 1 (unacceptable) to 5 (excellent). Sensory parameters were evaluated by application of the formulation between the fingertips and rubbed into the skin. The samples were assessed at room temperature and sensorial evaluation was conducted after 24 hours of product storage. The results were analysed using the statistical programme Origin Pro 2021b SR1 (OriginLab Corporation, Northampton, MA, USA).

4.1.2.8 Optical microscopy image collection

A NIKON Eclipse Ti-S (Tokyo, Japan) optical microscope equipped with a NIKON D610 digital camera was used. Pictures were collected with the Camera Control Pro software, using a 40x objective magnification.

4.1.3 Results

4.1.3.1 FucoPol's safety

FucoPol's safety for incorporation into cosmetic products was assessed by the HRIPT test that evaluated the biopolymer's skin compatibility and allergic potential. The absence of adverse reactions in the initial three weeks of contact or after the final challenge contact allowed to confirm that the repeated application of the FucoPol aqueous solution on the skin of the volunteers did not induce irritation or allergic reaction and showed good skin compatibility. Hence, FucoPol can be considered a dermatologically validated hypoallergenic ingredient that is safe for cosmetic formulations.

4.1.3.2 Characterization of the FucoPol-based cream

4.1.3.2.1 Physicochemical characterization

After preparation, samples of the F-cream were placed at different temperatures (4, 20 and 30 °C) to evaluate the formulation's stability over a period of 60 days. The prolonged stability of an emulsion is a decisive factor to consider its suitability for pharmaceutical/cosmetic applications [391]. Storage at different temperatures allowed to evaluate the emulsion's behaviour upon storage under different conditions.

The F-cream presented a yellowish white colour (Figure 4.1.1a) and a slight lemon odour due the *Citrus limon* peel oil added as fragrance, with no visible changes compared to the freshly prepared formulation. The EI (100%), homogeneous texture, colour, and odour of the F-cream was maintained throughout the 60-day storage period, with no visible oil/water phase separation, at all tested temperatures (Figure 4.1.2a). The results showed that, up to 60 days of storage, there were no breaking mechanisms for the samples kept at 4 °C and at 30 °C, which maintained their stability without phase separation after the centrifugation cycle (Figure 4.1.2b). Contrarily, the sample kept at 20 °C presented phase separation, thus indicating density differences between the oil and water phases [305].

Microscopy analysis of the F-cream samples after 24 h showed dispersed oil droplets at all storage temperatures (Figure 4.1.1a-b), characteristic of O/W systems [183,184], in agreement with the high electrical conductivity values (138-282 $\mu\text{S}/\text{cm}$) displayed by the samples (Figure 4.1.3a) [276,305,392]. However, there was an evident decrease of the conductivity after 60 days of storage (from 282 $\mu\text{S}/\text{cm}$ to 138 $\mu\text{S}/\text{cm}$) for the samples stored at 20 °C (Figure 4.1.3a). Unstable emulsions have been reported to present variation in electrical conductivity [306]. This result is in agreement with the phase separation observed in the centrifuge test (Figure 4.1.2b). Although an increase in the conductivity values was noticed for the samples preserved at 4 °C (from 186 $\mu\text{S}/\text{cm}$ to 282 $\mu\text{S}/\text{cm}$) and 30 °C (from 155 $\mu\text{S}/\text{cm}$ to 282 $\mu\text{S}/\text{cm}$), it did not affect the systems.

Section 4. Validation of the FucoPol-based Cream: Bioactive Properties and Sensorial Evaluation

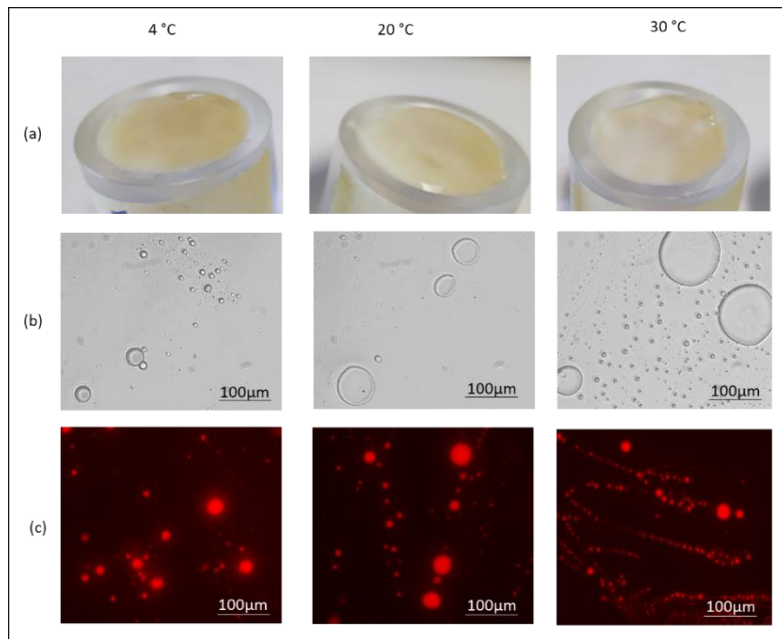


Figure 4.1.1. FucoPol-based cream (F-cream) after 24 hours at different temperatures: (a) F-cream appearance, (b) phase contrast and (c) fluorescence optical microscopic (100x) images of the samples after Nile Blue A staining.

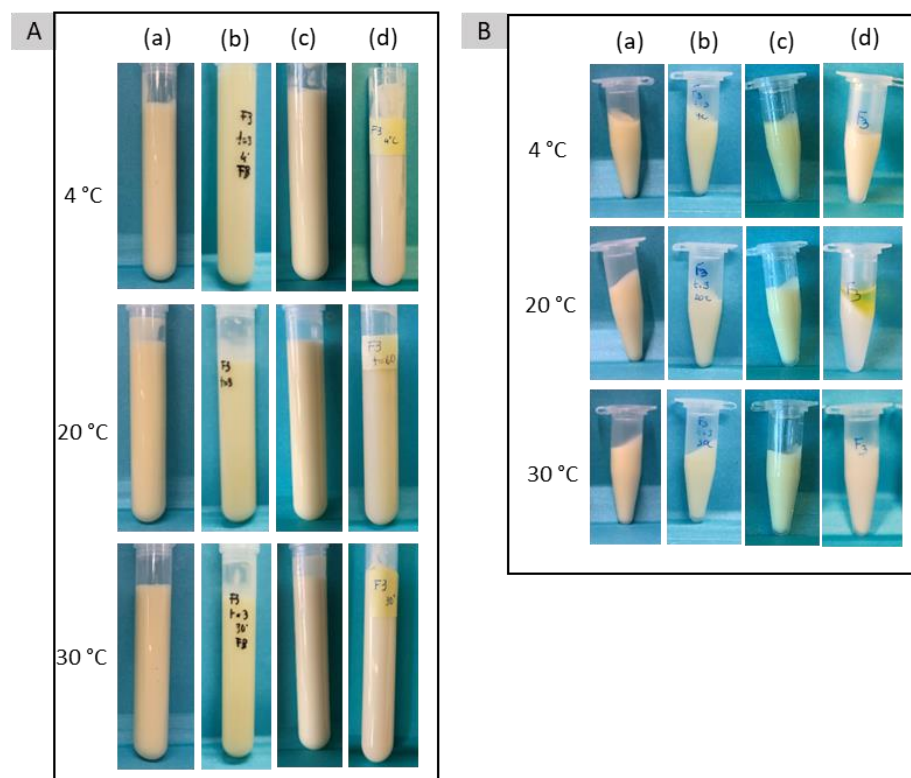


Figure 4.1.2. (A) Emulsification index over storage period of (a) t=1, (b) t=3, (c) t=7, (d) t=60 days, and (B) samples submitted to the centrifugation test.

The F-cream had a pH of 5.88 at 24 h and the observed pH variations (5.88–6.19) were not significant (Figure 4.1.3a) at the different tested temperatures. The observed pH values are compatible with human skin pH [393,394], supporting the use of the F-cream as a topical cosmetic formulation.

In terms of droplet size, there were some interesting variations which could explain the observed stability for F-cream at different temperatures (Figure 4.1.1a-b). At 20 °C, the average droplet size presented its highest value ($22.4 \pm 1.73 \mu\text{m}$), remaining constant during the storage period, with minor changes ($22.9 \pm 0.66 \mu\text{m}$). At 4 °C, the droplet size increased from $12.9 \pm 1.37 \mu\text{m}$, at 1 day, to $16.5 \pm 2.58 \mu\text{m}$ after 3 days, and to $17.3 \pm 0.78 \mu\text{m}$ after 60 days of storage. At 30 °C, the formed droplets also increased during the first 7 days of storage, from $14.1 \pm 0.85 \mu\text{m}$ to $18.6 \pm 0.32 \mu\text{m}$, remaining stable for the rest of the storage period. Apparently, the storage temperature affects the droplet formation mechanism, in which cold storage temperatures lead to smaller droplets and to the fastest droplet size stabilization, which was obtained after 3 days at 4 °C *versus* 7 days at 30 °C. Despite this possible thermal effect on droplet size stabilization, the final values obtained at 4 and 30 °C are similar. At higher temperatures, the droplet coalescence mechanism is favoured, due to a lower inter-droplet liquid viscosity. Moreover, higher temperatures lead to increased O/W electrostatic repulsion. Therefore, the fastest stabilization of droplet size at lower temperatures is related to the lower size of the formed droplets, which present lower tendency for droplet coalescence [395]. Lower droplet size has been correlated with stable emulsions [191,309,375].

Smaller droplet sizes and lower PI values (< 0.3) are responsible for higher stability [191,294,308–310] avoiding the gravitational separation [396,397]. As shown in Figure 4.1.3b, the PI values of all samples were higher than 0.3 [276,309], being ranged between 2.7–3.3 independently of the storage time and the temperature. The PI values are in agreement with the microscopic observation (Figure 4.1.1a-b), in which it is possible to note various droplets with different sizes indicating considerable polydisperse droplet sizes. As expected, the Zeta-potential values were negative at all tested conditions, which can be attributed to the presence of the negatively charged carboxylate groups [272] present in FucoPol macromolecule.

For all studied conditions, the Zeta-potential was stable during 3-days (ranged between -69 mV to -72 mV) (Figure 4.1.1a-b). Afterwards an increase was observed at 4 °C (from -69 mV to -28.3 mV) and at 30 °C (from -70 mV to -42 mV), while a decrease was observed at 20 °C (from -70 mV to -99 mV). Nonetheless, the Zeta-potential agrees to the reported range ($+25 < \text{mV} < -25$) for stable emulsions [294].

Section 4. Validation of the FucoPol-based Cream: Bioactive Properties and Sensorial Evaluation

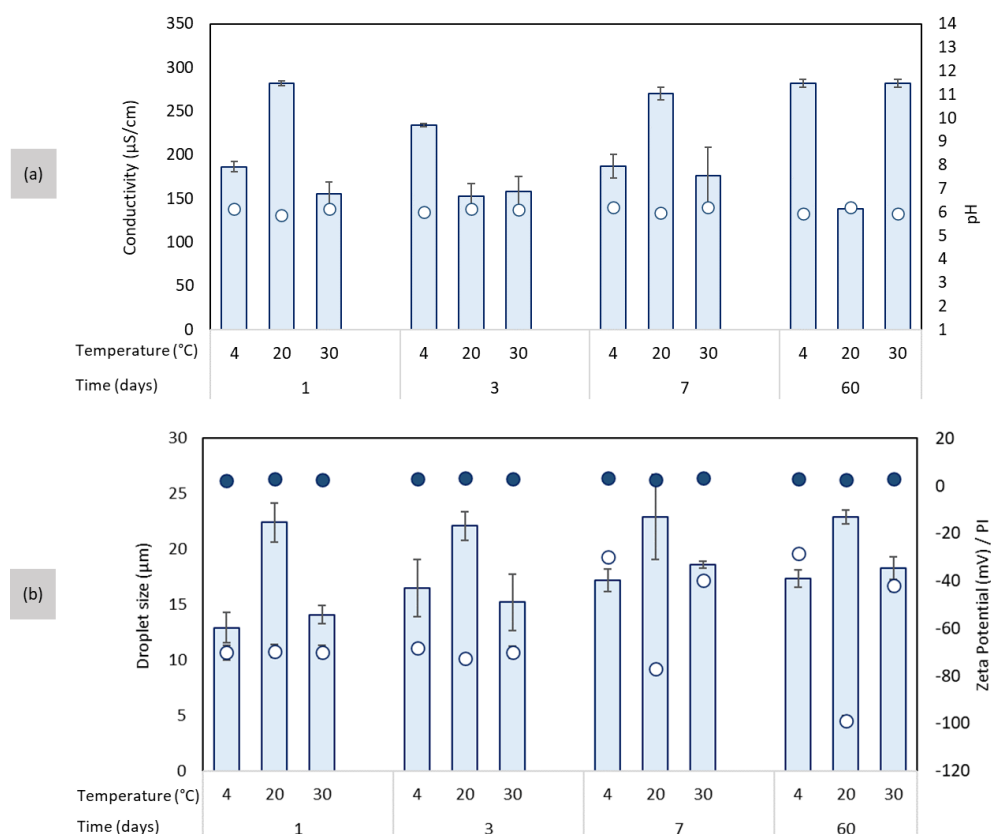


Figure 4.1.3. (a) pH (open circles) and conductivity (blue bars) and (b) droplet size (blue bars), Zeta-potential (open circles), and PI (closed circles) for F-cream during the storage period (t=1, 3, 7, 60 days) at different temperatures (4 °C, 20 °C and 30 °C).

4.1.3.2.2 Apparent viscosity and viscoelastic properties

Structural deformation resistance during standardized shearing procedure is measured by rotational shear tests. F-cream formulation presented a non-Newtonian (shear-thinning) behaviour (Figure 4.1.4) as viscosity gradually decreased under shear rate, a characteristic attributed to their semi-flexible molecular structure [204,235,394]. The storage time apparently affects the viscosity of the formulation since, after 60-days, a slight decrease at shear rate 2.3 s^{-1} (38 Pa.s to 22 Pa.s) for F-cream stored at 20 °C and at 30 °C (43 Pa.s to 38 Pa.s). Viscosity reduction may result from the diffusion of internal aqueous phase to the outer aqueous phase or globules breach induced by higher shear stress [398]. On the other hand, after 60 days of storage for F-cream at 4 °C the viscosity increases from 28 Pa.s to 38 Pa.s at the same shear rate, which can be attributed to the increase of emulsion viscosity at lower temperatures, an effect reported before by several authors [305,399], being enhanced after a long exposure to low temperature.

Section 4. Validation of the FucoPol-based Cream: Bioactive Properties and Sensorial Evaluation

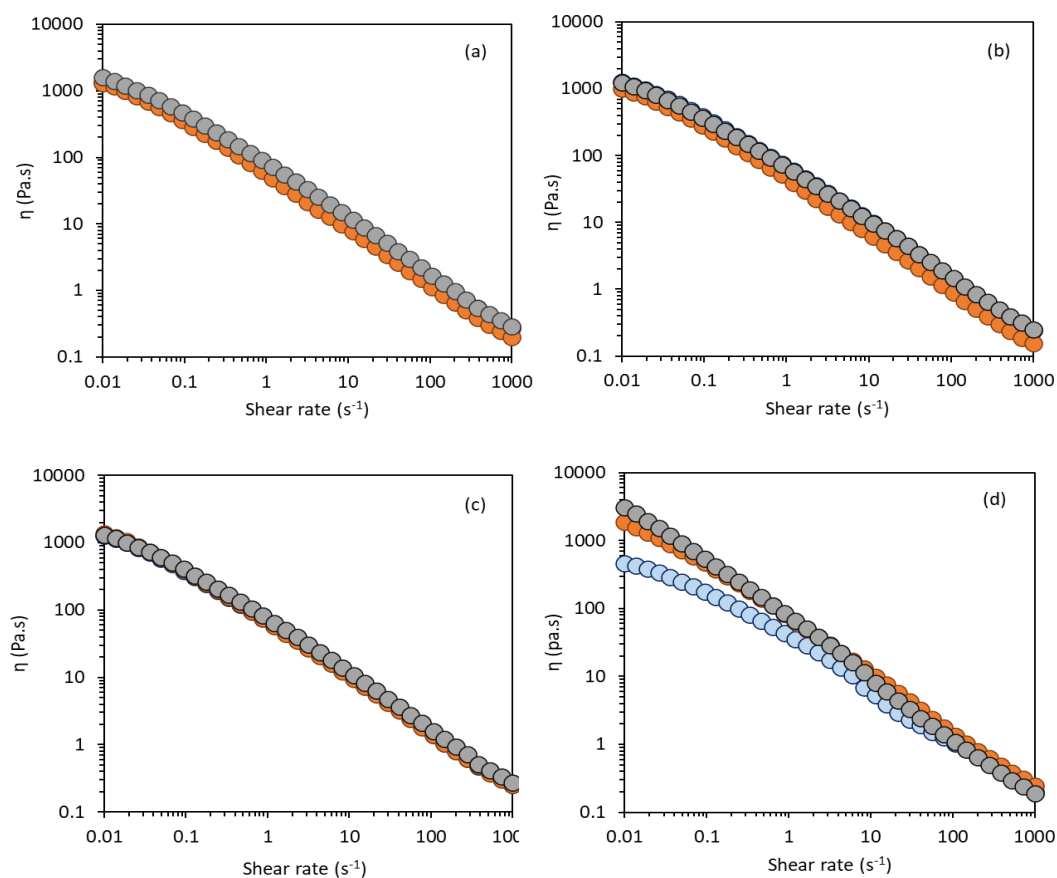


Figure 4.1.4. Flow curves for FucoPol-based cream during the storage time (days) at different temperatures (°C): (a) t=1, (b) t=3, (c) t=7. (d) t=60; 4 °C (orange circles), 20 °C (blue circles), and 30 °C (grey circles).

Oscillatory tests were performed to infer about the F-cream viscoelastic behaviour at different time and temperature storage. The obtained mechanical spectra (Figure 4.1.5) showed a solid-like behaviour [191] (weakly structured gel) for all conditions tested, with the storage modulus higher than the loss modulus ($G' > G''$ at 0.1 Hz). At the end of storage (Figure 4.1.5d), an increase of G' and G'' at 4 °C and 30°C (from 159 Pa to 454 Pa, and from 159 Pa to 3241 Pa at 0.1 Hz, respectively) was observed indicating that at these temperatures F-cream present a stronger network [235,273,316] with higher stability. Emulsions with higher elasticity ($G' \gg G''$) are usually more stable [400]. For F-cream stored at 20 °C a significant decrease of G' and G'' with a crossover at 0.01 Hz (Figure 4.1.5d) indicated that formulation loses stability during the storage time probably caused by weaker droplets interactions which ultimately results in system destabilization [400]. These results are in agreement with physico-chemical and viscosity results.

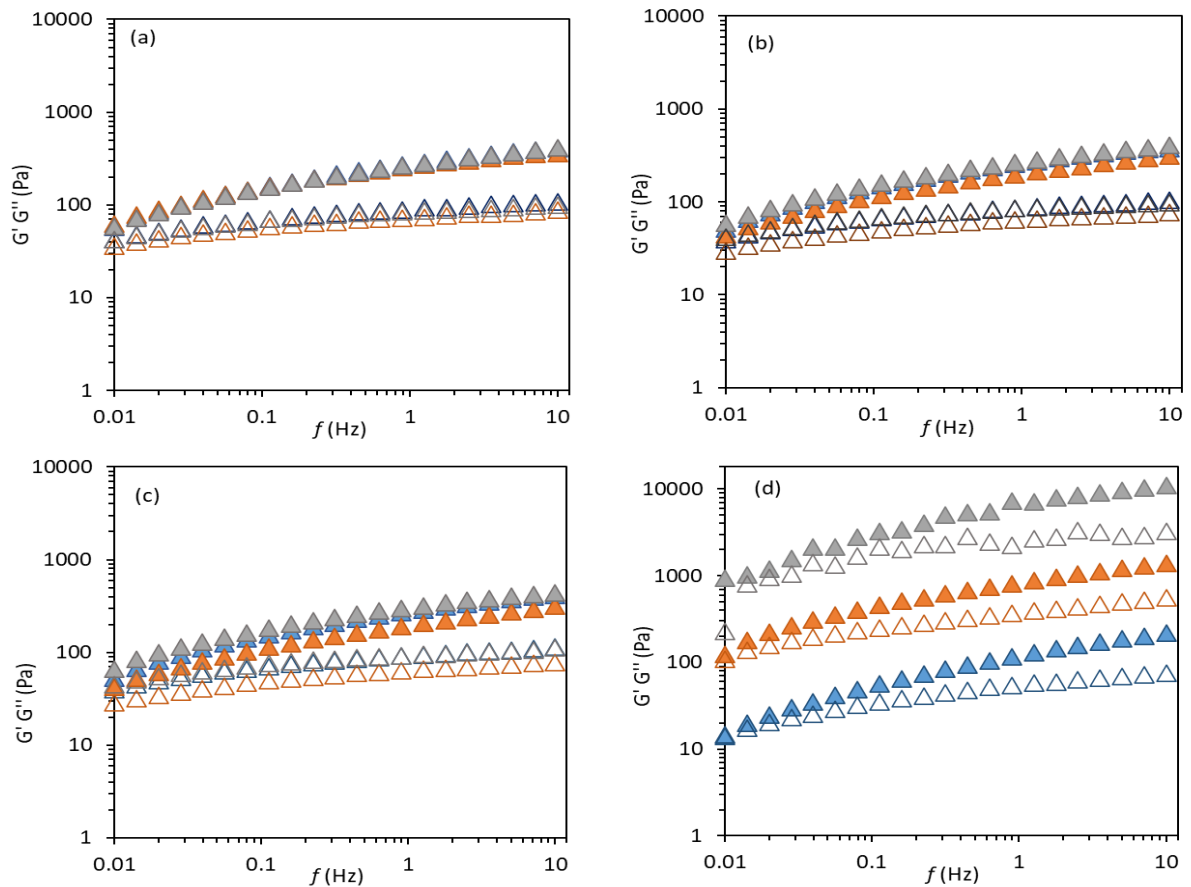


Figure 4.1.5. Mechanical spectrum for the FucoPol-based cream during the storage time (days) at different temperatures ($^{\circ}\text{C}$): (a) $t=1$, (b) $t=3$, (c) $t=7$. (d) $t=60$; 4 $^{\circ}\text{C}$ (orange), 20 $^{\circ}\text{C}$ (blue), and 30 $^{\circ}\text{C}$ (grey). G' (closed triangle) and G'' (open triangle).

4.1.3.3 Textural assessment

Most textural parameters (Table 4.1.2) seem to be affected by both the storage temperature and duration. In terms of firmness, an initial increase until 3 days of storage was observed, followed by an accentuated decrease until 60 days, which was more obvious for the sample stored at 20 $^{\circ}\text{C}$ (from 0.147 to 0.047 N). Sample consistency presented a similar behaviour as its firmness, with the consistency loss being more significant also at 20 $^{\circ}\text{C}$ (from 0.469 to 0.117 mJ). There was also an initial increase of adhesiveness at all tested temperatures, which was maintained between 3 and 7 days of storage at 20 $^{\circ}\text{C}$ but decreased at 30 $^{\circ}\text{C}$ and 4 $^{\circ}\text{C}$. Between days 7 and 60 of the storage period, this parameter presented oscillating behaviour: decreased at 20 $^{\circ}\text{C}$ (from 0.420 to 0.191 mJ); maintained at 30 $^{\circ}\text{C}$ (0.341–0.388 mJ); and increased at 4 $^{\circ}\text{C}$ (from 0.225 to 0.381 mJ). The cohesiveness of the samples was not affected by temperature nor storage duration (0.9–1.0 N). Consumers are generally interested in products with good spreadability, which is determined by the firmness and consistency parameters [268]. In addition, an acceptable spreadability leads to the correct use of the formulation, ensuring the uniform scattering of the active substance on the skin [203,204]. Therefore, the F-cream stored at 20 $^{\circ}\text{C}$ could be proposed

as a suitable candidate for consumer's acceptance, despite not being as stable as F-creams stored at different temperatures.

Table 4.1.2. Textural parameters for F-cream during the storage period (days) at different temperatures (°C).

Time (days)	1			3			7			60		
Temperature (°C)	4	20	30	4	20	30	4	20	30	4	20	30
Firmness (N)	0.103	0.111	0.106	0.188	0.147	0.233	0.108	0.150	0.143	0.117	0.047	0.091
Consistency (mJ)	0.195	0.280	0.239	0.544	0.469	0.664	0.279	0.346	0.316	0.321	0.117	0.380
Cohesiveness (N)	0.876	0.938	0.898	0.994	1.012	0.964	0.952	1.003	1.044	0.983	0.944	0.930
Adhesiveness (mJ)	0.129	0.232	0.257	0.346	0.382	0.517	0.225	0.420	0.341	0.381	0.191	0.388

4.1.3.4 Comparison of FucoPol-based cream with Bioderm® Prototype™ cream anti-wrinkles

Bioderm® Prototype™ is an anti-wrinkle and anti-age face cream that provides skin firming and hydration, with hyaluronic acid and α -tocopherol in its composition (www.bioderm.com; www.galenicpharmacy.gr/en-gb/bioderm-prototype-intensive-anti-wrinkle-anti-age-cream-50ml).

Prototype™ cream presents a SPF20 protection index and a pH value of 4.87. Comparing the rheological and texture properties (Table 4.1.3), Prototype™ cream presented higher G' and G'' than the F-cream (2828 Pa and 1816 Pa at $f=0.1$ Hz, respectively) than the F-cream (203 Pa and 68.7 Pa, at $f=0.1$ Hz, respectively), indicating a stronger network for the commercial formulation [235,273,316]. This behaviour suggests an elastic over viscous predominance, with a structure supported by physical bonds between the macromolecules [204]. However, a more structured system influences the spreading behaviour of the cream [191], and Prototype™ presented higher firmness (0.129 N) and consistency (0.792 mJ) than the F-cream (0.047 N and 0.117 mJ, respectively). The corresponding higher spreadability of the F-cream might render it more easily acceptable by the consumers [268].

Table 4.1.3. Rheological parameters and textural parameters of the F-cream stored for 60 days at room temperature (20 °C) and Bioderm® Prototype™. Apparent viscosity (η , measured at 2.30 s^{-1}) and viscoelastic parameters (G' , G'') at room temperature (20 °C). G' -storage/elastic modulus and G'' - loss/viscous moduli at $f=0.1$ Hz.

Cream	pH	Conductivity ($\mu\text{s}/\text{cm}$)	Droplet size (μm)	Rheological Parameters			Textural Parameters			
				η (Pa.s)	G' (Pa)	G'' (Pa)	Firmness (N)	Consistency (mJ)	Cohesiveness (N)	Adhesiveness (mJ)
Bioderm® Prototype™	4.87	287	2.99	21.82	2828	1816	0.129	0.792	0.961	0.398
F-cream (60 days)	6.19	138	22.9	14.2	203	68.7	0.047	0.117	0.943	0.192

4.1.3.5 Antioxidant activity

The skin antioxidant system is constantly challenged to protect its extensive area from exogenous radical attacks [401,402]. Therefore, the utilization of daily care products incorporated with antioxidant ingredients is essential to prevent and attenuate skin aging, with the cosmetic industry widely searching for new compounds to use in the formulation of such products [65,403].

A FRAP assay was employed to assess the $\text{Fe}^{3+} \rightarrow \text{Fe}^{2+}$ conversion as a direct measure of an antioxidant effect. Figure 4.1.6a shows the 595-nm absorption data by employing the TPTZ assay to directly measure the ferric-reducing antioxidant power of the α -tocopherol-containing F-cream and Trolox, a water-soluble analogue of α -tocopherol. It was previously shown [49] that a Hill binding model can be applied to polysaccharide-containing formulations, providing the effective concentration value necessary to achieve 50% of the maximal antioxidant power at a given concentration (EC_{50}) in ferric-reducing experiments. The antioxidant data was then modelled according to non-specific Hill binding dynamics and the results are shown in Figure 4.1.6b. Linear regression and Hill theoretical fitting, along with the EC_{50} and the Hill binding coefficient of molecule-ligand cooperativity (H) parameters are shown in Table 4.1.4.

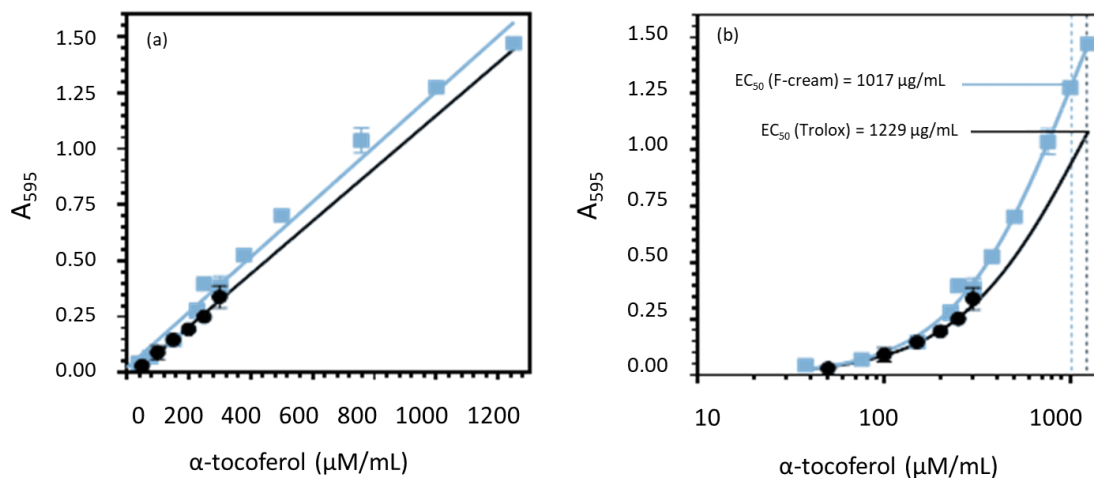


Figure 4.1.6. Ferric-reducing antioxidant potential of FucoPol-based cream (blue), in comparison with Trolox (black): (a) Antioxidant potential follows a dose-dependent linear response, as reported by 595 nm absorption (Trolox: $y=1.182 \times 10^{-3}x - 0.031$, $R^2=0.9905$ | F-cream: $y=1.235 \times 10^{-3}x + 0.023$, $R^2=0.9864$). (b) Hill binding model reveals an increased slope in FucoPol-based cream antioxidant power, suggestive of synergistic effects. The x-axis is presented in log-scale.

Table 4.1.4. Linear regression and Hill model parameters determined for Trolox and FucoPol-based Cream

Linear regression		Hill model	
Trolox	F-cream	Trolox	F-cream
$y=1.182 \times 10^{-3}x-0.031$	$y=1.235 \times 10^{-3}x+0.023$	$EC_{50} = 1229 \mu\text{M}$ $H = 1.258$	$EC_{50} = 1017 \mu\text{M}$ $H = 1.370$
$R^2=0.9905$	$R^2=0.9864$	$R^2 = 0.9606$	$R^2 = 0.9950$

The F-cream and Trolox both show a linear dose-dependent response in reducing Fe^{3+} -TPTZ. The similar regression slopes (1.235×10^{-3} and 1.182×10^{-3} , respectively) suggest that the chemical substance responsible for the antioxidant effect in the F-cream formulation is largely α -tocopherol. However, a slightly increased slope could indicate a potentially synergistic effect in the F-cream that either (i) potentiates α -tocopherol activity or (ii) is complemented by a second antioxidant agent in its composition. The former hypothesis would result in an exponential dose-dependent response, whilst the latter would be a cumulative but linear response. It has been previously shown that FucoPol has an antioxidant effect [49] with greater expression at higher concentrations. This upper-tailed accentuation of the antioxidant effect was proposed to be due to smaller antioxidant molecules that have higher diffusivity in viscous solutions to be able to quench Fe^{3+} species before high molecular-weight polymers.

Analysis of non-specific Hill binding (Figure 4.1.6b) reveals that the F-cream has a lower effective concentration and higher binding cooperativity ($EC_{50}=1017 \mu\text{M}$, $H=1.370$) than Trolox ($EC_{50}=1229 \mu\text{M}$, $H=1.258$). The visibly increased slope of F-cream in Figure 4.1.6b compared to Trolox suggests an enhanced antioxidant power at higher α -tocopherol concentrations that does not vary linearly with the amount of α -tocopherol present. At $227 \mu\text{M}$ of F-cream, the dose-dependent response becomes increasingly exponential and diverges from the Hill slope of Trolox. According to the Hill equation, H can be correlated with receptor-ligand stoichiometry. Positive cooperativity ($H > 1$, in which the binding of a first ligand facilitates the binding of a second in adjacent free receptors) is observed for both Trolox ($H=1.258$) and F-cream ($H=1.370$). A higher H for F-cream suggests increased binding synergism, despite equivalent α -tocopherol concentrations. In summary, these observations agree with a synergistic effect on the expression of antioxidant activity in the multimolecular emulsion system F-cream.

These results suggest that the F-cream is a robust formulation because FucoPol acts not only as an emulsifier but also as an active ingredient with antioxidant effect and as oxidation protector of other formulation ingredients [369], protecting vitamins that oxidize easily in aqueous media, such as vitamin C [404].

4.1.3.6 Cytotoxicity evaluation

Materials for skin care applications must meet several requirements, including its biocompatibility. The cytotoxicity of a material when in contact with skin tissue is a major concern that could

compromise the whole application of a product as a topical use product [405]. Although all formulation components, including FucoPol, were demonstrated as non-cytotoxic [59,246,281,287,288,293], the assessment of cell viability when exposed to the F-cream should be assessed. Particularly, FucoPol was shown to be non-cytotoxic for HaCaT cells at concentrations up to 0.5 mg/mL [52,57] and for Vero cells at concentrations up to 10 mg/mL [52,57]. Hence, the cytotoxic effect of the F-cream was evaluated and compared to that of Boderm® Prototype™ HaCaT cells (recommended by the ISO 10993-5), were used for testing both samples at different formulation concentrations (100, 50, 25, 12.5, 6.25, 3.12, 1.56 and 0.78 mg/mL) obtained by diluting the formulations in cell culture medium. Figure 4.1.7 presents the viability of the cells after being exposed to F-cream aqueous suspensions for 48 h, showing a cytotoxic effect (cell viability decreased below 70%) for formulation concentrations above 12.5 mg/mL. Boderm® Prototype™ suspensions, tested under identical conditions, apparently had a higher impact on cell metabolism, exhibiting a significantly lower cell viability ($90\pm 3\%$) for a concentration of only 0.78 mg/mL (Figure 4.1.7). Given these results, the F-cream arises as a promising formulation, with better biocompatibility than Boderm® Prototype™.

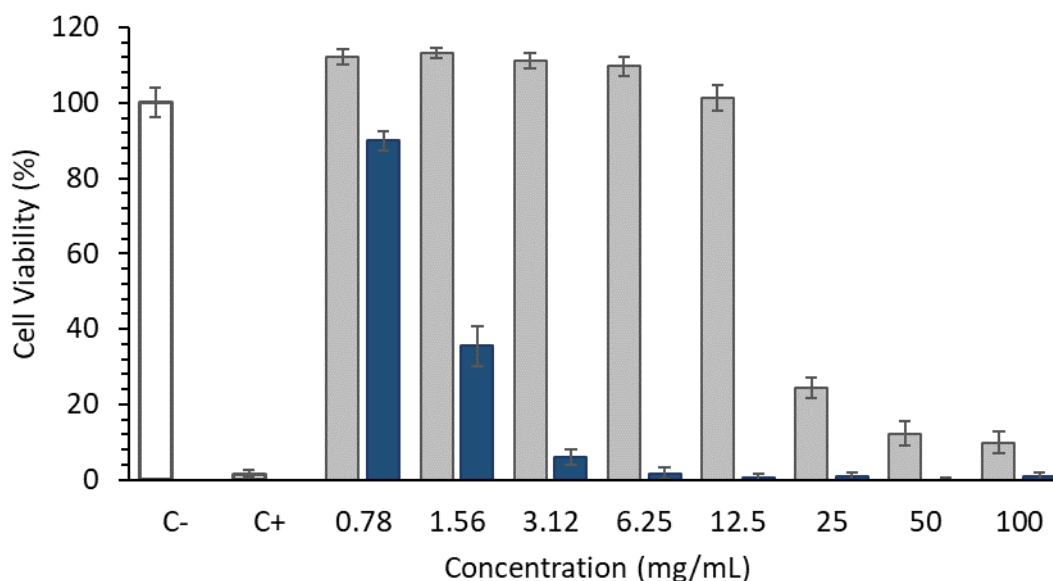


Figure 4.1.7. Cell viability of HaCaT cells after exposure to aqueous suspensions of the F-cream (gray bars) and Prototype™ Boderm® (blue bars) during 48 h. C-, negative control (DMEM High); C+, positive control (DMEM High + 10% DMSO).

4.1.3.7 Wound healing assay

The ability of the F-cream to promote cell migration upon inducing a tear on skin cells (fibroblasts and keratinocytes) monolayers was evaluated for aqueous suspensions at different concentrations (2.5,

Section 4. Validation of the FucoPol-based Cream: Bioactive Properties and Sensorial Evaluation

5 and 10 mg/mL), within the range proven to be non-cytotoxic (Figure 4.1.7). Cell migration assessment was performed by microscope observation of HFFF2 and HaCaT cells after 16 and 24 h (Figures 4.1.8 and 4.1.9, respectively); and was expressed as a percentage of wound closure (Table 4.1.5). For all F-cream concentrations, the cell structure was intact. However, it appears that fibroblast cells have migrated faster when exposed to an F-cream concentration of 2.5 mg/mL, reflecting a positive effect on the wound healing process. After 16 h, a wound closure of $46 \pm 6\%$ was already noticeable, increasing to $70 \pm 7\%$ at 24 h. These values are higher than the ones observed for the control samples at 16 and 24 h ($43 \pm 4\%$ and $53 \pm 8\%$, respectively) (Table 4.1.5). Similarly, for keratinocytes, an F-cream concentration of 10 mg/mL led to higher cell migration ($95 \pm 7\%$ gap closure after 16 h, and $99.92 \pm 0.15\%$ after 24 h), above the values observed for the control ($90 \pm 7\%$ and $97.5 \pm 0.9\%$, respectively) (Table 4.1.5). These results are in agreement with the literature since it has already been shown that the presence of FucoPol enhances the wound healing process in keratinocyte cells [52]. These also reensure that, depending on the concentration of F-cream, this formulation could be used in skin care applications for skin regeneration.

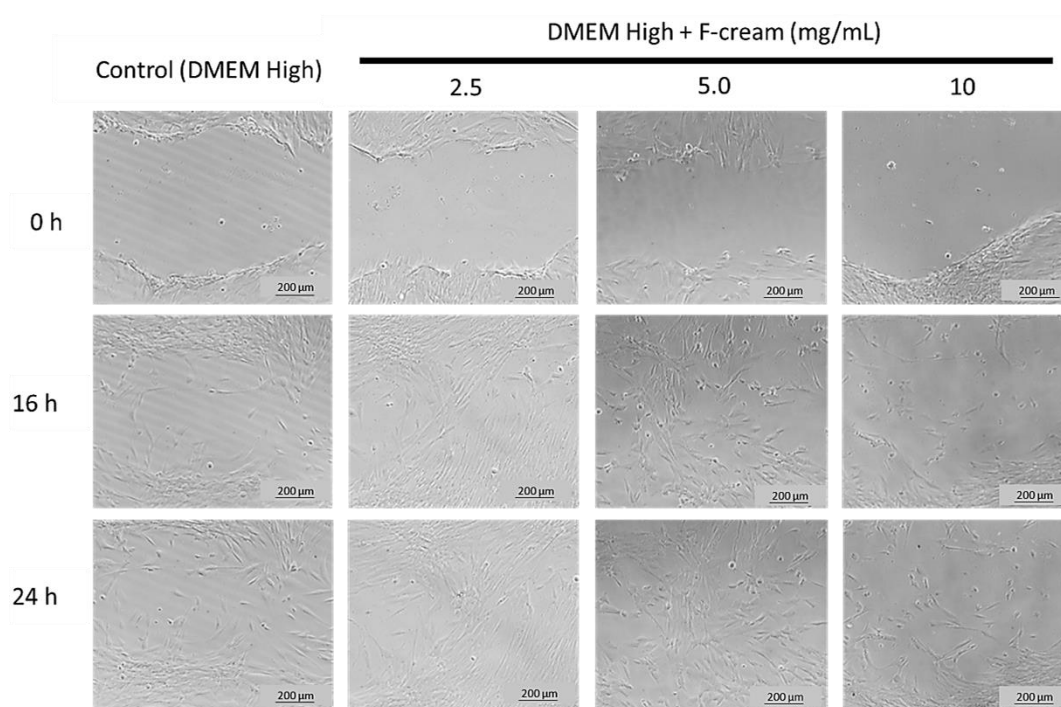


Figure 4.1.8. Microscope images of the wound healing assessment for HFFF2 cells post scratch (0 h) and after being exposed to DMEM (Control) and to DMEM supplemented with five different concentrations of F3 formulation (2.5, 5 and 10 mg/mL) for 16 h and 24 h.

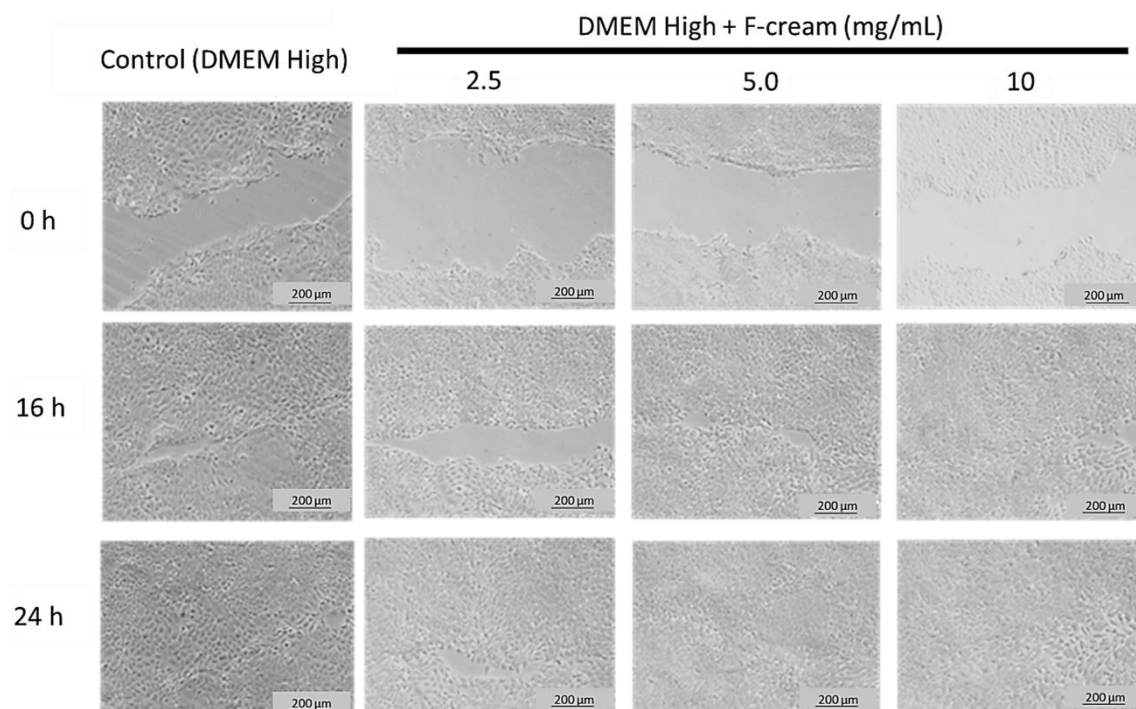


Figure 4.1.9. Microscope images of the wound healing assessment for HaCaT cells post scratch (0 h) and after being exposed to DMEM High (Control) and to DMEM High supplemented with five different concentrations of F-cream formulation (2.5, 5.0 and 10 mg/mL) for 16 h and 24 h.

Table 4.1.5. Cell migration of HFFF2 and HaCaT cell after exposure to F-cream aqueous suspensions, for 16 and 24 h after application of a scratch in the cells' monolayer. Results expressed in percentage of wound closure relatively to time 0 h.

Cell Line	Time (hours)	Wound Closure (%)			
		Control	F-cream (mg/mL)		
			2.5	5	10
Fibroblasts	16	42.84 ± 4.07	46.08 ± 6.02	28.09 ± 3.84	23.38 ± 0.89
	24	52.80 ± 7.60	69.94 ± 7.44	42.92 ± 2.13	47.06 ± 0.21
keratinocytes	16	90.36 ± 6.74	79.66 ± 7.00	88.80 ± 10.09	94.99 ± 6.90
	24	97.50 ± 0.87	96.99 ± 2.36	98.20 ± 2.73	99.92 ± 0.15

4.1.3.8 Photoprotective activity

Several cosmetic products possess photoprotective effects, such as skin care creams for premature skin aging prevention, and the cosmetics' industry is heavily interested in the discovery of new photoprotective ingredients [406,407]. The absorptive capacity of formulation F-cream was tested *in vitro* to

assess its biological photoprotective ability. To mimic a sunscreen applying setting, a surface of adhered Vero cells was exposed to a 0.5 mm layer of either F-cream or Boderm® Prototype™ aqueous suspensions. Figure 4.1.10 shows the metabolic viability of Vero cells post-exposure to both formulations and 254-nm irradiation for 30 minutes, that mimics sunlight exposure.

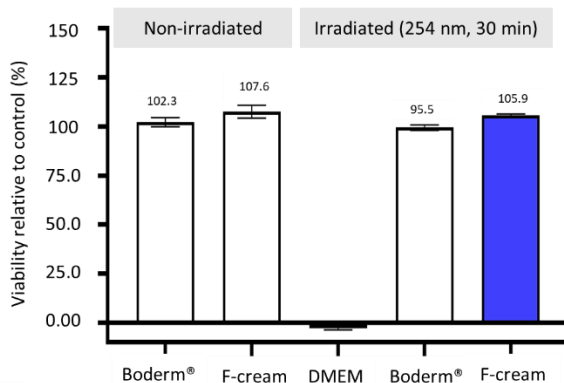


Figure 4.1.10. Metabolic viability of Vero cells exposed to Boderm® Prototype™ and F-cream aqueous suspensions (1:5 dilution), under 254 nm irradiation or no irradiation. Percentual data shown above bars is relative to the non-irradiated DMEM control condition.

The non-irradiated conditions all show maximal performance, with no significant impact on cell viability. There is, however, a slight enhancement of cell proliferation when exposed to the FucoPol-containing formulation F-cream, a phenomenon observed before [49,58]. A 254-nm radiation exposure for only 30 minutes is impactful to cell viability: metabolic activity, as evaluated by the resazurin reduction assay, of exposed cells cultured in DMEM is nil. Even at a 5-fold dilution, there is a maximal performance of the F-cream, with cell viability achieving 105.9%. This formulation presents similar results to the Boderm® Prototype™ sample, at the same dilution (99.5%), while also being a chemically simplified version of standard sunscreen formulations. Given that cell viability is assessed 24 hours after radiation exposure, it already accounts for delayed radiation-induced effects on cell healthiness. Thus, the F-cream is a good candidate for implementation as a photoprotective formulation with a simplified, bio-based chemical composition.

Figure 4.1.11 shows the morphological appearance of Vero cells under all media tested, both in non-irradiated (Figure 4.1.11a) and 254-nm irradiated conditions (Figure 4.1.11b). The effects of UV irradiation are clearly visible in the control group (DMEM). Without irradiation, cells cultured in DMEM growth media have a polygonal aspect, with high degree of attachment, visible cell-cell boundaries, and a structured internal disposition of organelles. When irradiated, cells burst and detached, leaving only residual detritus of non-attached cellular material (viability is effectively 0%). Exposure protection with either Boderm® Prototype™ or F-cream creates a visible photoprotection effect on cell morphology. Overall, cells preserve their polygonal aspect, cell-cell boundaries are distinguishable and

cellular attachment is highly preserved. In summary, F-cream is a suitable candidate for an anti-aging application both in terms of effective photoprotection and cellular preservation.

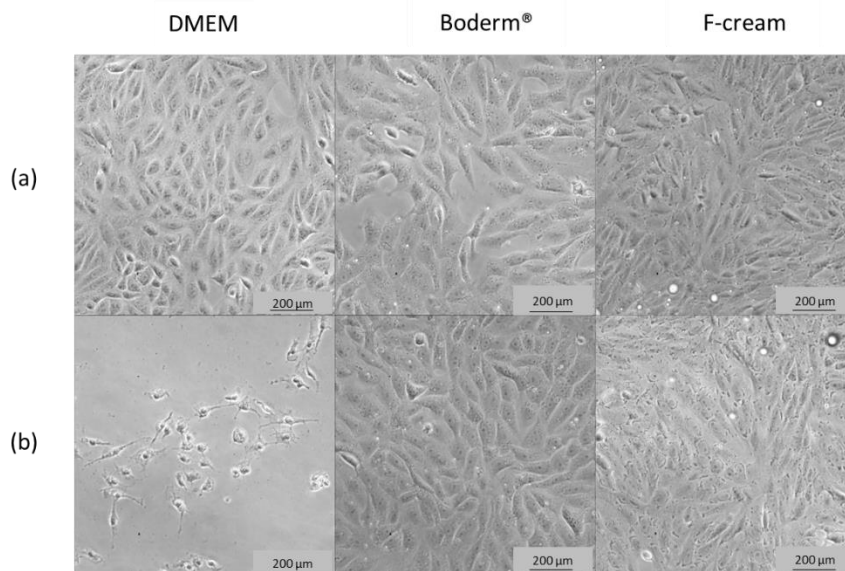


Figure 4.1.11. Morphological appearance of Vero cells in the *in vitro* photoprotection assay with Boderm® Prototype™ and F-cream aqueous suspensions (1:5 dilution): (a) non-irradiated cells, (b) Irradiated at 254-nm irradiation, for 30 min. DMEM is shown as control medium.

4.1.3.9 Sensorial analysis

The interaction between a consumer and a cosmetic product involves a cognitive process composed by two important stages: (1) consumers' perception regarding product organoleptic characteristics (colour, perfume, and texture), the first step for the acceptance or disapproval depending on the sensory assessment performed by the consumer; (2) the posterior processing of the assessment to attribute a symbolical value or positive emotion related to the product, through this specific physiological process. Therefore, the marketing strategies of several cosmetic companies rely on the acknowledgment of the consumers' needs and desires to develop a targeted and suitable product [408]. In this sense, the evaluation of a product's sensory characteristics is indispensable before, during and after application (Figure 4.1.12). Regarding visual aspect, most volunteers agreed that the F-cream presented appealing appearance, which was scored as 4.3. In terms of application and spreadability, the volunteers considered that the cream is easy to apply and spreadable. The volunteers also considered that the formulation provide softness and hydration to the skin, scored 4.5 and 4.3, respectively. Regarding greasiness and tackiness, the volunteers considered that the formulation leaves the skin slightly oily and tacky. Most volunteers noted a fresh effect after application. Concerning the formulation odour, the volunteers presented opposing opinions, whilst some did not report a distinguishable smell, others smelled olive oil or lemon or rancidness. Other volunteers felt an odour change when applied to the skin. The opinion of the volunteers was unanimous regarding the inexistence of residues after application to the skin. Overall, the

Section 4. Validation of the FucoPol-based Cream: Bioactive Properties and Sensorial Evaluation

formulation had a positive acceptance and, although some features require improvement, the feedback was encouraging. Consumers are generally concerned with product performance, the decisive factor in the choice and purchase processes. Considering the obtained feedback in this questionnaire, it can be concluded that, after addressing the odour issue, this formulation presents very promising characteristics to be commercialized as a hydrating cream.

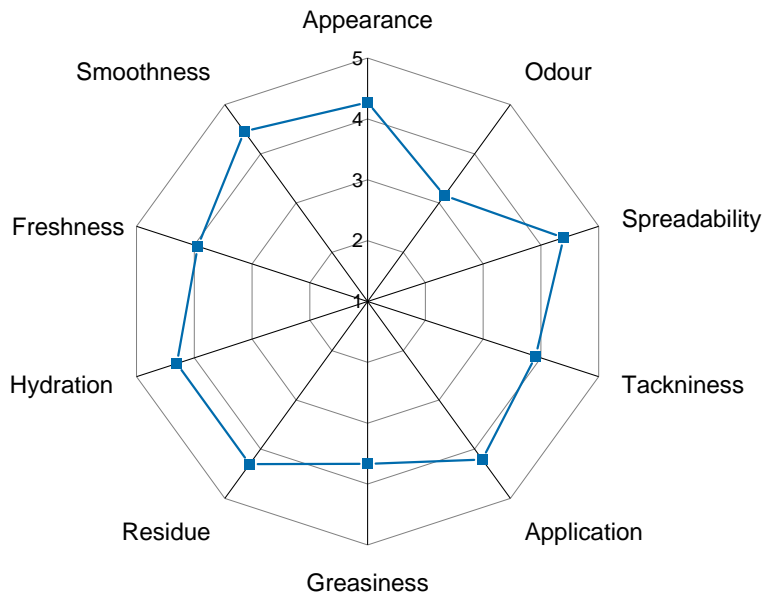


Figure 4.1.12. Sensorial analysis (immediate sensation).

4.1.4 Conclusion

The F-cream formulation is a very promising contender as a cosmetic product for topical application, with anti-aging, skin regenerator, antioxidant and photoprotection properties. It was demonstrated that the storage period and the temperature slightly affected the formulation's physical-chemical, rheological and textural properties. The F-cream stored at 20°C for two months presented satisfactory macroscopic appearance, forming a stable system with minor losses in viscosity, and possessing interesting values of consistency and firmness concordant with spreadable products (higher consumer acceptance). The F-cream might be made more stable by increasing the homogenization time, creating smaller droplet sizes. The formulation was established as a fitting antioxidant cream that enhanced α -tocopherol antioxidant power, with FucoPol contributing to its antioxidant activity. Furthermore, the F-cream was not cytotoxic, conferred photoprotection to irradiated cells, suggesting its use as a stand-alone anti-aging cream, or incorporated in other formulations to intensify their UV-blocking capacity. The F-cream was effective in cellular preservation, contributing to the cell proliferation and migration process. In addition, the F-cream presented appealing sensorial characteristics, with the odour being the characteristic still requiring improvement.

This page was intentionally left blank

5. CONCLUDING REMARKS AND FUTURE WORK

This page was intentionally left blank

Section 5. Concluding Remarks and Future Work

The formulation of cosmetic emulsions is a complex process that requires a lot of investigation time. The composition, ingredients' selection, and interaction between them, reflect the final product's performance and its effect on the skin. Ingredient selection is a challenging process due to several variables: ingredients' safety and function; stability of final formulation; and consumers' preferences. Several ingredients play a fundamental role in the formula to fulfil all the requirements, such as moisturizing, physical stability, chemical inertness, safety, and efficacy profile, while maintaining optimal sensory attribute. An ingredient that can perform several functions in a cosmetic formulation is an asset to the company that produces it.

This thesis aimed at developing stable FucoPol-based emulsified formulations, with suitable physicochemical and biological properties for their utilization as cosmetic creams.

FucoPol, produced by 73100, Lda., has already given sufficient scientific evidence to support its application in cosmetic and pharmaceutical formulations, which makes this biopolymer a high-value ingredient. Nevertheless, its downstream process must be upgraded to reduce FucoPol production costs. In this sense, the study described in Chapter 1 of Section 2 was carried out to optimize the FucoPol extraction process to make the product more profitable while maximizing its yield. These findings demonstrate a significant improvement in the downstream procedure increasing FucoPol's recovery, while reducing water consumption and operation time, key criteria in terms of process economic and environmental sustainability. Moreover, those changes improved the biopolymer's rheological properties, known to significantly impact FucoPol's utilization in cosmetic or pharmaceutical products. In the Chapter 2 of Section 2, polymer deacetylation was successfully achieved, showing some differences compared to native FucoPol. There was a significant reduction of d-FucoPol aqueous solutions' apparent viscosity, which was also affected by the ionic strength and the temperature. These features are advantageous compared to xanthan gum, as it does not require chemical treatment to enhance its properties. Nonetheless, for drug delivery application, the d-FucoPol seems to be more promising than native FucoPol, because the deacetylation confers pH resistance to FucoPol.

The preliminary studies described in Chapter 1 of Section 3, revealed that FucoPol showed a proper emulsion forming and stabilizing capacity for different oils used in cosmetic industry. The interaction between FucoPol, olive oil, and α -tocopherol content was successfully studied by RSM allowing the development of emulsions with high emulsification index. These findings showed FucoPol's high performance as an emulsifier for olive oil/ α -tocopherol, which are supported by an effective impact on the physicochemical and structural characteristics of the emulsions. Formulation of FucoPol-based emulsions was developed in Chapter 2 of Section 3, allowing emulsions with desired organoleptic and structural characteristics. After comparison with several available commercial products, the optimized formulation showed the desired criteria of the thin emulsion system and the physicochemical properties and stability indicate its suitability for cosmeceutical applications. The Chapter 3 of Section 3 revealed a negative effect of L-ascorbic acid in FucoPol-based emulsion, regardless of the cosmetic oil used. Although resulting in particle size reduction, the presence of L-ascorbic acid in the aqueous phase resulted in O/W systems with lower physical stability, as demonstrated by the decrease of the emulsions' apparent viscosity, firmness, cohesiveness and adhesivity, as well viscoelastic behaviour change. This

Section 5. Concluding Remarks and Future Work

study was complemented by a validation of final formulation in Section 4. The stability tests proved that formulation has a satisfactory stability during the shelf life (2 months), and *in vitro* studies proved its non-cytotoxic effect, as well having a photoprotective and regenerative effect.

In summary, a FucoPol-based emulsion system was successfully developed as a potential cosmetic lotion. Its development included the optimization of composition, manufacturing process, and physicochemical characteristics; formulation stability studies and *in vitro* studies to evaluate the cytotoxicity, photoprotection and wound healing effect; and sensory analysis. In this context, the RSM proved to be an effective tool for the screening ingredient content in all development stages.

In conclusion, FucoPol has been demonstrated to act as an emulsifier agent, emollient, and thickening agent. Moreover, FucoPol can also be added to formulations to act as an active agent with photoprotective, antioxidant, and skin regenerative effects. In this sense, FucoPol possess a high-market value because it is a versatile ingredient and more research and development using FucoPol may rise the industry attention towards this biopolymer. From 73100, Lda. point of view, FucoPol should be looked at as an asset to commercialize as an ingredient for dermatological formulation developers or should be even used by 73100, Lda. to develop its own applications in case that is the company's strategic view. Academically, this thesis enhanced the available knowledge about FucoPol, not only by the development of upgraded downstream procedures (which can also save 73100, Lda. money by reducing operation costs, i.e., water consumption and operation time), but also showed the biopolymer applicability to use in topical formulations, as well as its interaction mechanisms with other ingredients (olive oil, α -tocopherol, and L-ascorbic acid). FucoPol must be considered a valuable ingredient suitable to use in several applications, both pharmaceutical and cosmetic, given its distinctive properties.

As a natural follow-up from the present study, the scale-up production to a pilot scale using a mini-plant pilot reactor to increase the volume of the lab scale. Regarding the FucoPol-based creams, a 6-month shelf-life assessment and antimicrobial activity control, as recommended by the International Standard ISO 11930:2019, would complement the formulations' characterization. To provide more information on the stabilization of emulsions, the multiple light scattering can be useful. Additionally, physicochemical characterization could be complemented by performing structural studies using X-ray photoelectron spectroscopy and NMR spectroscopy. Determination of hydrophile-lipophile balance (HLB) in emulsion, and olive oil/water interfacial tension measurements would provide a useful complementary result.

In vitro permeation studies could be performed to evaluate the capacity for the systemic absorption of α -tocopherol after emulsion application on the skin. Supplementary *in vivo* studies involving a Human Repeat Insult Patch test to evaluate the irritation/allergic reactions of the product, determination of hydration performance with epidermal capacitance evaluation, and, to evaluate the biodistribution of ingredients, bioluminescence imaging studies could be performed after skin application.

Other objectives will be the composition adjustment, with ingredient content adjust and/or addition of new ingredients to ensure physical stability during the cosmetic shelf life; directing the FucoPol-containing formulations for therapeutic use, with targeted delivery of drugs; and formulation

Section 5. Concluding Remarks and Future Work

preparation using a cold process to minimize the energy consumption. Regarding applications, the development of different formulations with alternative oils, such as soybean, avocado, and grapeseed oils (among others) might be explored. Moreover, it is also possible the design and development of creams for specific skin types (with higher or lower oiliness), as well as the development of skin regeneration creams with anti-wrinkle effect. Independently of the desired application, the organoleptic properties of the designed creams might also require research and development to improve important characteristics such as odour, oiliness, and colour.

This page was intentionally left blank

REFERENCES

1. Shanmugam, M.; Abirami, R.G. Microbial Polysaccharides - Chemistry and Applications. *Journal of Biologically Active Products from Nature* **2019**, *9*, 73–78, doi:10.1080/22311866.2019.1571944.
2. Yildiz, H.; Karatas, N. Microbial Exopolysaccharides: Resources and Bioactive Properties. *Process Biochemistry* **2018**, *72*, 41–46, doi:10.1016/j.procbio.2018.06.009.
3. Sutherland, I. A Sticky Business. Microbial Polysaccharides: Current Products and Future Trends. *Microbiology today* **2002**, *29*, 70–71.
4. Freitas, F.; Alves, V.; Reis, M.A.M. Bacterial Polysaccharides: Production and Applications in Cosmetic Industry. *Polysaccharides* **2014**, 1–24, doi:10.1007/978-3-319-03751-6.
5. Balkrishna, A.; Agarwal, V.; Kumar, G.; Gupta, A.K. Applications of Bacterial Polysaccharides with Special Reference to the Cosmetic Industry. *Microbial Bioprospecting for Sustainable Development* **2018**, 189–202, doi:10.1007/978-981-13-0053-0_9.
6. Kanlayavattanukul, M.; Lourith, N. Biopolysaccharides for Skin Hydrating Cosmetics. In *Polysaccharides: Bioactivity and Biotechnology in Springer International Publishing*; Ramawat, K.G.; Mé-rillon J.-M., Eds.; Springer International Publishing: Switzerland, **2015**, Chapter 60, 1867–1892, doi.org/10.1007/978-3-319-03751-6_29-1.
7. Bom, S.; Jorge, J.; Ribeiro, H.M.; Marto, J. A Step Forward on Sustainability in the Cosmetics Industry: A Review. *J Clean Prod* **2019**, *225*, 270–290, doi:10.1016/j.jclepro.2019.03.255.
8. Sahota, A. Introduction to Sustainability. In *Sustainability: How the Cosmetics Industry is Greening Up*; Sahota, A., Ed.; Wiley, **2013**, Chapter 1, 1–15, doi:10.1002/9781118676516.ch1.
9. Ammala, A. Biodegradable Polymers as Encapsulation Materials for Cosmetics and Personal Care Markets. *Int J Cosmet Sci* **2013**, *35*, 113–124, doi:10.1111/ics.12017.
10. Lei, S.; Edmund, T.F. Polysaccharides, Microbial. *Encyclopedia of Microbiology* **2019**, 660–678, doi:10.1016/B978-0-12-809633-8.13102-4.
11. Kumar, A.S.; Mody, K.; Jha, B. Bacterial Exopolysaccharides - A Perception. *J Basic Microbiol* **2007**, *47*, 103–117, doi:10.1002/jobm.200610203.
12. Roca, C.; Alves, V.D.; Freitas, F.; Reis, M.A.M. Exopolysaccharides Enriched in Rare Sugars: Bacterial Sources, Production, and Applications. *Front Microbiol* **2015**, *6*, 1–7, doi:10.3389/fmicb.2015.00288.
13. Ahmad, N.H.; Mustafa, S.; Man, Y.B.C. Microbial Polysaccharides and Their Modification Approaches: A Review. *Int J Food Prop* **2015**, *18*, 332–347, doi:10.1080/10942912.2012.693561.
14. Sandford, P.A.; Cottrell, I.W.; Pettitt, D.J. Microbial Polysaccharides: New Products and Their Commercial Applications. *Pure and Applied Chemistry* **1984**, *56*, 879–892, doi:10.1351/pac198456070879.
15. BeMiller, J.N. Polysaccharides: Properties. In *Carbohydrate chemistry for food scientists*; BeMiller JN, Ed., 3rd ed. Duxford: Elsevier; 2019, 103–57, **2019**, ISBN 9780128120699.

16. Lohmann, D. Structural Diversity and Functional Versatility of Polysaccharides. *Kluwer Academic Publishers* **1990**, 333–348.
17. M'sakni, N.H.; Majdoub, H.; Roudesli, S.; Picton, L.; Cerf, D.; Rihouey, C.; Morvan, C. Composition, Structure and Solution Properties of Polysaccharides Extracted from Leaves of *Mesembryanthemum crystallinum*. *Eur Polym J* **2006**, *42*, 786–795, doi:10.1016/j.eurpolymj.2005.09.014.
18. Bhavani, A.L.; Nisha, J. Dextran - The Polysaccharide with Versatile Uses. *Int J Pharma Bio Sci* **2010**, *1*, 569–573.
19. Savary, G.; Grisel, M.; Picard, C. Cosmetics and personal care products. In: *Natural polymers*; Olatunji O, Ed.; Cham: Springer International Publishing, **2016**, 219–61.
20. Owh, C.; Chee, P.; Loh, X. A Global Analysis of the Personal Care Market. In *Polymers for personal products and cosmetics*; Loh, X., Ed.; Royal Society of Chemistry: Cambridge, **2016**, 1–17.
21. Alves, V.D.; Torres, C.A.V.; Freitas, F. Bacterial Polymers as Materials for the Development of Micro/Nanoparticles. *International Journal of Polymeric Materials and Polymeric Biomaterials* **2016**, *65*, 211–224, doi:10.1080/00914037.2015.1103239.
22. Gallegos, A.M.A.; Carrera, S.H.; Parra, R.; Keshavarz, T.; Iqbal, H.M.N. Bacterial Cellulose: A Sustainable Source to Develop Value-Added Products – A Review. *Bioresources* **2016**, *11*, 5641–5655, doi:10.15376/BIORES.11.2.5641-5655.
23. Alves, T.F.R.; Morsink, M.; Batain, F.; Chaud, M.V.; Almeida, T.; Fernandes, D.A.; Silva, C.F.; Souto, E.B. Applications of Natural, Semi-Synthetic, and Synthetic Polymers in Cosmetic Formulations Thais. *Cosmetics* **2020**, *7*, 1–16.
24. Lima Fontes, M.; Meneguim, A.B.; Tercjak, A.; Gutierrez, J.; Cury, B.S.F.; Santos, A.M.; Ribeiro, S.J.L.; Barud, H.S. Effect of *in Situ* Modification of Bacterial Cellulose with Carboxymethylcellulose on Its Nano/Microstructure and Methotrexate Release Properties. *Carbohydr Polym* **2018**, *179*, 126–134, doi:10.1016/j.carbpol.2017.09.061.
25. Öner, E.T.; Hernández, L.; Combie, J. Review of Levan Polysaccharide: From a Century of Past Experiences to Future Prospects. *Biotechnol Adv* **2016**, *34*, 827–844, doi:10.1016/j.biotechadv.2016.05.002.
26. Fallacara, A.; Baldini, E.; Manfredini, S.; Vertuani, S. Hyaluronic Acid in the Third Millennium. *Polymers (Basel)* **2018**, *10*, doi:10.3390/polym10070701.
27. Pavicic, T.; Gauglitz, G.G.; Lersch, P.; Schwach-Abdellaoui, K.; Malle, B.; Korting, H.C.; Farwick, M. Efficacy of Cream-Based Novel Formulations of Hyaluronic Acid of Different Molecular Weights in Anti-Wrinkle Treatment. *Journal of Drugs in Dermatology* **2011**, *10*, 990–1000.
28. Prajapati, V.D.; Jani, G.K.; Zala, B.S.; Khutliwala, T.A. An Insight into the Emerging Exopolysaccharide Gellan Gum as a Novel Polymer. *Carbohydr Polym* **2013**, *93*, 670–678, doi:10.1016/j.carbpol.2013.01.030.
29. Ullah, H.; Santos, H.A.; Khan, T. Applications of Bacterial Cellulose in Food, Cosmetics and Drug Delivery. *Cellulose* **2016**, *23*, 2291–2314, doi:10.1007/s10570-016-0986-y.

30. Domżał-Kędzia, M.; Lewińska, A.; Jaromin, A.; Weselski, M.; Pluskota, R.; Łukaszewicz, M. Fermentation Parameters and Conditions Affecting Levan Production and its Potential Applications in Cosmetics. *Bioorg Chem* **2019**, *93*, 102787, doi:10.1016/j.bioorg.2019.02.012.
31. Siqueira, E.C.; Rebouças, J. de S.; Pinheiro, I.O.; Formiga, F.R. Levan-Based Nanostructured Systems: An Overview. *Int J Pharm* **2020**, *580*, doi:10.1016/j.ijpharm.2020.119242.
32. Bukhari, S.N.A.; Roswandi, N.L.; Waqas, M.; Habib, H.; Hussain, F.; Khan, S.; Sohail, M.; Ramli, N.A.; Thu, H.E.; Hussain, Z. Hyaluronic Acid, a Promising Skin Rejuvenating Biomedicine: A Review of Recent Updates and Pre-Clinical and Clinical Investigations on Cosmetic and Nutricosmetic Effects. *Int J Biol Macromol* **2018**, *120*, 1682–1695, doi:10.1016/j.ijbiomac.2018.09.188.
33. Huynh, A.; Priefer, R. Hyaluronic Acid Applications in Ophthalmology, Rheumatology, and Dermatology. *Carbohydr Res* **2020**, *489*, 107950, doi:10.1016/j.carres.2020.107950.
34. Poetschke, V.J.; Hschwaiger, H.; Steckmeier, S.; Ruzicka, T.; Gauglitz, G.G. Anti-Wrinkle Creams with Hyaluronic Acid: How Effective Are They? *MMW Fortschr Med* **2016**, *158*, 1–6.
35. Lochhead, R.Y. The Use of Polymers in Cosmetic Products. In *Cosmetic science and technology: theoretical principles and applications*; Sakamoto, K., Lochhead, R., Maibach, H., Yamashita, Y., Eds.; Elsevier Inc.: Amsterdam, **2017**; 171–221; ISBN 9780128020548.
36. Jindal, N.; Khattar, J.S. Microbial Polysaccharides in Food Industry. In *Biopolymers for food design*; Grumezescu AM, Holban AM. Eds.; Elsevier Inc., **2018**, 95–123, ISBN 9780128115015.
37. Dubuisson, P.; Picard, C.; Grisel, M.; Savary, G. How Does Composition Influence the Texture of Cosmetic Emulsions? *Colloids Surf A Physicochem Eng Asp* **2018**, *536*, 38–46, doi:10.1016/j.colsurfa.2017.08.001.
38. Zia, K.M.; Tabasum, S.; Khan, M.F.; Akram, N.; Akhter, N.; Noreen, A.; Zuber, M. Recent Trends on Gellan Gum Blends with Natural and Synthetic Polymers: A Review. *Int J Biol Macromol* **2018**, *109*, 1068–1087, doi:10.1016/j.ijbiomac.2017.11.099.
39. Alves, V.D.; Freitas, F.; Torres, C.A.V.; Cruz, M.; Marques, R.; Grandfils, C.; Gonçalves, M.P.; Oliveira, R.; Reis, M.A.M. Rheological and Morphological Characterization of the Culture Broth During Exopolysaccharide Production by *Enterobacter* sp . *Carbohydr Polym* **2010**, *81*, 758–764, doi:10.1016/j.carbpol.2009.09.006.
40. Reis, M.A.M.; Oliveira, R.; Freitas, F.; Alves, V. Fucose-containing Bacterial Biopolymer, **2011**, WO2011073874A4.
41. Freitas, F.; Alves, V.D.; Torres, C.A.V.; Cruz, M.; Sousa, I.; João, M.; Ramos, A.M.; Reis, M.A.M. Fucose-containing Exopolysaccharide Produced by the Newly Isolated *Enterobacter* strain A47 DSM 23139. *Carbohydr Polym* **2011**, *83*, 159–165, doi:10.1016/j.carbpol.2010.07.034.
42. Torres, C.A.V.; Marques, R.; Antunes, S.; Alves, V.D.; Sousa, I.; Maria, A.; Oliveira, R.; Freitas, F.; Reis, M.A.M. Kinetics of Production and Characterization of the Fucose-containing Exopolysaccharide from *Enterobacter* A47. *J Biotechnol* **2011**, *156*, 261–267, doi:10.1016/j.jbiotec.2011.06.024.
43. Torres, C.A.V.; Antunes, S.; Ricardo, A.R.; Grandfils, C.; Alves, V.D.; Freitas, F.; Reis, M.A.M.M. Study of the Interactive Effect of Temperature and pH on Exopolysaccharide Production by

- Enterobacter* A47 using Multivariate Statistical Analysis. *Bioresour Technol* **2012**, *119*, 148–156, doi:10.1016/j.biortech.2012.05.106.
44. Freitas, F.; Alves, V.D.; Gouveia, A.R.; Pinheiro, P.; Torres, C.A.V.; Grandfils, C.; Reis, M.A.M. Controlled Production of Exopolysaccharides from *Enterobacter* A47 as a Function of Carbon Source with Demonstration of their Film and Emulsifying Abilities. *Appl Biochem Biotechnol* **2014**, *172*, 641–657, doi:10.1007/s12010-013-0560-0.
 45. Antunes, S.; Freitas, F.; Sevrin, C.; Grandfils, C.; Reis, M.A.M. Production of FucoPol by *Enterobacter* A47 using Waste Tomato Paste By-Product as Sole Carbon Source. **2017**, *227*, 66–73, doi:10.1016/j.biortech.2016.12.018.
 46. Antunes, S.; Freitas, F.; Alves, V.D.; Grandfils, C.; Reis, M.A.M. Conversion of Cheese Whey into a Fucose- and Glucuronic Acid-Rich Extracellular Polysaccharide by *Enterobacter* A47. *J Biotechnol* **2015**, *210*, 1–7, doi:10.1016/j.jbiotec.2015.05.013.
 47. Concórdio-Reis, P.; Pereira, J.R.; Torres, C.A.V.; Sevrin, C. Effect of Mono- and Dipotassium Phosphate Concentration on Extracellular Polysaccharide Production by the Bacterium *Enterobacter* A47. *Process Biochemistry journal* **2018**, *75*, 16–21, doi:10.1016/j.procbio.2018.09.001.
 48. Torres, C.A.V.; Marques, R.; Ferreira, A.R. v; Antunes, S.; Grandfils, C.; Freitas, F.; Reis, M.A.M. Impact of Glycerol and Nitrogen Concentration on *Enterobacter* A47 Growth and Exopolysaccharide Production. *Int J Biol Macromol* **2014**, *71*, 81–86, doi:10.1016/j.ijbiomac.2014.04.012.
 49. Guerreiro, B.M.; Silva, J.C.; Lima, J.C.; Reis, M.A.M.; Freitas, F. Antioxidant Potential of the Bio-Based Fucose-Rich Polysaccharide FucoPol Supports its Use in Oxidative Stress-Inducing Systems. *Polymers (Basel)* **2021**, *13*, doi:10.3390/polym13183020.
 50. Torres, C.A.V.; Ferreira, A.R.V.; Freitas, F.; Reis, M.A.M.; Coelho, I.; Sousa, I.; Alves, V.D. Rheological Studies of the Fucose-rich Exopolysaccharide FucoPol. *Int J Biol Macromol* **2015**, *79*, 611–617, doi:10.1016/j.ijbiomac.2015.05.029.
 51. Rodrigues, T. Preparation and Characterization of Hydrogels Based on Biopolymers: FucoPol and Chitin-Glucan Complex (CGC). **2020**, 1–81.
 52. Concórdio-Reis, P.; Pereira, C.V.; Batista, M.P.; Sevrin, C.; Grandfils, C.; Marques, A.C.; Fortunato, E.; Gaspar, F.B.; Matias, A.A.; Freitas, F.; Reis, M.A.M. Silver Nanocomposites Based on the Bacterial Fucose-Rich Polysaccharide Secreted by *Enterobacter* A47 for Wound Dressing Applications: Synthesis, Characterization and *In Vitro* Bioactivity. *Int J Biol Macromol* **2020**, *163*, 959–969, doi:10.1016/j.ijbiomac.2020.07.072.
 53. Lourenço, S.C.; Torres, C.A.V.; Nunes, D.; Duarte, P.; Freitas, F.; Reis, M.A.M.; Fortunato, E.; Moldão-Martins, M.; Beirão, L.; Alves, V.D. Using a Bacterial Fucose-Rich Polysaccharide as Encapsulation Material of Bioactive Compounds. *Int J Biol Macromol* **2017**, *104*, 1099–1106, doi:10.1016/j.ijbiomac.2017.07.023.
 54. Cruz, M.; Freitas, F.; Torres, C.A.V.; Reis, M.A.M.; Alves, V.D. Influence of Temperature on the Rheological Behaviour of a New Fucose-Containing Bacterial Exopolysaccharide. *Int J Biol Macromol* **2011**, *48*, 695–699, doi:10.1016/j.ijbiomac.2011.02.012.

55. Antunes, S.A. Biological Conversion of Industrial By-Products/Wastes into Value-Added Bacterial Exopolysaccharides. *PQDT - Global* **2018**.
56. Ferreira, A.R.V.; Torres, C.A.V.; Freitas, F.; Reis, M.A.M.; Alves, V.D.; Coelho, I.M. Biodegradable Films Produced from the Bacterial Polysaccharide FucoPol. *Int J Biol Macromol* **2014**, *71*, 111–116, doi:10.1016/j.ijbiomac.2014.04.022.
57. Guerreiro, B.M.; Freitas, F.; Lima, J.C.; Silva, J.C.; Dionísio, M.; Reis, M.A.M. Demonstration of the Cryoprotective Properties of the Fucose-containing Polysaccharide FucoPol. *Carbohydr Polym* **2020**, *245*, 116500, doi:10.1016/j.carbpol.2020.116500.
58. Guerreiro, B.M.; Freitas, F.; Lima, J.C.; Silva, J.C.; Reis, M.A.M. Photoprotective Effect of the Fucose-containing Polysaccharide FucoPol. *Carbohydr Polym* **2021**, *259*, doi:10.1016/j.carbpol.2021.117761.
59. Fialho, L.; Araújo, D.; Alves, V.D.; Roma-Rodrigues, C.; Baptista, V.; Fernandes, A.R.; Freitas, F.; Reis, M.A.M. Cation-Mediated Gelation of the Fucose-rich Polysaccharide FucoPol: Preparation and Characterization of Hydrogel Beads and Their Cytotoxicity Assessment. *International Journal of Polymeric Materials and Polymeric Biomaterials* **2021**, *70*, 90–99, doi:10.1080/00914037.2019.1695205.
60. Vásquez-González, Y.; Prieto, C.; Stojanovic, M.; Torres, C.A.V.; Freitas, F.; Arturo, J. Preparation and Characterization of Electrospun Polysaccharide FucoPol-Based Nanofiber Systems. *Molecules* **2022**, *12*, 1–15.
61. Cañedo-Dorantes, L.; Cañedo-Ayala, M. Skin Acute Wound Healing: A Comprehensive Review. *Int J Inflamm* **2019**, *2019*, 1–15.
62. Lai-Cheong, J.E.; McGrath, J.A. Structure and Function of Skin, Hair and Nails. *Medicine (United Kingdom)* **2013**, *41*, 317–320, doi:10.1016/j.mpmed.2013.04.017.
63. Monteiro-Riviere, N.A. Structure and Function of Skin. *Toxicology of the Skin* **2010**, 1–18, doi:10.5005/jp/books/11954_1.
64. Long C.C. Common skin disorders and their topical treatment. In *Dermatological and transdermal formulations*; Walters KA, Ed.; New York: Informa Healthcare, **2002**, 41–58.
65. Kusumawati I, Indrayanto G. Natural Antioxidants in Cosmetics. *Stud Nat Prod Chem.* **2013**; *40*: 485–505, ISBN 9780444596031.
66. Prow, T.W.; Grice, J.E.; Lin, L.L.; Faye, R.; Butler, M.; Becker, W.; Wurm, E.M.T.; Yoong, C.; Robertson, T.A.; Soyer, H.P.; Roberts, M.S. Nanoparticles and Microparticles for Skin Drug Delivery. *Adv Drug Deliv Rev* **2011**, *63*, 470–491, doi:10.1016/j.addr.2011.01.012.
67. Lawton S. Skin 1: The Structure and Functions of the Skin. *Nursing Times [online]* **2019**, *115*, 30–33.
68. Moser, K.; Kriwet, K.; Naik, A.; Kalia, Y.N.; Guy, R.H. Passive Skin Penetration Enhancement and its Quantification *In Vitro*. *European Journal of Pharmaceutics and Biopharmaceutics* **2001**, *52*, 103–112, doi:10.1016/S0939-6411(01)00166-7.

69. Jungersted, J.M.; Hellgren, L.I.; Jemec, G.B.E.; Agner, T. Lipids and Skin Barrier Function - A Clinical Perspective. *Contact Dermatitis* **2008**, *58*, 255–262, doi:10.1111/j.1600-0536.2008.01320.x.
70. Grubauer, G.; Feingold, K.R.; Harris, R.M.; Elias, P.M. Lipid Content and Lipid Type as Determinants of the Epidermal Permeability Barrier. *J Lipid Res* **1989**, *30*, 89–96, doi:10.1016/s0022-2275(20)38401-7.
71. Williams, A.C.; Barry, B.W. Penetration Enhancers. *Adv Drug Deliv Rev* **2012**, *64*, 128–137, doi:10.1016/j.addr.2012.09.032.
72. Lane, M.E. Skin Penetration Enhancers. *Int J Pharm* **2013**, *447*, 12–21, doi:10.1016/j.ijpharm.2013.02.040.
73. Szumała, P.; Macierzanka, A. Topical Delivery of Pharmaceutical and Cosmetic Macromolecules Using Microemulsion Systems. *Int J Pharm* **2022**, *615*, doi:10.1016/j.ijpharm.2022.121488.
74. Wu, Y.-W.; Ta, G.H.; Lung, Y.-C.; Weng, C.F.; Leong, M.K. In Silico Prediction of Skin Permeability Using a Two-QSAR Approach. *Int J Mol Sci* **2022**, *14*, doi:10.3390/ijms20133170.
75. Nohynek, G.J.; Antignac, E.; Re, T.; Toutain, H. Safety Assessment of Personal Care Products/Cosmetics and their Ingredients. *Toxicol Appl Pharmacol* **2010**, *243*, 239–259, doi:10.1016/j.taap.2009.12.001.
76. Patil, A.; Ferritto, M.S. Polymers for Personal Care and Cosmetics: Overview. In *Polymers for Personal Care and Cosmetics*; Patil, A., Ferritto, M.S., Eds.; ACS Symposium Series: Washington, 2013; Vol. 1148, 3–11, ISBN 9780841229051.
77. Bilal, M.; Iqbal, H.M.N. New Insights on Unique Features and Role of Nanostructured Materials in Cosmetics. *Cosmetics* **2020**, *7*, 1–16, doi:10.3390/cosmetics7020024.
78. EC The European Parliament and the Council of the European Union. Regulation No. 1223/2009 of the European Parliament and of the Council of 30 November 2009 on Cosmetic Products Available online: <https://eur-lex.europa.eu/LexUriServ/LexUriServ.do?uri=OJ:L:2009:342:0059:0209:en:PDF>.
79. Halla, N.; Fernandes, I.P.; Heleno, S.A.; Costa, P.; Boucherit-Otmani, Z.; Boucherit, K.; Rodrigues, A.E.; Ferreira, I.C.F.R.; Barreiro, M.F. Cosmetics Preservation: A Review on Present Strategies. *Molecules* **2018**, *23*, 1–41, doi:10.3390/molecules23071571.
80. Wanjari, N.; Waghmare, J. A Review on Latest Trend of Cosmetics-Cosmeceuticals. *International Journal of Pharma Research & Review IJPRR* **2015**, *4*, 45–51.
81. Gao, X.H.; Zhang, L.; Wei, H.; Chen, H.D. Efficacy and Safety of Innovative Cosmeceuticals. *Clin Dermatol* **2008**, *26*, 367–374, doi:10.1016/j.clindermatol.2008.01.013.
82. Aranaz, I.; Acosta, N.; Civera, C.; Elorza, B.; Mingo, J.; Castro, C.; Gandía, M. de los L.; Caballero, A.H. Cosmetics and Cosmeceutical Applications of Chitin, Chitosan and Their Derivatives. *Polymers (Basel)* **2018**, *10*, doi:10.3390/polym10020213.
83. Hosoi, J.; Koyama, J.; Ozawa, T. New Aspects of Cosmetics and Cosmetic Science. In *Cosmetic Science and Technology: Theoretical Principles and Applications*; Sakamoto, K., Lochhead, R.Y., Maibach, H.I., Yuji, Y., Eds.; Elsevier Inc., **2017**; 87–100, ISBN 978-0-12-802005-0.
84. Lautenschäger, H. INCI - Declaration. *Kosmetische Praxis* **2002**, 50–53.

85. Costa, R.; Santos, L. Delivery Systems for Cosmetics - From Manufacturing to the Skin of Natural Antioxidants. *Powder Technol* **2017**, *322*, 402–416, doi:10.1016/j.powtec.2017.07.086.
86. Ferreira, S.M.; Falé, Z.; Santos, L. Sustainability in Skin Care: Incorporation of Avocado Peel Extracts in Topical Formulations. *Molecules* **2022**, *27*, 1–16, doi:10.3390/molecules27061782.
87. Fodil-Bourahla, I.; Bizbiz, L.; Schoevaert, D.; Robert, A.M.; Robert, L. Effect of L-Fucose and Fucose-Rich Oligo- and Polysaccharides (FROP-s) on Skin Aging: Penetration, Skin Tissue Production and Fibrillogenesis. *Biomedicine and Pharmacotherapy* **2003**, *57*, 209–215, doi:10.1016/S0753-3322(03)00047-7.
88. Rakuša, Ž.T.; Roškar, R. Quality Control of Vitamins A and E and Coenzyme Q10 in Commercial Anti-Ageing Cosmetic Products. *Cosmetics* **2021**, *8*, 9–12, doi:10.3390/cosmetics8030061.
89. Lautenschlager, H. Additives in Cosmetic Products. *Kosmetische Praxis* **2004**, 8–10.
90. Lautenschäger, H. Active Agents, the Effective Skin Care - Smoothing the Skin and Providing Overall Protection. *Kosmetische Praxis* **2003**, 6–8.
91. Azorín, C.; Benedé, J.L.; Chisvert, A.; Salvador, A. Green, Rapid and Simultaneous Determination of ‘Alternative Preservatives’ in Cosmetic Formulations by Gas Chromatography-Mass Spectrometry. *J Pharm Biomed Anal* **2022**, *209*, 114493, doi:10.1016/j.jpba.2021.114493.
92. Mendoza, D.J.; Maliha, M.; Raghuwanshi, V.S.; Browne, C.; Mouterde, L.M.M.; Simon, G.P.; Allais, F.; Garnier, G. Diethyl Sinapate-Grafted Cellulose Nanocrystals as Nature-Inspired UV Filters in Cosmetic Formulations. *Mater Today Bio* **2021**, *12*, 100126, doi:10.1016/j.mtbio.2021.100126.
93. Lintner, K.; Mas-Chamberlin, C.; Mondon, P.; Peschard, O.; Lamy, L. Cosmeceuticals and Active Ingredients. *Clin Dermatol* **2009**, *27*, 461–468, doi:10.1016/j.clindermatol.2009.05.009.
94. Buchmann, S. Main Cosmetic Vehicles. In *Handbook of Cosmetic Science and Technology*; Barel, A.O., Paye, M., Maibach, H.I., Eds.; Marcel Dekker: New York, **2002**.
95. Epstein, H. Cosmeceutical Vehicles. *Clin Dermatol* **2009**, *27*, 453–460, doi:10.1016/j.clindermatol.2009.05.007.
96. Mason, T.G.; Wilking, J.N.; Meleson, K.; Chang, C.B.; Graves, S.M. Nanoemulsions: Formation, Structure, and Physical Properties. *Journal of Physics Condensed Matter* **2006**, *18*, doi:10.1088/0953-8984/18/41/R01.
97. Souto, E.B.; Cano, A.; Martins-Gomes, C.; Coutinho, T.E.; Zielińska, A.; Silva, A.M. Microemulsions and Nanoemulsions in Skin Drug Delivery. *Bioengineering* **2022**, *9*, 1–22, doi:10.3390/bioengineering9040158.
98. Burguera, J.L.; Burguera, M. Analytical Applications of Emulsions and Microemulsions. *Talanta* **2012**, *96*, 11–20, doi:10.1016/j.talanta.2012.01.030.
99. Hu, Y.T.; Ting, Y.; Hu, J.Y.; Hsieh, S.C. Techniques and Methods to Study Functional Characteristics of Emulsion Systems. *J Food Drug Anal* **2017**, *25*, 16–26, doi:10.1016/j.jfda.2016.10.021.
100. Tadros, T. Application of Rheology for Assessment and Prediction of the Long-Term Physical Stability of Emulsions; *Advances in Colloid and Interface Science* **2004**, 108-109, 227–258. doi:10.1016/j.cis.2003.10.025.

101. Goodarzi, F.; Zendejboudi, S. A Comprehensive Review on Emulsions and Emulsion Stability in Chemical and Energy Industries. *Canadian Journal of Chemical Engineering* **2019**, *97*, 281–309, doi:10.1002/cjce.23336.
102. Bouyer, E.; Mekhloufi, G.; Rosilio, V.; Grossiord, J.L.; Agnely, F. Proteins, Polysaccharides, and their Complexes used as Stabilizers for Emulsions: Alternatives to Synthetic Surfactants in the Pharmaceutical Field? *Int J Pharm* **2012**, *436*, 359–378, doi:10.1016/j.ijpharm.2012.06.052.
103. Tadros, T.F. Emulsion Formation, Stability, and Rheology. In *Emulsion Formation, Stability, and Rheology*; Tadros, T.F., Ed.; Wiley-VCH Verlag GmbH & Co. KGaA., **2013**, 1-75, doi:10.1002/9783527647941.ch1.
104. Costa, M.; Paiva-Martins, F.; Losada-Barreiro, S.; Bravo-Díaz, C. Modeling Chemical Reactivity at the Interfaces of Emulsions: Effects of Partitioning and Temperature. *Molecules* **2021**, *26*, doi:10.3390/molecules26154703.
105. Martins, D.; Estevinho, B.; Rocha, F.; Dourado, F.; Gama, M. A Dry and Fully Dispersible Bacterial Cellulose Formulation as a Stabilizer for Oil-in-Water Emulsions. *Carbohydr Polym* **2020**, *230*, 115657, doi:10.1016/j.carbpol.2019.115657.
106. Singh, S.; Lohani, A.; Mishra, A.K.; Verma, A. Formulation and Evaluation of Carrot Seed Oil-Based Cosmetic Emulsions. *Journal of Cosmetic and Laser Therapy* **2019**, *21*, 99–107, doi:10.1080/14764172.2018.1469769.
107. Fu, W.; Liu, Y.; Yang, C.; Wang, W.; Wang, M.; Jia, Y. Stabilization of Pickering Emulsions by Bacterial Cellulose Nanofibrils. *Key Eng Mater* **2015**, *645*, 1247–1254, doi:10.4028/www.scientific.net/KEM.645-646.1247.
108. Freitas, F.; Alves, V.D.; Reis, M.A.M. Advances in Bacterial Exopolysaccharides: From Production to Biotechnological Applications. *Trends Biotechnol* **2011**, *29*, 388–398, doi:10.1016/j.tibtech.2011.03.008.
109. Baptista, S.; Freitas, F. Bacterial Polysaccharides: Cosmetic Applications. In *Polysaccharides of Microbial Origin*; Oliveira, J., Radhouani, H., Reis, R.L., Eds.; Springer Nature AG: Cham, Switzerland, **2021**, 1–42 ISBN 9783030357344.
110. Huang, R.; He, Q.; Ma, J.; Ma, C.; Xu, Y.; Song, J.; Sun, L.; Wu, Z.; Huangfu, X. Quantitative Assessment of Extraction Methods for Bound Extracellular Polymeric Substances (B-EPSs) Produced by *Microcystis* sp. and *Scenedesmus* sp. *Algal Res* **2021**, *56*, 102289, doi:10.1016/j.algal.2021.102289.
111. Nadzir, M.M.; Nurhayati, R.W.; Idris, F.N.; Nguyen, M.H. Biomedical Applications of Bacterial Exopolysaccharides: A Review. *Polymers (Basel)* **2021**, *13*, 1–25, doi:10.3390/polym13040530.
112. Siddharth, T.; Sridhar, P.; Vinila, V.; Tyagi, R.D. Environmental Applications of Microbial Extracellular Polymeric Substance (EPS): A Review. *J Environ Manage* **2021**, *287*, 112307, doi:10.1016/j.jenvman.2021.112307.
113. Taberner, A.; Cardea, S. Microbial Exopolysaccharides as Drug Carriers. *Polymers (Basel)* **2020**, *12*, doi:10.3390/POLYM12092142.

114. Tiwari, S.; Kavitate, D.; Devi, P.B.; Halady Shetty, P. Bacterial Exopolysaccharides for Improvement of Technological, Functional and Rheological Properties of Yoghurt. *Int J Biol Macromol* **2021**, *183*, 1585–1595, doi:10.1016/j.ijbiomac.2021.05.140.
115. Donot, F.; Fontana, A.; Baccou, J.C.; Schorr-Galindo, S. Microbial Exopolysaccharides: Main Examples of Synthesis, Excretion, Genetics and Extraction. *Carbohydr Polym* **2012**, *87*, 951–962, doi:10.1016/j.carbpol.2011.08.083.
116. Feng, C.; Lotti, T.; Canziani, R.; Lin, Y.; Tagliabue, C.; Malpei, F. Extracellular Biopolymers Recovered as Raw Biomaterials from Waste Granular Sludge and Potential Applications: A Critical Review. *Science of the Total Environment* **2021**, *753*, 142051, doi:10.1016/j.scitotenv.2020.142051.
117. Freitas, F.; Alves, V.D.; Carvalheira, M.; Costa, N.; Oliveira, R.; Reis, M.A.M. Emulsifying Behaviour and Rheological Properties of the Extracellular Polysaccharide Produced by *Pseudomonas oleovorans* Grown on Glycerol Byproduct. *Carbohydr Polym* **2009**, *78*, 549–556, doi:10.1016/j.carbpol.2009.05.016.
118. Meireles, I.T.; Portugal, C.; Alves, V.D.; Crespo, J.G.; Coelho, I.M. Impact of Biopolymer Purification on the Structural Characteristics and Transport Performance of Composite Polysaccharide Membranes for Pervaporation. *J Memb Sci* **2015**, *493*, 179–187, doi:10.1016/j.memsci.2015.07.011.
119. Macedo, M.G.; Lacroix, C.; Gardner, N.J.; Champagne, C.P. Effect of Medium Supplementation on Exopolysaccharide Production by *Lactobacillus rhamnosus* RW-9595M in Whey Permeate. *Int Dairy J* **2002**, *12*, 419–426, doi:10.1016/S0958-6946(01)00173-X.
120. Patel, A.K.; Laroche, C.; Marcati, A.; Ursu, A.V.; Jubeau, S.; Marchal, L.; Petit, E.; Djelveh, G.; Michaud, P. Separation and Fractionation of Exopolysaccharides from *Porphyridium cruentum*. *Bioresour Technol* **2013**, *145*, 345–350, doi:10.1016/j.biortech.2012.12.038.
121. Ziadi, M.; Bouzaïene, T.; M’Hir, S.; Zaafouri, K.; Mokhtar, F.; Hamdi, M.; Boisset-Helbert, C. Evaluation of the Efficiency of Ethanol Precipitation and Ultrafiltration on the Purification and Characteristics of Exopolysaccharides Produced by Three Lactic Acid Bacteria. *Biomed Res Int* **2018**, *2018*, doi:10.1155/2018/1896240.
122. Charcosset, C. Membrane Processes in Biotechnology: An Overview. *Biotechnol Adv* **2006**, *24*, 482–492, doi:10.1016/j.biotechadv.2006.03.002.
123. Hooshdar, P.; Kermanshahi, R.K.; Ghadam, P.; Khosravi-Darani, K. A Review on Production of Exopolysaccharide and Biofilm in Probiotics like *Lactobacilli* and Methods of Analysis. *Biointerface Res Appl Chem* **2020**, *10*, 6058–6075, doi:10.33263/BRIAC105.60586075.
124. Li, H.; Li, Z.; Xiong, S.; Zhang, H.; Li, N.; Zhou, S.; Liu, Y.; Huang, Z. Pilot-Scale Isolation of Bioactive Extracellular Polymeric Substances from Cell-Free Media of Mass Microalgal Cultures Using Tangential-Flow Ultrafiltration. *Process Biochemistry* **2011**, *46*, 1104–1109, doi:10.1016/j.procbio.2011.01.028.
125. Ferreira, A.R. v.; Torres, C.A.V.; Freitas, F.; Sevrin, C.; Grandfils, C.; Reis, M.A.M.; Alves, V.D.; Coelho, I.M. Development and Characterization of Bilayer Films of FucoPol and Chitosan. *Carbohydr Polym* **2016**, *147*, 8–15, doi:10.1016/j.carbpol.2016.03.089.

126. Ferreira, A.R.V.; Torres, C.A.V.; Freitas, F.; Reis, M.A.M.; Alves, V.D.; Coelho, I.M. Biodegradable Films Produced from the Bacterial Polysaccharide FucoPol. *Int J Biol Macromol* **2014**, *71*, 111–116, doi:10.1016/j.ijbiomac.2014.04.022.
127. Araújo, D.; Concórdio-Reis, P.; Marques, A.C.; Sevrin, C.; Grandfils, C.; Alves, V.D.; Fortunato, E.; Reis, M.A.M. Demonstration of the Ability of the Bacterial Polysaccharide FucoPol to Flocculate Kaolin Suspensions. **2020**, *3330*, doi:10.1080/09593330.2018.1497710.
128. Concórdio-Reis, P.; Reis, M.A.M.; Freitas, F. Biosorption of Heavy Metals by the Bacterial Exopolysaccharide FucoPol. *applied sciences* **2020**, *10*, 6708.
129. Tang, D.S.; Yin, G.M.; He, Y.Z.; Hu, S.Q.; Li, B.; Li, L.; Liang, H.L.; Borthakur, D. Recovery of Protein from Brewer's Spent Grain by Ultrafiltration. *Biochem Eng J* **2009**, *48*, 1–5, doi:10.1016/j.bej.2009.05.019.
130. Péterszegi, G.; Fodil-Bourahla, I.; Robert, A.M.; Robert, L. Pharmacological Properties of Fucose. Applications in Age-Related Modifications of Connective Tissues. *Biomedicine and Pharmacotherapy* **2003**, *57*, 240–245, doi:10.1016/S0753-3322(03)00028-3.
131. Vanhooren, P.T.; Vandamme, E.J. L-Fucose: Occurrence, Physiological Role, Chemical, Enzymatic and Microbial Synthesis. *Journal of Chemical Technology and Biotechnology* **1999**, *74*, 479–497, doi:10.1002/(SICI)1097-4660(199906)74:6<479:AID-JCTB76>3.0.CO;2-E.
132. Iyer, A.; Mody, K.; Jha, B. Characterization of an Exopolysaccharide Produced by a Marine Enterobacter *Cloacae*. *Indian J Exp Biol* **2005**, *43*, 467–471.
133. Gómez-Ordóñez, E.; Rupérez, P. FTIR-ATR Spectroscopy as a Tool for Polysaccharide Identification in Edible Brown and Red Seaweeds. *Food Hydrocoll* **2011**, *25*, 1514–1520, doi:10.1016/j.foodhyd.2011.02.009.
134. Asgher, M.; Urooj, Y.; Qamar, S.A.; Khalid, N. Improved Exopolysaccharide Production from *Bacillus licheniformis* MS3: Optimization and Structural/Functional Characterization. *Int J Biol Macromol* **2020**, *151*, 984–992, doi:10.1016/j.ijbiomac.2019.11.094.
135. Synytsya, A.; Kim, W.J.; Kim, S.M.; Pohl, R.; Synytsya, A.; Kvasnička, F.; Čopíková, J.; il Park, Y. Structure and Antitumour Activity of Fucoidan Isolated from Sporophyll of Korean Brown Seaweed *Undaria pinnatifida*. *Carbohydr Polym* **2010**, *81*, 41–48, doi:10.1016/j.carbpol.2010.01.052.
136. Liyaskina, E.V.; Rakova, N.A.; Kitykina, A.A.; Rusyaeva, V.V.; Toukach, P.V.; Fomenkov, A.; Vainauskas, S.; Roberts, R.J.; Revin, V.V. Production and Characterization of the Exopolysaccharide from Strain *Paenibacillus polymyxa* 2020. *PLoS One* **2021**, *16*, 1–25, doi:10.1371/journal.pone.0253482.
137. Chambi, D.; Romero-Soto, L.; Villca, R.; Orozco-Gutiérrez, F.; Vega-Baudrit, J.; Quillaguamán, J.; Hatti-Kaul, R.; Martín, C.; Carrasco, C. Exopolysaccharides Production by Cultivating a Bacterial Isolate from the Hypersaline Environment of Salar de Uyuni (Bolivia) in Pretreatment Liquids of Steam-Exploded Quinoa Stalks and Enzymatic Hydrolysates of Curupaú Sawdust. *Fermentation* **2021**, *7*, 1–16, doi:10.3390/fermentation7010033.

138. Yang, X.; Li, L. The Relationship between Charge Intensity and Bioactivities/Processing Characteristics of Exopolysaccharides from Lactic Acid Bacteria. *Lwt* **2021**, *153*, 112345, doi:10.1016/j.lwt.2021.112345.
139. Wang, J.; Salem, D.R.; Sani, R.K. Two New Exopolysaccharides from a Thermophilic Bacterium *Geobacillus* sp. WSUCF1: Characterization and Bioactivities. *N Biotechnol* **2021**, *61*, 29–39, doi:10.1016/j.nbt.2020.11.004.
140. Ayyash, M.; Stathopoulos, C.; Abu-Jdayil, B.; Esposito, G.; Baig, M.; Turner, M.S.; Baba, A.S.; Apostolopoulos, V.; Al-Nabulsi, A.; Osaili, T. Exopolysaccharide Produced by Potential Probiotic *Enterococcus faecium* MS79: Characterization, Bioactivities and Rheological Properties Influenced by Salt and PH. *Lwt* **2020**, *131*, 109741, doi:10.1016/j.lwt.2020.109741.
141. Xu, L.; Dong, M.; Gong, H.; Sun, M.; Li, Y. Effects of Inorganic Cations on the Rheology of Aqueous Welan, Xanthan, Gellan Solutions and Their Mixtures. *Carbohydr Polym* **2015**, *121*, 147–154, doi:10.1016/j.carbpol.2014.12.030.
142. Morris, E.R. Shear-Thinning of “Random Coil” Polysaccharides: Characterisation by Two Parameters from a Simple Linear Plot. *Carbohydr Polym* **1990**, *13*, 85–96, doi:10.1016/0144-8617(90)90053-U.
143. Torres, C.A.V. Engineering of Bacterial Exopolysaccharides: From Synthesis to Properties. **2012**.
144. Willumsen, P.A.; Karlson, U. Screening of Bacteria, Isolated from PAH-Contaminated Soils, for Production of Biosurfactants and Bioemulsifiers. *Biodegradation* **1996**, *7*, 415–423, doi:10.1007/bf00056425.
145. Calero, N.; Muñoz, J.; Cox, P.W.; Heuer, A.; Guerrero, A. Influence of Chitosan Concentration on the Stability, Microstructure and Rheological Properties of O/W Emulsions Formulated with High-Oleic Sunflower Oil and Potato Protein. *Food Hydrocoll* **2013**, *30*, 152–162, doi:10.1016/j.foodhyd.2012.05.004.
146. Tafuro, G.; Costantini, A.; Baratto, G.; Francescato, S.; Semenzato, A. Evaluating Natural Alternatives to Synthetic Acrylic Polymers: Rheological and Texture Analyses of Polymeric Water Dispersions. *ACS Omega* **2020**, *5*, 15280–15289, doi:10.1021/acsomega.0c01306.
147. Baptista, S.; Torres, C.A.V.; Sevrin, C.; Grandfils, C.; Reis, M.A.M.; Freitas, F. Extraction of the Bacterial Extracellular Polysaccharide FucoPol by Membrane-Based Methods : Efficiency and Impact on Biopolymer Properties. *Polymers (Basel)* **2022**, 1–16.
148. Xu, L.; Qiu, Z.; Gong, H.; Zhu, C.; Li, Z.; Li, Y.; Dong, M. Rheological Behaviors of Microbial Polysaccharides with Different Substituents in Aqueous Solutions: Effects of Concentration, Temperature, Inorganic Salt and Surfactant. *Carbohydr Polym* **2019**, *219*, 162–171, doi:10.1016/j.carbpol.2019.05.032.
149. Jeong, J.P.; Kim, Y.; Hu, Y.; Jung, S. Bacterial Succinoglycans: Structure, Physical Properties, and Applications. *Polymers (Basel)* **2022**, *14*, 1–21, doi:10.3390/polym14020276.
150. Chokboribal, J.; Tachaboonyakiat, W.; Sangvanich, P.; Ruangpornvisuti, V.; Jettanacheawchankit, S.; Thunyakitpisal, P. Deacetylation Affects the Physical Properties and Bioactivity of Acemannan,

- an Extracted Polysaccharide from *Aloe vera*. *Carbohydr Polym* **2015**, *133*, 556–566, doi:10.1016/j.carbpol.2015.07.039.
151. Zhang, F.; Cai, X.; Ding, L.; Wang, S. Effect of PH, Ionic Strength, Chitosan Deacetylation on the Stability and Rheological Properties of O/W Emulsions Formulated with Chitosan/Casein Complexes. *Food Hydrocoll* **2021**, *111*, 106211, doi:10.1016/j.foodhyd.2020.106211.
 152. Du, X.; Li, J.; Chen, J.; Li, B. Effect of Degree of Deacetylation on Physicochemical and Gelation Properties of Konjac Glucomannan. *Food Research International* **2012**, *46*, 270–278, doi:10.1016/j.foodres.2011.12.015.
 153. Jin, W.; Song, R.; Xu, W.; Wang, Y.; Li, J.; Shah, B.R.; Li, Y.; Li, B. Analysis of Deacetylated Konjac Glucomannan and Xanthan Gum Phase Separation by Film Forming. *Food Hydrocoll* **2015**, *48*, 320–326, doi:10.1016/j.foodhyd.2015.02.007.
 154. Ridout, M.J.; Brownsey, G.J.; York, G.M.; Walker, G.C.; Morris, V.J. Effect of O-Acyl Substituents on the Functional Behaviour of *Rhizobium meliloti* Succinoglycan. *Int J Biol Macromol* **1997**, *20*, 1–7, doi:10.1016/S0141-8130(96)01140-3.
 155. Bajaj, I.B.; Survase, S.A.; Saudagar, P.S.; Singhal, R.S. Gellan Gum: Fermentative Production, Downstream Processing and Applications. *Food Technol Biotechnol* **2007**, *45*, 341–354.
 156. Huang, G.; Xie, J.; Shuai, S.; Wei, S.; Chen, Y.; Guan, Z.; Zheng, Q.; Yue, P.; Wang, C. Nose-to-Brain Delivery of Drug Nanocrystals by Using Ca²⁺ Responsive Deacetylated Gellan Gum Based in Situ-Nanogel. *Int J Pharm* **2021**, *594*, 120182, doi:10.1016/j.ijpharm.2020.120182.
 157. Wang, L.; Xiang, D.; Li, C.; Zhang, W.; Bai, X. Effects of Deacetylation on Properties and Conformation of Xanthan Gum. *J Mol Liq* **2022**, *345*, 117009, doi:10.1016/j.molliq.2021.117009.
 158. Riaz, T.; Iqbal, M.W.; Jiang, B.; Chen, J. A Review of the Enzymatic, Physical, and Chemical Modification Techniques of Xanthan Gum. *Int J Biol Macromol* **2021**, *186*, 472–489, doi:10.1016/j.ijbiomac.2021.06.196.
 159. Veiga-Santos, P.; Oliveira, L.M.; Cereda, M.P.; Alves, A.J.; Scamparini, A.R.P. Mechanical Properties, Hydrophilicity and Water Activity of Starch-Gum Films: Effect of Additives and Deacetylated Xanthan Gum. *Food Hydrocoll* **2005**, *19*, 341–349, doi:10.1016/j.foodhyd.2004.07.006.
 160. Abdou, E.S.; Nagy, K.S.A.; Elsabee, M.Z. Extraction and Characterization of Chitin and Chitosan from Local Sources. *Bioresour Technol* **2008**, *99*, 1359–1367, doi:10.1016/j.biortech.2007.01.051.
 161. Knidri, H.; Belaabed, R.; Addaou, A.; Laajeb, A.; Lahsini, A. Extraction, Chemical Modification and Characterization of Chitin and Chitosan. *Int J Biol Macromol* **2018**, *120*, 1181–1189, doi:10.1016/j.ijbiomac.2018.08.139.
 162. Kjartansson, G.T.; Zivanovic, S.; Kristbergsson, K.; Weiss, J. Sonication-Assisted Extraction of Chitin from North Atlantic Shrimps (*Pandalus Borealis*). *J Agric Food Chem* **2006**, *54*, 5894–5902, doi:10.1021/jf060646w.
 163. Guetta, O.; Mazeau, K.; Auzely, R.; Milas, M.; Rinaudo, M. Structure and Properties of a Bacterial Polysaccharide Named Fucogel. *Biomacromolecules* **2003**, *4*, 1362–1371, doi:10.1021/bm030033h.
 164. Pinto, E.P.; Furlan, L.; Vendruscolo, C.T. Chemical Deacetylation Natural Xanthan (Jungbunzlauer®). *Polimeros* **2011**, *21*, 47–52, doi:10.1590/S0104-14282011005000005.

165. Lima, C.S.; Rabelo, S.C.; Ciesielski, P.N.; Roberto, I.C.; Rocha, G.J.M.; Driemeier, C. Multiscale Alterations in Sugar Cane Bagasse and Straw Submitted to Alkaline Deacetylation. *ACS Sustain Chem Eng* **2018**, *6*, 3796–3804, doi:10.1021/acssuschemeng.7b04158.
166. Herasimenka, Y.; Cescutti, P.; Impallomeni, G.; Rizzo, R. Exopolysaccharides Produced by *Inquilinus limosus*, a New Pathogen of Cystic Fibrosis Patients: Novel Structures with Usual Components. *Carbohydr Res* **2007**, *342*, 2404–2415, doi:10.1016/j.carres.2007.07.012.
167. Paz-Samaniego, R.; Carvajal-Millan, E.; Brown-Bojorquez, F.; Rascón-Chu, A.; López-Franco, Y.L.; Sotelo-Cruz, N.; Lizardi-Mendoza, J. Gelation of Arabinoxylans from Maize Wastewater — Effect of Alkaline Hydrolysis Conditions on the Gel Rheology and Microstructure. *Wastewater Treatment Engineering* **2015**, doi:10.5772/61022.
168. Kavitate, D.; Balyan, S.; Devi, P.B.; Shetty, P.H. Evaluation of Oil-in-Water (O/W) Emulsifying Properties of Galactan Exopolysaccharide from *Weissella confusa* KR780676. *J Food Sci Technol* **2020**, *57*, 1579–1585, doi:10.1007/s13197-020-04262-3.
169. Martins, D.; Rocha, C.; Dourado, F.; Gama, M. Bacterial Cellulose-Carboxymethyl Cellulose (BC:CMC) Dry Formulation as Stabilizer and Texturizing Agent for Surfactant-Free Cosmetic Formulations. *Colloids Surf A Physicochem Eng Asp* **2021**, *617*, 126380, doi:10.1016/j.colsurfa.2021.126380.
170. Kwon, C.; Lee, S.; Jung, S. Matrix-Assisted Laser Desorption/Ionization Time-of-Flight Mass Spectrometric Behavior of Succinoglycan Monomers, Dimers, and Trimers Isolated from *Sinorhizobium meliloti* 1021. *Carbohydr Res* **2011**, *346*, 2308–2314, doi:10.1016/j.carres.2011.07.023.
171. Marsh, C.A. Chemistry of D-Glucuronic Acid and its Glycosides. In *Glucuronic Acid Free and Combined*; Dutton, G.J., Ed.; Elsevier Inc., **1966**; 3–136, ISBN 9780123955012.
172. Du, X.; Zhang, J.; Lv, Z.; Ye, L.; Yang, Y.; Tang, Q. Chemical Modification of an Acidic Polysaccharide (TAPA1) from *Tremella aurantialba* and Potential Biological Activities. *Food Chem* **2014**, *143*, 336–340, doi:10.1016/j.foodchem.2013.07.137.
173. Wang, F.; Wang, Y.J.; Sun, Z. Conformational Role of Xanthan Gum in its Interaction with Guar Gum. *J Food Sci* **2002**, *67*, 3289–3294, doi:10.1111/j.1365-2621.2002.tb09580.x.
174. Khouryieh, H.A.; Herald, T.J.; Aramouni, F.; Alavi, S. Intrinsic Viscosity and Viscoelastic Properties of Xanthan/Guar Mixtures in Dilute Solutions: Effect of Salt Concentration on the Polymer Interactions. *Food Research International* **2007**, *40*, 883–893, doi:10.1016/j.foodres.2007.03.001.
175. Li, S.; Xiong, Q.; Lai, X.; Li, X.; Wan, M.; Zhang, J.; Yan, Y.; Cao, M.; Lu, L.; Guan, J.; Zhang D., Lin, Y. Molecular Modification of Polysaccharides and Resulting Bioactivities. *Compr Rev Food Sci Food Saf* **2016**, *15*, 237–250, doi:10.1111/1541-4337.12161.
176. Madruga, L.Y.C.; Câmara, P.C.F.; Marques, N. do N.; Balaban, R. de C. Effect of Ionic Strength on Solution and Drilling Fluid Properties of Ionic Polysaccharides: A Comparative Study between Na-Carboxymethylcellulose and Na-Kappa-Carrageenan Responses. *J Mol Liq* **2018**, *266*, 870–879, doi:10.1016/j.molliq.2018.07.016.

177. Zhou, F.; Wu, Z.; Chen, C.; Han, J.; Ai, L.; Guo, B. Exopolysaccharides Produced by *Rhizobium radiobacter* S10 in Whey and Their Rheological Properties. *Food Hydrocoll* **2014**, *36*, 362–368, doi:10.1016/j.foodhyd.2013.08.016.
178. Barbosa, A.I.; Coutinho, A.J.; Costa Lima, S.A.; Reis, S. Marine Polysaccharides in Pharmaceutical Applications: Fucoidan and Chitosan as Key Players in the Drug Delivery Match Field. *Mar Drugs* **2019**, *17*, doi:10.3390/md17120654.
179. Singhvi, G.; Hans, N.; Shiva, N.; Kumar Dubey, S. Xanthan Gum in Drug Delivery Applications. In *Natural Polysaccharides in Drug Delivery and Biomedical Applications*; Nayak, A.K.; Hasnain, M.S., Eds; Elsevier Inc., **2019**, 121–144, ISBN 9780128170557.
180. Li, L.; Liao, B.Y.; Thakur, K.; Zhang, J.G.; Wei, Z.J. The Rheological Behavior of Polysaccharides Sequentially Extracted from *Polygonatum cyrtonema* Hua. *Int J Biol Macromol* **2018**, *109*, 761–771, doi:10.1016/j.ijbiomac.2017.11.063.
181. Ji, Y.H.; Liao, A.M.; Huang, J.H.; Thakur, K.; Li, X.L.; Hu, F.; Wei, Z.J. The Rheological Properties and Emulsifying Behavior of Polysaccharides Sequentially Extracted from *Amana edulis*. *Int J Biol Macromol* **2019**, *137*, 160–168, doi:10.1016/j.ijbiomac.2019.06.202.
182. Tako, M.; Nakamura, S. Rheological Properties of Deacetylated Xanthan. *Agric Biol Chem* **1984**, *48*, 2987–2993.
183. Baptista, S.; Pereira, J.R.; Gil, C.V.; Torres, C.A.V.; Reis, M.A.M.; Freitas, F. Development of Olive Oil and α -Tocopherol Containing Emulsions Stabilized by FucoPol: Rheological and Textural Analyses. *Polymers (Basel)* **2022**, *14*, 1–17.
184. McClements, D.J. Critical Review of Techniques and Methodologies for Characterization of Emulsion Stability. *Crit Rev Food Sci Nutr* **2007**, *47*, 611–649, doi:10.1080/10408390701289292.
185. Akbari, S.; Nour, A.H. Emulsion Types, Stability Mechanisms and Rheology: A Review. *International Journal of Innovative Research and Scientific Studies* **2018**, *1*, 14–21.
186. Lata Yadav, K.; Kumar Rahi, D.; Kumar Soni, S. Bioemulsifying Potential of Exopolysaccharide Produced by an Indigenous Species of *Aureobasidium pullulans* RYLF10., doi:10.7287/peerj.preprints.726v1.
187. Kavitate, D.; Balyan, S.; Devi, P.B.; Shetty, P.H. Interface between Food Grade Flavour and Water Soluble Galactan Biopolymer to Form a Stable Water-in-Oil-in-Water Emulsion. *Int J Biol Macromol* **2019**, *135*, 445–452, doi:10.1016/j.ijbiomac.2019.05.199.
188. Huang, Z.; Zong, M.H.; Lou, W.Y. Effect of Acetylation Modification on the Emulsifying and Antioxidant Properties of Polysaccharide from *Milletia speciosa* Champ. *Food Hydrocoll* **2022**, *124*, 107217, doi:10.1016/j.foodhyd.2021.107217.
189. Li, X.; Xia, W. Effects of Concentration, Degree of Deacetylation and Molecular Weight on Emulsifying Properties of Chitosan. *Int J Biol Macromol* **2011**, *48*, 768–772, doi:10.1016/j.ijbiomac.2011.02.016.

190. Blanco, L.F.; Rodriguez, M.S.; Schulz, P.C.; Agulló, E. Influence of the Deacetylation Degree on Chitosan Emulsification Properties. *Colloid Polym Sci* **1999**, *277*, 1087–1092, doi:10.1007/s003960050495.
191. Bom, S.; Fitas, M.; Martins, A.M.; Pinto, P.; Ribeiro, H.M.; Marto, J. Replacing Synthetic Ingredients by Sustainable Natural Alternatives: A Case Study Using Topical O/W Emulsions. *Molecules* **2020**, *25*, doi:10.3390/molecules25214887.
192. Heydari, A.; Razavi, S.M.A. Evaluating High Pressure-Treated Corn and Waxy Corn Starches as Novel Fat Replacers in Model Low-Fat O/W Emulsions: A Physical and Rheological Study. *Int J Biol Macromol* **2021**, *184*, 393–404, doi:10.1016/j.ijbiomac.2021.06.052.
193. Zhang, W.; Liu, L. Study on the Formation and Properties of Liquid Crystal Emulsion in Cosmetic. *Journal of Cosmetics, Dermatological Sciences and Applications* **2013**, *03*, 139–144, doi:10.4236/jcdsa.2013.32022.
194. Gamonpilas, C.; Pongjaruvat, W.; Fuongfuchat, A.; Methacanon, P.; Seetapan, N.; Thamjedsada, N. Physicochemical and Rheological Characteristics of Commercial Chili Sauces as Thickened by Modified Starch or Modified Starch/Xanthan Mixture. *J Food Eng* **2011**, *105*, 233–240, doi:10.1016/j.jfoodeng.2011.02.024.
195. Hoque, M.S.; Benjakul, S.; Prodpran, T. Effect of Heat Treatment of Film-Forming Solution on the Properties of Film from Cuttlefish (*Sepia pharaonis*) Skin Gelatin. *J Food Eng* **2010**, *96*, 66–73, doi:10.1016/j.jfoodeng.2009.06.046.
196. Khairunnisa, S.; Junianto; Zahidah; Rostini, I. The Effect of Glycerol Concentration as a Plasticizer on Edible Films Made from Alginate towards its Physical Characteristic. *World Sci News* **2018**, *112*, 130–141.
197. Khoirunnisa, A.R.; Joni, I.M.; Panatarani, C.; Rochima, E.; Praseptiangga, D. UV-Screening, Transparency and Water Barrier Properties of Semi Refined Iota Carrageenan Packaging Film Incorporated with ZnO Nanoparticles. *AIP Conf Proc* **2018**, *1927*, doi:10.1063/1.5021234.
198. Kędzierska, M.; Blilid, S.; Miłowska, K.; Kołodziejczyk-Czepas, J.; Katir, N.; Lahcini, M.; el Kadib, A.; Bryszewska, M. Insight into Factors Influencing Wound Healing Using Phosphorylated Cellulose-Filled-Chitosan Nanocomposite Films. *Int J Mol Sci* **2021**, *22*, 1–18, doi:10.3390/ijms222111386.
199. Jin, W.; Song, R.; Xu, W.; Wang, Y.; Li, J.; Shah, B.R.; Li, Y.; Li, B. Analysis of Deacetylated Konjac Glucomannan and Xanthan Gum Phase Separation by Film Forming. *Food Hydrocoll* **2015**, *48*, 320–326, doi:10.1016/j.foodhyd.2015.02.007.
200. Kurt, A. Rheology of Film-Forming Solutions and Physical Properties of Differently Deacetylated Salep Glucomannan Film. *Food and Health* **2019**, *5*, 175–184, doi:10.3153/fh19019.
201. Alves, V.D.; Ferreira, A.R.; Costa, N.; Freitas, F.; Reis, M.A.M.; Coelho, I.M. Characterization of Biodegradable Films from the Extracellular Polysaccharide Produced by *Pseudomonas*

- oleovorans* Grown on Glycerol Byproduct. *Carbohydr Polym* **2011**, *83*, 1582–1590, doi:10.1016/j.carbpol.2010.10.010.
202. Kurek, M.; Galus, S.; Debeaufort, F. Surface, Mechanical and Barrier Properties of Bio-Based Composite Films Based on Chitosan and Whey Protein. *Food Packag Shelf Life* **2014**, *1*, 56–67, doi:10.1016/j.fpsl.2014.01.001.
203. Tafuro, G.; Costantini, A.; Baratto, G.; Busata, L.; Semenzato, A. Rheological and Textural Characterization of Acrylic Polymer Water Dispersions for Cosmetic Use. *Ind Eng Chem Res* **2019**, *58*, 23549–23558, doi:10.1021/acs.iecr.9b05319.
204. Tafuro, G.; Costantini, A.; Baratto, G.; Francescato, S.; Busata, L.; Semenzato, A. Characterization of Polysaccharidic Associations for Cosmetic Use: Rheology and Texture Analysis. *Cosmetics* **2021**, *8*, doi:10.3390/cosmetics8030062.
205. Gilbert, L.; Picard, C.; Savary, G.; Grisel, M. Rheological and Textural Characterization of Cosmetic Emulsions Containing Natural and Synthetic Polymers: Relationships between Both Data. *Colloids Surf A Physicochem Eng Asp* **2013**, *421*, 150–163, doi:10.1016/j.colsurfa.2013.01.003.
206. Lochhead, R.Y. The Role of Polymers in Cosmetics: Recent Trends. *ACS Symposium Series* **2007**, *961*, 3–56, doi:10.1021/bk-2007-0961.ch001.
207. Filipovic, M.; Lukic, M.; Djordjevic, S.; Krstonosic, V.; Pantelic, I.; Vuleta, G.; Savic, S. Towards Satisfying Performance of an O/W Cosmetic Emulsion: Screening of Reformulation Factors on Textural and Rheological Properties using General Experimental Design. *Int J Cosmet Sci* **2017**, *39*, 486–499, doi:10.1111/ics.12402.
208. Abolhasani, S.; Ahmadpour, A.; Rohani Bastami, T.; Yaqubzadeh, A. Facile Synthesis of Mesoporous Carbon Aerogel for the Removal of Ibuprofen from Aqueous Solution by Central Composite Experimental Design (CCD). *J Mol Liq* **2019**, *281*, 261–268, doi:10.1016/j.molliq.2019.02.084.
209. Wang, Y.X.; Lu, Z.X. Optimization of Processing Parameters for the Mycelial Growth and Extracellular Polysaccharide Production by *Boletus Spp.* ACCC 50328. *Process Biochemistry* **2005**, *40*, 1043–1051, doi:10.1016/j.procbio.2004.03.012.
210. Yin, X.; You, Q.; Jiang, Z. Optimization of Enzyme Assisted Extraction of Polysaccharides from *Tricholoma matsutake* by Response Surface Methodology. *Carbohydr Polym* **2011**, *86*, 1358–1364, doi:10.1016/j.carbpol.2011.06.053.
211. Sun, Y.; Liu, J.; Kennedy, J.F. Application of Response Surface Methodology for Optimization of Polysaccharides Production Parameters from the Roots of *Codonopsis pilosula* by a Central Composite Design. *Carbohydr Polym* **2010**, *80*, 949–953, doi:10.1016/j.carbpol.2010.01.011.
212. Ahmadi, M.; Vahabzadeh, F.; Bonakdarpour, B.; Mofarrah, E.; Mehranian, M. Application of the Central Composite Design and Response Surface Methodology to the Advanced Treatment of Olive Oil Processing Wastewater Using Fenton's Peroxidation. *J Hazard Mater* **2005**, *123*, 187–195, doi:10.1016/j.jhazmat.2005.03.042.

213. Lundstedt, Torbjorn.; Seifert, Elisabeth.; Abramo, Lisbeth.; Thelin, Bernt.; Nystrom, Asa.; Petersen, Jarle.; Bergman, R. Experimental Design and Optimization. *Chemometrics and Intelligent Laboratory Systems* **1998**, 3–40, doi:10.1007/978-3-540-49148-4_3.
214. Roosta, M.; Ghaedi, M.; Daneshfar, A.; Sahraei, R.; Asghari, A. Optimization of the Ultrasonic Assisted Removal of Methylene Blue by Gold Nanoparticles Loaded on Activated Carbon Using Experimental Design Methodology. *Ultrason Sonochem* **2014**, 21, 242–252, doi:10.1016/j.ultsonch.2013.05.014.
215. Fernandes, R.N.; Simiqueli, A.A.; Vidigal, M.C.T.R.; Minim, V.P.R.; Minim, L.A. Kinetic Stability of the Oil-in-Water Emulsions and Dynamic Interfacial Properties of Mixtures of Sucrose Esters and Polysaccharides. *Food Chem* **2021**, 357, doi:10.1016/j.foodchem.2021.129693.
216. Gaudin, T.; Rotureau, P.; Pezron, I.; Fayet, G. Investigating the Impact of Sugar-Based Surfactants Structure on Surface Tension at Critical Micelle Concentration with Structure-Property Relationships. *J Colloid Interface Sci* **2018**, 516, 162–171, doi:10.1016/j.jcis.2018.01.051.
217. Garti, N.; Leser, M.E. Emulsification Properties of Hydrocolloids. *Polym Adv Technol* **2001**, 12, 123–135, doi:10.1002/1099-1581(200101/02)12:1/2<123:AID-PAT105>3.0.CO;2-0.
218. Breitenbach, B.B.; Schmid, I.; Wich, P.R. Amphiphilic Polysaccharide Block Copolymers for PH-Responsive Micellar Nanoparticles. *Biomacromolecules* **2017**, 18, 2839–2848, doi:10.1021/acs.biomac.7b00771.
219. Jain, R.M.; Mody, K.; Joshi, N.; Mishra, A.; Jha, B. Production and Structural Characterization of Biosurfactant Produced by an Alkaliphilic Bacterium, *Klebsiella* sp.: Evaluation of Different Carbon Sources. *Colloids Surf B Biointerfaces* **2013**, 108, 199–204, doi:10.1016/j.colsurfb.2013.03.002.
220. Phulpoto, I.A.; Yu, Z.; Hu, B.; Wang, Y.; Ndayisenga, F.; Li, J.; Liang, H.; Qazi, M.A. Production and Characterization of Surfactin-like Biosurfactant Produced by Novel Strain *Bacillus nealsonii* S2MT and its Potential for Oil Contaminated Soil Remediation. *Microb Cell Fact* **2020**, 19, 1–12, doi:10.1186/s12934-020-01402-4.
221. Rodríguez-López, L.; López-Prieto, A.; Lopez-Álvarez, M.; Pérez-Davila, S.; Serra, J.; González, P.; Cruz, J.M.; Moldes, A.B. Characterization and Cytotoxic Effect of Biosurfactants Obtained from Different Sources. *ACS Omega* **2020**, 5, 31381–31390, doi:10.1021/acsomega.0c04933.
222. Sałek, K.; Euston, S.R. Sustainable Microbial Biosurfactants and Bioemulsifiers for Commercial Exploitation. *Process Biochemistry* **2019**, 85, 143–155, doi:10.1016/j.procbio.2019.06.027.
223. Bernardi, D.S.; Pereira, T.A.; Maciel, N.R.; Bortoloto, J.; Viera, G.S.; Oliveira, G.C.; Rocha-Filho, P.A. Formation and Stability of Oil-in-Water Nanoemulsions Containing Rice Bran Oil: *in Vitro* and *in Vivo* Assessments. *J Nanobiotechnology* **2011**, 9, 1–9, doi:10.1186/1477-3155-9-44.

224. Patel, V.R.; Dumancas, G.G.; Viswanath, L.C.K.; Maples, R.; Subong, B.J.J. Castor Oil: Properties, Uses, and Optimization of Processing Parameters in Commercial Production. *Lipid Insights* **2016**, *9*, 1–12, doi:10.4137/LPI.S40233.
225. Chu, C.C.; Nyam, K.L. Application of Seed Oils and Its Bioactive Compounds in Sunscreen Formulations. *JAOCS, Journal of the American Oil Chemists' Society* **2021**, *98*, 713–726, doi:10.1002/aocs.12491.
226. Maktabi, B.; Liberatore, M.W.; Baki, G. Meadowfoam Seed Oil as a Natural Dispersing Agent for Colorants in Lipstick. *Int J Cosmet Sci* **2021**, *43*, 484–493, doi:10.1111/ics.12724.
227. Smaoui, S.; Hlima, H.; Jarraya, R.; Kamoun, N.; Ellouze, R.; Damak, M. Cosmetic Emulsion from Virgin Olive Oil: Formulation and Bio-Physical Evaluation. *Afr J Biotechnol* **2012**, *11*, 9664–9671, doi:10.5897/ajb12.163.
228. Shkreli, R.; Terziu, R.; Memushaj, L.; Dharmo, K. Formulation and Stability Evaluation of a Cosmetics Emulsion Loaded with Different Concentrations of Synthetic and Natural Preservative. *Journal of Biological Studies* **2022**, *5*, 38–51, ISSN 2209-2560.
229. Laurent, S. A Study of I-Cyclodextrin-Stabilized Paraffin Oil / Water Emulsions. *J. Cosmet. Sci* **1999**, *50*, 15-22.
230. Ahmad, Z. The Uses and Properties of Almond Oil. *Complement Ther Clin Pract* **2010**, *16*, 10–12, doi:10.1016/j.ctcp.2009.06.015.
231. Slavica, Č.; Zec, G.; Nati, M.; Fotiri, M. Almond (*Prunus dulcis*) Oil. In *Fruit Oils: Chemistry and Functionality*; Ramadan, M.F., Ed.; Springer Nature Switzerland AG **2019**, doi: 10.1007/978-3-030-12473-1_6.
232. Gallardo, V.; Munoz, M.; Ruiz, M.A. Formulations of Hydrogels and Lipogels with Vitamin E. *J Cosmet Dermatol* **2005**, *4*, 187–192, doi:10.1111/j.1473-2165.2005.00310.x.
233. Mota, A.H.; Silva, C.O.; Nicolai, M.; Baby, A.; Palma, L.; Rijo, P.; Ascensão, L.; Reis, C.P. Design and Evaluation of Novel Topical Formulation with Olive Oil as Natural Functional Active. *Pharm Dev Technol* **2018**, *23*, 794–805, doi:10.1080/10837450.2017.1340951.
234. César, F.C.S.; Maia Campos, P.M.B.G. Influence of Vegetable Oils in the Rheology, Texture Profile and Sensory Properties of Cosmetic Formulations Based on Organogel. *Int J Cosmet Sci* **2020**, *42*, 494–500, doi:10.1111/ics.12654.
235. Nunes, A.; Gonçalves, L.; Marto, J.; Martins, A.M.; Silva, A.N.; Pinto, P.; Martins, M.; Fraga, C.; Ribeiro, H.M. Investigations of Olive Oil Industry By-Products Extracts with Potential Skin Benefits in Topical Formulations. *Pharmaceutics* **2021**, *13*, 1–20, doi:10.3390/pharmaceutics13040465.
236. Gorini, I.; Iorio, S.; Ciliberti, R.; Licata, M.; Armocida, G. Olive Oil in Pharmacological and Cosmetic Traditions. *J Cosmet Dermatol* **2019**, *18*, 1575–1579, doi:10.1111/jocd.12838.

237. Sandford, E.C.; Muntz, A.; Craig, J.P. Therapeutic Potential of Castor Oil in Managing Blepharitis, Meibomian Gland Dysfunction and Dry Eye. *Clin Exp Optom* **2021**, *104*, 315–322, doi:10.1111/cxo.13148.
238. Kaur, C.D.; Saraf, S. *In Vitro* Sun Protection Factor Determination of Herbal Oils Used in Cosmetics. *Pharmacognosy Res* **2010**, *2*, 22–25, doi:10.4103/0974-8490.60586.
239. Chuberre, B.; Araviiskaia, E.; Bieber, T.; Barbaud, A. Mineral Oils and Waxes in Cosmetics: An Overview Mainly Based on the Current European Regulations and the Safety Profile of These Compounds. *Journal of the European Academy of Dermatology and Venereology* **2019**, *33*, 5–14, doi:10.1111/jdv.15946.
240. Rodrigues, F.; Pimentel, F.B.; Oliveira, M.B.P.P. Olive By-Products: Challenge Application in Cosmetic Industry. *Ind Crops Prod* **2015**, *70*, 116–124, doi:10.1016/j.indcrop.2015.03.027.
241. Kaltsa, O.; Spiliopoulou, N.; Yanniotis, S.; Mandala, I. Stability and Physical Properties of Model Macro- and Nano/Submicron Emulsions Containing Fenugreek Gum. *Food Hydrocoll* **2016**, *61*, 625–632, doi:10.1016/j.foodhyd.2016.06.025.
242. Kaur, N.; Kaur, M.; Mahajan, M.; Jain, S.K. Development, Characterization and Evaluation of Nanocarrier Based Formulations of Antipsoriatic Drug “Acitretin” for Skin Targeting. *J Drug Deliv Sci Technol* **2020**, *60*, doi:10.1016/j.jddst.2020.102010.
243. Anchisi, C.; Maccioni, A.M.; Sinico, C.; Valenti, D. Stability Studies of New Cosmetic Formulations with Vegetable Extracts as Functional Agents. *Farmaco* **2001**, *56*, 427–431, doi:10.1016/S0014-827X(01)01055-2.
244. Jaiswal, P.V.; Ijeri, V.S.; Srivastava, A.K. Voltammetric Behavior of α -Tocopherol and its Determination Using Surfactant + Ethanol + Water and Surfactant + Acetonitrile + Water Mixed Solvent Systems. *Anal Chim Acta* **2001**, *441*, 201–206, doi:10.1016/S0003-2670(01)01119-9.
245. Alayoubi, A.; Kanthala, S.; Satyanarayanajois, S.D.; Anderson, J.F.; Sylvester, P.W.; Nazzal, S. Stability and *in Vitro* Antiproliferative Activity of Bioactive “Vitamin E” Fortified Parenteral Lipid Emulsions. *Colloids Surf B Biointerfaces* **2013**, *103*, 23–30, doi:10.1016/j.colsurfb.2012.10.003.
246. Fiume, M.M.; Bergfeld, W.F.; Belsito, D. v.; Hill, R.A.; Klaassen, C.D.; Liebler, D.C.; Marks, J.G.; Shank, R.C.; Slaga, T.J.; Snyder, P.W. Safety Assessment of Tocopherols and Tocotrienols as Used in Cosmetics. *Int J Toxicol* **2018**; *37*(Supplement 2), 61S-94S, ISBN 1091581818794.
247. Cieśla, J.; Koczańska, M.; Narkiewicz-Michalek, J.; Szymula, M.; Bieganowski, A. Effect of α -Tocopherol on the Properties of Microemulsions Stabilized by the Ionic Surfactants. *J Mol Liq* **2017**, *236*, 117–123, doi:10.1016/j.molliq.2017.04.015.
248. Gonçalves, G.M.S.; Maia Campos, P.M.B.G. Shelf Life and Rheology of Emulsions Containing Vitamin C and its Derivatives. *Revista de Ciências Farmaceuticas Basica e Aplicada* **2009**, *30*, 217–224.

249. Daher, C.C.; Fontes, I.S.; de Oliveira Rodrigues, R.; Azevedo De Brito Damasceno, G.; dos Santos Soares, D.; Flávio Soares Aragão, C.; Paula Barreto Gomes, A.; Ferrari, M. Development of O/W Emulsions Containing *Euterpe oleracea* Extract and Evaluation of Photoprotective Efficacy. *Brazilian Journal of Pharmaceutical Sciences* **2014**, *50*, 639–652, doi:10.1590/S1984-82502014000300024.
250. Infante, V.H.P.; Calixto, L.S.; Maia Campos, P.M.B.G. Physico-Mechanical Properties of Topical Formulations Based on Different Polymers. *Biomedical and Biopharmaceutical Research* **2019**, *16*, 213–222, doi:10.19277/bbr.16.2.214.
251. Vanti, G.; Grifoni, L.; Bergonzi, M.C.; Antiga, E.; Montefusco, F.; Caproni, M.; Bilia, A.R. Development and Optimisation of Biopharmaceutical Properties of a New Microemulgel of Cannabidiol for Locally-Acting Dermatological Delivery. *Int J Pharm* **2021**, *607*, 121036, doi:10.1016/j.ijpharm.2021.121036.
252. Moldovan, M.L.; Ionuț, I.; Bogdan, C. Cosmetic Products Containing Natural Based Emollients for Restoring Impaired Skin Barrier: Formulation and *In Vivo* Evaluation. *Farmacia* **2021**, *69*, 129–134, doi:10.31925/farmacia.2021.1.17.
253. Bergamante, V.; Ceschel, G.C.; Marazzita, S.; Ronchi, C.; Fini, A. Effect of Vehicles on Topical Application of *Aloe vera* and Arnica Montana Components. *Drug Deliv* **2007**, *14*, 427–432, doi:10.1080/10717540701202960.
254. Lee, W.C.; Yusof, S.; Hamid, N.S.A.; Baharin, B.S. Optimizing Conditions for Hot Water Extraction of Banana Juice Using Response Surface Methodology (RSM). *J Food Eng* **2006**, *75*, 473–479, doi:10.1016/j.jfoodeng.2005.04.062.
255. Hamzaoui, A.H.; Jamoussi, B.; M'nif, A. Lithium Recovery from Highly Concentrated Solutions: Response Surface Methodology (RSM) Process Parameters Optimization. *Hydrometallurgy* **2008**, *90*, 1–7, doi:10.1016/j.hydromet.2007.09.005.
256. Khuri, A.I.; Mukhopadhyay, S. Response Surface Methodology. *Wiley Interdiscip Rev Comput Stat* **2010**, *2*, 128–149, doi:10.1002/wics.73.
257. Huber, P. Sensory Measurement-Evaluation and Testing of Cosmetic Products. In *Cosmetic Science and Technology: Theoretical Principles and Applications*; Sakamoto, K., Locceed, R.; Mai-bach, Yamashita, Y., Eds.; H.I. Elsevier Inc., **2017**, doi:10.1016/B978-0-12-802005-0.00037-9.
258. Calvo, F.; Gómez, J.M.; Ricardez-Sandoval, L.; Alvarez, O. Integrated Design of Emulsified Cosmetic Products: A Review. *Chemical Engineering Research and Design* **2020**, *161*, 279–303, doi:10.1016/j.cherd.2020.07.014.
259. Marti-Mestres, G.; Nielloud, F. Emulsions in Health Care Applications-An Overview. *J Dispers Sci Technol* **2002**, *23*, 419–439, doi:10.1080/01932690208984214.
260. Cheng, Y.S.; Lam, K.W.; Ng, K.M.; Ko, R.K.M.; Wibowo, C. An Integrative Approach to Product Development-A Skin-Care Cream. *Comput Chem Eng* **2009**, *33*, 1097–1113, doi:10.1016/j.compchemeng.2008.10.010.

261. Vianna-Filho, R.P.; Petkowicz, C.L.O.; Silveira, J.L.M. Rheological Characterization of O/W Emulsions Incorporated with Neutral and Charged Polysaccharides. *Carbohydr Polym* **2013**, *93*, 266–272, doi:10.1016/j.carbpol.2012.05.014.
262. Tadros, T. Interparticle Interactions in Concentrated Suspensions and Their Bulk (Rheological) Properties. *Adv Colloid Interface Sci* **2011**, *168*, 263–277, doi:10.1016/j.cis.2011.05.003.
263. Quintana, J.M.; Califano, A.N.; Zaritzky, N.E.; P., P.; Franco, J.M. Linear and Nonlinear Viscoelastic Behavior of Oil-in-Water Emulsions Stabilized with Polysaccharides. *J Texture Stud* **2002**, *33*, 215–236.
264. Krstonošić, V.; Dokić, L.; Dokić, P.; Dapčević, T. Effects of Xanthan Gum on Physicochemical Properties and Stability of Corn Oil-in-Water Emulsions Stabilized by Polyoxyethylene (20) Sorbitan Monooleate. *Food Hydrocoll* **2009**, *23*, 2212–2218, doi:10.1016/j.foodhyd.2009.05.003.
265. Webb, E.B.; Koh, C.A.; Liberatore, M.W. High Pressure Rheology of Hydrate Slurries Formed from Water-in-Mineral Oil Emulsions. *Ind Eng Chem Res* **2014**, *53*, 6998–7007, doi:10.1021/ie5008954.
266. Rózańska, S.; Broniarz-Press, L.; Rózański, J.; Mitkowski, P.T.; Ochowiak, M.; Woziwodzki, S. Extensional Viscosity of o/w Emulsion Stabilized by Polysaccharides Measured on the Opposed-Nozzle Device. *Food Hydrocoll* **2013**, *32*, 130–142, doi:10.1016/j.foodhyd.2012.12.018.
267. Iqbal, S.; Xu, Z.; Huang, H.; Chen, X.D. Controlling the Rheological Properties of Oil Phases Using Controlled Protein-Polysaccharide Aggregation and Heteroaggregation in Water-in-Oil Emulsions. *Food Hydrocoll* **2019**, *96*, 278–287, doi:10.1016/j.foodhyd.2019.05.028.
268. Savary, G.; Grisel, M.; Picard, C. Impact of Emollients on the Spreading Properties of Cosmetic Products: A Combined Sensory and Instrumental Characterization. *Colloids Surf B Biointerfaces* **2013**, *102*, 371–378, doi:10.1016/j.colsurfb.2012.07.028.
269. Semenzato, A.; Costantini, A.; Baratto, G. Green Polymers in Personal Care Products: Rheological Properties of Tamarind Seed Polysaccharide. *Cosmetics* **2015**, *2*, 1–10, doi:10.3390/cosmetics2010001.
270. Li, Z.; Dai, L.; Wang, D.; Mao, L.; Gao, Y. Stabilization and Rheology of Concentrated Emulsions Using the Natural Emulsifiers Quillaja Saponins and Rhamnolipids. *J Agric Food Chem* **2018**, *66*, 3922–3929, doi:10.1021/acs.jafc.7b05291.
271. Caritá, A.C.; Resende de Azevedo, J.; Vinícius Buri, M.; Bolzinger, M.A.; Chevalier, Y.; Riske, K.A.; Ricci Leonardi, G. Stabilization of Vitamin C in Emulsions of Liquid Crystalline Structures. *Int J Pharm* **2021**, *592*, doi:10.1016/j.ijpharm.2020.120092.
272. Melanie, H.; Taarji, N.; Zhao, Y.; Khalid, N.; Neves, M.A.; Kobayashi, I.; Tuwo, A.; Nakajima, M. Formulation and Characterisation of O/W Emulsions Stabilised with Modified Seaweed Polysaccharides. *Int J Food Sci Technol* **2020**, *55*, 211–221, doi:10.1111/ijfs.14264.

273. Medina-Torres, L.; Calderas, F.; Sanchez-Olivares, G.; Nuñez-Ramirez, D.M. Rheology of Sodium Polyacrylate as an Emulsifier Employed in Cosmetic Emulsions. *Ind Eng Chem Res* **2014**, *53*, 18346–18351, doi:10.1021/ie503406a.
274. Calvo, F.; Gómez, J.M.; Ricardez-Sandoval, L.; Alvarez, O. Integrated Design of Emulsified Cosmetic Products: A Review. *Chemical Engineering Research and Design* **2020**, *161*, 279–303, doi:10.1016/j.cherd.2020.07.014.
275. Favero, J.S.; Santos, V.; Weiss-Angeli, V.; Gomes, L.B.; Veras, D.G.; Dani, N.; Mexias, A.S.; Bergmann, C.P. Evaluation and Characterization of Melo Bentonite Clay for Cosmetic Applications. *Appl Clay Sci* **2019**, *175*, 40–46, doi:10.1016/j.clay.2019.04.004.
276. Afifah, S.N.; Azhar, S.; Ashari, S.E.; Salim, N. Development of a Kojic Monooleate-Enriched Oil-in-Water Nanoemulsion as a Potential Carrier for Hyperpigmentation Treatment. *Int J Nanomedicine* **2018**, *13*, 6465–6479, doi:10.2147/IJN.S171532.
277. Khan, B.A.; Akhtar, N.; Mena, A.; Mena, F. A Novel *Cassia fistula* (L.)-Based Emulsion Elicits Skin Anti-Aging Benefits in Humans. *Cosmetics* **2015**, *2*, 368–383, doi:10.3390/cosmetics2040368.
278. Semenzato, A.; Costantini, A.; Meloni, M.; Maramaldi, G.; Meneghin, M.; Baratto, G. Formulating O/W Emulsions with Plant-Based Actives: A Stability Challenge for an Effective Product. *Cosmetics* **2018**, *5*, 1–11, doi:10.3390/cosmetics5040059.
279. Martinez, R.M.; Magalhães, W.V.; Sufi, B. da S.; Padovani, G.; Nazato, L.I.S.; Velasco, M.V.R.; Lannes, S.C. da S.; Baby, A.R. Vitamin E-loaded Bigels and Emulsions: Physicochemical Characterization and Potential Biological Application. *Colloids Surf B Biointerfaces* **2021**, *201*, doi:10.1016/j.colsurfb.2021.111651.
280. Lin, T.K.; Zhong, L.; Santiago, J.L. Anti-Inflammatory and Skin Barrier Repair Effects of Topical Application of Some Plant Oils. *Int J Mol Sci* **2018**, *19*, doi:10.3390/ijms19010070.
281. Andersen, A.F. Final Report on the Safety Assessment of Cetearyl Alcohol, Cetyl Alcohol, Isostearyl Alcohol, Myristyl Alcohol, and Behenyl Alcohol. *Int J Toxicol* **1988**, *7*, 359–413, doi:10.3109/10915818809023137.
282. Djuris, J.; Vasiljevic, D.; Jokic, S.; Ibric, S. Application of D-Optimal Experimental Design Method to Optimize the Formulation of O/W Cosmetic Emulsions. *Int J Cosmet Sci* **2014**, *36*, 79–87, doi:10.1111/ics.12099.
283. Dastbaz, Z.; Ashrafizadeh, S.N. Preparation, Stabilization, and Characterization of Polyisobutylene Aqueous Suspension. *Colloid Polym Sci* **2020**, *298*, 1335–1347, doi:10.1007/s00396-020-04727-z.
284. Huynh, A.; Abou-Dahech, M.S.; Reddy, C.M.; O’Neil, G.W.; Chandler, M.; Baki, G. Alkenones, a Renewably Sourced, Biobased Wax as an SPF Booster for Organic Sunscreens. *Cosmetics* **2019**, *6*, doi:10.3390/cosmetics6010011.

285. Martins, M.S.; Ferreira, M.S.; Almeida, I.F.; Sousa, E. Occurrence of Allergens in Cosmetics for Sensitive Skin. *Cosmetics* **2022**, *9*, 1–13, doi:10.3390/cosmetics9020032.
286. Motia, S.; Bouchikhi, B.; Llobet, E.; Bari, N. Synthesis and Characterization of a Highly Sensitive and Selective Electrochemical Sensor Based on Molecularly Imprinted Polymer with Gold Nanoparticles Modified Screen-Printed Electrode for Glycerol Determination in Wastewater. *Talanta* **2020**, *216*, 120953, doi:10.1016/j.talanta.2020.120953.
287. Becker, L.C.; Bergfeld, W.F.; Belsito, D. v.; Hill, R.A.; Klaassen, C.D.; Liebler, D.C.; Marks, J.G.; Shank, R.C.; Slaga, T.J.; Snyder, P.W.; Gill, L.J., Heldreth, B. Safety Assessment of Glycerin as Used in Cosmetics. *Int J Toxicol* **2019**, *38*, 6S-22S, doi:10.1177/1091581819883820.
288. Fiume, M.M.; Heldreth, B.; Bergfeld, W.F.; Belsito, D. v.; Hill, R.A.; Klaassen, C.D.; Liebler, D.; Marks, J.G.; Shank, R.C.; Slaga, T.J.; Snyder, P.W.; Andersen, A. Safety Assessment of Triethanolamine and Triethanolamine-Containing Ingredients as Used in Cosmetics. *Int J Toxicol* **2013**, *32*, 59S-83S, doi:10.1177/1091581813488804.
289. Gupta, N.; Dubey, A.; Prasad, P. Roy, A. Formulation and Evaluation of Herbal Fairness Cream Comprising Hydroalcoholic Extracts of *Pleurotus ostreatus*, *Glycyrrhiza glabra* and *Camellia sinensis*. *Pharmaceutical and Biosciences Journal* **2015**, *3*, 40–45, doi:10.20510/ukjpb/3/i3/89410.
290. Isabella, E.; Pohan, T. Formulation of Oil-in-Water Cream from Mangosteen (*Garcinia mangostana* L.) Pericarp Extract Preserved by Gamma Irradiation. *Atom Indonesia* **2013**, *39*, 136–144, doi:10.17146/aij.2013.256.
291. Kusumawati, L.A.I.; Dewi, E.N.A.; Xenograf, O.C.; Rifrianasari, K.; Hidayat, M.A. Tyrosinase Inhibition Assay and Skin Whitening Cream Formulation of Edamame Extract (Glycine Max). *International Journal of Pharmacognosy and Phytochemical Research* **2015**, *7*, 1167–1171.
292. Soni, M.G.; Taylor, S.L.; Greenberg, N.A.; Burdock, G.A. Evaluation of the Health Aspects of Methyl Paraben: A Review of the Published Literature. *Food and Chemical Toxicology* **2002**, *40*, 1335–1373, doi:10.1016/S0278-6915(02)00107-2.
293. Matwiejczuk, N.; Galicka, A.; Brzóška, M.M. Review of the Safety of Application of Cosmetic Products Containing Parabens. *Journal of Applied Toxicology* **2020**, *40*, 176–210, doi:10.1002/jat.3917.
294. Jaslina, N.F.; Faujan, N.H.; Mohamad, R.; Ashari, S.E. Effect of Addition of PVA / PG to Oil-in-Water Nanoemulsion Kojic Monooleate Formulation on Droplet Size : Three-Factors Response Surface. *Cosmetics* **2020**, *7*, 2–15.
295. Yu, L.; Li, S.; Stubbs, L.P.; Lau, H.C. Effects of Salinity and Ph on the Stability of Clay-Stabilized Oil-in-Water Pickering Emulsions. *SPE Journal* **2021**, *26*, 1402–1421, doi:10.2118/203825-PA.
296. Berenguer, D.; Sosa, L.; Alcover, M.; Sessa, M.; Halbaut, L.; Guillén, C.; Fisa, R.; Calpena-Campmany, A.C.; Riera, C. Development and Characterization of a Semi-Solid Dosage Form of

- Meglumine Antimoniate for Topical Treatment of Cutaneous Leishmaniasis. *Pharmaceutics* **2019**, *11*, doi:10.3390/pharmaceutics11110613.
297. Gore, E.; Picard, C.; Savary, G. Spreading Behavior of Cosmetic Emulsions: Impact of the Oil Phase. *Biotribology* **2018**, *16*, 17–24, doi:10.1016/j.biotri.2018.09.003.
298. Aziz, A.A.; Nordin, F.N.M.; Zakaria, Z.; Abu Bakar, N.K. A Systematic Literature Review on the Current Detection Tools for Authentication Analysis of Cosmetic Ingredients. *J Cosmet Dermatol* **2022**, *21*, 71–84, doi:10.1111/jocd.14402.
299. Vidhyalakshmi, R.; Valli Nachiyar, C.; Narendra Kumar, G.; Sunkar, S.; Badsha, I. Production, Characterization and Emulsifying Property of Exopolysaccharide Produced by Marine Isolate of *Pseudomonas fluorescens*. *Biocatal Agric Biotechnol* **2018**, *16*, 320–325, doi:10.1016/j.bcab.2018.08.023.
300. Liebert, M.A. Final Report on the Safety Assessment of Oleic Acid, Lauric Acid, Palmitic Acid, Myristic Acid, and Stearic Acid. *Int J Toxicol* **1987**, *6*, 321–401, doi:10.3109/10915818709098563.
301. Ahmad, I.; Sheraz, M.A.; Ahmed, S.; Shaikh, R.H.; Vaid, F.H.M.; Khattak, S.U.R.; Ansari, S.A. Photostability and Interaction of Ascorbic Acid in Cream Formulations. *AAPS PharmSciTech* **2011**, *12*, 917–923, doi:10.1208/s12249-011-9659-1.
302. Dammak, M.; ben Hlima, H.; Smaoui, S.; Fendri, I.; Michaud, P.; Ayadi, M.A.; Abdelkafi, S. Conception of an Environmentally Friendly O/W Cosmetic Emulsion from Microalgae. *Environmental Science and Pollution Research* **2022**, doi:10.1007/s11356-022-20824-8.
303. Dąbrowska, M.; Nowak, I. Lipid Nanoparticles Loaded with Selected Iridoid Glycosides as Effective Components of Hydrogel Formulations. *Materials* **2021**, *14*, 1–23, doi:10.3390/ma14154090.
304. Martínez-Pla, J.J.; Martín-Biosca, Y.; Sagrado, S.; Villanueva-Camañas, R.M.; Medina-Hernández, M.J. Evaluation of the pH Effect of Formulations on the Skin Permeability of Drugs by Biopartitioning Micellar Chromatography. *J Chromatogr A* **2004**, *1047*, 255–262, doi:10.1016/j.chroma.2004.07.011.
305. Khan, B.A.; Akhtar, N.; Khan, H.; Braga, V. de A. Development, Characterization and Antioxidant Activity of Polysorbate Based O/W Emulsion Containing Polyphenols Derived from *Hippophae rhamnoides* and *Cassia fistula*. *Brazilian Journal of Pharmaceutical Sciences* **2013**, *49*, 763–773, doi:10.1590/S1984-82502013000400016.
306. Masmoudi, H.; Dréau, Y. le; Piccerelle, P.; Kister, J. The Evaluation of Cosmetic and Pharmaceutical Emulsions Aging Process Using Classical Techniques and a New Method: FTIR. *Int J Pharm* **2005**, *289*, 117–131, doi:10.1016/j.ijpharm.2004.10.020.
307. Calvo, F.; Gómez, J.M.; Ricardez-Sandoval, L.; Alvarez, O. Integrated Design of Emulsified Cosmetic Products: A Review. *Chemical Engineering Research and Design* **2020**, *161*, 279–303, doi:10.1016/j.cherd.2020.07.014.

308. Niu, F.; Han, B.; Fan, J.; Kou, M.; Zhang, B.; Feng, Z.J.; Pan, W.; Zhou, W. Characterization of Structure and Stability of Emulsions Stabilized with Cellulose Macro/Nano Particles. *Carbohydr Polym* **2018**, *199*, 314–319, doi:10.1016/j.carbpol.2018.07.025.
309. Estanqueiro, M.; Conceição, J.; Amaral, M.H.; Sousa Lobo, J.M. Characterization, Sensorial Evaluation and Moisturizing Efficacy of Nanolipidgel Formulations. *Int J Cosmet Sci* **2014**, *36*, 159–166, doi:10.1111/ics.12109.
310. Karbstein, H.; Schubert, H. Developments in the Continuous Mechanical Production of Oil-in-Water Macro-Emulsions. *Chemical Engineering and Processing: Process Intensification* **1995**, *34*, 205–211, doi:10.1016/0255-2701(94)04005-2.
311. Venkataramani, D.; Tsulaia, A.; Amin, S. Fundamentals and Applications of Particle Stabilized Emulsions in Cosmetic Formulations. *Adv Colloid Interface Sci* **2020**, *283*, 102234, doi:10.1016/j.cis.2020.102234.
312. Gullapalli, R.P.; Sheth, B.B. Influence of an Optimized Non-Ionic Emulsifier Blend on Properties of Oil-in-Water Emulsions. *European Journal of Pharmaceutics and Biopharmaceutics* **1999**, *48*, 233–238, doi:10.1016/S0939-6411(99)00048-X.
313. Dapčević Hadnadev, T.; Dokić, P.; Krstonošić, V.; Hadnadev, M. Influence of Oil Phase Concentration on Droplet Size Distribution and Stability of Oil-in-Water Emulsions. *European Journal of Lipid Science and Technology* **2013**, *115*, 313–321, doi:10.1002/ejlt.201100321.
314. Bhattacharjee, S. DLS and Zeta Potential - What They Are and What They Are Not? *Journal of Controlled Release* **2016**, *235*, 337–351, doi:10.1016/j.jconrel.2016.06.017.
315. Dickinson, E. Hydrocolloids and Emulsion Stability. In *Handbook of hydrocolloids*; Phillips, G. O.; Williams, P. A., Eds.; Woodhead Publishing Limited **2009**, 23–49, ISBN 9781845695873.
316. Paximada, P.; Tsouko, E.; Kopsahelis, N.; Koutinas, A.A.; Mandala, I. Bacterial Cellulose as Stabilizer of o/w Emulsions. *Food Hydrocoll* **2016**, *53*, 225–232, doi:10.1016/j.foodhyd.2014.12.003.
317. Douguet, M.; Picard, C.; Savary, G.; Merlaud, F.; Loubat-bouleuc, N.; Grisel, M. Spreading Properties of Cosmetic Emollients Use of Synthetic Skin Surface to Elucidate Structural Effect. *Colloids Surf B Biointerfaces* **2017**, *154*, 307–314, doi:10.1016/j.colsurfb.2017.03.028.
318. César, F.C.S.; Maia Campos, P.M.B.G. Influence of Vegetable Oils in the Rheology, Texture Profile and Sensory Properties of Cosmetic Formulations Based on Organogel. *Int J Cosmet Sci* **2020**, *42*, 494–500, doi:10.1111/ics.12654.
319. Enescu, C.D.; Bedford, L.M.; Potts, G.; Fahs, F. A Review of Topical Vitamin C Derivatives and their Efficacy. *J Cosmet Dermatol* **2022**, *21*, 2349–2359, doi:10.1111/jocd.14465.
320. Gosenca, M.; Obreza, A.; Pečar, S.; Gašperlin, M. A New Approach for Increasing Ascorbyl Palmitate Stability by Addition of Non-Irritant Co-Antioxidant. *AAPS PharmSciTech* **2010**, *11*, 1485–1492, doi:10.1208/s12249-010-9507-8.

321. Maia Campos, P.M.B.G.; Gianeti, M.D.; Camargo, F.B.; Gaspar, L.R. Application of Tetra-Iso-palmitoyl Ascorbic Acid in Cosmetic Formulations: Stability Studies and *in vivo* Efficacy. *European Journal of Pharmaceutics and Biopharmaceutics* **2012**, *82*, 580–586, doi:10.1016/j.ejpb.2012.08.009.
322. Ravetti, S.; Clemente, C.; Brignone, S.; Hergert, L.; Allemandi, D.; Palma, S. Ascorbic Acid in Skin Health. *Cosmetics* **2019**, *6*, 6–13, doi:10.3390/COSMETICS6040058.
323. Farahmand, S.; Tajerzadeh, H.; Farboud, E.S. Formulation and Evaluation of a Vitamin C Multiple Emulsion. *Pharm Dev Technol* **2006**, *11*, 255–261, doi:10.1080/10837450500464172.
324. Telang, P. Vitamin C in Dermatology. *Indian Dermatol Online J* **2013**, *4*, 143, doi:10.4103/2229-5178.110593.
325. Sheraz, M.A.; Ahmed, S.; Ahmad, I.; Shaikh, R.H.; Vaid, F.H.M.; Iqbal, K. Formulation and Stability of Ascorbic Acid in Topical Preparations. *Systematic Reviews in Pharmacy* **2011**, *2*, 86–90, doi:10.4103/0975-8453.86296.
326. Yi, N.; Chiang, Z. Topical Vitamin C and the Skin. *Jcad Journal of Clinical and Aesthetic Dermatology* **2017**, *14*, 14–17.
327. Khalid, N.; Kobayashi, I.; Neves, M.A.; Uemura, K.; Nakajima, M. Preparation and Characterization of Water-in-Oil Emulsions Loaded with High Concentration of L-Ascorbic Acid. *LWT - Food Science and Technology* **2013**, *51*, 448–454, doi:10.1016/j.lwt.2012.11.020.
328. Yuan, J.P.; Chen, F. Degradation of Ascorbic Acid in Aqueous Solution. *J Agric Food Chem* **1998**, *46*, 5078–5082, doi:10.1021/jf9805404.
329. Sheraz, M.; Khan, M.; Ahmed, S.; Kazi, S.; Ahmad, I. Stability and Stabilization of Ascorbic Acid. *Household and Personal Care Today* **2015**, *10*, 22–25.
330. Macan, A.M.; Kraljević, T.G.; Raić-malić, S. Therapeutic Perspective of Vitamin C and its Derivatives. *Antioxidants* **2019**, *8*, doi:10.3390/antiox8080247.
331. Lin, J.Y.; Selim, M.A.; Shea, C.R.; Grichnik, J.M.; Omar, M.M.; Monteiro-Riviere, N.A.; Pinnell, S.R. UV Photoprotection by Combination Topical Antioxidants Vitamin C and Vitamin E. *J Am Acad Dermatol* **2003**, *48*, 866–874, doi:10.1067/mjd.2003.425.
332. Gallarate, M.; Carlotti, M.E.; Trotta, M.; Bovo, S. On the Stability of Ascorbic Acid in Emulsified Systems for Topical and Cosmetic Use. *Int J Pharm* **1999**, *188*, 233–241, doi:10.1016/S0378-5173(99)00228-8.
333. Caritá, A.C.; Fonseca-Santos, B.; Shultz, J.D.; Michniak-Kohn, B.; Chorilli, M.; Leonardi, G.R. Vitamin C: One Compound, Several Uses. Advances for Delivery, Efficiency and Stability. *Nanomedicine* **2020**, *24*, 102117, doi:10.1016/j.nano.2019.102117.
334. Raschke, T.; Koop, U.; Düsing, H.J.; Filbry, A.; Sauermann, K.; Jaspers, S.; Wenck, H.; Wittern, K.P. Topical Activity of Ascorbic Acid: From *In Vitro* Optimization to *in vivo* Efficacy. *Skin Pharmacol Physiol* **2004**, *17*, 200–206, doi:10.1159/000078824.

335. Jacques, C.; Genies, C.; Bacqueville, D.; Tourette, A.; Borotra, N.; Chaves, F.; Sanches, F.; Gaudry, A.L.; Bessou-Touya, S.; Duplan, H. Ascorbic Acid 2-Glucoside: An Ascorbic Acid Pro-Drug with Longer-Term Antioxidant Efficacy in Skin. *Int J Cosmet Sci* **2021**, *43*, 691–702, doi:10.1111/ics.12745.
336. Alhasso, B.; Ghori, M.U.; Conway, B.R. Systematic Review on the Effectiveness of Essential and Carrier Oils as Skin Penetration Enhancers in Pharmaceutical Formulations. *Sci Pharm* **2022**, *90*, doi:10.3390/scipharm90010014.
337. Jiang, Q.; Wu, Y.; Zhang, H.; Liu, P.; Yao, J.; Yao, P.; Chen, J.; Duan, J. Development of Essential Oils as Skin Permeation Enhancers: Penetration Enhancement Effect and Mechanism of Action. *Pharm Biol* **2017**, *55*, 1592–1600, doi:10.1080/13880209.2017.1312464.
338. Herman, A.; Herman, A.P. Essential Oils and Their Constituents as Skin Penetration Enhancer for Transdermal Drug Delivery: A Review. *Journal of Pharmacy and Pharmacology* **2015**, *67*, 473–485, doi:10.1111/jphp.12334.
339. Morteza-Semnani, K.; Saeedi, M.; Akbari, J.; Eghbali, M.; Babaei, A.; Hashemi, S.M.H.; Nokhodchi, A. Development of a Novel Nanoemulgel Formulation Containing Cumin Essential Oil as Skin Permeation Enhancer. *Drug Deliv Transl Res* **2022**, *12*, 1455–1465, doi:10.1007/s13346-021-01025-1.
340. Chen, J.; Jiang, Q.D.; Wu, Y.M.; Liu, P.; Yao, J.H.; Lu, Q.; Zhang, H.; Duan, J.A. Potential of Essential Oils as Penetration Enhancers for Transdermal Administration of Ibuprofen to Treat Dysmenorrhoea. *Molecules* **2015**, *20*, 18219–18236, doi:10.3390/molecules201018219.
341. Nawaz, A.; Khan, G.M.; Shah, S.U.; Shah, K.U.; Rehman, A.; Hussain, A. Preparation and Evaluation of Clotrimazole Matrix Type Patch: Effect of Olive Oil on Drug Penetration across Rabbit Skin. *Proceedings of the Pakistan Academy of Sciences* **2011**, *48*, 95–100.
342. Ruiz, A.; Arias, J.L.; Gallardo, V. Skin Creams Made with Olive Oil. In *Olives and Olive Oil in Health and Disease Prevention*; Watson, R.; Preedy, V., Eds.; Elsevier Inc., **2010**; ISBN 9780123744203.
343. Chaiyana, W.; Leelapornpisid, P.; Phongpradist, R.; Kiattisin, K. Enhancement of Antioxidant and Skin Moisturizing Effects of Olive Oil by Incorporation into Microemulsions. *Nanomaterials and Nanotechnology* **2016**, *6*, 1–8, doi:10.1177/1847980416669488.
344. Mahmood, H.S.; Alaayedi, M.; Ashoor, J.A.; Alghurabi, H. The Enhancement Effect of Olive and Almond Oils on Permeability of Nimesulide as Transdermal Gel. *International Journal of Pharmaceutical Research* **2019**, *11*, 1200–1206.
345. Hasan, Z.A.; Almousawy, J.M.M.; Alghurabi, H.S.K. The Effect of Almond Oil on the Permeability of Ketoprofen Hydrogel. *International Journal of Applied Pharmaceutics* **2020**, *12*, 65–69, doi:10.22159/ijap.2020v12i2.35896.
346. Xylia, P.; Chrysargyris, A.; Tzortzakis, N. Ascorbic Acid , and Chitosan on Fresh-Cut Lettuce Preservation. *Foods* **2021**, *10*, 1–21.

347. Doucet, O.; Ferrero, L.; Garcia, N.; Zastrow, L. O/W Emulsion and W/O/W Multiple Emulsion : Physical Characterization and Skin Pharmacokinetic Comparison in the Delivery. *Int J Cosmet Sci* **1998**, *295*, 283–295.
348. Ruiz-Domínguez, M.L.; Raigón, M.D.; Prohens, J. Diversity for Olive Oil Composition in a Collection of Varieties from the Region of Valencia (Spain). *Food Research International* **2013**, *54*, 1941–1949, doi:10.1016/j.foodres.2013.06.023.
349. Ramirez-Tortosa, M.C.; Granados, S.; Quiles, J.L. Chemical Composition, Types and Characteristics of Olive Oil. In *Olive Oil and Health*; Quiles, J.L., M.Carmen, R.T., Parven, Y., Eds.; CAB International: London, **2006**; Vol. 10, 1–375, ISBN 9781845930684.
350. Blekas, G.; Tsimidou, M.; Boskou, D. Olive Oil Composition. In *Olive oil*; **2006**; ISBN 9781439832028.
351. Carrillo, C.A.; Nypelö, T.E.; Rojas, O.J. Cellulose Nanofibrils for One-Step Stabilization of Multiple Emulsions (W/O/W) Based on Soybean Oil. *J Colloid Interface Sci* **2015**, *445*, 166–173, doi:10.1016/j.jcis.2014.12.028.
352. Pinnell, S.R.; Yang, H.; Omar, M.; Riviere, N.M.; DeBuys, H. v.; Walker, L.C.; Wang, Y.; Levine, M. Topical L-Ascorbic Acid: Percutaneous Absorption Studies. *Dermatologic Surgery* **2001**, *27*, 137–142, doi:10.1046/j.1524-4725.2001.00264.x.
353. Ascenso, A.; Simões, S.; Marto, J.; Ribeiro, H.M.; Almeida, A.J. Colloidal Disperse Systems: Microemulsions and Nanoemulsions. In *Nanocarriers for Drug Delivery*; Eloy, J.O., Abriata, J.P., Marchetti, J.M., Eds.; Springer, Cham.: Switzerland, **2021**, ISBN 9783030633882.
354. Li, P.H.; Lu, W.C. Effects of Storage Conditions on the Physical Stability of D-Limonene Nanoemulsion. *Food Hydrocoll* **2016**, *53*, 218–224, doi:10.1016/j.foodhyd.2015.01.031.
355. Tal-Figiel, B. The Formation of Stable W/O, O/W, W/O/W Cosmetic Emulsions in an Ultrasonic Field. *Chemical Engineering Research and Design* **2007**, *85*, 730–734, doi:10.1205/cherd06199.
356. Eh Suk, V.R.; Khalid, K.; Misran, M. Preparation and Characterization of Ylang-Ylang (*Cananga Odorata*) Essential Oil and Ascorbic Acid Loaded Olive Oil-in-Water Emulsion. *Chiang Mai Journal of Science* **2019**, *46*, 353–360.
357. Kundu, P.; Kumar, V.; Mishra, I.M. Study the Electro-Viscous Effect on Stability and Rheological Behavior of Surfactant-Stabilized Emulsions. *J Dispers Sci Technol* **2018**, *39*, 384–394, doi:10.1080/01932691.2017.1320668.
358. Aveyard, R.; Clint, J.H.; Nees, D.; Paunov, V.N. Compression and Structure of Monolayers of Charged Latex Particles at Air/Water and Octane/Water Interfaces. *Langmuir* **2000**, *16*, 1969–1979, doi:10.1021/la990887g.
359. Fazal, W.; Musa, K.B.; Mohsan, N.; Khakemin, K. Comparison of Some Physico-Chemical Properties of Different Oils Available in the Local Market in Pakistan. *International Journal of Recent Research Aspects* **2015**, *2*, 93-98.

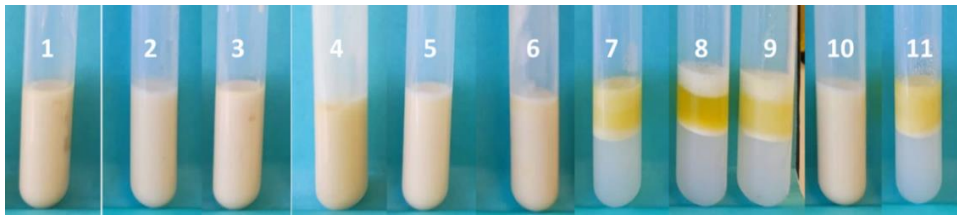
360. Brito, A.C.F.; Sierakowski, M.R.; Reicher, F.; Feitosa, J.P.A.; de Paula, R.C.M. Dynamic Rheological Study of *Sterculia striata* and Karaya Polysaccharides in Aqueous Solution. *Food Hydrocoll* **2005**, *19*, 861–867, doi:10.1016/j.foodhyd.2004.10.035.
361. Abdolmaleki, K.; Mohammadifar, M.A.; Mohammadi, R.; Fadavi, G.; Meybodi, N.M. The Effect of pH and Salt on the Stability and Physicochemical Properties of Oil-in-Water Emulsions Prepared with Gum Tragacanth. *Carbohydr Polym* **2016**, *140*, 342–348, doi:10.1016/j.carbpol.2015.12.081.
362. Saiki, Y.; Horn, R.G.; Prestidge, C.A. Droplet Structure Instability in Concentrated Emulsions. *J Colloid Interface Sci* **2008**, *320*, 569–574, doi:10.1016/j.jcis.2008.01.014.
363. Thanasukarn, P.; Pongsawatmanit, R.; McClements, D.J. Influence of Emulsifier Type on Freeze-Thaw Stability of Hydrogenated Palm Oil-in-Water Emulsions. *Food Hydrocoll* **2004**, *18*, 1033–1043, doi:10.1016/j.foodhyd.2004.04.010.
364. Morganti, P.; Morganti, G.; Gagliardini, A.; Lohani, A. From Cosmetics to Innovative Cosmeceuticals—Non-Woven Tissues as New Biodegradable Carriers. *Cosmetics* **2021**, *8*, 1–19, doi:10.3390/cosmetics8030065.
365. Mahendra, C.K.; Teng, L.; Tan, H.; Mahendra, C.K.; Ser, H.; Pusparajah, P.; Htar, T.T.; Chuah, L.; Yap, W.H.; Tang, S.Y. The Potential of Sky Fruit as an Anti-Aging and Wound Healing Cosmeceutical Agent. *Cosmetics* **2021**, *8*, 1–15.
366. Charles Dorni, A.I.; Amalraj, A.; Gopi, S.; Varma, K.; Anjana, S.N. Novel Cosmeceuticals from Plants—An Industry Guided Review. *J Appl Res Med Aromat Plants* **2017**, *7*, 1–26, doi:10.1016/j.jarmap.2017.05.003.
367. Mishra, A.K.; Mishra, A.; Chattopadhyay, P. Herbal Cosmeceuticals for Photoprotection from Ultraviolet B Radiation: A Review. *Tropical Journal of Pharmaceutical Research* **2011**, *10*, 351–360, doi:10.4314/tjpr.v10i3.7.
368. Yaghoubi, A.; Ghojazadeh, M.; Abolhasani, S.; Alikhah, H.; Khaki-Khatibi, F. Correlation of Serum Levels of Vitronectin, Malondialdehyde and Hs-CRP With Disease Severity in Coronary Artery Disease. *J Cardiovasc Thorac Res* **2015**, *7*, 113–117, doi:10.15171/jcvtr.2015.24.
369. Frazão, D.F.; Martins-Gomes, C.; Steck, J.L.; Keller, J.; Delgado, F.; Gonçalves, J.C.; Bunzel, M.; Pintado, C.M.B.S.; Díaz, T.S.; Silva, A.M. Labdanum Resin from *Cistus Ladanifer* L.: A Natural and Sustainable Ingredient for Skin Care Cosmetics with Relevant Cosmeceutical Bioactivities. *Plants* **2022**, *11*, 1477, doi:10.3390/plants11111477.
370. Simon, H.U.; Haj-Yehia, A.; Levi-Schaffer, F. Role of Reactive Oxygen Species (ROS) in Apoptosis Induction. *Apoptosis* **2000**, *5*, 415–418, doi:10.1023/A:1009616228304.
371. Zanatta, C.F.; Mitjans, M.; Urgatondo, V.; Rocha-Filho, P.A.; Vinardell, M.P. Photoprotective Potential of Emulsions Formulated with Buriti Oil (*Mauritia flexuosa*) against UV Irradiation on Keratinocytes and Fibroblasts Cell Lines. *Food and Chemical Toxicology* **2010**, *48*, 70–75, doi:10.1016/j.fct.2009.09.017.

372. Gasparrini, M.; Forbes-Hernandez, T.Y.; Afrin, S.; Alvarez-Suarez, J.M.; González-Paramàs, A.M.; Santos-Buelga, C.; Bompadre, S.; Quiles, J.L.; Mezzetti, B.; Giampieri, F. A Pilot Study of the Photoprotective Effects of Strawberry-based Cosmetic Formulations on Human Dermal Fibroblasts. *Int J Mol Sci* **2015**, *16*, 17870–17884, doi:10.3390/ijms160817870.
373. Sirerol, J.A.; Feddi, F.; Mena, S.; Rodriguez, M.L.; Sirera, P.; Aupí, M.; Pérez, S.; Asensi, M.; Ortega, A.; Estrela, J.M. Topical Treatment with Pterostilbene, a Natural Phytoalexin, Effectively Protects Hairless Mice against UVB Radiation-Induced Skin Damage and Carcinogenesis. *Free Radic Biol Med* **2015**, *85*, 1–11, doi:10.1016/j.freeradbiomed.2015.03.027.
374. Bissett, D.L.; Oblong, J.E.; Berge, C.A. Niacinamide: A B Vitamin That Improves Aging Facial Skin Appearance. *Dermatol Surg* **2005**, *31*, 860–866, doi:10.1111/j.1524-4725.2005.31732.
375. Hoang, H.T.; Moon, J.Y.; Lee, Y.C. Natural Antioxidants from Plant Extracts in Skincare Cosmetics: Recent Applications, Challenges and Perspectives. *Cosmetics* **2021**, *8*, 1–24, doi:10.3390/cosmetics8040106.
376. Rattanawitpong, P.; Wanitphakdeedecha, R.; Bumrungrert, A.; Maiprasert, M. Anti-Aging and Brightening Effects of a Topical Treatment Containing Vitamin C, Vitamin E, and Raspberry Leaf Cell Culture Extract: A Split-Face, Randomized Controlled Trial. *J Cosmet Dermatol* **2020**, *19*, 671–676, doi:10.1111/jocd.13305.
377. Zerbinati, N.; Sommatis, S.; Maccario, C.; di Francesco, S.; Capillo, M.C.; Rauso, R.; Herrera, M.; Bencini, P.L.; Guida, S.; Mocchi, R. The Anti-Ageing and Whitening Potential of a Cosmetic Serum Containing 3-o-Ethyl-l-Ascorbic Acid. *Life* **2021**, *11*, doi:10.3390/life11050406.
378. Silva, S.; Ferreira, M.; Oliveira, A.S.; Magalhães, C.; Sousa, M.E.; Pinto, M.; Sousa Lobo, J.M.; Almeida, I.F. Evolution of the Use of Antioxidants in Anti-Ageing Cosmetics. *Int J Cosmet Sci* **2019**, *41*, 378–386, doi:10.1111/ics.12551.
379. Huang, C.K.; Miller, T.A. The Truth about Over-the-Counter Topical Anti-Aging Products: A Comprehensive Review. *Aesthet Surg J* **2007**, *27*, 402–412, doi:10.1016/j.asj.2007.05.005.
380. Pisoschi, A.M.; Pop, A.; Iordache, F.; Stanca, L.; Predoi, G.; Serban, A.I. Oxidative Stress Mitigation by Antioxidants - An Overview on Their Chemistry and Influences on Health Status. *Eur J Med Chem* **2021**, *209*, 112891, doi:10.1016/j.ejmech.2020.112891.
381. Bujak, T.; Zagórska-dziok, M.; Ziemińska, A.; Nizioł-lukaszewska, Z.; Wasilewski, T.; Hordyjewicz-baran, Z. Antioxidant and Cytoprotective Properties of Plant Extract from Dry Flowers as Functional Dyes for Cosmetic Products. *Molecules* **2021**, *26*, 1–25, doi:10.3390/molecules26092809.
382. Sharmeen, J.B.; Mahomoodally, F.M.; Zengin, G.; Maggi, F. Essential Oils as Natural Sources of Fragrance Compounds for Cosmetics and Cosmeceuticals. *Molecules* **2021**, *26*, doi:10.3390/molecules26030666.
383. Guzmán, E.; Lucia, A. Essential Oils and Their Individual Components in Cosmetic Products. *Cosmetics* **2021**, *8*, 1–28, doi:10.3390/cosmetics8040114.

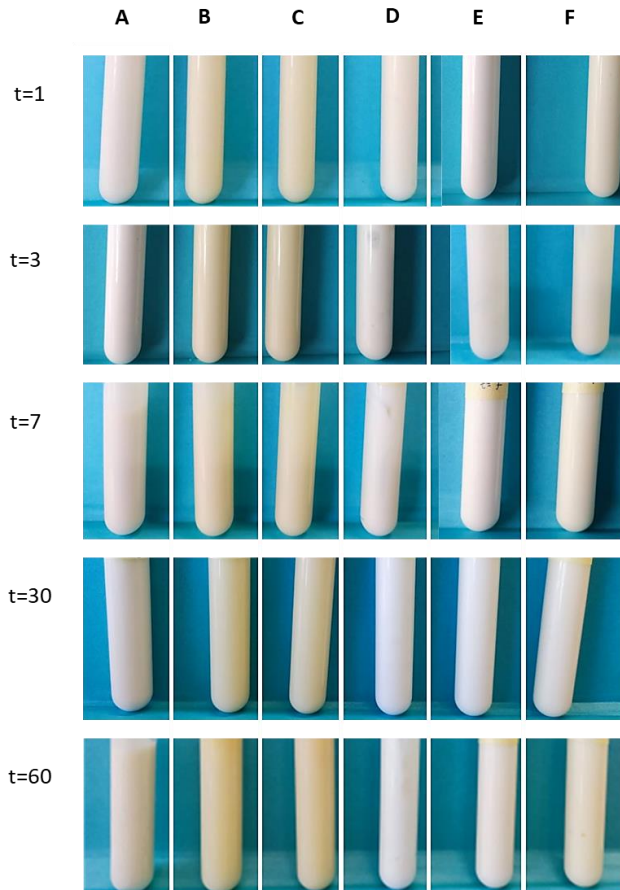
384. Marzulli, F.N.; Maibach, H.I. Contact Allergy: Predictive Testing in Man. *Contact Dermatitis* **1976**, *2*, 1–17, doi:10.1111/j.1600-0536.1976.tb02972.x.
385. Fregert, S.; Bandmann, H.-J. Patch Testing. Springer Berlin Heidelberg: Berlin/Heidelberg, 1975; ISBN 978-3-540-07229-4.
386. Hulme, E.C.; Trevethick, M.A. Ligand Binding Assays at Equilibrium: Validation and Interpretation. *Br J Pharmacol* **2010**, *161*, 1219–1237, doi:10.1111/j.1476-5381.2009.00604.x.
387. Bourne, R. ImageJ. *Fundamentals of Digital Imaging in Medicine* **2010**, *9*, 185–188, doi:10.1007/978-1-84882-087-6_9.
388. Zhou, X.; Ruan, Q.; Ye, Z.; Chu, Z.; Xi, M.; Li, M.; Hu, W.; Guo, X.; Yao, P.; Xie, W. Resveratrol Accelerates Wound Healing by Attenuating Oxidative Stress-Induced Impairment of Cell Proliferation and Migration. *Burns* **2021**, *47*, 133–139, doi:10.1016/j.burns.2020.10.016.
389. Evans, P.M.; Woodbine, L.; Riballo, E.; Gennery, A.R.; Hubank, M.; Jeggo, P.A. Radiation-Induced Delayed Cell Death in a Hypomorphic Artemis Cell Line. *Hum Mol Genet* **2006**, *15*, 1303–1311, doi:10.1093/hmg/ddl050.
390. Vieira, T.; Carvalho Silva, J.; Botelho do Rego, A.M.; Borges, J.P.; Henriques, C. Electrospun Biodegradable Chitosan Based-Poly(Urethane Urea) Scaffolds for Soft Tissue Engineering. *Materials Science and Engineering C* **2019**, *103*, 109819, doi:10.1016/j.msec.2019.109819.
391. Maruno, M.; Rocha-Filho, P.A. O/W Nanoemulsion after 15 Years of Preparation: A Suitable Vehicle for Pharmaceutical and Cosmetic Applications. *J Dispers Sci Technol* **2010**, *31*, 17–22, doi:10.1080/01932690903123775.
392. Pereira, T.A.; Guerreiro, C.M.; Maruno, M.; Ferrari, M.; Rocha-Filho, P.A. Exotic Vegetable Oils for Cosmetic O/W Nanoemulsions: *in vivo* Evaluation. *Molecules* **2016**, *21*, 1–16, doi:10.3390/molecules21030248.
393. Schmid-Wendtner, M.H.; Korting, H.C. The pH of the Skin Surface and Its Impact on the Barrier Function. *Skin Pharmacol Physiol* **2006**, *19*, 296–302, doi:10.1159/000094670.
394. Pereira, J.; Gonçalves, R.; Barreto, M.; Dias, C.; Carvalho, F.; Almeida, A.J.; Ribeiro, H.M.; Marto, J. Development of Gel-in-Oil Emulsions for Khellin Topical Delivery. *Pharmaceutics* **2020**, *12*, doi:10.3390/pharmaceutics12050398.
395. Bera, B.; Khazal, R.; Schroën, K. Coalescence Dynamics in Oil-in-Water Emulsions at Elevated Temperatures. *Sci Rep* **2021**, *11*, 1–10, doi:10.1038/s41598-021-89919-5.
396. Hong, I.K.; Kim, S.I.; Lee, S.B. Effects of HLB Value on Oil-in-Water Emulsions: Droplet Size, Rheological Behavior, Zeta-Potential, and Creaming Index. *Journal of Industrial and Engineering Chemistry* **2018**, *67*, 123–131, doi:10.1016/j.jiec.2018.06.022.
397. Querol, N.; Barreneche, C.; Cabeza, L.F. Storage Stability of Bimodal Emulsions vs. Monomodal Emulsions. *Applied Sciences (Switzerland)* **2017**, *7*, doi:10.3390/app7121267.
398. Mahmood, T.; Akhtar, N. Stability of a Cosmetic Multiple Emulsion Loaded with Green Tea Extract. *The Scientific World Journal* **2013**, *2013*, doi:10.1155/2013/153695.

399. Lim, C.; Basri, M.; Omar, D.; Abdul Rahman, M.; Salleh, A.; Raja Abdul Rahman, R. Physico-chemical Characterization of Nonionic Surfactants in Oil-in-Water (O/W) Nano-Emulsions for New Pesticide Formulations. *Int J Appl Sci Technol* **2011**, *1*, 131–142.
400. Masmoudi, H.; Piccerelle, P.; le Dréau, Y.; Kister, J. A Rheological Method to Evaluate the Physical Stability of Highly Viscous Pharmaceutical Oil-in-Water Emulsions. *Pharm Res* **2006**, *23*, 1937–1947, doi:10.1007/s11095-006-9038-x.
401. Badea, G.; Lăcătușu, I.; Badea, N.; Ott, C.; Meghea, A. Use of Various Vegetable Oils in Designing Photoprotective Nanostructured Formulations for UV Protection and Antioxidant Activity. *Ind Crops Prod* **2015**, *67*, 18–24, doi:10.1016/j.indcrop.2014.12.049.
402. Kehrer, J.P.; Klotz, L.O. Free Radicals and Related Reactive Species as Mediators of Tissue Injury and Disease: Implications for Health. *Critical Reviews in Toxicology* **2015**, *45* (9), 1-34, 10.3109/10408444.2015.1074159.
403. Mota, G.S.T. da; Arantes, A.B.; Sacchetti, G.; Spagnoletti, A.; Ziosi, P.; Scalambra, E.; Vertuani, S.; Manfredini, S. Antioxidant Activity of Cosmetic Formulations Based on Novel Extracts from Seeds of Brazilian *Araucaria angustifolia* (Bertoll) Kuntze. *Journal of Cosmetics, Dermatological Sciences and Applications* **2014**, *04*, 190–202, doi:10.4236/jcdsa.2014.43027.
404. Segall, A.I.; Moyano, M.A. Stability of Vitamin C Derivatives in Topical Formulations Containing Lipoic Acid, Vitamins A and E. *Int J Cosmet Sci* **2008**, *30*, 453–458, doi:10.1111/j.1468-2494.2008.00473.x.
405. Castro, K.C.; Campos, M.G.N.; Mei, L.H.I. Hyaluronic Acid Electrospinning: Challenges, Applications in Wound Dressings and New Perspectives. *Int J Biol Macromol* **2021**, *173*, 251–266, doi:10.1016/j.ijbiomac.2021.01.100.
406. Guillerme, J.B.; Couteau, C.; Coiffard, L. Applications for Marine Resources in Cosmetics. *Cosmetics* **2017**, *4*, 1–15, doi:10.3390/cosmetics4030035.
407. Séhédic, D.; Hardy-Boismartel, A.; Couteau, C.; Coiffard, L.J.M. Are Cosmetic Products Which Include an SPF Appropriate for Daily Use? *Arch Dermatol Res* **2009**, *301*, 603–608, doi:10.1007/s00403-009-0974-2.
408. Pensé-Lhéritier, A.M. Recent Developments in the Sensorial Assessment of Cosmetic Products: A Review. *Int J Cosmet Sci* **2015**, *37*, 465–473, doi:10.1111/ics.12223.

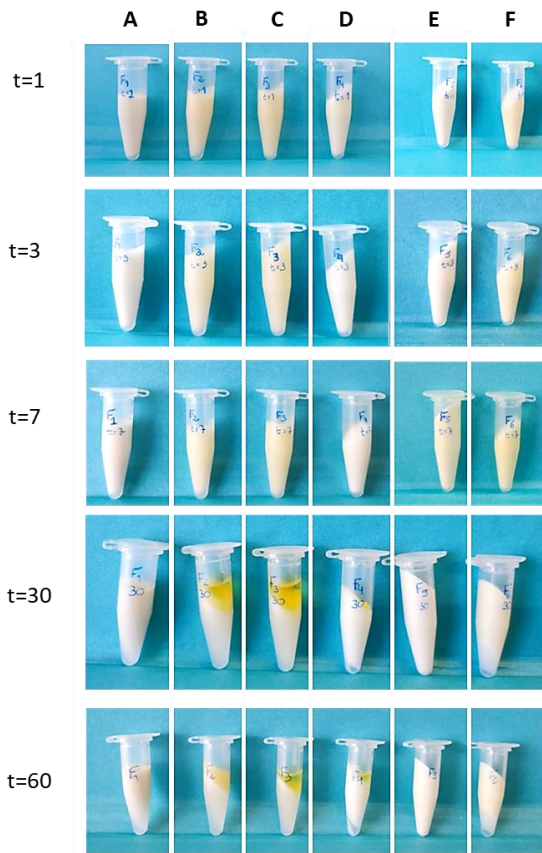
APPENDIX



A.1. Emulsions prepared using RSM after 24 h of preparation.



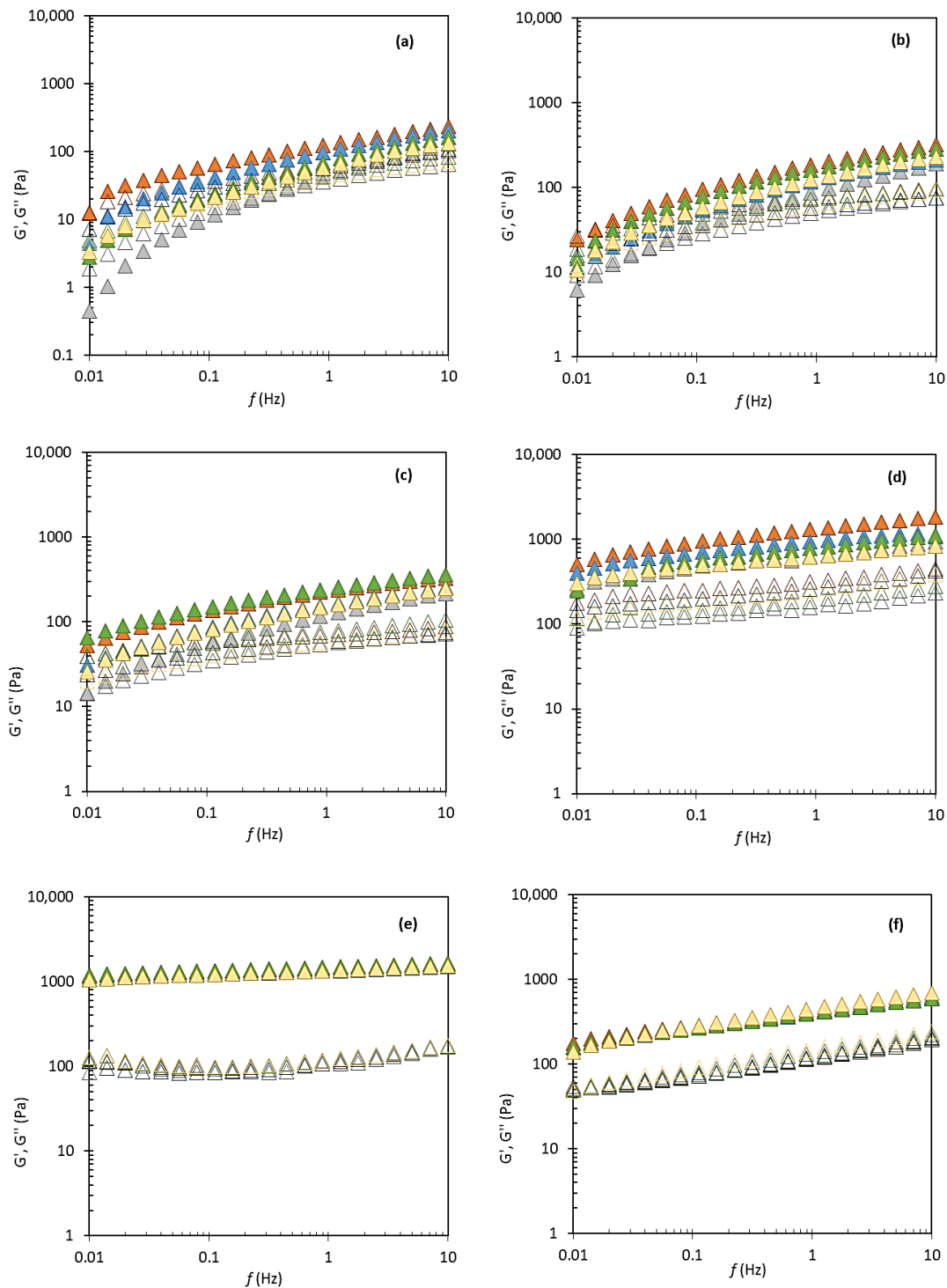
A.2. Emulsification index (EI=100%) for formulations A, B, C, D, E, F during the storage times: t=1, t=3, t=7, t=30, and t=60.



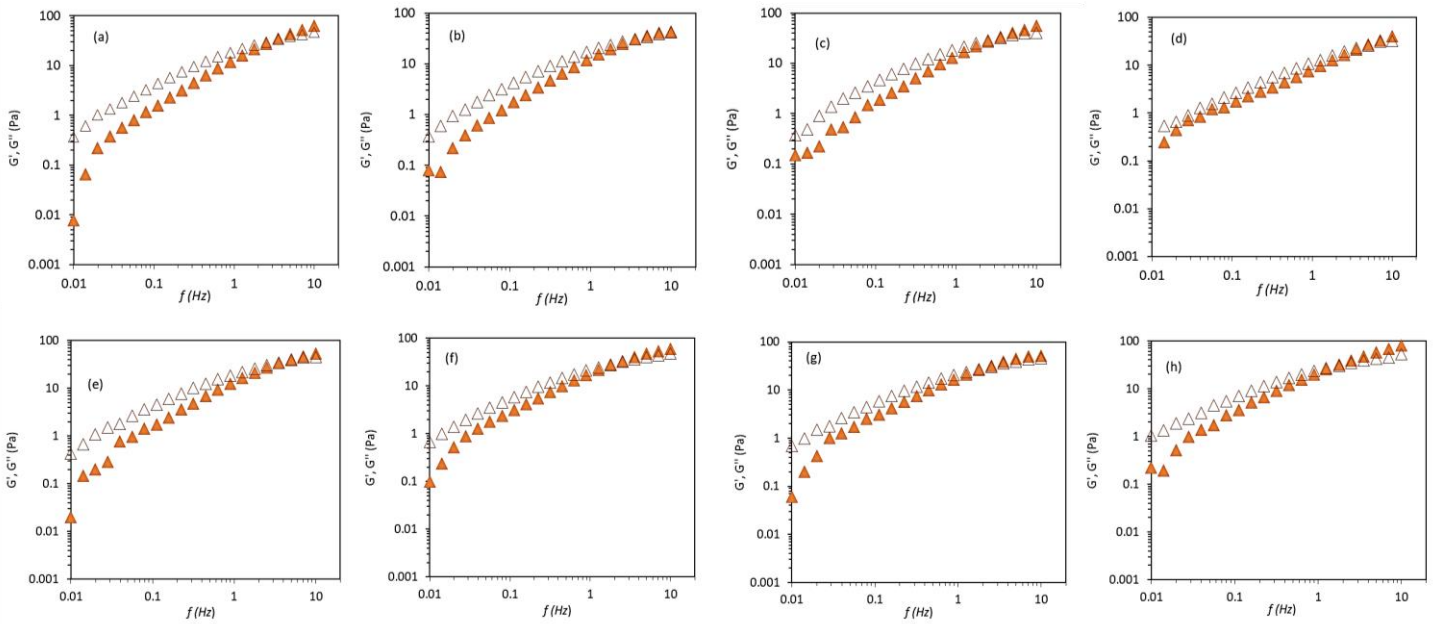
A.3. Centrifugation test for formulations A, B, C, D, E, F during the storage times: t=1, t=3, t=7, t=30, and t=60.



A.4. Centrifugation test for commercial formulations: (1) Cien® Body lotion, (2) Sephora® Hand cream, (3) Shiseido® Primer, (4) Uriage® Pruriced.



A.5. Mechanical spectrum for formulations A (a), B (b), C (c), D (d), E (e), and F (f) during the storage times; $t=1$ (orange), $t=3$ (blue), $t=7$ (green), $t=30$ (yellow), and $t=60$ (gray). G' (closed triangle) and G'' (open triangle).



A.6. Mechanical spectrum for the FucoPol-based emulsions. The top row represents emulsions with *Olea europaea* fruit oil with different L-ascorbic acid concentration: (a) 5.0 wt.%, (b) 8.0 wt.%, (c) 10 wt.%, and (d) 15 wt.%. The bottom row represents the emulsions with *Prunus amygdalus dulcis* oil with different L-ascorbic acid concentration: (e) 5.0 wt.%, (f) 8.0 wt.%, (g) 10 wt.%, and (h) 15 wt.%. G' (open triangle) and G'' (closed triangle).

A.7. Sensory analysis of moisturizing cream

This questionnaire aims at the characterization of FucoPol-based moisturizer. To do this, we ask that you answer some questions after product application. Your identity will not be disclosed, and we thank you in advance for your cooperation. These products do not contain any medicine in its composition, being solely moisturizing cosmetic products for face/body application. Please, place some product between your fingertips, assess how it feels and then apply the product on the back of the hand in circular movements until it disappears, answering the following questions on a scale from 1 (unacceptable) to 5 (excellent).

Sex: Male ____ Female ____

Age: <25 ____ 25-39 ____ 40-60 ____ >60 ____

Please rate from 1-5 the following questions:

- a. How do you rate product appearance? _____
- b. How do you rate product odour? _____
- c. How do you rate product spreading on the skin? _____
- d. How do you rate product tackiness? (How sticky is it?) _____
- e. How did you feel after product application? _____
- f. After product application, how do you rate your skin feel, in terms of oiliness? _____
- g. After product application, how do you rate the white residue trail? _____
- h. After product application, how do you rate your skin smoothness? _____
- i. After product application, how do you rate your skin hydration? _____
- j. After product application, how do you rate your skin freshness? _____



2022

SÍLVIA DE ALMEIDA BAPTISTA

DEVELOPMENT AND CHARACTERIZATION OF COSMETIC APPLICATIONS
FOR FUCOPOL

